Australian Government
Geoscience Australia

Record 2013/28 | **GeoCat** 76664

Yilgarn Craton–Officer Basin–Musgrave Province Seismic and MT Workshop

Edited by N.L. Neumann

Yilgarn Craton–Officer Basin–Musgrave Province Seismic and MT Workshop

GEOSCIENCE AUSTRALIA
RECORD 2013/28

Edited by N.L. Neumann

Australian Government
Geoscience Australia

Geological Survey of
Western Australia

Department of Resources, Energy and Tourism

Minister for Resources and Energy: The Hon Gary Gray AO MP
Secretary: Mr Blair Comley, PSM

Geoscience Australia
Chief Executive Officer: Dr Chris Pigram
This paper is published with the permission of the CEO, Geoscience Australia

ISSN 1448-2177 (Print)
ISSN 2201-702X (PDF)

ISBN 978-1-922201-60-7 (Print)
ISBN 978-1-922201-61-4 (PDF)

GeoCat 76664

Bibliographic reference:

Full volume
Neumann, N.L. (ed.) 2013. *Yilgarn Craton–Officer Basin–Musgrave Province Seismic and MT Workshop*. Record 2013/28. Geoscience Australia: Canberra.

Individual abstract example
Duan, J., Milligan, P.R., & Fomin, T. 2013. 'Electrical resistivity distribution from magnetotelluric data in the Yilgarn Craton, western Officer Basin and western Musgrave Province' in Neumann, N.L. (ed.) *Yilgarn Craton–Officer Basin–Musgrave Province Seismic and MT Workshop*. Geoscience Australia Record 2013/28. Geoscience Australia: Canberra, pp. 9–23.

Version: 1307

Acknowledgements

We would like to thank the Ngaanyatjarra Council, the Shire of Ngaanyatjarraku and the indigenous people of the Ngaanyatjarra lands for their assistance and hospitality during the acquisition of these geophysical surveys.

Contents

Acknowledgements iii

1 11GA-YO1 Yilgarn Craton–Officer Basin–Musgrave Province seismic survey - acquisition and processing 1
Introduction 1
Seismic acquisition 1
Seismic reflection processing 3
Conclusions 7
Acknowledgements 7
References 8

2 Electrical resistivity distribution from magnetotelluric data in the Yilgarn Craton, western Officer Basin and western Musgrave Province 9
Introduction 9
Data acquisition 9
Data processing 10
Analysis of data dimensionality and geoelectric strike 11
Analysis of magnetic transfer function data 14
Analysis of MT data responses 15
One-dimensional inversion of YOM data 17
Two-dimensional inversion of YOM data 18
Three-dimensional inversion of YOM data 19
Discussion and conclusion 20
Acknowledgements 21
References 22

3 Geological setting and interpretation of the southwest half of deep seismic reflection line 11GA-YO1: Yamarna Terrane of the Yilgarn Craton and the western Officer Basin 24
Introduction and aims of the seismic survey 24
Seismic and MT acquisition and processing 29
Geological setting 29
Geological interpretation of the southwestern part of seismic line 11GA-YO1 39
Summary 46
Acknowledgements 46
References 47

4 Geological setting and interpretation of the northeastern half of deep seismic reflection line 11GA-YO1: west Musgrave Province and the Bentley Supergroup 51
Introduction 51
Tectonic subdivisions of the west Musgrave Province 53
Lithological subdivisions of the west Musgrave Province 56
Detailed geology and geological history of the west Musgrave Province 58
The 1085–1040 Ma Giles Event, Warakurna Supersuite and Ngaanyatjarra Rift 69
Geological interpretation of the northeastern part of seismic line 11GA-YO1 80
Acknowledgements 89

References....90
5 Geophysical investigation and 3D geological model of the Yilgarn Craton–Officer Basin–Musgrave Province region....96
Introduction....96
Input data....97
Geophysical studies....104
3D geological model....118
Concluding remarks....127
Acknowledgements....127
References....128
6 Four-dimensional architecture of the west Musgrave Province....130
Introduction....130
The west Musgrave Province....130
The Mount West Orogeny....131
The Musgrave Orogeny....132
The Ngaanyatjarra Rift (NR)....132
Post-NR tectonics....133
Methods....133
Tectonic architecture of the west Musgrave Province....141
Summary....146
Acknowledgements....147
References....148
7 Numerical modelling of the west Musgrave Province during Musgrave Orogeny....151
Introduction....151
Numerical method....152
Results....153
Conclusions....156
Acknowledgments....156
References....157
8 The nature of the lithosphere in the vicinity of the Yilgarn Craton–Officer Basin–Musgrave Province (11GA-YO1) seismic line....158
Introduction....158
Crustal Structure....160
Surface Wave tomography....163
Discussion and Conclusions....165
Acknowledgements....165
References....166
9 Geodynamic implications of the Yilgarn Craton–Officer Basin–Musgrave Province (YOM) deep seismic reflection survey: part of a ~1800 km transect across Western Australia from the Pinjarra Orogen to the Musgrave Province....168
Introduction....168
Moho....173
Crustal architecture....176
Crustal sutures and major faults....184
Geodynamic Implications....185
Transect across Western Australia....188

Summary 190
Acknowledgements 190
References 191
10 The YOM seismic survey: Implications for mineral systems in the Yilgarn Craton–Officer Basin–Musgrave Province region 197
Introduction 197
Mineral Systems 198
Gold and Komatiite-hosted Nickel in the Yamarna Terrane 199
The Manunda Basin 202
Giles Event & Warakurna LIP magmatic Ni-Cu-PGE mineral system 203
Hydrothermal gold and base-metal mineral systems in the Bentley Supergroup 205
Iron Oxide Copper-Gold (IOCG) mineral systems 206
Summary 206
Acknowledgements 207
References 208

1 11GA-YO1 Yilgarn Craton–Officer Basin–Musgrave Province seismic survey - acquisition and processing

J. Holzschuh

Minerals and Natural Hazards Division, Geoscience Australia, GPO Box 378, Canberra, ACT 2601.

Josef.Holzschuh@ga.gov.au

Introduction

Geoscience Australia in collaboration with the Geological Survey of Western Australia (GSWA), contracted Terrex Seismic to collect the Yilgarn Craton–Officer Basin–Musgrave Province (YOM) Deep Seismic Reflection Survey data in May and June 2011. Deep seismic reflection data and gravity readings were acquired along the 484 km YOM seismic line. Magnetotelluric (MT) data (Duan et al., 2013) were also acquired along the seismic line. The survey was funded by Geoscience Australia's Onshore Energy Security Program together with GSWA under the Royalties for Regions Exploration Incentive Scheme. The aims of the survey were to image and help evaluate the architecture and deep structure of the northeast Yilgarn Craton and Musgrave Province, and the western Officer Basin and the relationship between the Yamarna Terrane and the western Musgrave Province beneath it.

Seismic acquisition

The reflection seismic survey acquisition commenced on 30 May 2011, from Warakurna, Western Australia and continued south west along the Great Central Road to Tjukayirla, Laverton Shire, Western Australia ending on 26 June 2011. The location of the line is shown in Figure 1.1. Acquisition parameters for the survey are shown in Table 1.1. Most of the seismic data were collected with a 300 live channels spread over 12 km with the source array located at the centre of the spread. For most of the line the maximum offset receiver groups were 6 km from the source. No stations were pegged or surveyed through the Warburton aboriginal community from stations 6555 to 6669. Geophones were laid to the edge of the town. Vibrator Points (VPs) were shot to the edge of the town and then across the gap to the west of the town with the geophones spread to the east, followed by the spread to the west and the VPs to the east. This provided far offset data across the Warburton gap which infilled the deeper data beneath the gap providing far offset data for the 4.6 km Warburton gap, with a maximum offset of 14.5 km.

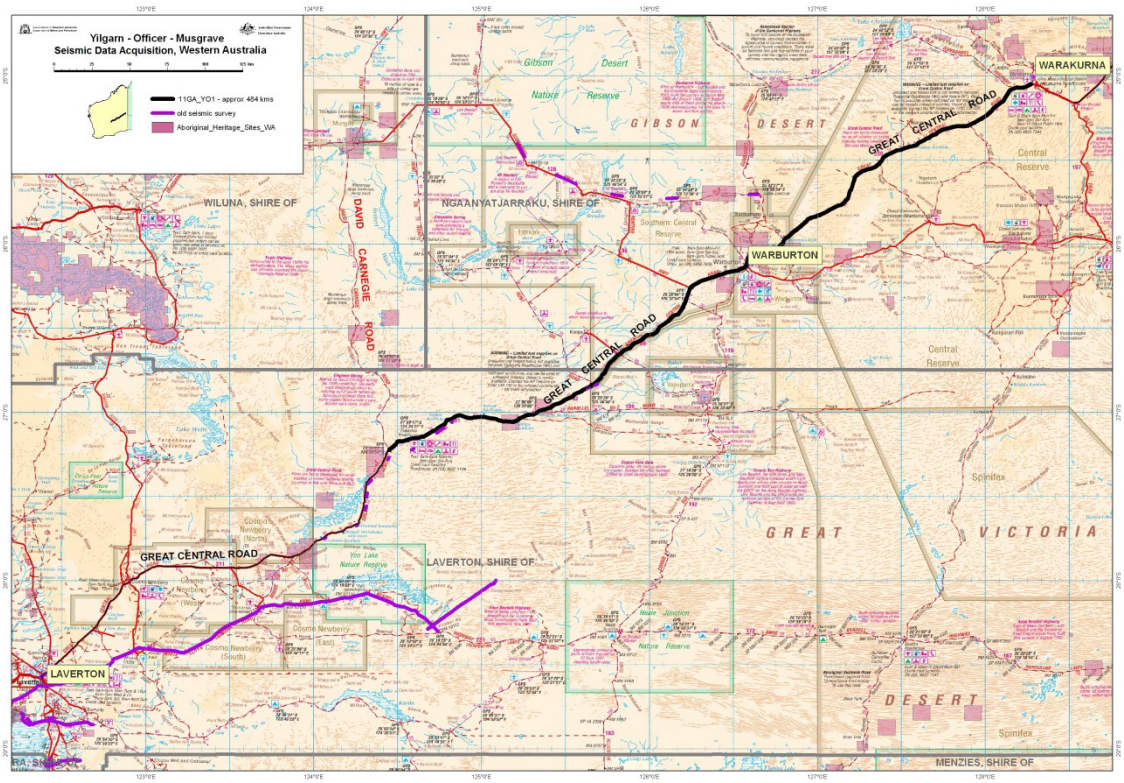

Figure 1.1 *Location of the Yilgarn Craton–Officer Basin–Musgrave Province seismic and MT line.*

The seismic data were recorded using a Sercel 428XL recording system in SEG-D demultiplexed format. The recording system cross-correlated each of the 3 recorded sweeps for each VP with its respective reference sweep and stacked the cross-correlated sweeps, creating a single 20 s record for each VP. After station 4911, 22 s data were recorded as possible moho reflections were visible on the field stack at close to 20 s. An average survey production rate of 216 VPs or 17.3 km per day was achieved.

Table 1.1 *Acquisition parameters used for the 11GA-YO1 seismic survey.*

Line	11GA-YO1
Source type	3 IVI Hemi-50 vibrators
Source array	15 m pad-to-pad, 15 m moveup
Sweep length	3 x 12 s
Sweep frequency	6–64 Hz, 10–96 Hz, 8–80 Hz
Vibration Point (VP) interval	80 m
Receiver group	12 geophones @ 3.3 m spacing
Group interval	40 m
Number of recorded channels	300
Fold (nominal)	75
Record length	20 s and 22 s @ 2 ms

Seismic reflection processing

The reflection seismic data for the YOM survey was processed by the Seismic Acquisition and Processing team of the Onshore Energy and Minerals Division of Geoscience Australia, using the Paradigm Disco/Focus processing software on a Red Hat Enterprise Linux Sun Fire X4600 M2 server. The basic processing sequence applied to the data is shown in Table 1.2. A reduced processing stream was used in the field to produce field stacks to QC and monitor data quality while the survey was in progress. As the line was essentially a 2D transect, it was processed using algorithms that are based on assumed 2D geometry. This 2D assumption has implications for processing and for the interpretation of the resulting processed data, which is explained in the description of the key processing steps.

Table 1.2 *Seismic reflection processing sequence for line 11GA-YO1.*

Crooked line geometry definition (CDP interval 20 m)
SEG-D to SEG-Y to Disco format conversion, resample to 4 ms
Quality control displays
Inner trace edits
Common midpoint sort
Gain recovery (spherical divergence)
Spectral equalisation over 8 to 92 Hz (1000 ms AGC gate)
Application of floating datum residual refraction statics
Velocity Analysis
Application of automatic residual statics
Normal moveout correction and variable percentage stretch mute
Band pass filter
Offset regularisation and dip moveout (DMO) correction
Common midpoint stack
Omega-x migration
Signal coherency enhancement (digistack 0.5 and fkpower)
Application of mean datum statics, datum 600 m, replacement velocities 5900 m/s, 2500 m/s and 4600 m/s at stations 1000–6900, 6900–11200, and 11200–13105 respectively.
Trace amplitude scaling for display

Crooked line geometry definition

The seismic line followed the Great Central Road and hence was not straight. To process crooked line data using the Common Depth Point (CDP) method, it is necessary to bin the data into common midpoint gathers based on a calculated CDP line. The CDP line a curve of best fit through the source-receiver midpoints which optimises the fold of the data. Each trace (source-receiver pair) is allocated to the nearest CDP bin to its midpoint. The CDP bins were defined to be 20 metres along the line, and 1800 m wide across the line. The effect of the bin size and midpoint scatter within the bin is most critical at shallow depths. Where the line has sharp bends, there is likely to be smearing and poor

resolution of shallow data. The effect of bends on deeper data can also be significant, depending of the relative directions of the seismic line and the dip of the structures to be imaged. The CDP line was processed as if it was straight, ignoring the effects of changing azimuth along the line. This simplification of the processing to a 2D geometry right at the start of the processing sequence is reasonable for large sections of the line which are relatively straight, however, it is not possible to correctly migrate, and therefore correctly image, reflections at significant bends in the line.

Refraction statics

Variations in surface elevation, weathering layer depth and weathering layer velocity can produce significant time delays in land seismic data. Variations over a short distance relative to the spread length can degrade the stack, as the reflections do not align across the traces to be stacked. Variations over distances longer than a spread length will not significantly affect the stack quality, but can introduce spurious long wavelength structure on the stacked reflections. Static corrections are applied in the processing stream in order to remove these effects. Static corrections for the YOM reflection seismic processing were calculated based on picking first break refracted arrivals from shot records and creating a near surface refractor model of the weathering layer. The refraction statics were applied in two stages using a floating datum. An intermediate step of automatic residual statics produced fine tuning of the corrections. The final statics were calculated relative to a datum of 600 m (AHD).

Once the first breaks for the line have been picked and edited and the number of layers to be modelled is selected, the refractor model can be calculated. Usually, a one or two layer model can provide a suitable solution to the modelling of the weathering. For the YOM line, single layer models were selected as best representing the weathering and varied across the seismic line. Over the Musgrave section northeast of Warburton the replacement velocity used was 5900 m/s (stations 1000–6900). Southwest of Warburton over the Officer Basin the replacement velocity used was 2500 m/s (stations 6900–11200), and on the southwest end of the line a replacement velocity of 4600 m/s was used (stations 11200–13105).

Spectral equalisation

Spectral Equalisation is a process used to sharpen the reflection wavelet and suppress low frequency energy, primarily ground roll energy, which is surface wave energy that is generated by the vibrators. The frequency spectrum of the data is flattened over a specified frequency range and within a specified time gate. The high energy, low frequency ground roll is thereby reduced relative to the higher frequency energy of the reflections. The resulting data has better resolution, particularly in the shallow (0 – 2 s) section. The selection of appropriate frequency range and time gate is based on selective testing and spectral analysis of the data.

Normal moveout correction

Normal moveout (NMO) correction removes time variations across CDP gathers by adjusting for the time delays caused by increasing offset between source and receivers across the gather. The NMO correction is applied as a stacking velocity which best aligns the reflections in the CDP gather. Constant velocity stacks were used to define the stacking velocity field, producing a velocity field varying in time and space (along the line) which maximises the stack response of the data.

When applying NMO correction far offset data will be stretched and an artificial increase in wavelength appears. This is relatively large for horizontal reflections with low stacking velocities. The data that are over-stretched are muted, this is called stretch-mute. Numerous NMO stretch mute percentages and velocities were tested. The stretch mute velocities and percentages changed significantly along the seismic line.

The velocity boxes annotated on the seismic sections are the final velocities picked from the normal moveout gathers with all corrections except the mean refraction statics applied, i.e. velocities were applied prior to moving the data to its final datum.

Dip moveout correction

Dip moveout (DMO) correction, also known as partial prestack migration, adjusts the NMO correction for the increase in stacking velocity as structural dip increases, and has the effect of correcting the NMO to account for different dips occurring along the line. The process effectively moves reflection energy between traces within and between CDP gathers based on apparent dip of the reflections, and creates a new set of DMO-corrected CDP gathers. After DMO, intersecting dipping and flat reflections will correctly stack with the same stacking velocity. DMO is a very computer intensive processing step.

Common midpoint stack

Common midpoint stack is simply the summing of traces in a CDP gather to produce a single trace at the CDP location. The traces in the gather are aligned by the NMO and DMO processes to sum optimally. Stacking the data improves the signal to noise ratio of the data by $\sqrt{n}$, where n is the number of traces summed (the fold). A nominal fold of 75 resulted from the acquisition geometry for the YOM survey.

Post-stack time migration

Migration is the final processing step and moves dipping reflections to their most likely lateral positions. Reflections that appear as dipping on the stack section will be moved up dip and shortened after migration. Diffraction hyperbolas resulting from discontinuities, such as terminations of reflectors at faults, and which are visible on the stack section, should collapse to a small region after migration. However, areas of poor signal to noise ratio, sharp bends and boundaries of high amplitude and low amplitude (strong and weak) reflections in the line can produce artefacts in the data which will not migrate successfully. The main parameters to be selected when performing migration are the velocity field and dip ranges to process. The velocity field used is usually a percentage of the stacking velocity. Tests are run on different percentages of the stacking velocities and the optimum migration velocity is selected for different sections along the seismic line.

The final migrated time section should have dipping reflections in the correct spatial location. The Omega-X (frequency-space) migration algorithm used to process the YOM data is a finite difference approximation to the monochromatic wave equation, as described in Yilmaz (2001). The effect of migration on the stacked data is illustrated in Figure 1.2 which shows stack and migrated images of part of the Officer Basin. The lower image shows how the migration process collapses diffraction energy and moves dipping reflectors to the correct location.

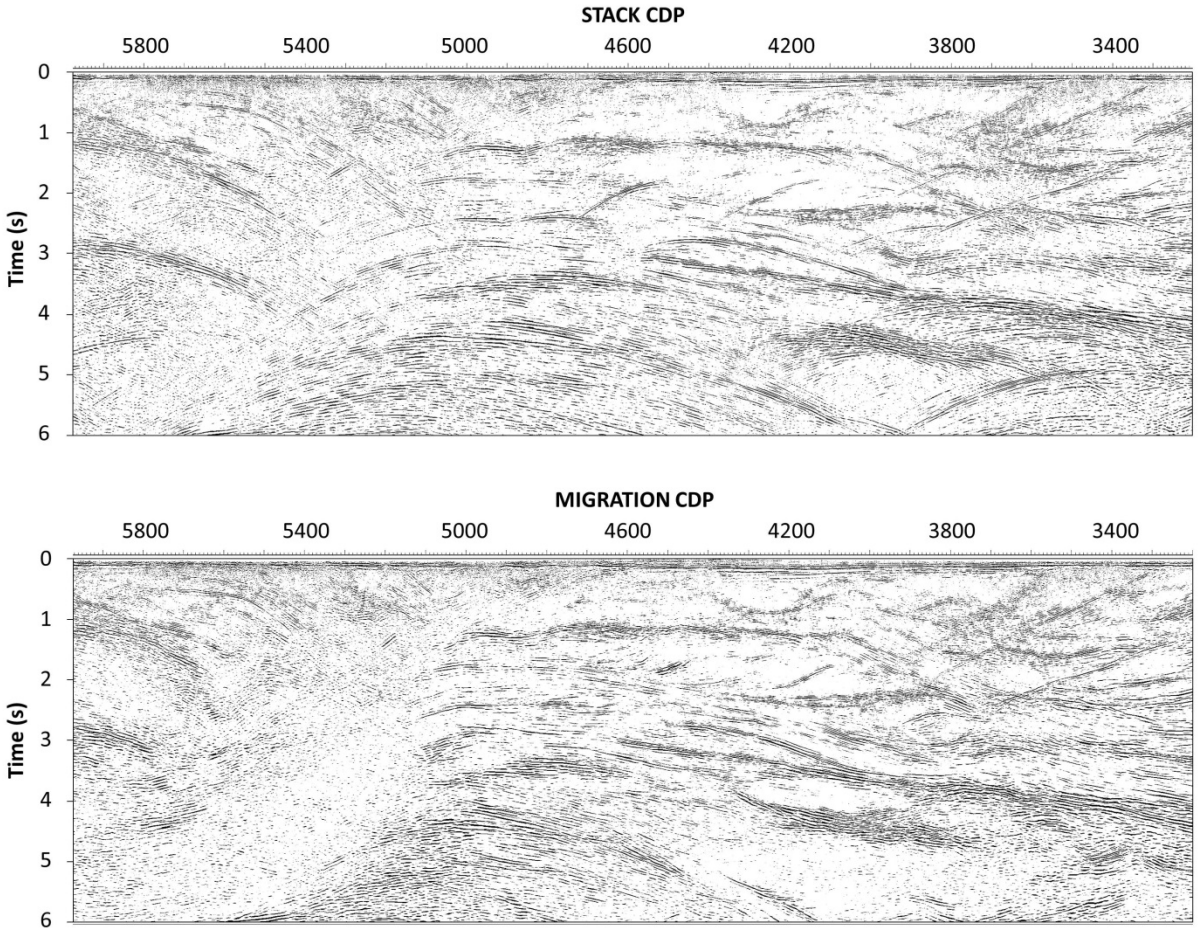

Figure 1.2 *Final stacked (upper) and migrated (lower) sections for part of YOM seismic line.*

Warburton data gap processing

Across the Warburton town no geophones or source stations were used and only far offset data exists, creating a data gap in the upper 2 s. The data acquired across this Warburton gap have a maximum offset of 14.5 km. When applying NMO and DMO the stretch-mute effect had to be reduced to allow maximum imaging of these far offset data in the top 3 s.

Across the Warburton gap the data are not continuous with adjacent data in the top 2 s. Applying DMO did not show up any further dipping reflections but only smeared the data in the top 2 s, so DMO was not applied to the gap data. Migration also smeared the data and a very low migration velocity of 2000 m/s was applied to the gap data. A surgical mute was applied in the final plot to remove migration smearing edge effects along the edges of the Warburton gap in the top 2 s.

Signal enhancement

Coherency filters were applied to the data to enhance reflections for the final display images.

Regions of low reflectivity

In some regions, the data appeared weak or low reflectivity and have some correlation with Cretaceous units, green region in Figure 1.3 (CDPs 14000 to 22500) suggesting source energy and/or reflected energy penetration problems at the near surface. This geology is discussed in more detail in Korsch et al. (2013). Otherwise this indicates a change in reflectivity at these locations at depth.

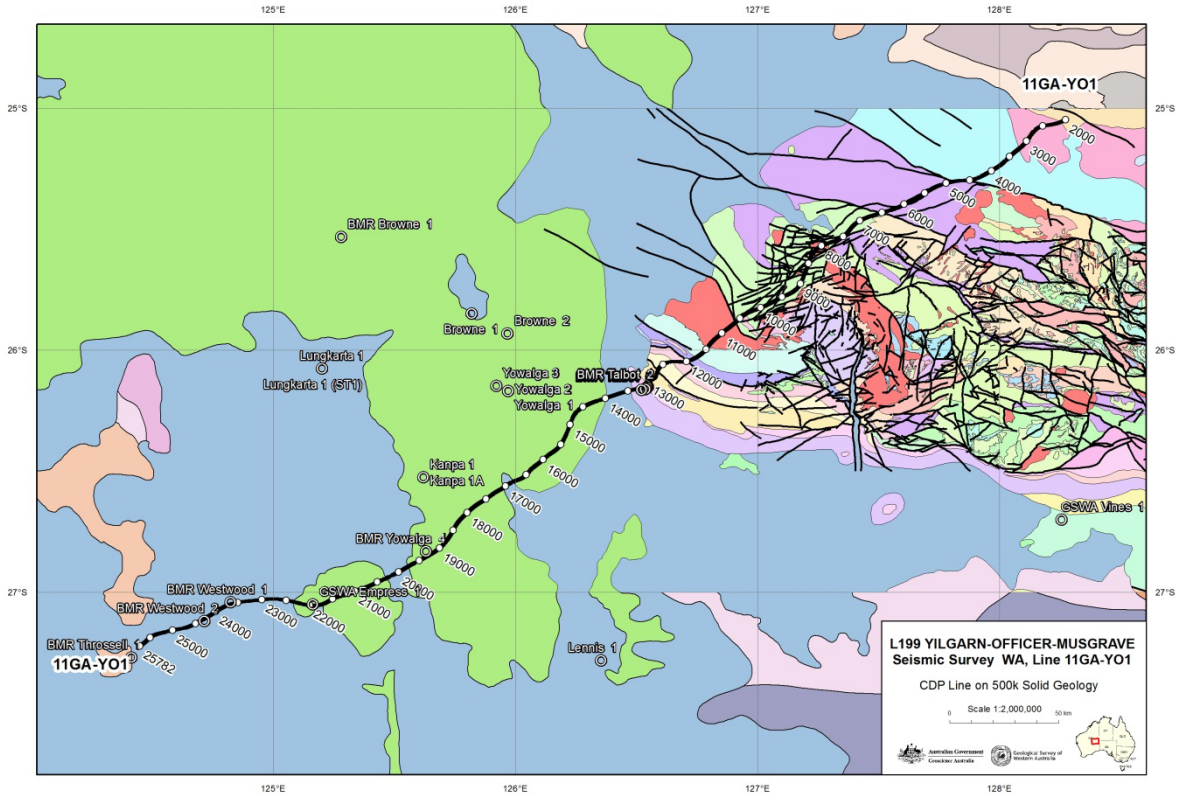

Figure 1.3 *Solid geology map showing the YOM seismic line and CDP locations.*

Conclusions

484 km of 75 fold deep seismic reflection data were acquired along the Great Central Road from near the NT border towards Laverton, WA, in May and June 2011. The YOM traverse spanned parts of the Musgrave Province, the Officer Basin and the Yilgarn Craton. For most of the seismic line, the seismic data provide images of the full depth of the crust through this region. The processed data provide valuable information on the nature of the major crustal structures and sedimentary layering in this area, and is of a quality that meets the scientific objectives of the project.

Acknowledgements

This document is modified from Costelloe and Holzschuh (2010). Land access was organised by Jenny Maher, field data QC and data processing was done by Josef Holzschuh.

References

Costelloe, R., and Holzschuh, J., 2010. *GOMA (Gawler Craton–Officer Basin–Musgrave Province–Amadeus Basin) Seismic and MT Workshop 2010*. Geoscience Australia Record 2010/39, 1–6.

Duan, J., Milligan, P.R., and Fomin, T., 2013. Electrical resistivity distribution from magnetotelluric data in the Yilgarn Craton, western Officer Basin and western Musgrave Province. In: Neumann, N.L. (editor), *Yilgarn Craton–Officer Basin–Musgrave Province (YOM) Seismic and MT Workshop*. Geoscience Australia Record 2013/28, 9–23.

Korsch, R.J., Blewett, R.S., Pawley, M.J., Carr, L.K., Hocking, R.M., Neumann, N.L., Smithies, R.H, Quentin de Gromard, R., Howard, H.M., Kennett, B.L.N., Aitken, A.R.A., Holzschuh, J., Duan, J., Goodwin, J.A., Jones, T., Gessner, K., and Gorczyk, W., 2013. Geological setting and interpretation of the southwest half of deep seismic reflection line 11GA-YO1: Yamarna Terrane of the Yilgarn Craton and the western Officer Basin. In: Neumann, N.L. (editor), *Yilgarn Craton–Officer Basin–Musgrave Province (YOM) Seismic and MT Workshop*. Geoscience Australia Record 2013/28, 24–50.

Yilmaz, O., 2001. Seismic Data Analysis. Society of Exploration Geophysicists, Tulsa, Oklahoma.

2 Electrical resistivity distribution from magnetotelluric data in the Yilgarn Craton, western Officer Basin and western Musgrave Province

J.Duan, P.R.Milligan, and T.Fomin

Minerals and Natural Hazards Division, Geoscience Australia, GPO Box 378, Canberra, ACT 2601.

Jingming.Duan@ga.gov.au

Introduction

As part of the Australian Government's Onshore Energy Security Program, Geoscience Australia in collaboration with the Geological Survey of Western Australia, acquired magnetotelluric (MT) data during May–June 2011 along the 484 km deep crustal seismic reflection transect 11GA-YO1, referred to as the Yilgarn Craton–Officer Basin–Musgrave Province (YOM) survey (see Figure 2.1 for location map). The MT profile extends from the Yamarna Terrane in the north-eastern Yilgarn Craton, across the western Officer Basin, to the western Musgrave Province. The purpose of the MT survey is to map the electrical resistivity distribution and to improve scientific understanding of the Earth's crust and upper mantle in this region. The MT data complement the YOM deep crustal seismic reflection survey, other geophysical data and geological data. The aim is to provide additional geological understanding by using multi-disciplinary earth imaging techniques in the region.

Data acquisition

MT data were measured at 72 broadband MT sites and 31 long-period MT sites along the seismic line (see Figure 2.2). The average site spacing was approximately 5–10 km for broadband data and 10–15 km for long period data. Data from most sites were good quality since there is little cultural noise in this region. The instrumentation used for measuring magnetic data included two induction coils for the higher frequencies (broadband data) and three-component fluxgate magnetometers for the lower frequencies (long-period data). The electric field components were indirectly measured through the potential difference voltage between two separated electrodes along the designed direction. GPS provided accurate timing for correlation of the observed magnetic and electric field measurements at each site, and synchronisation between simultaneous sites for the purposes of remote-referencing reduce uncorrelated noise. More than three sites were usually deployed at a time to enable this remote-referencing. Data quality control was conducted in the field during the data acquisition period.

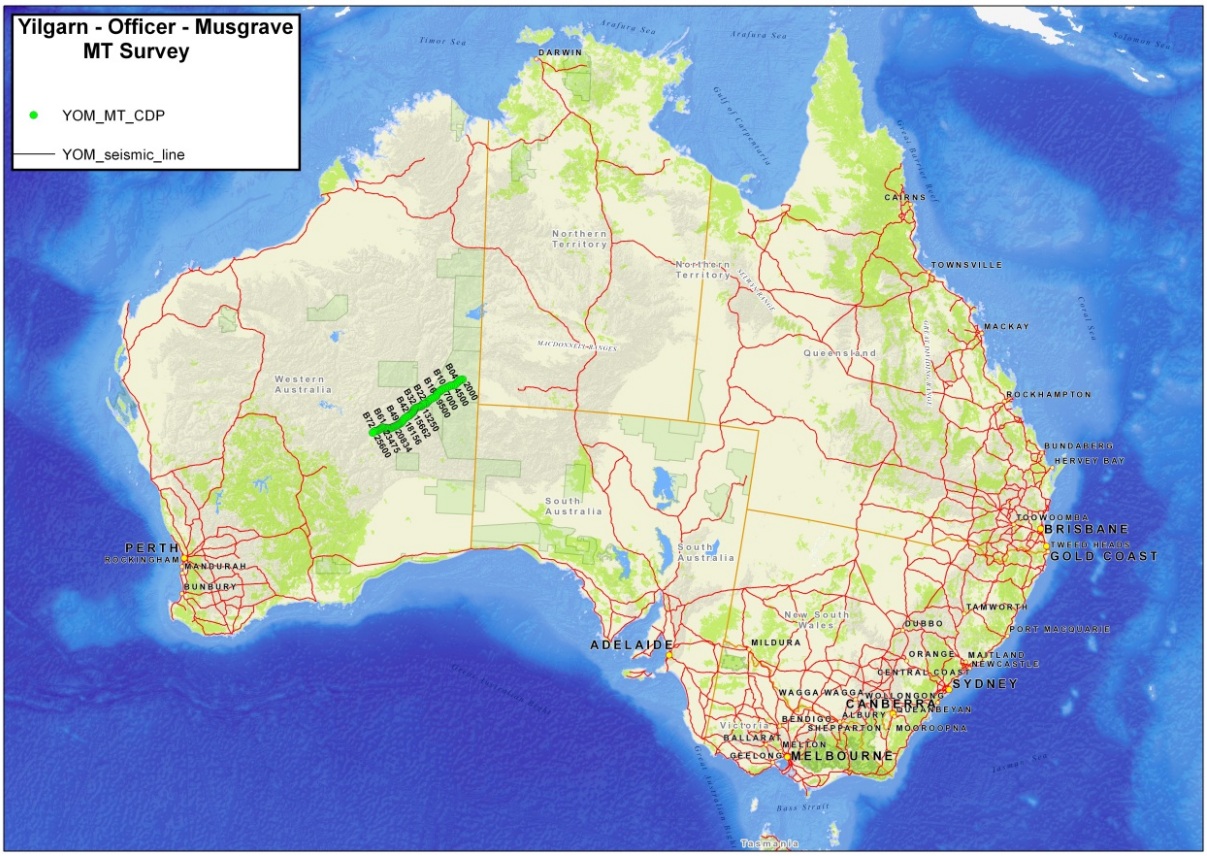

Figure 2.1 *Location of YOM MT survey (green line) plotted on a topography map from Geoscience Australia.*

At each broadband site, induction coils were used to measure the magnetic fields in two orthogonal horizontal directions (north-south and east-west). The horizontal electric fields were measured using two orthogonal dipoles (north-south and east-west) with an average length of 50 m in an L-shaped configuration. Electrodes were buried to reduce any temperature variations, and to ensure a wet environment to provide a low contact resistance. MT data were recorded as four channels of time series at a sampling rate of 1000 Hz, which gives an effective frequency bandwidth of approximately 300−0.01 Hz. The broadband survey was used to gain information within the upper crust, thus deployments of 20–50 hours were sufficient.

At each long-period MT site, magnetic data were acquired in three orthogonal directions (two horizontal and one vertical) with a fluxgate magnetometer. Electric field acquisition remained the same as for broadband. Data were recorded as five channels of time series at a sampling rate of 10 Hz. The sensitivity range of the fluxgate magnetometers is 0.2–0.0001 Hz. Long-period data was used for identifying regional features in the crust and upper mantle, with a longer recording period of 7 days being required for the deeper penetration of signals.

Data processing

Pre-processing of the MT time-series data is a manual selection process to remove contaminated data, such as spikes or obvious disturbances. The MT processing fundamentally involves Fourier transformation of the electric and magnetic field time-series data into the frequency domain for deriving the complex impedance tensor of the subsurface. The impedance tensor links the horizontal

components of electric and magnetic fields in the frequency domain and contains the Earth's resistivity information beneath the measurement point. The apparent resistivity and phase as a function of frequency are derived from the impedance tensor. The common approach uses the robust processing technique (Egbert et al., 1986, 1997; Chave et al., 1987, 2004; Larsen et al., 1996; Smirnov, 2003) coupled with remote reference technique (Gamble et al., 1979). The impedance tensor of the YOM MT survey was derived by using the algorithm BIRRP of Chave et al. (1987, 2004) with remote reference data when available. This method uses robust statistics to remove non-Gaussian data outliers and errors. Coherence analysis of the behaviour of the electric field as the magnetic field changes with time was carried out for assessing data quality during the processing stage. Apparent resistivity and phase were also determined for each site. Long-period and broadband MT data of coincident location sites were merged into single responses (prefix BL *) to obtain these estimates, covering periods of 0.005 s to about 10000 s for these sites. The rest of the broadband MT data (prefix B*) covers periods of 0.005 s to 100 s (Figure 2.3 shows some examples).

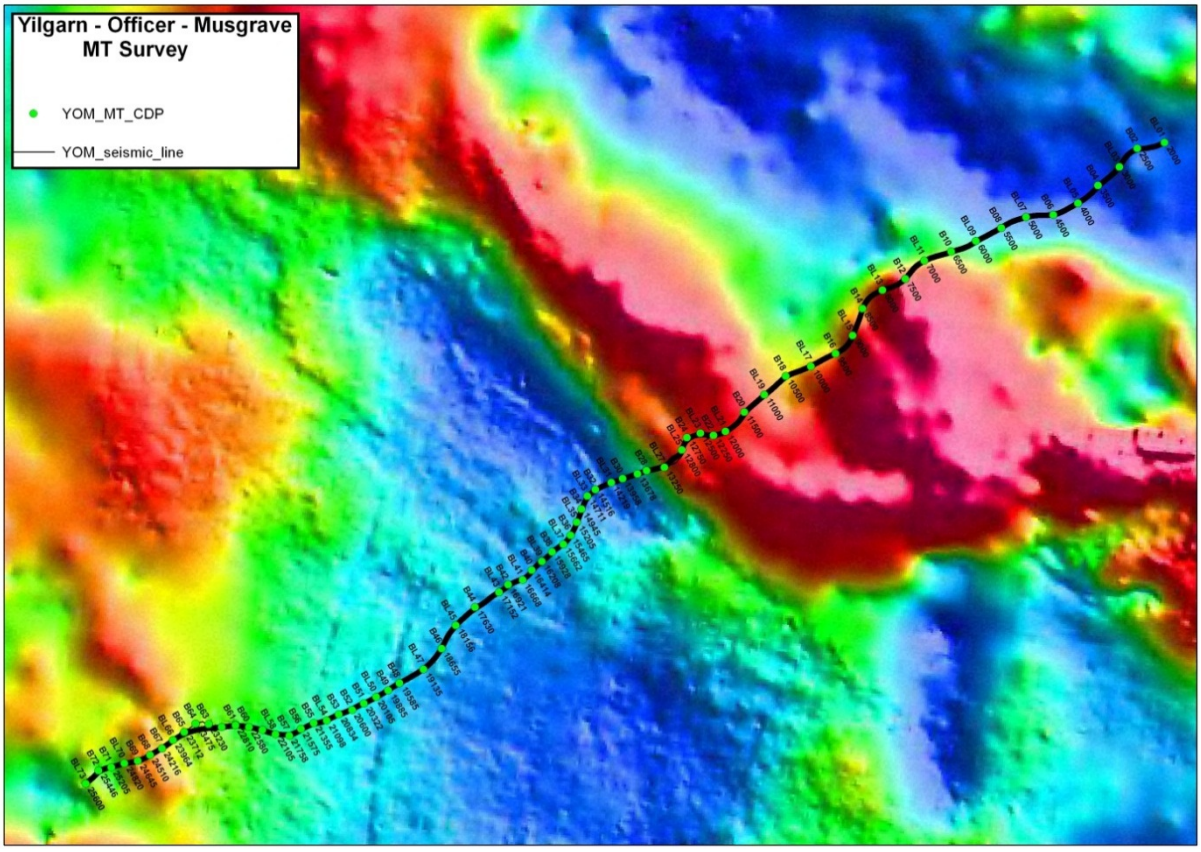

Figure 2.2 *MT sites plotted on a gravity anomaly map (Wynne, 2009). Black line is the seismic transect with common depth point (CDP) locations.*

Analysis of data dimensionality and geoelectric strike

The processed data should carefully analyse prior to inverting any conductivity model. The analysis of the impedance tensor is necessary in order to understand the basic electrical properties in the region. These properties (e.g. the dimensionality, electrical strike direction, and data distortion) have considerable effects on the inversion results. A successful analysis may be crucial to decide appropriate model assumptions and can prevent misinterpretation of the data with inadequate

assumptions. MT impedance tensor analysis techniques have become a standard tool, which may be classified into mathematical decompositions and physical decompositions. Many methods have been developed to determine the dimensionality, strike direction and galvanic distortion of an investigation region (e.g. Swift, 1967; Bahr, 1988; Groom et al., 1989, 1991; McNeice et al., 2001; Caldwell et al., 2004; Becken et al., 2004; Mart et al., 2009).

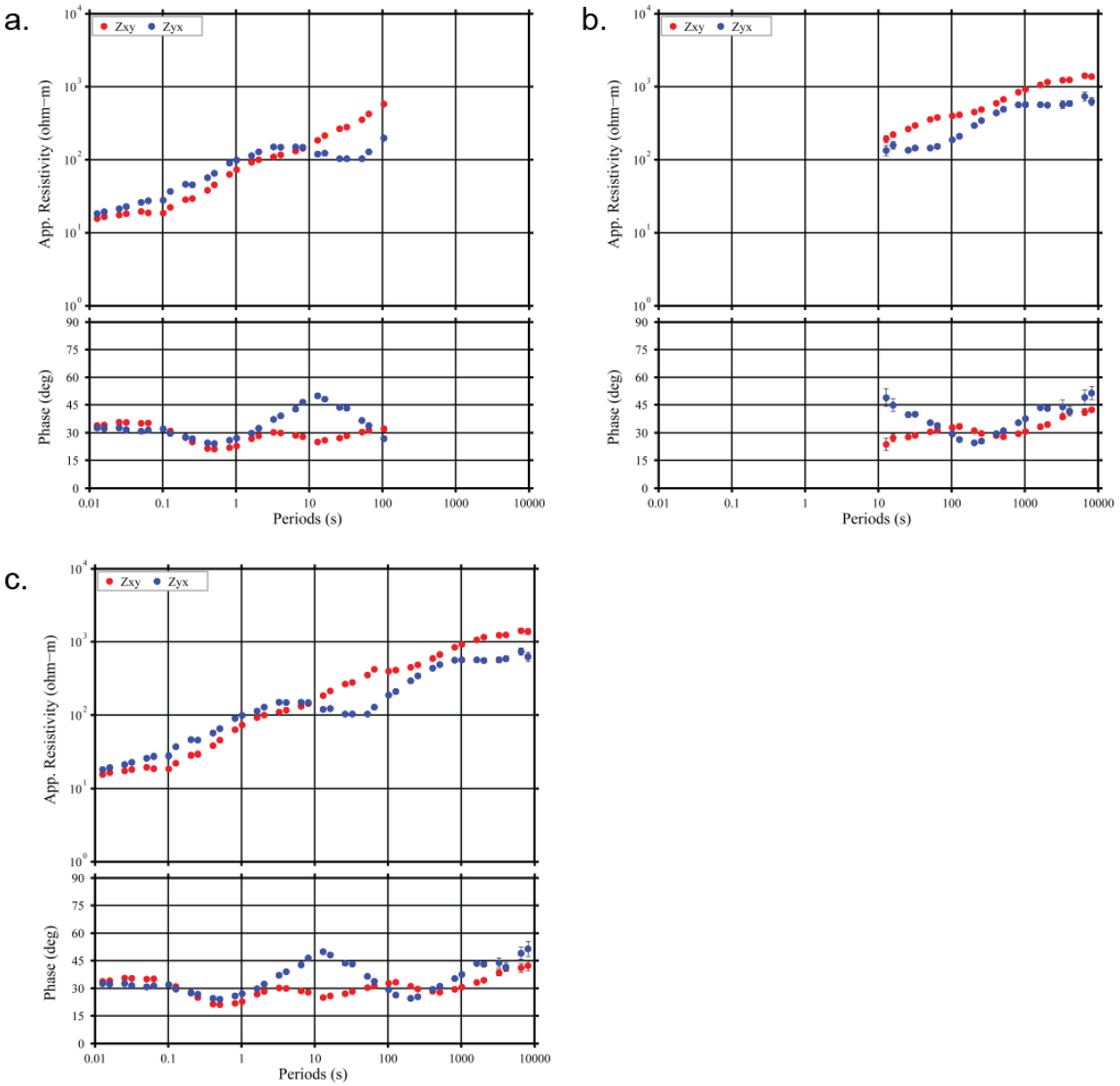

Figure 2.3 *Examples of a) broadband data response where X axis = range of periods, Y axis = apparent resistivity value (top image) and phase in degrees (bottom image), b) long period data where X axis = range of periods, Y axis = apparent resistivity value (top image) and phase in degrees (bottom image), and c) merged data response where X axis = range of periods, Y axis = apparent resistivity value (top image) and phase in degrees (bottom image).*

Ellipticity parameters after Becken and Burkhard (2004) provided information on the directionality and dimensionality of the YOM MT data (Figure 2.4). This decomposition technique separates local and regional parameters under the assumption that the regional structure is mostly two-dimensional (2D) and the local structure causes only galvanic scattering of the electric fields. It examines the MT full ellipticity parameters of the impedance tensor in terms of ellipses and subsequently enables rotation to

the coordinate system in which the ellipticities are minimised. If the minimal ellipticities are close to zero, the existence of a regional 2D resistivity distribution can be assumed. Otherwise, impedance tensor are elliptically polarized in any coordinate system which suggests a strong three-dimensional (3D) resistivity distribution. In practice, real data rarely exhibit an exactly 2D impedance tensor, but 2D impedance tensors exist at least over a certain frequency range. A structure which acts as part of the regional inductive structure at high frequencies may act as a frequency independent distortion structure at much lower frequencies (Groom et al., 1989).

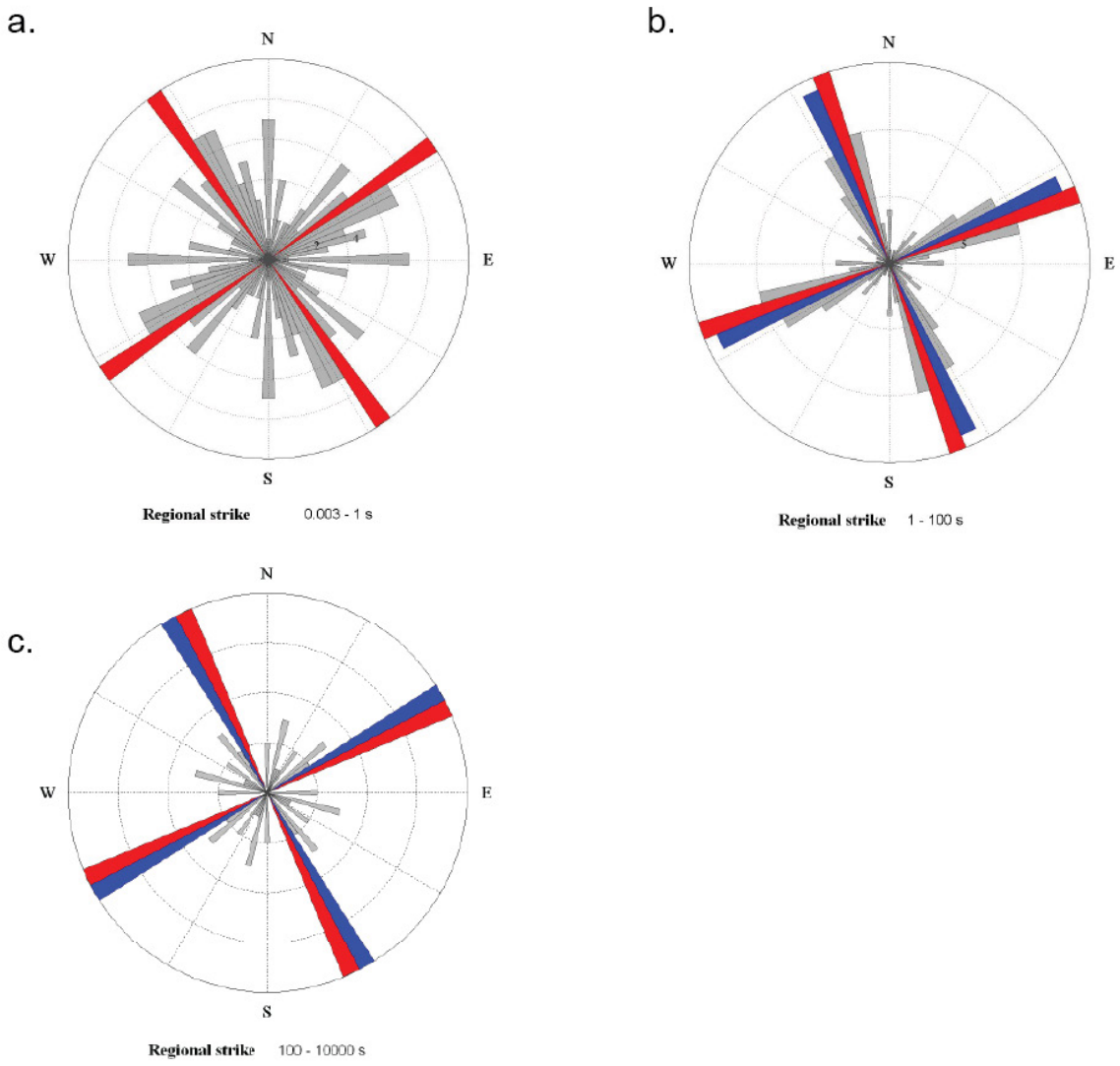

Figure 2.4 *Regional strike directions in a rose diagram at periods of a) 0.003 s to 1 s, b) 1 s to 100 s, and c) 100 s to 10000 s.*

The analysis demonstrates that multiple geoelectric strike directions exist along the YOM profile. The principal strike directions are about N25°W to N40°W or N50°E to N65°E with 90° ambiguity. The principal strike direction will be either perpendicular or parallel to the strike of the strong distortion structure. This 90° ambiguity in geoelectric strike direction cannot be resolved from the analysis information alone. External information is required to resolve this ambiguity, such as, magnetic induction vectors, geological surface strike of major terrane boundaries, and other geophysical data.

The WALDIM method of Marti et al. (2005, 2009) was used for the dimensionality and invariant analysis of YOM MT data. The statistical distribution of dimensionality and distortion has been carefully calculated and examined. Most data from the south-western section (between site BL73 to BL27) exhibit one-dimensional (1D) or 2D character at periods less than 10 s, 2D and weak 3D behaviour at periods less than 100 s, and 3D behaviour at other longer periods. The data from the north-eastern section (between site BL25 to BL01) show 2D and weak 3D effects at periods less than 10 s and 3D character at most longer periods. The 3D effects may be caused by the distorted response of a 2D regional structure, strong 3D structure or a combination of both. The 3D behaviour creates a challenge for 2D inversion since a 2D assumption is not valid for the north-eastern section. Various estimates of strike angle and phase sensitivity skew have also been computed in the analysis.

The phase tensor analysis (Caldwell et al., 2004) technique was also applied to determine the strike direction and dimensionality of YOM MT data. This technique calculates the phase tensor independently and depicts it graphically as an ellipse. The phase tensor ellipses enable determination of 1D, 2D and 3D behaviour respectively in a direct way. In the 2D case, the electric strike direction is either parallel or perpendicular to the major axis of the ellipse. Again the 90° ambiguity needs additional information to resolve. The observed strike directions and dimensionality of YOM data are similar that obtained from the ellipticity parameters method and the WALDIM method.

Analysis of magnetic transfer function data

The magnitude of the magnetic transfer function varies depends upon the strength of the induced current and the distance of the measuring site from the induced current (Figure 2.5). The high magnitudes (yellow and green colours) at periods great than 10 s beneath sites BL01 to BL31 and at periods great than 100 s beneath sites BL50 to BL73 correspond with high degrees of data complexity and 3D geoelectric behaviour beneath these sites from dimensionality analysis. They imply uncertainty and instability when performing 2D inversion in these regions. In contrast to these high magnitudes, a region with low magnitudes is observed beneath stations BL35 to BL47, which coincide simple 1D or 2D structures (blue colour) in this region.

The induction arrows (Parkinson, 1959) of different periods (10 s to 10000 s) from long-period MT data are shown along the entire profile in Figure 2.6. Several features can be observed from the characters of the induction arrows for different periods. Long induction arrows from sites BL50 to BL73 are pointing to north-east at most periods. Long induction arrows from BL11 to BL31 are pointing to south-west at most periods. The induction arrows with small lengths from sites BL31 to BL50 are not pointing in any obvious direction, which could be the cause for larger induction vectors reversals at this area. The above features suggest a lower resistivity zone beneath the sites BL31 to BL50.

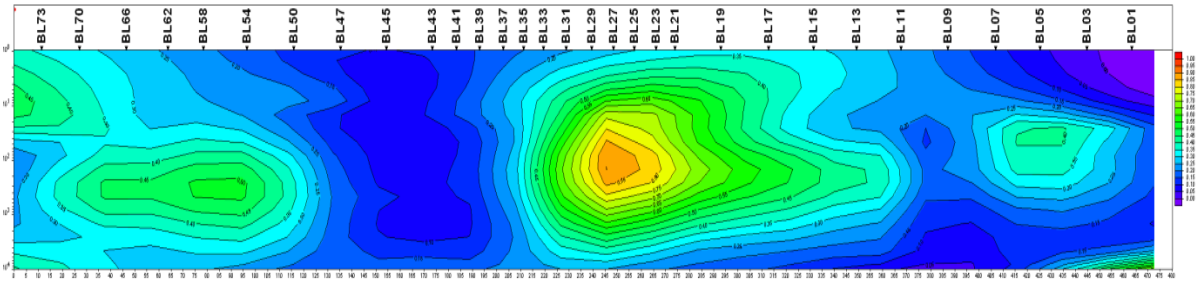

Figure 2.5 *Magnitudes of the magnetic transfer function for the YOM long period data. X axis - MT sites along the profile, Y axis - range of periods from 1 s (top) to 10^4 s (bottom). Colour scale for magnitude from 0 to 1 (red), green is about 0.5.*

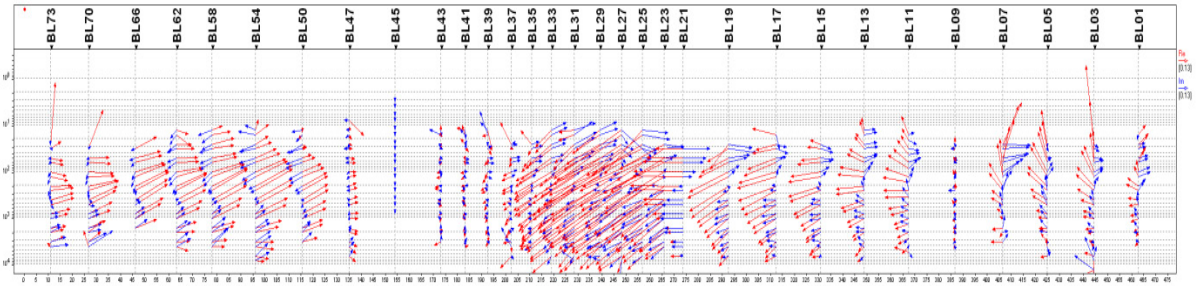

Figure 2.6 *Induction arrow (vectors) of the magnetic transfer function from YOM long period MT data (the real vectors with red colour are pointing to conducting anomalies; the imaginary arrows are blue colour). X axis - MT sites along the profile, Y axis - range of periods from 1 s (top) to 10^4 s.*

Analysis of MT data responses

Analysing the impedance tensor from each site prior to inversion enables evaluation of the complexity of the data and contributes to the inversion strategy. Apparent resistivity and phase from each site can be visualised as pseudo-sections, which are obtained from values of apparent resistivity and phase at each site along the profile. The pseudo-section presents the traverse line on the horizontal axis and period (frequency) on a logarithmic scale vertical axis. The higher frequencies plot on the top of the section and the lower frequencies plot at the bottom, representing the shallow to deeper layers. These images give a qualitative impression of resistivity and phase variations with depth along the profile. Unlike apparent resistivity, phase is not affected by galvanic distortion static-shift. A phase angle above 45º may indicate a conductive structure, while a phase angle below 45º may indicate a resistivity structure.

The pseudo-sections of YOM rotated data are presented for both of transverse magnetic (TM) mode and transverse electric (TE) mode data (Figure 2.7 and Figure 2.8). The information can be used to constrain 2D or 3D inversions and provides a baseline for the results of inversion. The main electrical structures from the pseudo-section should be present in a successful inversion model. The pseudo sections of TM and TE mode data exhibit the following major features:

- In the northeastern section of the profile (between sites BL01 and BL23), the pseudo-sections of phase from both modes data indicate a very high resistivity region at 0.01 s to 10 s. The pseudo-sections of apparent resistivity from both modes show some differences. The TE mode data indicate continuous higher resistivity features at periods great than 1 s, where the TM mode data show resistivity structures for several different regions in the period range 1–1000 s.

- In the southwestern region of the profile (between sites BL29 and BL73), both TM and TE modes data indicate a highly conductive layer with apparent resistivity values less than 10 ohm.m for periods in the range of 0.01–100 s along the south-western part of the profile. They also show a higher resistivity zone beneath sites BL61 to BL73 at periods 0.1–1000 s. For longer periods (100–10000 s), the pseudo-sections of TE mode data indicates much higher resistivity structures, where the TM mode data appear less resistive in the south-western section. This discrepancy maybe related to different induction depth of the two modes.
- Data from both modes show a common feature - an electrical resistivity boundary is clearly suggested at about sites BL23 to BL29.

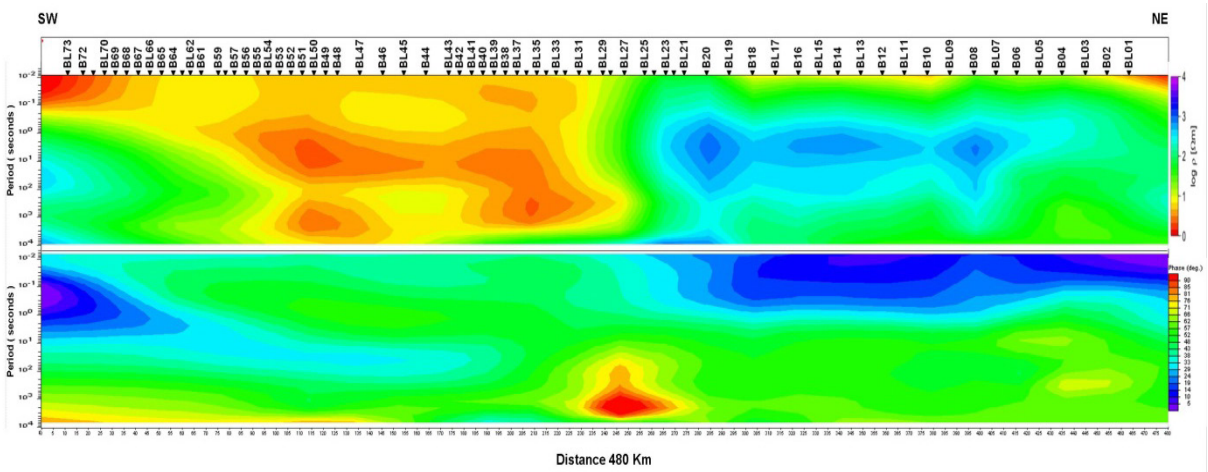

Figure 2.7 *Pseudo-sections of apparent resistivity (top image) and phase (bottom image) from TM mode data. X axis - MT sites along the profile, Y axis - range of periods from 10^{-2} s (top; shallowest) to 10^{4} s (bottom, deepest). Colour scale for phase is red for 90º, green for 45 º, and dark blue for 0º.*

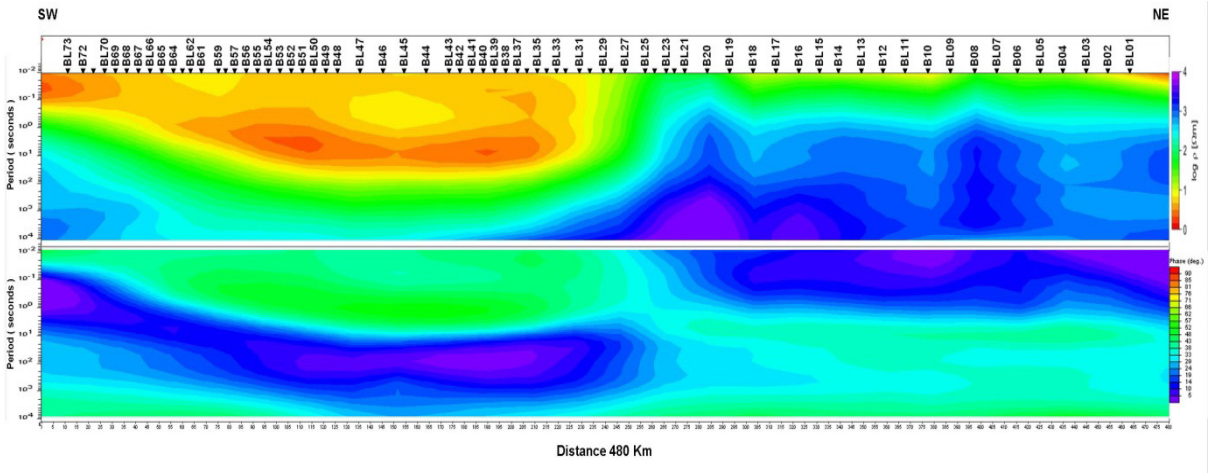

Figure 2.8 *Pseudo-sections of apparent resistivity and phase from TE mode data. X and Y axis are same as Figure 2.7.*

One-dimensional inversion of YOM data

1D MT inversions are an important step to assist in 2D inversion. 1D resistivity structure at each site can be used to examine or constrain the results from a 2D model. The Bostick 1D inversion (Bostick, 1977) and Occam 1D inversion (Constable et al., 1987) were performed for both modes of YOM data. The two different inversion algorithms produced similar 1D models (see Figure 2.9 and Figure 2.10 for results from 1D Occam inversion). The 1D models show a good fit between the measured data and the modelled responses generally. The 1D models give an approximate view of the depth of the penetration of the MT signal and the resistivity structure at each site along the profile. The information was used to determine starting parameters for the 2D inversion and help examining the reliability of resistivity feature from the results of 2D inversion. The 1D resistivity models indicate several major features. The north-eastern section of the profile show much higher resistivity than the south-western section generally. Some lower resistivity features appear beneath sites BL01–BL05 and BL15–BL17 in the north-eastern section of the profile. A shallow conductive structure at sites BL27 to BL70 is indicated by both 1D models. A middle crustal structure with higher resistivity may be located between stations BL54 to BL73 at the south-western end of the profile. The MT signals from stations BL25 to BL54 have less penetration than at other sites. This may be caused by the very high conductive structure beneath these sites.

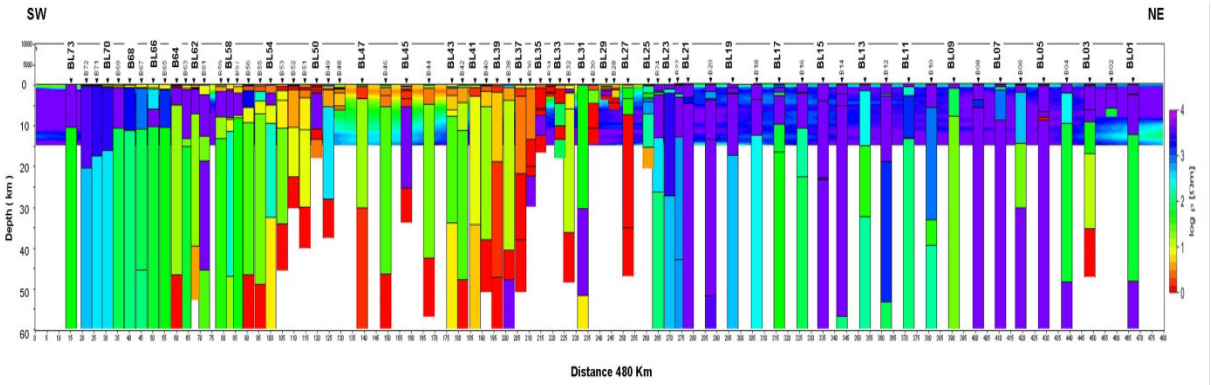

Figure 2.9 *1D model of TM mode data from Occam inversion.*

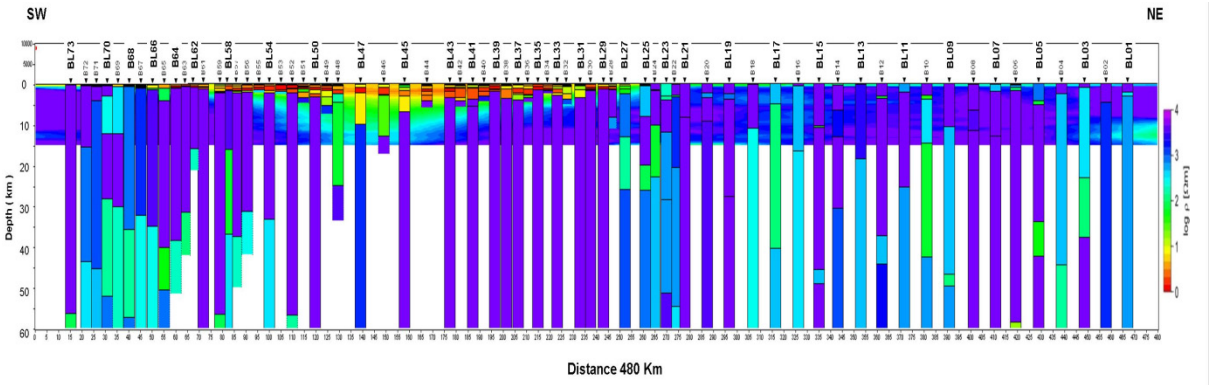

Figure 2.10 *1D model of TE mode data from Occam inversion.*

Two-dimensional inversion of YOM data

The MT inverse problem is nonlinear and ill-posed. It converts a finite set of noisy MT data into a resistivity model of the subsurface of the Earth. Non-uniqueness is to be expected for the 2D inversion. If a solution can be found, then an infinite set of models may also be found. Additional constraints have to be applied to limit the range of acceptable models. The common features, showing repeatability in all models from different inversions, should have a greater degree of confidence. Known geological information, geophysical data and other data are desirable to constraint the model.

A 2D assumption and geoelectric strike of N35°W were applied to the YOM MT dataset. All data were rotated to the strike direction. 3D geoelectric effects and galvanic distortion were neglected. Some noisy data were removed at this stage. Although the single strike direction was assumed for this study, multiple different strike directions exist along the profile. A perfectly 2D situation did not exist in this region; hence, the strike direction and the dimensionality of the data did not fit exactly to the theoretical 2D models as used by 2D inversion algorithms. Based on the results of the 1D models and the data analysis, a strategy and reasonable starting model were constructed for the 2D inversion.

The 2D inversion was performed using the non-linear conjugate gradient (NLCG) algorithm of Rodi and Mackie (2001). Many different models were generated by using different input data and wide range inversion parameters. The TE mode, TM mode and Tipper data (vertical magnetic field transfer function) from different period ranges (broadband data, long period data, merged data and subset data) were inverted respectively and together to emphasize different structures in the crust and upper mantle. Different starting models and meshes were also tested for the 2D inversion. The aim of these inversions was to test the impacts of different input data and parameters on the inversion result, and to test robustness of models. The results of these inversions demonstrated that different input data and inversion parameters had significant impact on the resulting inversion model, but the main features were presented in most models.

Two models obtained from jointly inverting all data with different smoothness levels are presented in Figure 2.11 and Figure 2.13. The model in Figure 2.11 is much smoother than the model in Figure 2.12. There is always a trade-off between smoothness of the model and fitting data. Increasing smoothness of the model leads to decrease data fitting, which means some detail of electrical structures may miss out. On other hand, emphasizing data fitting can produce rough models (contain more features), but some features can be wrong due to data error. The data fit of the 2D models is generally acceptable with the overall normalized RMS (Root Mean Square) 3.4 and RMS 2.8 respectively, but some higher RMS up to 8 occur at some sites in the northeastern part of the section. They may cause by the strong distortion in the data or 3D effects.

The main larger-scale features of the two models are described as below:

- The northeastern region (between sites BL01 to BL25) of the profile appear to have much higher resistivity than the southwestern region. Some structures with resistivity values about 10000 Ωm extend from shallow upper crust to upper mantle.
- One resistive region with a resistivity value less than 500 Ωm in the middle and low crust is beneath sites BL01– BL07.
- A conductive layer (up to about 4 km) with less than 10 Ωm resistivity value is found beneath sites BL27 to BL73 in the southwestern region.
- A crustal higher resistivity region is beneath BL58 to BL73 with a resistivity value about 5000 Ωm.

- Several electrical resistivity boundaries have been suggested along the profile. For example, between sites BL25 to BL41.

The main features of the 2D model are in good agreement with the MT data responses. However, the 2D models show weak points and uncertainty. There are some differences in features between different models, especially, features in the north-eastern region. For example, the shape of higher resistivity structure between BL07 to BL27 changes in different models. The variation may be caused by the data distortion, complexity of dimensionality and the 3D effects. The dimensionality analysis suggested uncertainty and instability of inversion in this area.

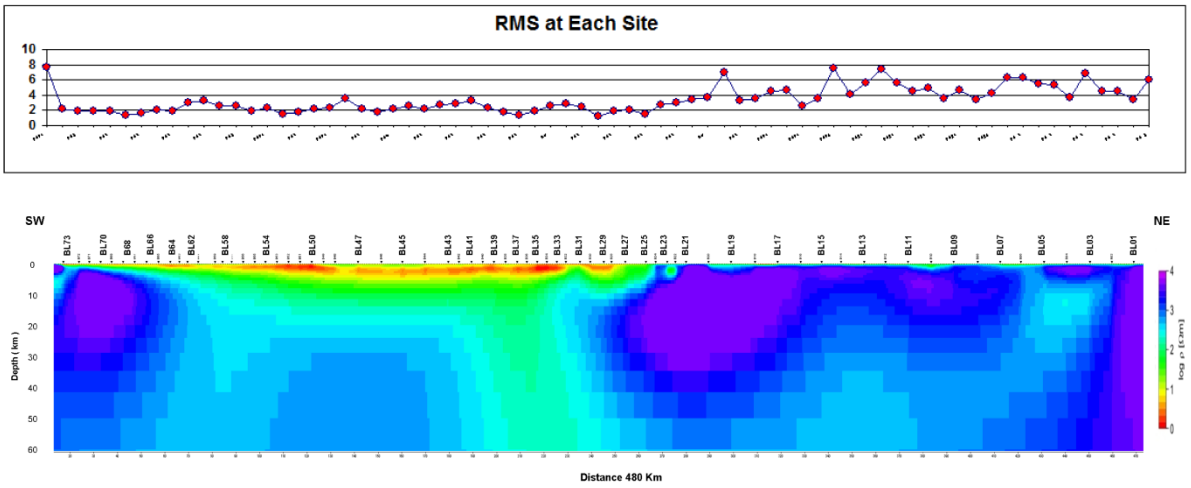

Figure 2.11 *2D model of all data from NLCG inversion, RMS = 3.4.*

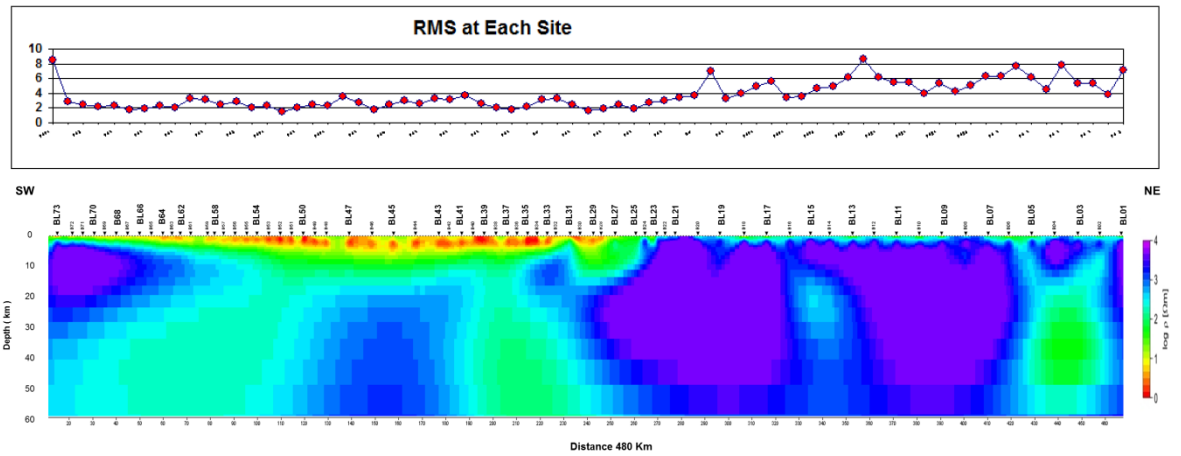

Figure 2.12 *2D model of all data from NLCG inversion, RMS = 2.8.*

Three-dimensional inversion of YOM data

2D MT interpretation of 3D data can be a guide to a reasonable geological interpretation in many cases. There is always a need to consider which of the structures presented in the 2D model are real and which are artificial due to the error of interpreting 3D structures as 2D. To determine the quality of the 2D interpretation of the YOM MT data, a new 3D inversion algorithm ModEM (Egbert and Kelbert,

2012) was applied to the data for extracting geoelectric information from near 3D environment. The advantage of 3D inversion was that it is no longer required to make simplifying assumption on the geoelectric strike direction and dimensionality. The orientation of the 3D model was along the YOM MT profile. The full impedance tensors were used for the inversion. The mesh of the model was 79 x 79 horizontal elements and 34 vertical elements respectively. Two preliminary 3D models (Figure 2.13 – extracted along a straight line; and Figure 2.14 – extracted along seismic CDP localities) with different smoothness levels (and slightly different locations) show that the main large-scale features are similar to the features obtained from 2D inversion. This gives considerable confidence with the main features. However, some features seem to be overestimated, which may be caused by the visualisation scheme or the lower resolution of 3D model (due to the coarser grid).

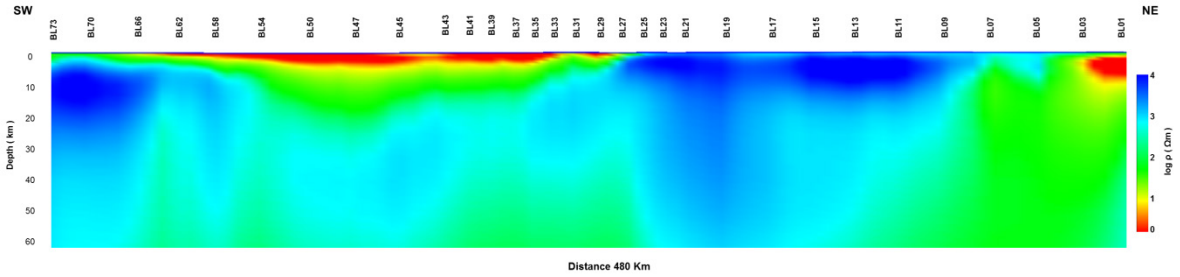

Figure 2.13 *Cross section of smooth 3D model extracted along a straight line from ModEM, RMS = 4.55.*

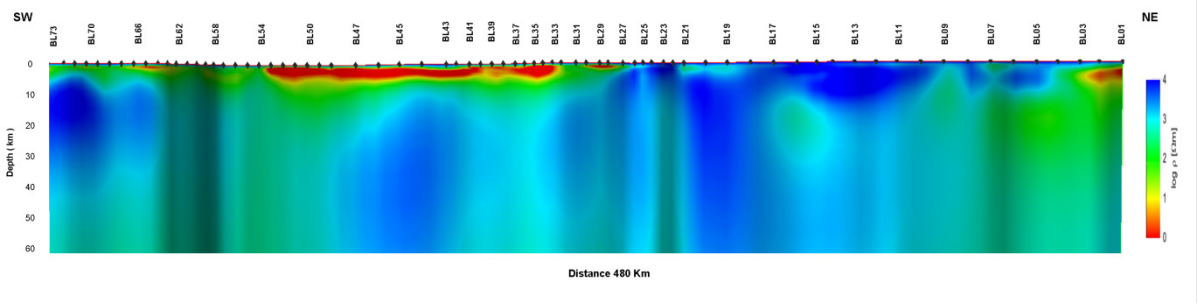

Figure 2.14 *Cross section of 3D model extracted along seismic CDP localities from ModEM, RMS = 3.86.*

Discussion and conclusion

This paper presents an overview of the YOM MT data acquisition, processing and inversion. The results of 2D inversion and 3D inversion indicate some consistent resistivity structures, which appear on most models. The common features, with repeatability from many different inversion approaches and different geophysical studies (seismic and potential field data), can be trusted as robust features. The YOM model shows several major resistive structures, which may relate to geological features in the crust.

In the northeastern region, resistivity models from sites BL01 to BL07 present a lower resistivity region in the middle and low crust. A southwest-dipping boundary in the resistivity model at about BL07 approximates with the location of the Woodroffe Thrust. Sites BL07 to BL25 appear as very high resistivity of about 10000 Ωm in the upper and low crust.

In the southwestern region (between sites BL27 to BL73), a shallow 1D conductive layer with resistivity value less than 10 Ωm locates beneath sites BL27 to BL70. This feature is appropriate for a

sedimentary basin and is interpreted to be the western Office Basin and Manunda Basin, which occurs beneath the Office Basin (see Korsch et al., 2013). The sediments have a length over 200 km along the MT profile and reach a thickness up to about 4 km. A crustal higher resistivity structure of about 5000 Ωm beneath sites BL58 to BL73 correlates with a gravity high (see Figure 2.2) and may be related, in part, to upper crustal greenstones and/or banded iron formations. A crustal resistive region with less than 1000 Ωm is beneath sites BL27 to BL54, and is coincident with a broad gravity low. The sharp contrast of resistivity at north-eastern boundary of this zone (at about site BL27) approximates to the boundary between the Yilgarn Craton and the Musgrave Province.

Although the MT result provides evidence of main features in the region, the inversion result should not be viewed as a unique final solution. The solution of MT inversion is non-unique and any resulting model is only a fit to the response data. Selecting models without prior information is challenging and the results always contain ambiguity. Always keep in mind that some resistivity structures are uncertain due to the data errors, distortion, and dimensionality complexity. Further work with applying prior information is required for the inversion, especially to solve small features and surface anomalies.

Acknowledgements

This paper forms part of a collaborative project between the Geological Survey of Western Australia and Geoscience Australia. We thank Jenny Maher, Aki Nakamura, Tim Jones, Emilio Extremera and Kiaran Smith for support and help with field acquisition.

References

Bahr, K., 1988. Interpretation of the magnetotelluric impedance tensor: regional induction and local telluric distortion. *Journal of Geophysics*, 62, 119–127.

Becken, M., and Burkhardt, H., 2004. An ellipticity criterion in magnetotelluric tensor analysis. *Geophysical Journal International*, 159, 69–82.

Bostick, F.X., 1977. A simple almost exact method of MT analysis, in Workshop on Electrical Methods in Geothermal Exploration, U.S. Geological Survey.

Caldwell, T.G., Bibby, H.M., and Brown, C., 2004. The magnetotelluric phase tensor. *Geophysical Journal International*, 158, 457–469.

Chave, A.D., Thompson, D.J., and Ander, M.E., 1987. On the robust estimation of power spectra, coherences and transfer functions. *Journal of Geophysical Research-Solid Earth*, 92, 633–648.

Chave, A.D., and Thomson, D.J., 2004. Bounded influence magnetotelluric response function estimation. *Geophysical Journal International*, 157, 988–1006.

Constable, S.C., Parker, R.L., and Constable, C.G, 1987. Occam's inversion: A practical algorithm for generating smooth models from electromagnetic sounding data. *Geophysics*, 52, 289–300.

Egbert, G.D., and Booker, J. R., 1986. Robust estimation of geomagnetic transfer functions. *Geophysical Journal of the Royal Astronomical Society*, 87, 173–194.

Egbert, G.D., 1997. Robust multiple-station magnetotelluric data processing. *Geophysical Journal International*, 130, 475–496.

Egbert, G.D., and Kelbert, A., 2012. Computational recipes for electromagnetic inverse problems. *Geophysical Journal International*, 189, 251–267.

Gamble, T.D., Goubau, W.M., and J. Clarke, 1979. Magnetotellurics with a remote magnetic reference. *Geophysics*, 44, 53–68.

Groom, R.W., and Bailey, R.C., 1989. Decomposition of magnetotelluric impedance tensors in presence of local three-dimensional galvanic distortion. *Journal of Geophysical Research*, 94, 1913–1925.

Groom, R.W., and Bailey, R.C., 1991. Analytic investigation of the effects of near surface 3D galvanic scatterers on MT tensor decompositions. *Geophysics*, 56, 496–518.

Korsch, R.J., Blewett, R.S., Pawley, M.J., Carr, L.K., Hocking, R.M., Neumann, N.L., Smithies, R.H, Quentin de Gromard, R., Howard, H.M., Kennett, B.L.N., Aitken, A.R.A., Holzschuh, J., Duan, J., Goodwin, J.A., Jones, T., Gessner, K., and Gorczyk, W., 2013. Geological setting and interpretation of the southwest half of deep seismic reflection line 11GA-YO1: Yamarna Terrane of the Yilgarn Craton and the western Officer Basin. In: Neumann, N.L. (editor), *Yilgarn Craton–Officer Basin–Musgrave Province (YOM) Seismic and MT Workshop*. Geoscience Australia Record 2013/28, 24–50.

Marti, A., Queralt, P., Jones, A.G., and Ledo, J., 2005. Improving Bahr's invariant parameters using the WAL approach. *Geophysical Journal International*, 163, 38–41.

Marti, A., Queralt, P., and Ledo, J., 2009. WALDIM: A code for the dimensionality analysis of magnetotelluric data using the rotational invariants of the magnetotelluric tensor. *Computers and Geosciences*, 35, 2295–2303.

McNeice, G., and Jones, A.G., 2001. Multi-site, multi-frequency tensor decomposition of magnetotelluric data. *Geophysics*, 66, 158–173.

Larsen, J. C., Mackie, R.L., Manzella, A., Fiordelisi, A., and Rieven, S., 1996. Robust smooth magnetotelluric transfer functions. *Geophysical Journal International*, 124, 801–819.

Parkinson, W.D., 1959. Directions of rapid geomagnetic fluctuations. *Geophysical Journal Royal Astronomical Society*, 2, 1–14.

Rodi, W., and Mackie, R.L., 2001. Nonlinear conjugate gradients algorithm for 2D magnetotelluric inversion. *Geophysics*, 66, 174–187.

Smirnov M.YU, 2003. Magnetotelluric data processing with a robust statistical procedure having a high breakdown point. *Geophysical Journal International*, 152, 1–7.

Swift, C. M., 1967. A magnetotelluric investigation of an electrical conductivity anomaly in the southwestern United States. Phd. Thesis, Mass. Inst. of Technol., Cambridge, 1967.

Wynne, P., 2009. Index of gravity surveys: 2nd edition. *Geoscience Australia Record*, 2009/007.

3 Geological setting and interpretation of the southwest half of deep seismic reflection line 11GA-YO1: Yamarna Terrane of the Yilgarn Craton and the western Officer Basin

R.J. Korsch[1], R.S. Blewett[1], M.J. Pawley[2], L.K. Carr[3], R.M. Hocking[4], N.L. Neumann[1], R.H. Smithies[4], R. Quentin de Gromard[4], H.M. Howard[4], B.L.N. Kennett[5], A.R.A. Aitken[6], J. Holzschuh[1], J. Duan[1], J.A. Goodwin[1], T. Jones[1], K. Gessner[4] and W. Gorczyk[6]

[1] Minerals and Natural Hazards Division, Geoscience Australia, GPO Box 378, Canberra, ACT 2601.
[2] Geological Survey of South Australia, Department of Manufacturing, Innovation, Trade, Resources and Energy, Level 4, 101 Grenfell Street, Adelaide, SA 5000.
[3] Energy Division, Geoscience Australia, GPO Box 378, Canberra, ACT 2601.
[4] Geological Survey of Western Australia, Department of Mines and Petroleum, 100 Plain Street, East Perth, WA 6004.
[5] Research School of Earth Sciences, The Australian National University, Canberra. ACT 0200.
[6] Centre for Exploration Targeting, School of Earth and Environment, The University of Western Australia, 35 Stirling Highway, Crawley, WA 6009.

Russell.Korsch@ga.gov.au

Introduction and aims of the seismic survey

As part of its Onshore Energy Security Program, Geoscience Australia, in conjunction with the Geological Survey of Western Australia under its Royalties for Regions Exploration Incentive Scheme, acquired 484 line km of vibroseis-source, deep-seismic reflection data along a single northeast–southwest traverse from the west Musgrave Province, across the western Officer Basin, to the Yamarna Terrane in the northeast Yilgarn Craton (Figures 3.1 to 3.4). The transect, line 11GA-YO1, referred to here as the YOM (Yilgarn Craton–Officer Basin–Musgrave Province) seismic line, was acquired during May and June 2011.

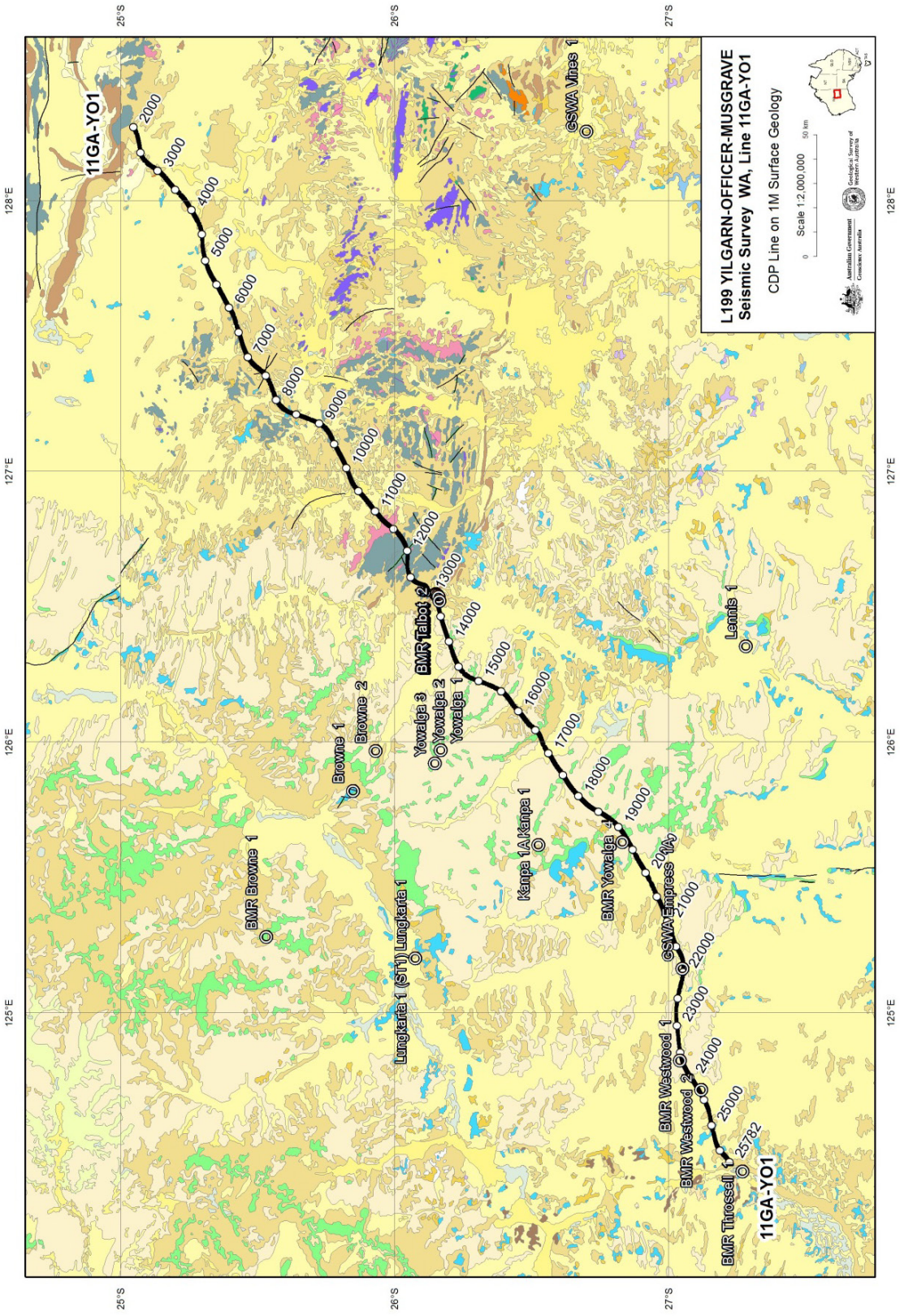

Figure 3.1 *Map showing the surface geology of the region covered by the YOM (11GA-YO1) seismic line, from the Yamarna Terrane in the northeastern Yilgarn Craton, across the western Officer Basin, to the west Musgrave Province. The surface geology is from the 1:1 000 000 scale geology map of Australia (Raymond, 2009, which also contains the legend). The seismic line has CDP stations labelled, and the locations of key drill holes are also shown.*

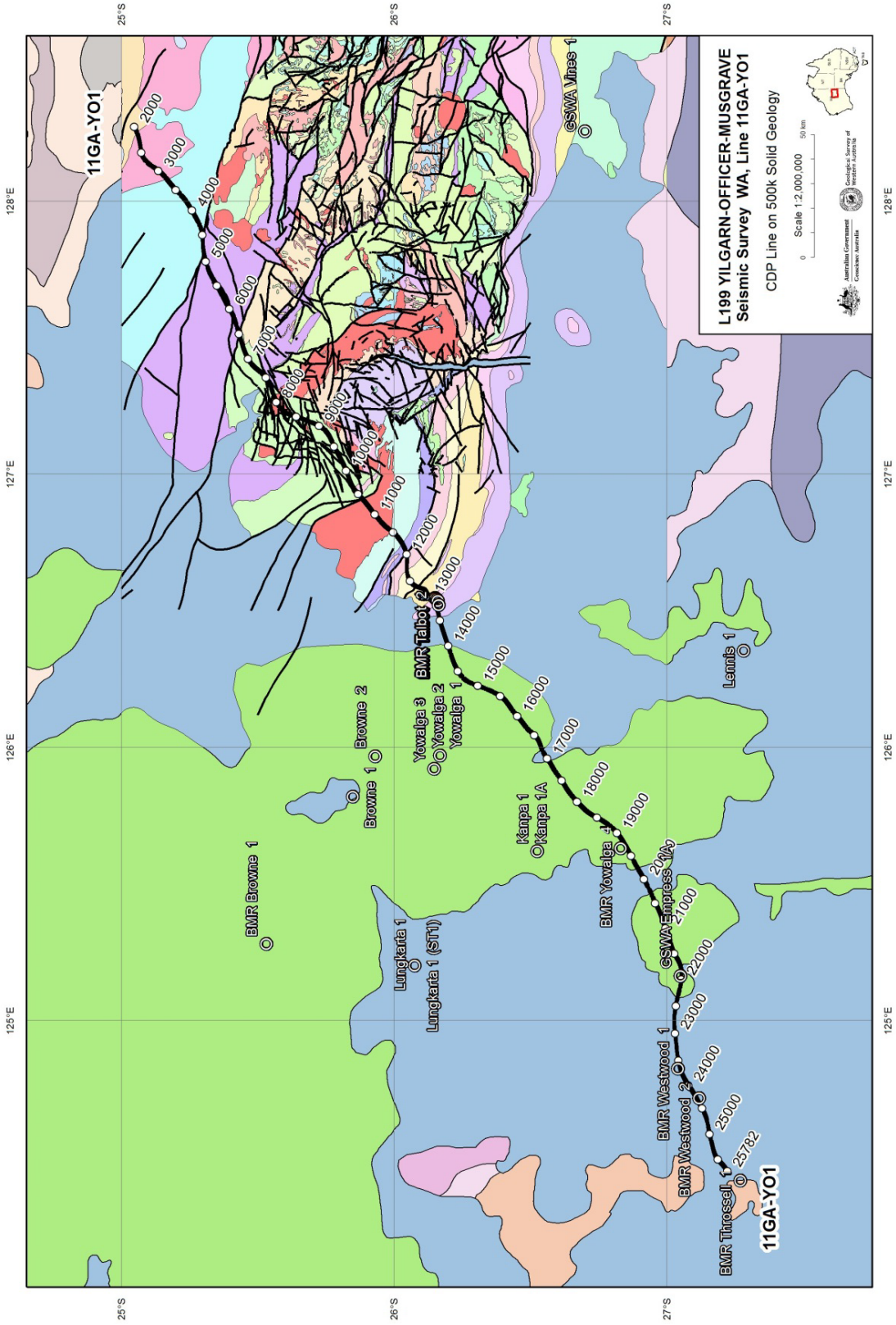

Figure 3.2 *Map showing the solid geology of the region covered by the YOM (11GA-YO1) seismic line, from the Yamarna Terrane in the northeastern Yilgarn Craton, across the western Officer Basin, to the west Musgrave Province. The solid geology is from the 1:500 000 scale solid geology map of Western Australia, which also contains the legend (Geological Survey of Western Australia, 2008; and unpublished data). The seismic line has CDP stations labelled, and the locations of key drill holes are also shown.*

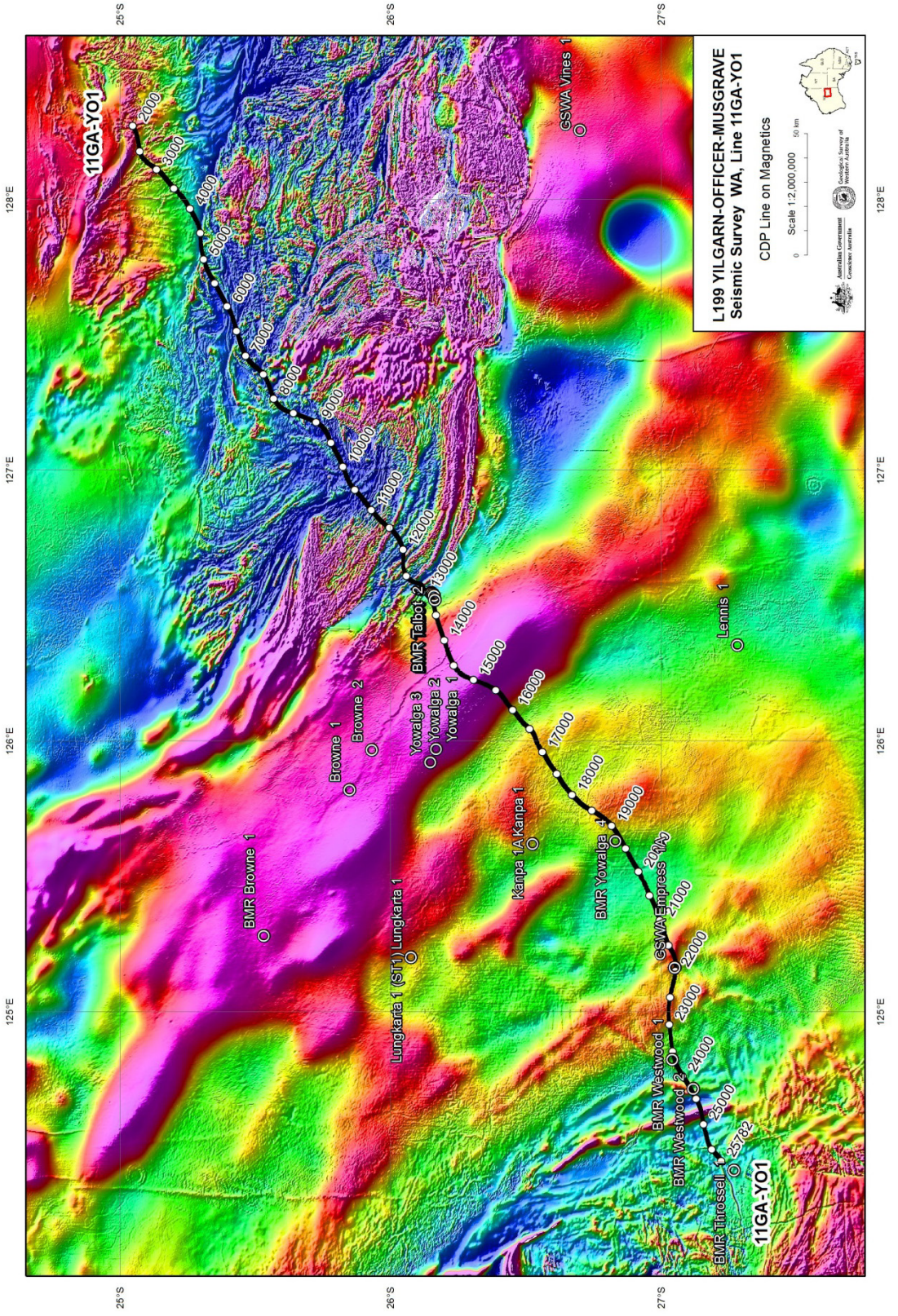

Figure 3.3 *Map showing regional aeromagnetic data for the region covered by the YOM (11GA-YO1) seismic line, from the Yamarna Terrane in the northeastern Yilgarn Craton, across the western Officer Basin, to the west Musgrave Province (extracted from Milligan et al., 2010). Warm colours are high magnetic intensities; cool colours are low magnetic intensities. The seismic line has CDP stations labelled, and the locations of key drill holes are also shown.*

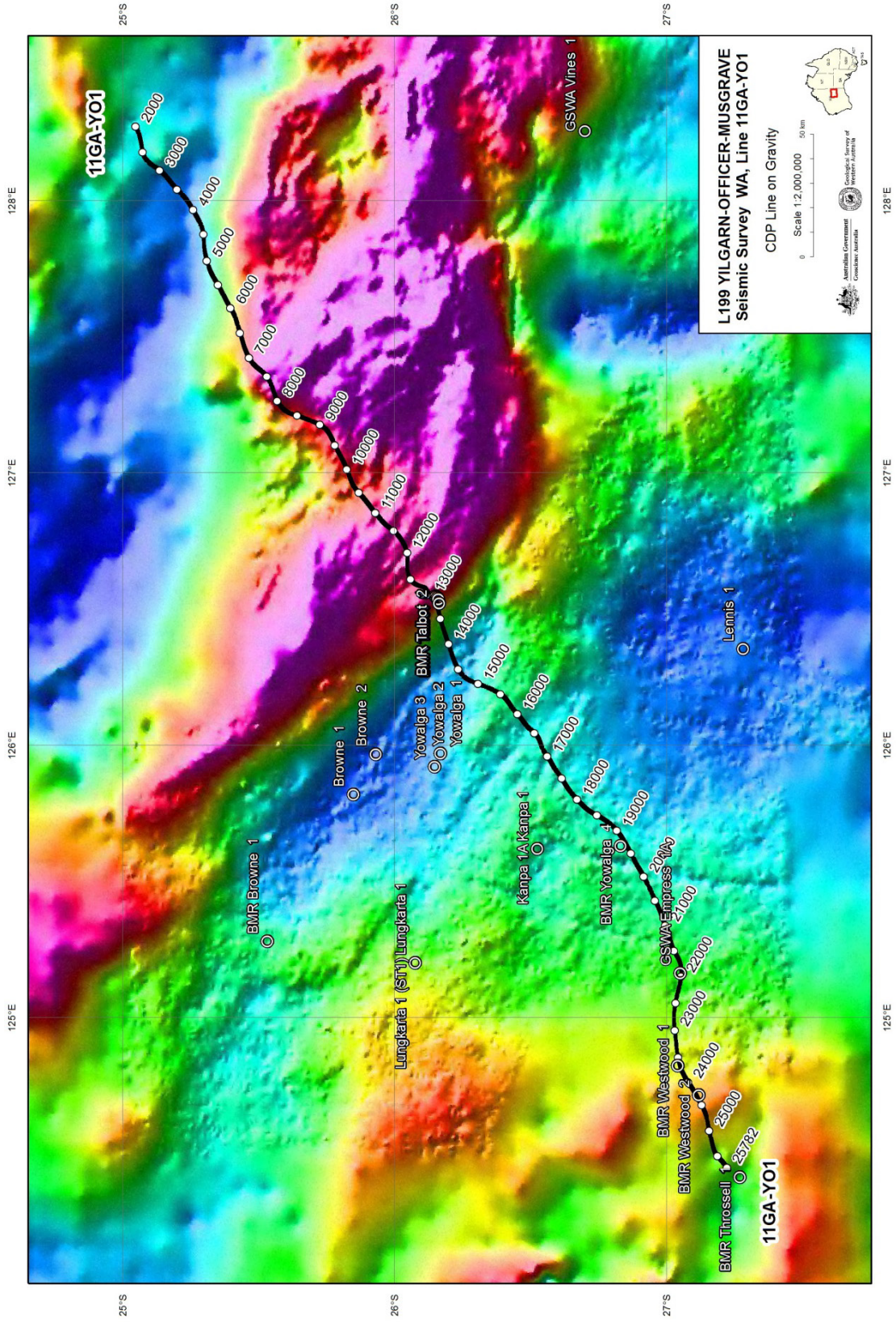

Figure 3.4 *Map showing a regional gravity image for the region covered by the YOM (11GA-YO1) seismic line, from the Yamarna Terrane in the northeastern Yilgarn Craton, across the western Officer Basin, to the west Musgrave Province (extracted from Bacchin et al., 2008). Warm colours are gravity highs, cool colours are gravity lows. The seismic line has CDP stations labelled, and the locations of key drill holes are also shown.*

The primary objective of the YOM survey was to produce a high quality seismic section across the western Officer Basin, one of Australia's underexplored frontier sedimentary basins. Additional objectives were to evaluate:

1. the architecture and deep structure of the Archean Yamarna Terrane, in the northeast Yilgarn Craton. This is both the easternmost and the least well understood terrane of the Yilgarn Craton, because it is largely hidden under younger cover,
2. the architecture and deep structure of the Mesoproterozoic west Musgrave Province, and,
3. the relationship between the Yilgarn Craton and the west Musgrave Province, beneath the western Officer Basin.

This dataset complements several previous deep seismic surveys in the Yilgarn Craton, particularly the 2010 Youanmi deep crustal reflection and MT survey (Wyche et al., 2013), the 2001 Northeast Yilgarn deep crustal seismic survey (lines 01AGS-NY1 and 01AGS-NY3; Goleby et al., 2004, 2006), and the 1991 Eastern Goldfields deep seismic survey (line BMR91-EGF01, commonly known as EGF1; Drummond et al., 1993, 2000; Swager et al., 1997). Combined with previous surveys, the YOM survey completes a comprehensive transect across most of south-central Western Australia, from near the coastline in the west to near the border with the Northern Territory in the east.

Here, we report the results of an initial geological interpretation of the seismic data across the southwest half of the line, covering the western Officer Basin and the Yilgarn Craton. A companion paper by Howard et al. (2013) presents the interpretation of the northeast half of the line, which crosses the west Musgrave Province.

Seismic and MT acquisition and processing

Seismic reflection and magnetotelluric (MT) data along the YOM line were acquired in 2011, with project management by the Seismic Acquisition and Processing Section from Geoscience Australia. For the seismic line, 75-fold seismic reflection data were acquired to 20 s and 22 s two-way travel time (TWT), providing an image of the crust and upper mantle to a depth of about 66 km (Figure 3.5). Details of the acquisition and processing techniques are provided in Holzschuh et al. (2013). We undertake conversion from two-way travel time to depth using an effective reflection velocity for the crust of 6000 ms^{-1}, so that 1 s TWT is approximately equal to 3 km depth, with the exception of sedimentary rocks in the western Officer Basin, where we assume velocities of 3200–4600 ms^{-1}. Because of the 2D nature of the seismic line, the orientations of structures, mentioned below, are apparent dips, and apparent dip directions. Crustal-scale MT data were collected along, or adjacent to, the seismic traverse and is described by Duan et al. (2013).

Geological setting

Geology of the northeast Yilgarn Craton

The Yilgarn Craton is divided into a series of terranes, with the easternmost Eastern Goldfields Superterrane (Eastern Goldfields Province; Gee et al., 1981) separated from the Youanmi Terrane which forms the core of the protocraton, by the Ida Fault (Cassidy et al., 2006). Cassidy et al. (2006) subdivided the Eastern Goldfields Superterrane into the western Kalgoorlie, central Kurnalpi, and eastern Burtville terranes.

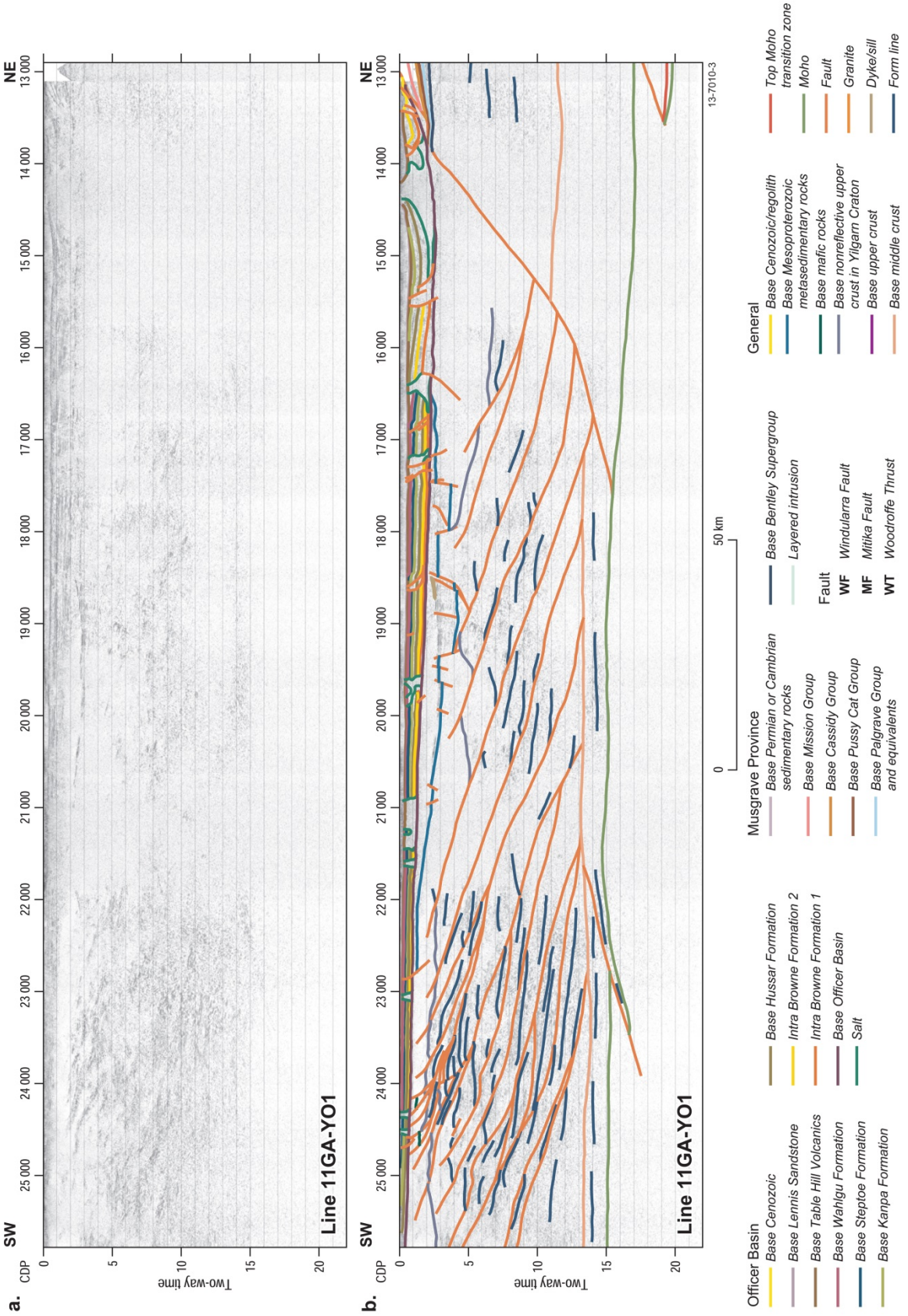

Figure 3.5 *Migrated seismic section for the southwestern half of seismic section 11GA-YO1, showing both uninterpreted and interpreted versions. Display is to 22 s TWT (~66 km) depth, and shows vertical scale equal to the horizontal scale, assuming an average crustal velocity of 6000 ms^{-1}.*

The Burtville Terrane is moderately to poorly exposed, but contains c. 2810 Ma supracrustal rocks along its western margin, which are significantly older than the < c. 2720 Ma greenstone rocks of the Kalgoorlie and Kurnalpi terranes (Cassidy et al., 2006). Recent geological mapping, geochronology, and isotopic analysis by the GSWA, however, indicate that the Burtville Terrane, as proposed by Cassidy et al. (2006), consists of two terranes, separated by the Yamarna Shear Zone (Pawley et al., 2012). These include a redefined Burtville Terrane to the west, and the Yamarna Terrane to the east.

The greenstone rocks of the Burtville Terrane consist of mafic to felsic volcanic and volcaniclastic rocks, and mafic intrusive rocks. These form a series of packages that have been dated at c. 2970–2910 Ma, c. 2815–2800 Ma, and c. 2775–2735 Ma (Pawley et al., 2012). Due to the poor, dispersed nature of the outcrop, it is difficult to determine how these packages relate to each other, as they are not systematically distributed. In contrast, the Yamarna Terrane appears to consist of a single cycle of ultramafic-mafic-felsic volcanic and siliciclastic rocks, from which felsic volcanic rocks of the Toppin Hill Formation have been dated at c. 2699–2677 Ma (Sircombe et al., 2007; Wingate et al., 2011).

Despite the differences between these two terranes, it is possible to find correlatives at the cratonic scale (Pawley et al., 2012). The greenstones in the Burtville Terrane are similar in age and character to the older greenstones in the Murchison Domain in the western Youanmi Terrane, and the greenstones of the Yamarna Terrane are similar in age and lithology to the rocks of the Kalgoorlie Terrane in the western part of the Eastern Goldfields Superterrane, in particular the upper basalt of the c. 2715–2692 Ma Kambalda Sequence and the c. 2686–2666 Ma felsic Kalgoorlie Sequence (e.g. Kositcin et al., 2008).

Aeromagnetic images suggest that there are several unexposed belts of greenstone and/or banded iron formation in the northeastern Yilgarn Craton, which are covered either by a thin succession of Permian or younger sedimentary deposits, or regolith. These include a hook-shaped belt to the north of the YOM seismic line, beneath the Ernest Giles Range, well to the east of the exposed rocks in the Yamarna Terrane (visible on the western edge of Figure 3.3, between 26ºS and 27ºS). This belt was drilled and found to consist of altered and sheared, interbedded banded iron-formation and mafic rocks, and was interpreted to be similar to the greenstone assemblage found much farther west in the Murchison Domain of the Youanmi Terrane (Greatland Gold, 2010), raising the possibility that there may be slivers of older (i.e. >2735 Ma) rocks under the basins which cover the eastern part of the craton (e.g. Van Kranendonk et al., 2012).

The age and rock characteristics of the terranes suggest that the Youanmi and Burtville terranes had a similar greenstone history prior to c. 2735 Ma, and were likely contiguous during this time. Extension after c. 2720 Ma resulted in separation of these two older crustal blocks, with magmatism and sedimentation occurring in the intervening Kalgoorlie and Kurnalpi terranes, and the outboard Yamarna Terrane (Pawley et al., 2012). The terrane-bounding Ida Fault and the Yamarna Shear Zone would have accommodated this extension (Czarnota et al., 2010; Pawley et al., 2012). Significantly, the Kalgoorlie, Kurnalpi, and Yamarna terranes contain scattered “basement” fragments, and older xenocrystic zircons which have similar age patterns to the Youanmi and Burtville terranes, suggesting that older crust underlies, and was incorporated into, the rocks of the younger terranes (Pawley et al., 2012).

The recent collection of Sm–Nd and Lu–Hf isotope data has provided insights into crustal growth processes in the Yilgarn Craton. The Sm–Nd isotopic data indicates that the Ida Fault is a major boundary which separates older average crustal ages in the Youanmi Terrane, from younger crustal ages in the Eastern Goldfields Superterrane (Champion and Cassidy, 2007). Similarly, new Lu–Hf isotope data collected by GSWA reveals that mantle extraction events occurred in the central Yilgarn Craton at c. 4200 Ma, c. 3500 Ma, and c. 3100 Ma, whereas only the two youngest mantle extraction

episodes are recorded in the Eastern Goldfields Superterrane (Wyche et al., 2012), suggesting that crustal formation in the east post-dated the earliest event in the protocraton. It also suggests that magmas in the Eastern Goldfields Superterrane had a substantial juvenile input, whereas those in the central Yilgarn Craton recorded reworking of older crust. Furthermore, the widespread occurrence of the c. 3500 Ma and c. 3100 Ma mantle extraction events indicate that several episodes of major, possibly plume-related, heating occurred right across the craton (Wyche et al., 2012). This supports the interpretation that the Burtville and Youanmi terranes had a common history extending back to at least c. 2960 Ma, and that crust of this age underlies the Kalgoorlie, Kurnalpi, and Yamarna terranes (Pawley et al., 2012).

Granites

Five main types of granites have been recognised in the Eastern Goldfields Superterrane (Champion and Sheraton, 1997), with most felsic magmatism occurring between c. 2720 Ma and 2630 Ma. Although there is overlap in their ages, the emplacement of the different granite types peaked at different times:

- High-HFSE granites are a minor phase (~5%), generally restricted to the Kurnalpi Terrane, which peaked between 2720 Ma and 2680 Ma.
- Mafic granites are a minor phase (~5%), with a peak between 2720 Ma and 2680 Ma, but decreasing until < 2655 Ma.
- High-Ca granites are the dominant granite type (~60%), occurring between 2720 Ma and 2655 Ma.
- Syenitic granites are a minor phase (~1%), ranging from 2675 Ma to < 2655 Ma, which are generally restricted to the Kurnalpi Terrane.
- Low-Ca granites are common (~25%), typically younger than 2655 Ma, and interpreted to be derived by recycling of the older granitoids.

Older granites, dating back to c. 2930 Ma, have been recognised across the Superterrane, but these are minor phases (see Pawley et al., 2012; and references therein).

Structural history

Numerous structural studies have been published for the Eastern Goldfields Superterrane, which differ in nomenclature, but generally recognise a similar sequence of deformation events (e.g. Swager, 1997; Blewett et al., 2010, and references therein). Extension (D1) between c. 2720 Ma and c. 2670 Ma was accompanied by deposition of the Kambalda Sequence. This was followed by several cycles of episodic transpression and extension/transtension, between c. 2665 and c. 2635 Ma (Blewett et al., 2010), including:

- D2 north-northwesterly-trending upright folding and thrust faulting at c. 2665 Ma,
- D3 northeasterly-directed extension at c. 2665–2655 Ma, resulting in shear zones which reached the base of the crust, extensional granite doming, and deposition of clastic sedimentary ‘late basins’ adjacent to the domes,
- D4a tightening of the north-northwesterly-trending folds and thrust faulting at c. 2655 Ma,
- D4b north-northwesterly-trending sinistral shearing and thrusting at c. 2655–2650 Ma, interpreted to result from minor rotation of the stress field, and,
- D5 north-trending dextral strike-slip shearing at 2650–2635 Ma.

Czarnota et al. (2010) ascribed most of the deformational history to tectonic switching at a convergent plate boundary, with the change in shearing attributed to variations in plate vectors. In contrast, the final deformational event, which involved locally-developed, minor vertical shortening with variable extension vectors, was attributed to thermal relaxation after c. 2630 Ma (Blewett et al., 2010).

A major feature of the Eastern Goldfields Superterrane is the development of north-northwest-trending shear zones and faults. A deep-crustal seismic traverse across the central part of the Eastern Goldfields Superterrane (Goleby et al., 2004) showed that the terrane-bounding Ockerburry and Hootanui fault systems, and the Yamarna Shear Zone are large-scale, east-dipping, listric structures that extend to the base of the crust. Such structures have long and complex histories. For example, the Yamarna Shear Zone preserves three phases of deformation:

- dextral strike-slip shearing in the footwall,
- tight to isoclinal folding and layer-parallel strike-slip shearing in the greenstones adjacent to the footwall, which is demonstrably contemporaneous with the footwall deformation, and,
- sinistral strike-slip shearing in the hangingwall to the east (Pawley et al., 2009).

Based on the age of the synkinematic Point Salvation Monzogranite, located in the footwall of the shear zone, the dextral strike-slip shearing can be constrained at c. 2664 Ma (Pawley et al., 2012). This age is older than the c. 2650–2635 Ma proposed for dextral transtension by Blewett et al. (2010), suggesting that deformation was diachronous across the eastern Yilgarn Craton.

Manunda Basin

The term Manunda Basin (new term after Manunda Rockhole) is proposed for a succession of sedimentary rocks beneath the Officer Basin, which have been intersected in drill holes and observed on previous seismic profiles, but not yet identified in outcrop within the region of the YOM seismic line.

A series of short seismic reflection lines were acquired in the western Officer Basin by the Bureau of Mineral Resources in 1972, some of which were located on, or very close to, the YOM seismic line. Preliminary interpretation indicated the presence of layered rocks up to 10,000 m thick in the central part of the basin (Harrison, 1973). Follow up work by Harrison and Zadoroznyj (1978) considered that the layered rocks imaged below the Officer Basin were possibly igneous and metamorphic rocks, which may be distinct from basement of the Yilgarn Craton, and that this package could consist of metasedimentary rocks intruded by mafic igneous rocks.

The mineral exploration drill hole WMC NJD1, located about 100 km south of the YOM seismic line, was drilled in 1981 to a depth of 517.37 m (Western Mining Corporation Limited, 1981). The drill hole intersected gently-dipping Neoproterozoic units of the Officer Basin to a depth of 376.85 m, then Mesoproterozoic or Paleoproterozoic metasedimentary rocks dipping at 50–70º to the bottom of the hole (Hocking, 2002). The pre-Officer Basin succession is divisible into an upper siliciclastic unit consisting of sandstone, siltstone and shale, and a lower unit consisting predominantly of sandstone. Both units have a weak crenulation cleavage defined by mica growth (Hocking, 2002).

Deep seismic reflection profile 01AGS-NY3, collected in 2001 across the northeast Yilgarn Craton (Goleby et al., 2003, 2004), passes across the location of WMC NJD 1. This seismic line, and the northeastern end of seismic line 01AGS-NY1, imaged a thick succession of usually gently deformed sedimentary rocks, extending down to a depth of about 2 s TWT (~4.5 km), beneath a relatively thin (up to ~400 m) succession in the Officer Basin. The succession is disrupted where WMC NJD 1

intersects seismic line 01AGS-NY3, and the dips in the succession of 50–70º are likely related to an adjacent fault. A recent interpretation of seismic line 01AGS-NY01 has suggested that the Mesoproterozoic succession in this seismic line can be subdivided into up to four discrete successions (Phoenix Oil and Gas Limited, 2011).

The Kanpa 1A petroleum exploration well was drilled ~25 km to the north of the YOM seismic line in 1983, to a total depth of 3803 m. The lowermost unit between 3671 m and 3803 m is intensely silicified sandstone with minor mudstone, and was interpreted as the Townsend Quartzite, the basal unit of the Officer Basin (Shell Company of Australia, Ltd, 1983; Townson, 1985). Grey et al. (2005) have since reassessed this unit as being basement below the Officer Basin. Some petroleum industry seismic lines collected during the early 1980s showed the presence of an older layered succession below the Officer Basin (Townson, 1985; see, for example, line N83–5 shown as Figure 5 in Perincek, 1996). These successions were interpreted to be limited in extent and to have a graben-like geometry (Townson, 1985; see modification by Iasky, 1990).

The stratigraphic drill holes GSWA Empress 1A (Stevens and Apak, 1999), which like the YOM seismic line is located on the Great Central Road, and GSWA Lancer 1 (Haines et al., 2004), about 230 km to the north of the YOM seismic line, also intersected older rocks below the Officer Basin. In GSWA Empress 1A, Stevens and Apak (1999) interpreted the interval from 1521.8 m to 1540 m (a mixed mudstone and mafic volcanic unit) as Lefroy Formation, a unit near the base of the Officer Basin succession, above siliciclastic and volcanic rocks which were interpreted as being pre-Officer Basin (1540–1624 m, TD). Re-examination of the core indicated that all the section below 1521.8 m is part of the Mesoproterozoic basement (Grey et al., 2005). A sample of basalt from 1602.0 m has a K–Ar whole rock age of 1058 ± 13 Ma (Amdel Limited, in Stevens and Apak, 1999). Assuming this age is a crystallisation age, and not due to later resetting, the basalt is equivalent in age to the Giles Event and the Bentley Supergroup of the west Musgrave Province (e.g. Evins et al., 2010; Howard et al., 2011), and possibly forms part of the Warakurna Large Igneous Province, as defined by Wingate et al. (2004). The quality of the drill core makes it is uncertain whether the basalt is a flow, forming part of the succession, or whether it is a younger sill intruding into an older succession.

In GSWA Lancer 1, quartzite below the Officer Basin (1478.9 m to 1501.2 m, TD) was assigned to the Cornelia Sandstone (Haines et al., 2004), which was correlated tentatively with rocks in the Edmund Basin by Hocking et al. (2000). Detrital zircons from a sandstone sample from 1490 m depth, and further samples of Cornelia Sandstone from outcrop, dated by SHRIMP, have provided maximum depositional ages of 1305 ± 14 Ma in GSWA Lancer 1 and 1279 ± 25 Ma in outcrop, suggesting a correlation with the Collier Basin (Bodorkos et al., 2006; Wingate and Bodorkos, 2007).

Several lithological correlations have been proposed between the sedimentary package forming the Manunda Basin and nearby sedimentary basins, including the Collier Basin, Edmund Basin, and possibly the Earaheedy Basin (see Hocking, 2002). As part of our project, in an attempt to clarify the correlations, four sandstones from the Manunda Basin intersected in WMC NJD 1, Kanpa 1 and GSWA Empress 1A, were sampled, and detrital zircons were analysed via SHRIMP U–Pb geochronology.

GA sample number 2152078 was collected from drill core between 504 m and 511 m in WMC NJD 1, and is fine-grained sandstone. Detrital zircons from this sample yield $^{207}Pb/^{206}Pb$ ages which range from ~2721 Ma to ~1255 Ma, with dominant age clusters at ~1780 Ma, at ~1670 Ma and at ~1310 Ma (Figure 3.6a). The youngest group of ages at ~1310 Ma can be used to define a maximum depositional age for this sample.

GA sample number 2152079 was collected from drill core between 1538.9 m and 1539.3 m in GSWA Empress 1A, and is a coarse-grained lithic sandstone. Detrital zircons from this sample yield $^{207}Pb/^{206}Pb$ ages which range from ~3428 Ma to ~1288 Ma, with dominant age clusters at ~1780 Ma and ~1680 Ma, and smaller peaks at ~1380 Ma and at ~1310 Ma (Figure 3.6b). The youngest age group of ~1310 Ma can be used to define a maximum depositional age for this sample.

GA sample number 2152080 was collected from drill core between 1546.2 m and 1546.6 m in GSWA Empress 1A, and is a very fine-grained sandstone to siltstone. Detrital zircons from this sample yield $^{207}Pb/^{206}Pb$ ages which range from ~2630 Ma to ~1285 Ma, with dominant age clusters at ~1800 Ma, at ~1750 Ma and at ~1670 Ma, and a large number of ages between ~1440 Ma and the youngest age of ~1285 Ma (Figure 3.6c). Within this range, the youngest age group of ~1315 Ma can be used to define a maximum depositional age for this sample.

GA sample number 2152081 was collected from drill cuttings between 3773 m and 3803 m in Kanpa 1A, and is a coarse-grained sandstone. Detrital zircons from this sample yield $^{207}Pb/^{206}Pb$ ages which range from ~2982 Ma to ~1692 Ma, with a large number of ages ranging between ~2750 and ~2600 Ma, and smaller age clusters at ~2000 Ma and ~1790 Ma (Figure 3.6d). The youngest group of ages at ~1790 Ma can be used to define a maximum depositional age for this sample.

Western Officer Basin

The western Officer Basin covers about 525 000 km^2 across South Australia and Western Australia, between the northeastern Yilgarn Craton and the west Musgrave Province. It is a Neoproterozoic to ?Devonian basin which formed part of the Centralian Superbasin (Walter et al., 1995). A detailed lithostratigraphy for the western Officer Basin was presented by Grey et al. (2005), based principally on drill hole and well log information, and outcrop observations from the northwestern part of the Officer Basin. The basin was deformed by the latest Neoproterozoic to earliest Cambrian Petermann Orogeny, the late Cambrian Delamerian Orogeny, and the Silurian–Carboniferous Alice Springs Orogeny. Geochemical evaluation of numerous minor oil and bitumen shows indicate the presence of at least one petroleum system in the basin in Western Australia (Ghori, 1998).

In the vicinity of the YOM seismic line, almost all of the Officer Basin is concealed beneath surface outcrops of Permian and Cretaceous sedimentary rocks of the Gunbarrel Basin (Hocking, 1994) and younger Cenozoic sediments and regolith (Figure 3.1). Near the southwestern end of the YOM seismic line, our interpretation is constrained by limited surface outcrops of the Archean Yilgarn Craton and Neoproterozoic Buldya Group, whereas near the northeastern part of the seismic line discussed here, outcrops of the Neoproterozoic Townsend Quartzite dip to the southwest above rocks of the Mesoproterozoic Bentley Supergroup developed on the west Musgrave Province, which together form basement to the Officer Basin. The northeastern margin of the basin was deformed by a younger deformational event, possibly the Petermann Orogeny or Delamerian Orogeny.

A thick, gently folded sandstone succession extends westwards from South Australia south of the Musgrave Province. This unit, the Wirrildar beds, postdates syn-Petermann Orogeny deformation, but predates the Late Cambrian Table Hill Volcanics, suggesting the gentle folding is due to the Delamerian Orogeny. It does not appear to be present as far west as the YOM seismic line.

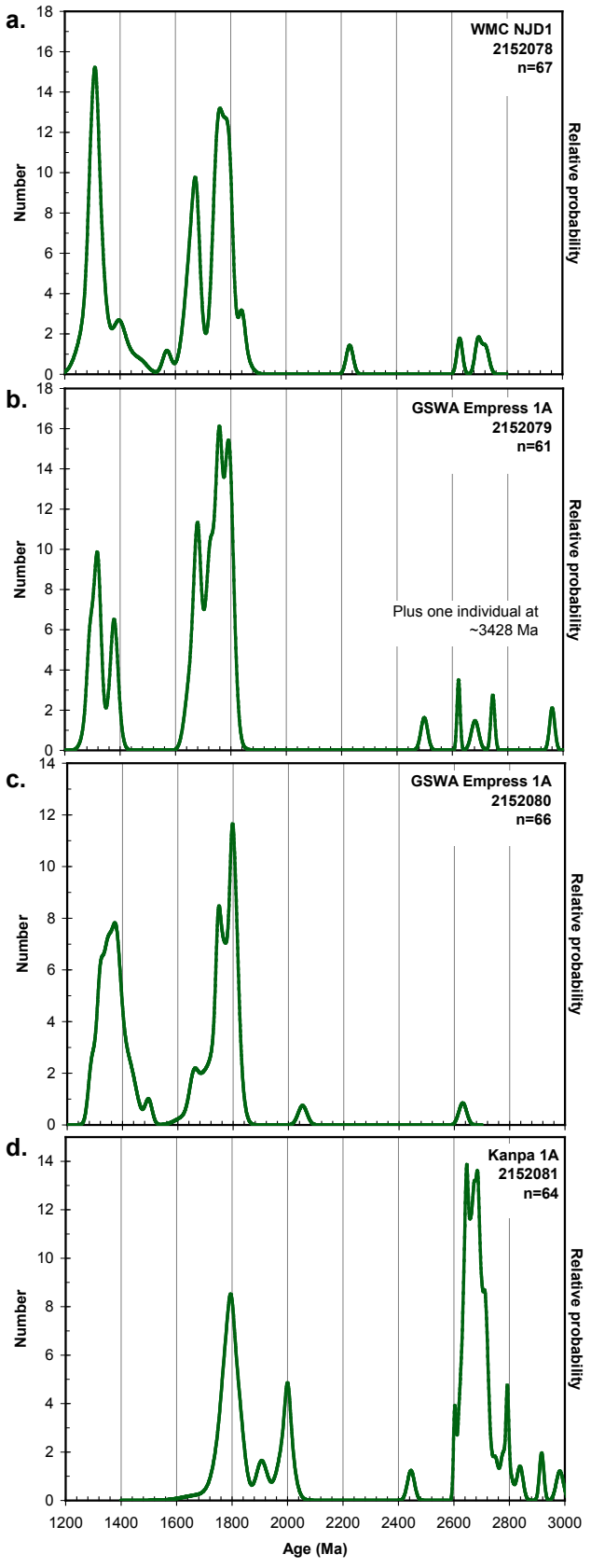

Figure 3.6 *Preliminary probability density diagrams of zircon analyses from drill hole samples a) WMC NJD 1, b) and c) GSWA Empress 1A, and d) Kanpa 1A, displayed as ^{204}Pb corrected $^{207}Pb/^{206}Pb$ ages.*

The interpretation of the Officer Basin in the YOM seismic line (Figure 3.7) is constrained stratigraphically by several petroleum exploration wells and stratigraphic drill holes located on or close to the seismic line, including Kanpa 1A, Yowalga 3, GSWA Empress 1A, BMR Westwood 1 and 2 and BMR Throssell 1. GSWA Empress 1A, located on the YOM seismic line, and Kanpa 1A, ~25 km to the north, intersected the base of the Officer Basin at 1522 m, and 3671 m, respectively (Grey et al., 2005). Yowalga 3, ~38 km to the north, reached 4200 m depth, still in the Browne Formation (Shell Development (Australia) Pty. Ltd., 1981). All three wells intersected a thick Neoproterozoic succession beneath the Cambrian Table Hill Volcanics and younger sediments (Figure 3.7).

Towards the base of the Officer Basin, the Browne Formation contains numerous evaporite horizons (halite, anhydrite and gypsum), with a cumulative thickness of several hundred metres. The evaporite deposits were mobilised during several tectonic events, leading Simeonova and Iasky (2005) to conclude that the major deformational mechanism in the western Officer Basin was halotectonics, which may also have formed a variety of hydrocarbon traps. In the vicinity of the YOM seismic line, Carlson et al. (2003) and Simeonova and Iasky (2005) developed a four-fold structural subdivision of the basin into, from northeast to southwest: marginal overthrusted zone, salt-ruptured zone, thrusted zone and western platform zone, although Carr et al. (2012) questioned their validity.

Within their salt-ruptured zone, Simeonova and Iasky (2005) described the Browne salt wall (Browne diapir of Jackson, 1976), a major, northwest-southeast trending salt structure extending for over 120 km in length. The Browne 1 well, ~70 km to the north of the YOM line, and the Browne 2 well, ~50 km to the north of the YOM seismic line, both penetrated this diapiric structure at shallow depths (133 m and 262 m, respectively) below Phanerozoic sedimentary units. The salt wall has been inferred to continue well to the south of the YOM line.

The Cambrian Table Hill Volcanics form part of the extensive Kalkarindji Large Igneous Province (Evins et al., 2009), and consist predominantly of basalt flows, and are up to 165 m thick. The unit forms a distinctive, highly-reflective, marker horizon on seismic sections (e.g. Simeonova and Iasky, 2005). A sample of basalt from the Empress 1A drill hole (depth 216 m) has a K–Ar whole rock age of 484 ± 4 Ma (Amdel Limited, in Stevens and Apak, 1999). Recently, Evins et al. (2009) obtained a $^{40}Ar/^{39}Ar$ plateau age of 505 ± 3 Ma on plagioclase from a basalt sample from the Empress 1A drill hole (depth 255 m). South of the Musgrave Province, nearer the South Australian border, there is an extensive sandstone succession between the Table Hill Volcanics and the glacigene Carboniferous–Permian Paterson Formation. This succession, the Lennis Sandstone and Wanna Formation, is otherwise unconstrained as to age, but appears to be aeolian at least in part.

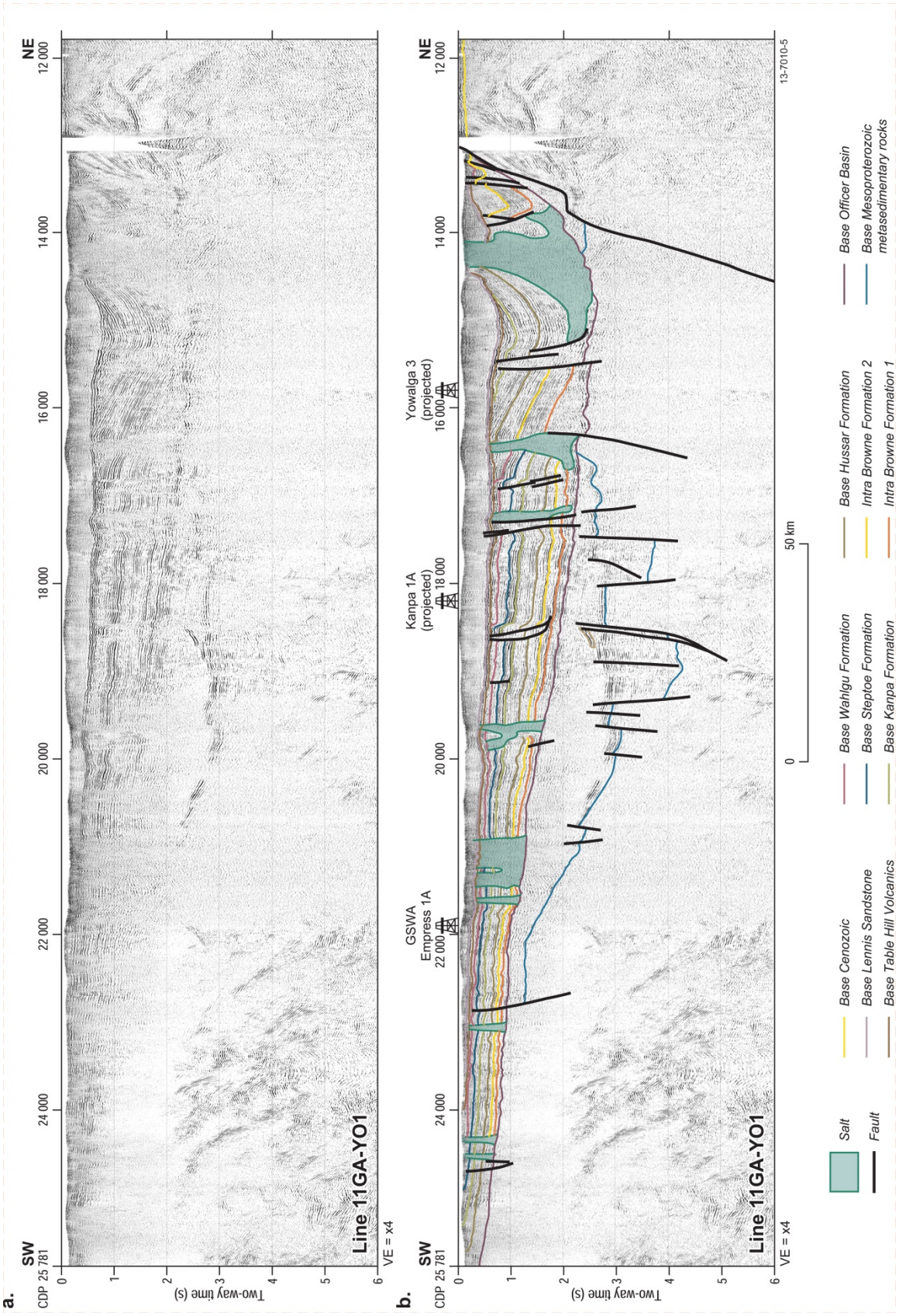

Figure 3.7 *Migrated seismic section for the southwestern half of seismic section 11GA-YO1, to a depth of 6 s TWT, showing both uninterpreted and interpreted versions for that part of the line across the western Officer Basin. Section is displayed with a vertical exaggeration of x4, assuming an average crustal velocity of 6000 ms^{-1}.*

Geological interpretation of the southwestern part of seismic line 11GA-YO1

The northeast–southwest orientation of the YOM seismic line is essentially perpendicular to the long axis of the main depocentre of the western Officer Basin, the strike of rocks in the Bentley Supergroup overlying the Musgrave Province, and to the orientation of the major magnetic and gravity anomalies in the region (Figures 3.3 and 3.4). In the vicinity of the YOM seismic line, the Yilgarn Craton is totally covered by the Officer Basin, and the Officer Basin and Musgrave Province are mostly concealed beneath younger Cenozoic, Cretaceous and Permian sedimentary deposits. Thus, the YOM seismic section provides an image of the subsurface architecture of the basin and basement provinces. The crust in the vicinity of the YOM seismic section has variable reflectivity, with some areas of the section containing very strong reflections, but other areas having only moderate to low reflectivity (Figure 3.5).

At the southwestern end of the YOM seismic line, for a distance of about 150 km between CDPs 18200 and 25780, the Mohorovičić discontinuity (Moho) is interpreted to occur at the base of a moderately to strongly reflective package, below which the nonreflective material is considered to represent the upper mantle (Figure 3.5). The interpreted Moho in this region is generally subhorizontal, at a depth of just over 15 s TWT (~45–46 km). At about CDP 22800, however, the Moho appears to be displaced by a shallow, southwest-dipping fault, with strong reflections in the footwall being mapped to a depth of at least 16.3 s TWT (~49 km) (Figure 3.5).

Northeast of about CDP 18200, the Moho is much less distinctive, but appears to be gently deepening towards the northeast, to a depth of about 16.2 s TWT (~49 km) at CDP 16400, and possibly to about 17 s TWT (~51 km) at about CDP 13400 (Figure 3.5). North of this point, beneath part of the Musgrave Province, the Moho has been mapped to a much deeper level (see Howard et al., 2013).

On the basis of seismic character and presence of discrete, crustal-scale structures, the crust in the YOM seismic section has been divided into six major components: the Officer Basin, the Manunda Basin, the Yamarna Terrane of the Yilgarn Craton, the Babool Seismic Province, the Musgrave Province and the Tikelmungulda Seismic Province (see Korsch et al., 2013a), the first four of which will be described in more detail below, and the remaining two described by Howard et al. (2013).

In the southwest half of the YOM seismic section, the upper crust can be subdivided into the Officer Basin, the Manunda Basin, and a very weakly reflective crust, which we infer to be the Yamarna Terrane of the Yilgarn Craton, based principally on surface geological mapping to the west of the seismic line and the interpretation of potential-field data (Figure 3.5). By comparison, the middle to lower crust, below the Yamarna Terrane, appears to have a very consistent seismic character, over a distance of about 200 km, which is very different in seismic character to that imaged in the upper crust. Because of the very distinct change in the seismic character at the boundary between the upper and middle crust, we here confine the Yamarna Terrane (*sensu stricto*) to only the upper crust, which is inferred to consist of the granite–greenstone units, and define its base as the contact between the relatively nonreflective upper crust and the package of strong reflections in the middle crust which have apparent dips to the northeast. We combine the middle and lower crust into the Babool Seismic Province (see below, and Korsch et al., 2013a).

Yamarna Terrane

Along the YOM seismic line, the Yamarna Terrane *sensu stricto* is only very weakly reflective, and varies in thickness from about 1.2 s TWT (~3–4 km) at about CDP 24000 to about 2.8 s TWT (~8 km)

at about CDP 20750 (Figure 3.5). Farther to the northeast, the weakly reflective package is interpreted to be part of the Yamarna Terrane, and it is inferred to be about 4.2 s TWT (~13 km) thick at about CDP 15800. Nevertheless, because there are no geological constraints, it is possible that most of the Archean upper crust, in the vicinity of the YOM seismic section, considered here to be part of the Yamarna Terrane, could be a separate, discrete terrane forming the northwesternmost part of the Yilgarn Craton. The weakly reflective character of the Yamarna Terrane observed in the YOM seismic section (Figure 3.5) is similar to that imaged in the upper crust on deep seismic line 01AGA-NY1, about 110 km to the southwest of the YOM line, across the western part of the Yamarna Terrane (Goleby et al., 2004; 2006).

It is difficult to determine the northeastern extent of the Yilgarn Craton in the YOM seismic line due to lack of crustal reflectivity below the Officer Basin to the north of about CDP 15600 (Figure 3.5). It is tentatively interpreted to extend to the Winduldarra Fault, which is inferred to be the boundary between the Yilgarn Craton and the Musgrave Province (see Korsch et al., 2013a).

The YOM seismic line crosses a strong, linear magnetic anomaly centred on CDP 24700, and one with a less intense magnetic signal centred on CDP 24340 (Figure 3.3). The first magnetic anomaly also coincides with a broad gravity high (Figure 3.4). We interpret these to be small, buried greenstone belts, and, although they are not reflective seismically, we infer their bases to be at about 3–4 km depth. The greenstone belts appear to be related to shear zones which cut deep into the crust, and can be traced to at least the top of the lower crust, at a depth of about 13.3 s TWT (~40 km) at about CDP 18900 (Figure 3.5). The magnetotelluric conductivity model for the YOM seismic line (Duan et al., 2013) indicates that the Yamarna Terrane is significantly more resistive than the overlying Officer Basin (Figure 3.8).

Babool Seismic Province

A highly reflective middle and lower crust has been imaged below the Yamarna Terrane (*sensu stricto*), and, as mentioned above, we use the term Babool Seismic Province (new name, after Babool Rockholes) to refer to the middle and lower crust in this region (Figure 3.5). The seismic province varies in thickness from about 11.7 s TWT (~35 km) at CDP 17600, to about 13.3 s TWT (~40 km) at about CDP 23950. As we have not been able to track these rocks to the surface, we have no direct constraints on their lithology or age. Also, we cannot demonstrate that this rock package forms part of the Yamarna Terrane, but having a different structural fabric. Hence, at this stage, we treat this seismic province as a discrete package of rocks which forms the current basement to the granite–greenstone rocks of the Yamarna Terrane. The majority of the Babool Seismic Province, down to a depth of approximately 13.3 s TWT (~40 km), is highly to moderately reflective, with abundant reflective surfaces having moderate (~30°) apparent dips to the northeast (Figure 3.5). Southwest-dipping reflections also occur, but are relatively rare. The reflections appear to sole onto the top of the lower crust at about 13.3 s TWT. Below this depth, the lower crust, down to the Moho, is also moderately reflective, but with the reflections being predominantly subhorizontal. The highly reflective middle to lower crust is indicative of much of the Yilgarn Craton, as imaged on previous deep seismic reflection lines across the Youanmi Terrane and the Eastern Goldfields Superterrane (e.g. Drummond et al., 2000; Goleby et al., 2004; Korsch et al., 2013b).

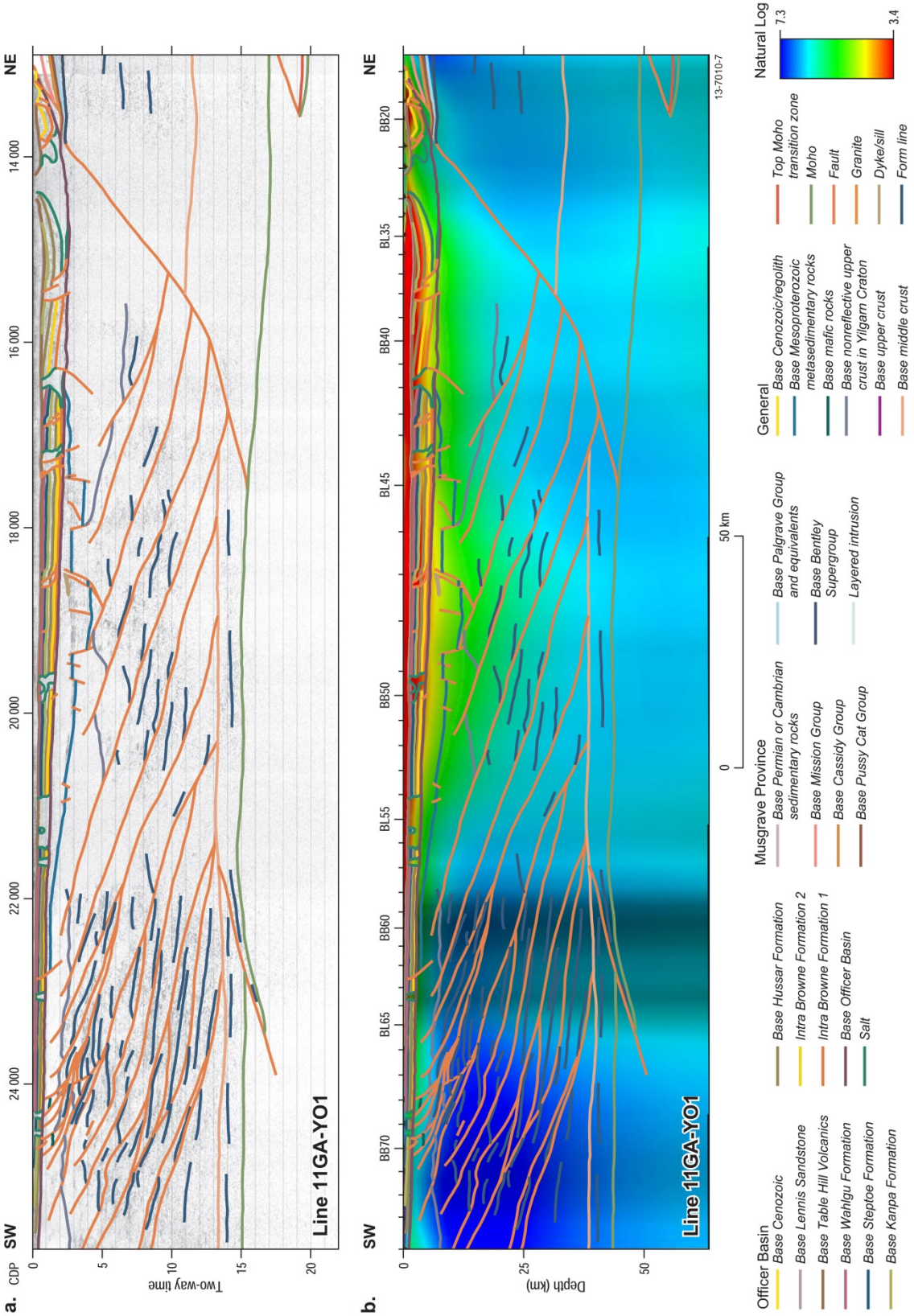

Figure 3.8 *Seismic interpretation (a) and magnetotelluric conductivity model (b) to a depth of 60 km, covering the southwest half of the YOM seismic traverse (see details in Duan et al., 2013). The display shows the vertical scale equal to the horizontal scale. Simplified line work from the interpretation of the seismic section in (a) is overlain on the MT model in (b).*

The northeast-dipping reflections are best developed, and hence more recognisable, towards the southwest end of the line (CDPs 21800 to 25400, Figure 3.5). These reflections often form anastomosing arrays, which may represent shear zones. Locally, the northeast-dipping reflections appear to be separated by sigmoidal reflections, suggesting an extensional sense of shear, that is, with top to the northeast. Nevertheless, there are numerous examples in the seismic section of reflections being truncated; these frequently have the geometry of hangingwall anticlines sitting on faults, indicating later contractional inversion on the extensional shear zones (see a good example at about 2.5 s TWT depth at CDP 23850, Figure 3.5).

There is a subvertical nonreflective zone about 20 km wide between about CDP 20800 and CDP 21800, which extends through most of the crust, although within it there are a series of weak, subhorizontal reflections at about 7–9 s TWT and also in the lower crust. This zone may be a result of the data acquisition, possibly due to poor surface coupling, because it is possible to approximately match the moderately-dipping reflections of the Babool Seismic Province across this zone, although the reflections are less pronounced to the northeast of this nonreflective zone. These reflections continue to the northeast to about CDP 15600 (Figure 3.5). The moderate to strong reflections in the middle crust, considered to represent the Babool Seismic Province, can be tracked as far to the northeast as about CDP 15600. There is a lack of reflectivity in the crust, beneath the Officer Basin, between about CDP 15600 and about CDP 13600, a distance of about 40 km. Reflections to the northeast of this are considered to form part of the Musgrave Province (Howard et al., 2013). Thus, it is difficult to determine the northeastern limit of the Babool Seismic Province in the YOM seismic line, which is tentatively interpreted to be the Winduldarra Fault (see Korsch et al., 2013a).

In the magnetotelluric conductivity model, the Babool Seismic Province is generally resistive, except for a more conductive zone dipping to the southeast, and overlapping with the subvertical nonreflective zone described above (Figure 3.8).

In the middle crust, there is a large structure at 7.7–8.5 s TWT at about CDP 25780, here termed the Throssell Shear Zone. This feature, if projected to the surface, would occur about 55 km to the west of the YOM seismic line, well to the east of the Yamarna Shear Zone, and hence still within the Yamarna Terrane.

Goleby et al. (2006) interpreted the Yamarna Shear Zone, the terrane boundary between the Yamarna and Burtville terranes, to cut deep in the crust on seismic line 01AGS-NY3, about 110 km to the south of the YOM seismic line. If projected to the north into the YOM seismic line, the Yamarna Shear Zone is likely to be deeper than about 12.5 s TWT, possibly soling onto the top of the lower crust. It is not possible, at this stage, to determine whether, in the YOM seismic section, there is a sliver of the Burtville Terrane deep in the crust at the western end of the line.

Manunda Basin

Beneath the Officer Basin, the YOM seismic line has provided an image of the geometry of the Manunda Basin, which is interpreted to occur between CDP 16500 and CDP 22800, a distance of over 125 km (Figures 3.5 and 3.7). The basin appears to consist of at least two graben, up to about 18 km wide, with thinner platforms on both sides, producing a geometry typical of a classic steer's head basin, with the subsidence being driven initially by mechanical extension, followed by thermal relaxation of the lithosphere (Dewey, 1982; White and McKenzie, 1988). The graben centred on CDP 19000 has a southwest-dipping, basin-bounding fault on its northeastern side, and shows some

growth of the graben-fill towards this fault. Elsewhere, the basin has been cut by a series of later minor extensional faults, best observed by displacements in the base of the basin (Figure 3.5).

The maximum depth to the base of the basin is about 4.2 s TWT (~10.5 km) at about CDP 19000, and the basin has a maximum thickness of 2.4 s TWT (~6000 m) at about this location (Figure 3.5). Thus, the basin in this area is thicker than where it was imaged in the 01AGS-NY1 and 01AGS-NY3 seismic lines (Goleby et al., 2003), where it has a maximum thickness of about 1.8 s TWT (~4500 m).

The basin can be subdivided into at least two, and possibly three, seismic stratigraphic sequences. The lower part of the graben contain a weakly layered sequence, which is overlain by a package of strong reflections. The package of strong reflections can be mapped as the basal unit on the adjacent platforms. The upper part of the basin forms a third sequence which is only weakly to moderately reflective (Figure 3.5). GSWA Empress 1A, drilled at CDP 21960 on the seismic line, penetrated about 103 m of the basin, which included about 58 m of basalt (Stevens and Apak, 1999); this is in an area of moderate reflections in the upper succession. The magnetotelluric conductivity model in the YOM seismic line (Duan et al., 2013) shows that conductivity decreases with depth in the Manunda Basin (Figure 3.8).

Western Officer Basin

The YOM seismic line provided an image across the western Officer Basin about 155 km long, from the southern end of the line to CDP 13020 (Figure 3.7). The seismic line shows an asymmetric geometry for the basin, with the sedimentary succession showing essentially a layer-cake stratigraphy, thickening gradually, from a thickness of about 0.3 s TWT (~480 m) at the southwest end of the section, to a maximum thickness of about 2.6 s TWT (~5200 m) at CDP 14800 just to southwest of outcrops of the Musgrave Province (Figure 3.7).

Stratigraphy

In the YOM seismic line, our interpretation of the stratigraphy of the western Officer Basin is constrained mainly by the lithological units intersected in the Empress 1A, Kanpa 1A and Yowalga 3 drill holes, and summarised by Grey et al. (2005). The basal unit of the western Officer Basin, the Townsend Quartzite, crops out at the northeastern edge of the basin, about 3 km to the southwest of Warburton, with a dip to the southwest of about 20º. This formation has limited distribution, as it has not been found in drill holes farther to the southwest. Instead, the Browne Formation rests directly on basement, which led Grey et al. (2005) to speculate that Townsend Quartzite may be present only adjacent to tectonically active margins of the basin. The succession is dominated by Neoproterozoic sedimentary rocks consisting of the Buldya Group (Townsend Quartzite, Browne, Hussar, Kanpa and Steptoe formations) and Wahlgu Formation, all of which appear to thicken to the northeast, towards the current margin of the basin (Figure 3.7). The Browne Formation, alone, is up to 1.7 s TWT (~3400 m) thick, at about CDP 16200.

The Pirrilyungka Formation (deposited during the Sturt glaciation, and separating the Buldya Group and Wahlgu Formation) may be present near the west Musgrave Province. This unit, to date recognised only in GSWA Vines 1 drill core (Haines et al., 2008), is probably equivalent to the Lupton Formation, a ?glacigene unit which overlies the Townsend Quartzite in outcrop, and may have been mismapped as Permian in some areas, based on outcrop trends and relationships. The overlying Wahlgu Formation was deposited during the Elatina glaciation, and crops out in the northwest Officer Basin. Both are dominated by diamictite, the former generally monomictic and grey, the later brownish

to varicoloured and polymictic (Haines et al., 2008). Aeolian Ediacaran sandstone of the Lungkarta Formation is present in Empress 1A and Vines 1, but cannot be differentiated from the glacigene units below on the YOM seismic section.

A very reflective couplet high in the seismic section is interpreted to represent strong contrasts in the velocities between the sedimentary rocks and the top and bottom of the Cambrian Table Hill Volcanics (Figure 3.7). Above the Table Hill Volcanics there is a weakly to nonreflective package up to 1000 m thick (Figure 3.7), consisting of the Cambrian–Ordovician Lenis Formation, Permian Paterson Formation and younger Cretaceous and Cenozoic sediments. Because of the lack of continuity in reflections within this package, we have not subdivided it on the seismic section.

A relatively thick Cenozoic palaeochannel has been imaged just to the south of Warburton (Figure 3.7). At about CDP 13340, the palaeochannel is about 0.3 s TWT (~300 m) thick, and forms one of the palaeodrainage systems in the region mapped by Allen (1997).

Unconformities

The basal contact of the Townsend Quartzite with the Mission Group of the Musgrave Province is nowhere exposed, but was considered by Daniels (1971) and Jackson and van de Graaff (1981) to be either conformable or disconformable near Warburton, because the strike and dip of the two units are essentially parallel. Farther to the east, it is considered to be an angular unconformity. Nevertheless, Daniels (1971) suggested that the contact possibly could be a decollement, based on regional outcrop fold patterns. In our interpretation of the YOM seismic line, we have mapped this contact as a fault (see below) (Figures 3.5 and 3.7).

In the YOM seismic section, a pronounced angular unconformity has been well imaged within the Officer Basin, at the base of the late Cambrian Table Hill Volcanics, particularly towards the northeastern end of the basin (Figure 3.7). At about CDP 13500, the Browne Formation is interpreted to sit directly below the unconformity, with the younger Neoproterozoic units being eroded. Farther south, the Hussar Formation (e.g. about CDP 14600), and Kanpa Formation (e.g. about CDP 15200) sit unconformably below the Table Hill Volcanics. Towards the southwestern end of the YOM seismic line, the Wahlgu Formation (deposited during the Elatina glaciation) and the Lungkarta Formation (an aeolian-dominated ?Ediacaran unit) sits below the Table Hill Volcanics with apparent conformity, but this surface is a disconformity representing a time gap of about 50–100 Ma (Figure 3.7).

Structures and Deformation

The thick succession and growth of the stratigraphic packages towards the northeastern end of the Officer Basin suggests that the basin was initially an extensional basin, with the northeastern margin probably being defined by a steep southwest-dipping, extensional growth fault, which was active at least during the deposition of the lower sedimentary succession (Browne, Hussar and Kanpa formations). The Winduldarra Fault, mapped as a major boundary in the crust (see Korsch et al., 2013a), was possibly the major basin-bounding fault during the extension which initiated the basin. Nevertheless, later contractional reactivation on this structure, possibly during the late Neoproterozoic Petermann Orogeny and/or the late Cambrian Delamerian Orogeny, has partially inverted the basin to produce the present-day geometry, with the basal Townsend Quartzite being brought to the present-day surface by this fault (Figure 3.7). Farther south, other faults which are now intruded by salt domes (see below) originally could have been extensional faults during the Neoproterozoic subsidence phase.

Shortening during the Petermann and/or Delamerian orogenies produced broad folds in the Neoproterozoic succession, between about CDP 17000 and the northeastern edge of the basin.

Several thrust faults displace the stratigraphy, often producing hangingwall anticlines in the upper part of the succession, for example, at about CDPs 15400, 16850 and 18550 (Figure 3.7). Although we have mapped a salt diapir at about CDP 16400, there is a displacement of the stratigraphy across it of up to 1 s TWT (~2000 m), and with significant changes in the thicknesses of the formations across it as well. The thickness changes imply the presence of a northeast-dipping extensional fault during deposition, and the large displacements suggest a significant amount of later contractional inversion. Our interpretation suggests that the diapir has utilised and obliterated the fault.

The thrust faults almost always dip to the northeast, although we have mapped two southwest-dipping thrusts at about CDP 13400, and a backthrust at CDP 13800. The thrust faults usually sole out in the lower part of the succession, interpreted in the seismic section as the Bowne Formation, which contains the thick evaporite horizons (Figure 3.7). Thus, the evaporitic unit has acted as a significant décollement, partitioning the deformation in the basin compared to the basement. The thrusts are much more common in the northeastern half of the basin and, in places, have facilitated the formation and emplacement of salt diapirs (see below). A significant period of erosion followed the orogenies, producing an unconformity surface prior to eruption of the Table Hills Volcanics at about 505 Ma.

As mentioned above, Carlson et al. (2003) and Simeonova and Iasky (2005, Figure 14, section B–B') described four discrete structural zones in the western Officer Basin in this region. Our interpretation suggests a blending of these zones, with the thrusts and salt diapirs being intimately related, and hence these features should not be used to define different structural zones.

Halotectonics

Several nonreflective areas imaged on the seismic section cut across the stratigraphy and are interpreted as salt diapirs or salt walls mobilised from evaporitic horizons in the Browne Formation (Figure 3.7). The Browne salt wall, imaged on the seismic section between CDPs 14200 and 14400, is the only salt structure near the YOM seismic line which has geological constraints, having been intersected in the Browne 1 and Browne 2 wells, to the north of the line. The salt dome has a distinctive seismic character (see also Simeonova and Iasky, 2005), and this pattern of reflectivity has been used to interpret the presence of several salt structures in the YOM seismic section, some of which are farther to the southwest than previously recognised (Figure 3.7).

Most of the salt structures appear to have formed during the Petermann Orogeny and/or Delamerian Orogeny, being related to thrust faults which formed during these orogenies. For most of the interpreted salt structures, the overlying Table Hill Volcanics are essentially subhorizontal, indicating no salt movement since eruption of the basalts in the late Cambrian. Nevertheless, at least two of the salt structures have had minor salt mobilisation since the Cambrian, with gentle doming of the Table Hill Volcanics and some of the younger sediments (e.g. about CDP 17300 and about CDP 19700) (Figure 3.7). Satellite imagery shows a characteristic bullseye pattern with apparent contortion at the core about 4.5 km east of about CDP 15000. Although not confirmed on the ground, the pattern is suggestive of a salt diapir with Browne Formation reaching the surface. Such diapirs are known to the northwest (Madley and Woolnough diapirs), and inferred from bullseye patterns, stratigraphic succession, and stromatolite occurrences to the southeast, in the Livesey Hills and north of Pirrilyungka Outstation (e.g. Jackson and van de Graaff, 1981).

The Browne salt wall, however, has penetrated the Table Hill Volcanics, almost reaching the present day surface (Figure 3.7). The Permian Paterson Formation is much thinner on top of the salt wall than in the surrounding areas, possibly due to erosion, suggesting that some of the mobilisation occurred in the Mesozoic and Cenozoic. Jackson and van de Graaff (1981) noted that Cenozoic duricrust is

buckled up around some diapirs which reach the surface, indicating Cenozoic salt movement. The magnetotelluric conductivity model for the YOM seismic line (Duan et al., 2013) shows that the Browne salt wall is more resistive than the adjacent sedimentary rocks in the Officer Basin (Figure 3.8).

Summary

The southwestern half of the YOM deep seismic reflection line (11GA-YO1) provides a northeast-southwest oriented image of the crust across the northeast part of the Yilgarn Craton and overlying Officer Basin, in a region where there is almost no exposure of these rocks. The Moho under this part of the YOM seismic line varies from a depth of about 45 km at the southwest end of the line to about 51 km in the northeast. A low-angle thrust fault has been interpreted to cut the Moho towards the southwest end of the line.

The Officer Basin is generally a subhorizontal package of sedimentary rocks, which thickens towards the northeast. In places, it has been disrupted by thrust faults and salt diapirs. Beneath the Officer Basin, the ?Mesoproterozoic Manunda Basin has a maximum thickness of about 6000 m and can be subdivided into at least three seismic stratigraphic sequences. Beneath both basins, the Yamarna Terrane of the Yilgarn Craton is only weakly to moderately reflective. It has been interpreted to have a maximum thickness of about 13 km, but is much thinner in most places. Beneath the Yamarna Terrane, strong reflections in the middle to lower crust have been referred to as the Babool Seismic Province. It is difficult to determine the northeastern boundary of the Yamarna Terrane and the Babool Seismic Province, but it is inferred to be the Winduldarra Fault.

Acknowledgements

This paper forms part of a collaborative project between Geoscience Australia and the Geological Survey of Western Australia. We thank the following for their contributions to the project: Jenny Maher and Tristan Kemp, for project management during the planning, acquisition and processing phase of the seismic data; Lindsay Highet, Weiping Zhang and Daniel McIlroy for producing the maps, digital versions of the interpretations of the seismic sections, and the figures of the seismic and MT sections, respectively; and Michael Doublier and Natalie Kositcin for their reviews of the manuscript. R. Hocking, H. Smithies, R. Quentin de Gromard, H. Howard and K. Gessner publish with the permission of the Executive Director of the Geological Survey of Western Australia.

References

Allen, A.D., 1997. Groundwater: the strategic resource - a geological perspective of groundwater occurrence and importance in Western Australia. *Geological Survey of Western Australia, Report* 50, 61p.

Bacchin, M., Milligan, P.R., Wynne, P., and Tracey, R., 2008. Gravity anomaly map of the Australian region (Third Edition), scale 1:5 000 000. *Geoscience Australia, Canberra*.

Blewett, R.S., Czarnota, K., and Henson, P.A., 2010. Structural-event framework for the eastern Yilgarn Craton, Western Australia, and its implications for orogenic gold. *Precambrian Research*, 183, 203–229.

Bodorkos, S., Love, G.J., Nelson, D.R., and Wingate, M.T.D., 2006. 149698: quartz sandstone, Cornelia Range. *Geological Survey of Western Australia, Geochronology Record* 617, 5p.

Carlsen, G.M., Simeonova, A.N., and Apak, S.N., 2003. Petroleum systems and exploration potential in the Officer Basin, Western Australia. *The APPEA Journal*, 43, 472–493.

Carr, L.K., Korsch, R.J., Mory, A.J., Hocking, R.M., Marshall, S.K., Costelloe, R.D., Holzschuh, J., and Maher, J.L., 2012. Structural and stratigraphic architecture of Western Australia's frontier onshore sedimentary basins: the Western Officer and Southern Carnarvon basins. *APPEA Journal and Conference Proceedings*, 52, 4p. (CD-ROM).

Cassidy, K.F., Champion, D.C., Krapež, B., Barley, M.E., Brown, S.J.A., Blewett, R.S., Groenewald, P.B., and Tyler, I.M., 2006. A revised geological framework for the Yilgarn Craton, Western Australia. *Geological Survey of Western Australia, Record* 2006/8, 8p.

Champion, D.C., and Sheraton, J.W., 1997. Geochemistry and Nd isotope systematics of Archaean granites of the Eastern Goldfields, Yilgarn Craton, Australia; implications for crustal growth processes. *Precambrian Research*, 83, 109–132.

Champion, D.C., and Cassidy, K.F., 2007. An overview of the Yilgarn Craton and its crustal evolution. In: Bierlein, F.P., and Knox-Robinson, C.M. (editors), Proceedings of Geoconferences (WA) Inc. Kalgoorlie '07 Conference. *Geoscience Australia, Record* 2007/14, 8–13.

Czarnota, K., Champion, D.C., Goscombe, B., Blewett, R.S., Cassidy, K.F., Henson, P.A., and Groenewald, P.B., 2010. Geodynamics of the eastern Yilgarn Craton. *Precambrian Research*, 183, 175–202.

Daniels, J.L., 1971. Talbot, Western Australia1: 250 000 Geological Series. *Bureau of Mineral Resources, Explanatory Notes* SG/52-9, 28p.

Dewey, J.F., 1982. Plate tectonics and the evolution of the British Isles. *Journal of the Geological Society, London,* 139, 371–412.

Drummond, B.J., Goleby, B.R., Swager, C.P., and Williams, P.R., 1993. Constraints on Archaean crustal composition and structure provided by deep seismic sounding in the Yilgarn Block. *Ore Geology Reviews,* 8, 117–124.

Drummond, B.J., Goleby, B.R., and Swager, C.P., 2000. Crustal signature of Late Archaean tectonic episodes in the Yilgarn craton, Western Australia: evidence from deep seismic sounding. *Tectonophysics,* 329, 193–221.

Duan, J., Milligan, P.R., and Fomin, T., 2013. Electrical resistivity distribution from magnetotelluric data in the Yilgarn Craton, western Officer Basin and western Musgrave Province. In: Neumann, N.L. (editor), *Yilgarn Craton–Officer Basin–Musgrave Province (YOM) Seismic and MT Workshop*. Geoscience Australia Record 2013/28, 9–23.

Evins, L.Z., Jourdan, F., and Phillips, D., 2009. The Cambrian Kalkarindji Large Igneous Province: Extent and characteristics based on new $^{40}Ar/^{39}Ar$ and geochemical data. *Lithos,* 110, 294–304.

Evins, P.M., Smithies, R.H., Howard, H.M., Kirkland, C.L., Wingate, M.T.D., and Bodorkos, S., 2010. Devil in the detail: The 1150–1000 Ma magmatic and structural evolution of the Ngaanyatjarra Rift, west Musgrave Province, Central Australia. *Precambrian Research*, 183, 572–588.

Gee, R.D., Baxter, J.L., Wilde, S.A., and Williams, I.R., 1981. Crustal development in the Archaean Yilgarn Block, Western Australia. In: Glover, J.E., and Groves, D.I. (editors), Archaean Geology. *Geological Society of Australia, Special Publication* 7, 43–56.

Geological Survey of Western Australia, 2008. 1:500 000 interpreted bedrock geology of Western Australia, 2008 Update. *Geological Survey of Western Australia, Perth.*

Ghori, K.A.R., 1998. Petroleum source-rock potential and thermal history of the Officer Basin, Western Australia. *Geological Survey of Western Australia, Record* 1998/3, 52p.

Goleby, B.R., Blewett, R.S., Groenewald, P.B., Cassidy, K.F., Champion, D.C., Jones, L.E.A., Korsch, R.J., Shevchenko, S., and Apak, S.N., 2003. The 2001 Northeastern Yilgarn deep seismic reflection survey. *Geoscience Australia Record*, 2003/28, 143p.

Goleby, B.R., Blewett, R.S., Korsch, R.J., Champion, D.C., Cassidy, K.F., Jones, L.E.A., Groenewald, P.B., and Henson, P.A., 2004. Deep seismic reflection profiling in the Archaean northeastern Yilgarn Craton, Western Australia: implications for crustal architecture and mineral potential. *Tectonophysics,* 388, 119–133.

Goleby, B.R., Blewett, R.S., Fomin, T., Fishwick, S., Reading, A.M., Henson, P.A., Kennett, B.L.N., Champion, D.C., Jones, L.E.A., Drummond, B.J., and Nicoll, M., 2006. An integrated multi-scale 3D seismic model of the Archaean Yilgarn Craton, Australia. *Tectonophysics,* 420, 75–90.

Greatland Gold, 2010. Proof of concept in initial drilling at Ernest Giles, A new large greenstone sequence discovered in the Eastern Goldfields of Western Australia. Greatland Gold Exploration Update 10 November 2010, http://www.greatlandgold.com/pdfs/20101110%20Exploration%20Update.pdf viewed on 23 December 2010.

Grey, K., Hocking, R.M., Stevens, M.K., Bagas, L., Carlsen, G.M., Irimies, F., Pirajno, F., Haines, P.W., and Apak, S.N., 2005. Lithostratigraphic nomenclature of the Officer Basin and correlative parts of the Paterson Orogen, Western Australia. *Geological Survey of Western Australia, Report* 93, 89p.

Haines, P.W., Mory, A.J., Stevens, M.K., and Ghori, K.A.R., 2004. GSWA Lancer 1 well completion report (basic data), Officer and Gunbarrel Basins, Western Australia. *Geological Survey of Western Australia, Record* 2004/10, 39p.

Haines, P.W., Hocking, R.M., Grey, K., and Stevens, M.K., 2008. Vines 1 revisited: are older Neoproterozoic glacial deposits preserved in Western Australia? *Australian Journal of Earth Sciences*, 55, 397–406.

Harrison, P.L., 1973. Officer Basin seismic survey, W.A., 1972. *Bureau of Mineral Resources, Record* 1973/62, 12p.

Harrison, P.L., and Zadoroznyj, I., 1978. Officer Basin, seismic, gravity, magnetic and radiometric survey. Western Australia 1972. *Bureau of Mineral Resources, Report* 191, 67p.

Hocking, R.M., 1994. Subdivisions of western Australian Neoproterozoic and Phanerozoic sedimentary basins. *Geological Survey of Western Australia, Record* 1994/4, 84p.

Hocking, R.M. (compiler), 2002. Drill hole WMC NJD 1, western Officer Basin, Western Australia: stratigraphy and petroleum geology. *Geological Survey of Western Australia, Record* 2002/18, 26p.

Hocking, R.M., Grey, K., Bagas, L., and Stevens, M.K., 2000. Mesoproterozoic stratigraphy in the Oldham Inlier, Little Sandy Desert, central Western Australia. *Geological Survey of Western Australia, Annual Review* 1999–2000, 49–56.

Holzschuh, J., 2013. 11GA-YO1 Yilgarn Craton–Officer Basin–Musgrave Province Seismic Survey – Acquisition and Processing. In: Neumann, N.L. (editor), *Yilgarn Craton–Officer Basin–Musgrave Province (YOM) Seismic and MT Workshop*. Geoscience Australia Record 2013/28, 1–8.

Howard, H.M., Werner, M, Smithies, R.H., Kirkland, C.L., Kelsey, D.L., Hand, M., Collins, A., Pirajno, F., Wingate, M.T.D., Maier, W.D., and Raimondo, T., 2011. The geology of the west Musgrave Province and the Bentley Supergroup – a field guide. *Geological Survey of Western Australia, Record* 2011/4, 119p.

Howard, H.M., Quentin de Gromard, R., Smithies, R.H., Kirkland, C.L., Korsch, R.J., Aitken, A.R.A., Gessner, K., Wingate, M.T.D., Blewett, R.S., Holzschuh, J., Kennett, B.L.N., Duan, J., Goodwin, J.A., Jones, T., Neumann, N.L., and Gorczyk , W., 2013. Geological setting and interpretation of the northeastern half of deep seismic reflection line 11GA-YO1: west Musgrave Province and the

Bentley Supergroup. In: Neumann, N.L. (editor), *Yilgarn Craton–Officer Basin–Musgrave Province (YOM) Seismic and MT Workshop*. Geoscience Australia Record 2013/28, 51–95.

Iasky, R.P., 1990. Officer Basin. *In:* Geology and mineral resources of Western Australia. *Geological Survey of Western Australia, Memoir* 3, 362–380.

Jackson, M.J., 1976. Browne, Western Australia 1:250 00 Geological Series. *Bureau of Mineral Resources, Explanatory Notes*, SG 151–8, 16p.

Jackson, M.J., and van de Graaff, W.J.E., 1981. Geology of the Officer Basin, Western Australia. *Bureau of Mineral Resources, Bulletin* 206, 102p.

Korsch, R.J., Blewett, R.S., Smithies, R.H., Quentin de Gromard, R., Howard, H.M., Pawley, M.J., Carr, L.K., Hocking, R.M., Neumann, N.L., Kennett, B.L.N., Aitken, A.R.A., Holzschuh, J., Duan, J., Goodwin, J.A., Jones, T., Gessner, K., and Gorczyk, W., 2013a. Geodynamic implications of the Yilgarn Craton–Officer Basin–Musgrave Province (YOM) deep seismic reflection survey: part of a ~1800 km transect across Western Australia from the Pinjarra Orogen to the Musgrave Province. In: Neumann, N.L. (editor), *Yilgarn Craton–Officer Basin–Musgrave Province (YOM) Seismic and MT Workshop*. Geoscience Australia Record 2013/28, 169–197.

Korsch, R.J., Blewett, R.S., Wyche, S., Zibra, I., Ivanic, T.J., Doublier, M.P., Romano, S.S., Pawley, M.P., Johnson, S.P., Van Kranendonk, M.J., Jones, L.E.A., Kositcin, N., Gessner, K., Hall, C.E., Chen, S.F., Patison, N., Kennett, B.L.N., Jones, T., Goodwin, J.A., Milligan, P.M., and Costelloe, R.D., 2013b. Geodynamic implications of the Youanmi and Southern Carnarvon deep seismic reflection surveys: a ~1300 km traverse from the Pinjarra Orogen to the eastern Yilgarn Craton. In: Wyche, S., Ivanic, I.J., and Zibra, I. (compilers), Youanmi and Southern Carnarvon seismic and magnetotelluric (MT) workshop. *Geological Survey of Western Australia, Record* 2013/6, 141–158.

Kositcin, N., Brown, S.J.A., Barley, M.E., Krapež, B., Cassidy, K.F., and Champion, D.C., 2008. SHRIMP U–Pb zircon age constraints on the Late Archaean tectonostratigraphic architecture of the Eastern Goldfields Superterrane, Yilgarn Craton, Western Australia. *Precambrian Research,* 161, 5–33.

Milligan, P.R., Franklin, R., Minty, B.R.S., Richardson, L.M., and Percival, P.J., 2010. Magnetic anomaly map of Australia (Fifth Edition), 1:5 000 000 scale. *Geoscience Australia, Canberra*.

Pawley, M.J., Romano, S.S., Hall, C.E., Wyche, S., and Wingate M.T.D., 2009. The Yamarna Shear Zone: a new terrane boundary in the northeastern Yilgarn Craton? *Geological Survey of Western Australia, Annual Review* 2007–08, 27–32.

Pawley, M.J., Wingate, M.T.D., Kirkland, C.L., Wyche, S., Hall, C.E., Romano, S.S., and Doublier, M.P., 2012. Adding pieces to the puzzle: episodic crustal growth and a new terrane in the northeast Yilgarn Craton, Western Australia. *Australian Journal of Earth Sciences*, 59, 603–623.

Perincek, D., 1996. The age of the Neoproterozoic–Palaeozoic sediments within the Officer Basin of the Centralian Super-Basin can be constrained by major sequence-boundary unconformities. *APPEA Journal*, 36, 61–79.

Phoenix Oil and Gas Limited, 2011. PHX701 – Western Officer Basin. Phoenix Oil and Gas Limited and FrOGTech Weekly Report - 4 February 2011, http://www.phoenixoilandgas.com.au/officer.php, viewed on 20 March 2013.

Raymond, O.L. (coordinator), 2009. Surface geology of Australia 1:1 million scale digital geology data. *Geoscience Australia, digital geology map*. https://www.ga.gov.au/products/servlet/controller?event=GEOCAT_DETAILS&catno=69455

Shell Company of Australia, Ltd, 1983. Kanpa-1/1A well completion report (Officer Basin, EP 178). Unpublished report, 70p.

Shell Development (Australia) Pty. Ltd., 1981. Yowalga-3 well completion report (Officer Basin, EP 178). Unpublished report, 61p.

Simeonova, A.P., and Iasky, R.P., 2005. Seismic mapping, salt deformation, and hydrocarbon potential of the central western Officer Basin, Western Australia. *Geological Survey of Western Australia, Report* 98, 51p.

Sircombe, K.N., Cassidy, K.F., Champion, D.C., and Tripp, G., 2007. Compilation of SHRIMP U–Pb geochronological data, Yilgarn Craton, Western Australia, 2004–2006. *Geoscience Australia, Record* 2007/01, 182p.

Stevens, M. K., and Apak, S.N. (compilers), 1999. GSWA Empress 1 and 1A well completion report, Yowalga Sub-basin, Officer Basin Western Australia. *Geological Survey of Western Australia, Record* 1999/4, 110p.

Swager, C.P., 1997. Tectono-stratigraphy of late Archaean greenstone terranes in the southern Eastern Goldfields, Western Australia. *Precambrian Research*, 83, 11–42.

Swager, C.P., Goleby, B.R., Drummond, B.J., Rattenbury, M.S., and Williams, P.R, 1997. Crustal structure of granite–greenstone terranes in the Eastern Goldfields, Yilgarn Craton, as revealed by seismic reflection profiling. *Precambrian Research,* 83, 43–56.

Townson, W.G., 1985. The subsurface geology of the western Officer Basin - results of Shell's 1980–1984 petroleum exploration campaign. *APEA Journal*, 25, 34–51.

Van Kranendonk, M.J., Ivanic, T.J., Wingate, M.T.D., Kirkland, C.L., and Wyche, S., 2012. Long-lived, autochthonous development of the Archean Murchison Domain, and implications for Yilgarn Craton tectonics. *Precambrian Research*, 229, 49–92.

Walter, M.R., Veevers, J.J., Calver, C.R., and Grey, K., 1995. Neoproterozoic stratigraphy of the Centralian Superbasin, Australia. *Precambrian Research,* 73, 173–196.

Western Mining Corporation Limited, 1981. Terminal report on the Neale temporary reserves 8165H, 8166H, 8167H, 8168H, and 8169H for the period 27 February 1981 to 9 November 1981. *Geological Survey Western Australia, Statutory Mineral Exploration Report*, Item 2752 A10540 (unpublished).

White, N., and McKenzie, D., 1988. Formation of the "steer's head" geometry of sedimentary basins by differential stretching of the crust and mantle. *Geology,* 16, 250–253.

Wingate, M.T.D., and Bodorkos, S., 2007. 181873: quartz sandstone, Lancer 1. *Geological Survey of Western Australia, Geochronology Record* 685, 6p.

Wingate, M.T.D., Pirajno, F., and Morris, P.A., 2004. Warakurna large igneous province: A new Mesoproterozoic large igneous province in west-central Australia. *Geology*, 32, 105–108.

Wingate, M.T.D., Kirkland, C.L., and Romano, S.S., 2011. 183150: metadacite, Central Bore. *Geological Survey of Western Australia, Geochronology Record* 950, 4p.

Wyche, S., Kirkland, C.L., Riganti, A., Pawley, M.J., Belousova, E., and Wingate, M.T.D., 2012. Isotopic constraints on stratigraphy in the central and eastern Yilgarn Craton, Western Australia. *Australian Journal of Earth Sciences*, 59, 657–670.

Wyche, S., Ivanic, T.J., and Zibra, I., 2013. Youanmi seismic and magnetotelluric (MT) workshop 2013: extended abstracts Preliminary edition. *Geological Survey of Western Australia Record* 2013/6.

4 Geological setting and interpretation of the northeastern half of deep seismic reflection line 11GA-YO1: west Musgrave Province and the Bentley Supergroup

H.M. Howard[1], R. Quentin de Gromard[1], R.H. Smithies[1], C.L. Kirkland[1], R.J. Korsch[2], A.R.A. Aitken[3], K. Gessner[1], M.T.D. Wingate[1], R.S. Blewett[2], J. Holzschuh[2], B.L.N. Kennett[4], J. Duan[2], J.A. Goodwin[2], T. Jones[2], N.L. Neumann[2] and W. Gorczyk[3]

[1] Geological Survey of Western Australia, Department of Mines and Petroleum, 100 Plain Street, East Perth, WA 6004.
[2] Minerals and Natural Hazards Division, Geoscience Australia, GPO Box 378, Canberra, ACT 2601.
[3] Centre for Exploration Targeting, School of Earth and Environment, The University of Western Australia, 35 Stirling Highway, Crawley, WA 6009.
[4] Research School of Earth Sciences, The Australian National University, Canberra. ACT 0200.

Heather.Howard@dmp.wa.gov.au

Introduction

The northeast-trending 11GA-YO1 (YOM) deep-seismic reflection line transects components of the Yilgarn Craton, the Officer Basin, and the Musgrave Province. Korsch et al. (2013) present the geological setting and interpretation of the southwestern half of the YOM deep-seismic reflection line, covering the Yamarna Terrane of the Yilgarn Craton and the western Officer Basin. Here, we present the geological setting and interpretation of the northeastern half of the YOM deep-seismic reflection line, covering the Musgrave Province (Figure 4.1). An introduction to the YOM deep-seismic reflection line, its aims, and discussion on seismic acquisition and processing are presented in Korsch et al. (2013) and are not repeated here. Below, we briefly outline some nomenclature relating to the Musgrave Province, describe the detailed geological evolution of the province, and outline the geological interpretation of that part of the YOM seismic line that images the province.

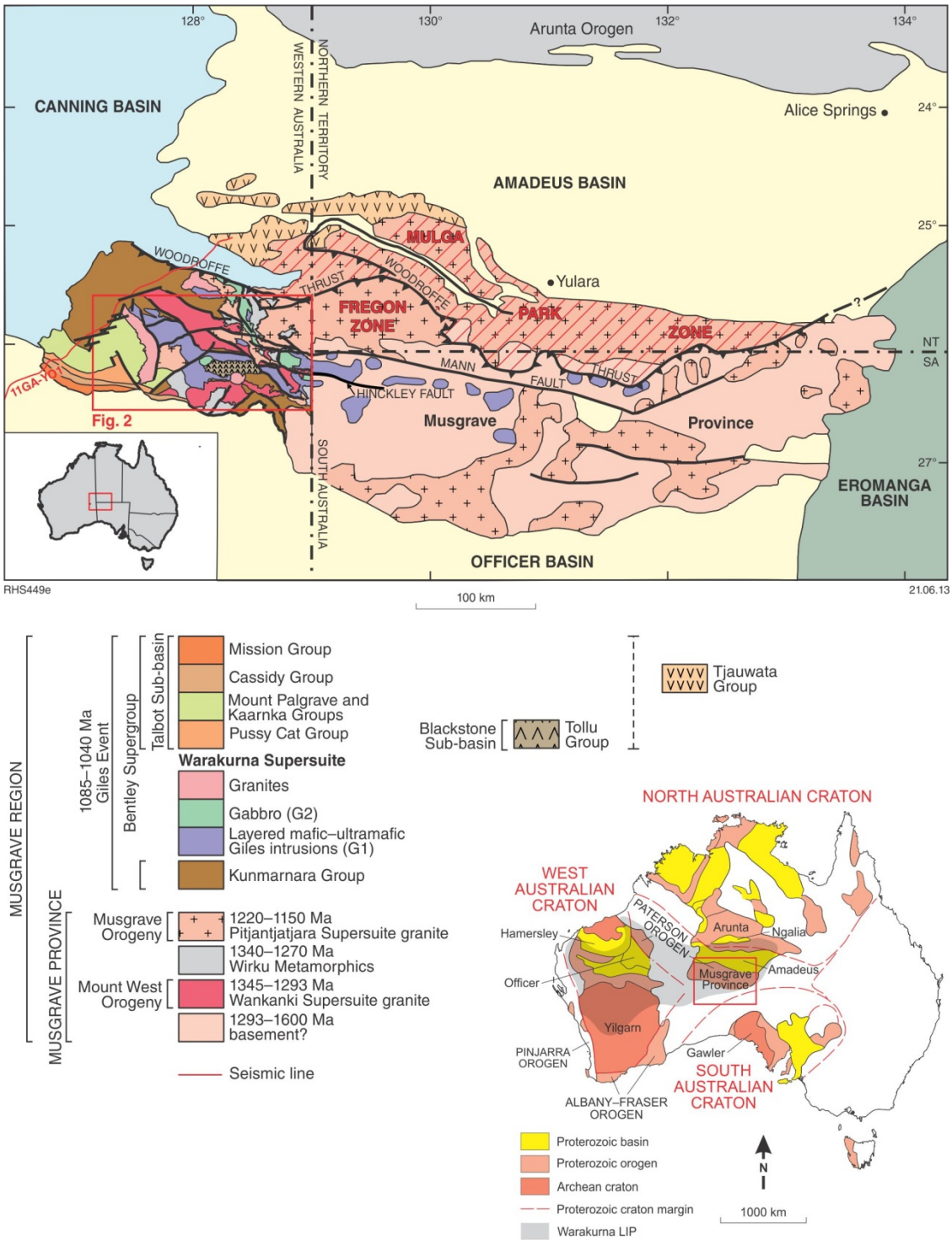

Figure 4.1 *Regional geological sketch of the Musgrave Province, modified from Glikson et al. (1996) and Edgoose et al. (2004).*

The term ‘Musgrave Province’ is used here to refer to all the meta-igneous and metasedimentary rocks affected by, or emplaced during the Mesoproterozoic Musgrave Orogeny. The province is located at the southeastern end of the Paterson Orogen, in central Australia, where it straddles the borders between the Northern Territory, Western Australia, and South Australia (Figure 4.1). It lies at the nexus of three Proterozoic structural trends formed by the amalgamation of the North, West, and

South Australian cratons (Figure 4.1), and is accordingly one of the most important regions in terms of the geological Proterozoic evolution of central Australia. Rocks within this region have a long and very complex geological history. The component of the Musgrave Province lying within Western Australia is referred to here as the west Musgrave Province.

During the 1085 Ma to 1040 Ma Giles Event, rocks of the Musgrave Province were intruded by rocks of the Warakurna Supersuite, and unconformably overlain by rocks of the Bentley Supergroup. The exposed and near-surface extent of the Musgrave Province is defined by the surrounding younger sedimentary basins (e.g. Edgoose et al., 2004) — namely, the Amadeus Basin to the north, Officer Basin to the south, and Canning Basin to the northwest (Figure 4.1).

The term Musgrave region is used in a geographical sense to denote the general area in which the Mesoproterozoic rocks of the Musgrave Province outcrop.

Tectonic subdivisions of the west Musgrave Province

The Musgrave Province was previously divided into zones with different structural and metamorphic characteristics, separated by major west- and west-northwest-striking faults that were last active during the c. 580 Ma to c. 530 Ma Petermann Orogeny (Camacho, 1989). In the north, the south-dipping Woodroffe Thrust (Figure 4.1) separates the northern amphibolite-facies Mulga Park Zone from the southern granulite-facies Fregon Zone (See Geological interpretation of the northeastern part of seismic line 11GA-YO1). Geochemical and geochronological similarities between these two zones indicate similar tectonic histories (Camacho and Fanning, 1995).

Within the Fregon Zone, Mesoproterozoic rocks to the north of the west-trending Mann Fault (Figure 4.1) have been multiply metamorphosed at granulite facies, and most have been deformed within the anastomosing west- to west-northwest-trending and shallow-dipping network of Petermann Orogeny-age mylonites that cut this part of the Musgrave Province. In the eastern part of the west Musgrave Province, the Fregon Zone shows a marked north to south decrease in the peak pressure of granulite-facies metamorphism. In the north, high-pressure metamorphism (10 kbar to 14 kbar; Scrimgeour and Close, 1999) during the Petermann Orogeny has masked the effects of Mesoproterozoic metamorphism (Scrimgeour and Close, 1999). To the south, where metamorphic overprints of Petermann Orogeny age are not as obvious, evidence for Mesoproterozoic high-temperature metamorphism, at much lower pressures, is preserved (Clarke et al., 1995a). In the west Musgrave Province, the boundary separating these two metamorphic styles lies close to the west-trending Mann Fault. Edgoose et al. (2004) speculated that this fault may further subdivide the Fregon Zone.

Walpa Pulka Zone, Tjuni Purlka Tectonic Zone, Mamutjarra Zone and Mitika area

Outcrop of the west Musgrave Province consists almost entirely of the Fregon Zone. Based on changes in the age and distribution of various rock types, and on the intensity and style of deformation, this part of the Fregon Zone has now been subdivided (Figures 4.2 and 4.3) into the Walpa Pulka Zone, Tjuni Purlka Tectonic Zone, Mamutjarra Zone and Mitika area (Smithies et al., 2009, 2010; Aitken et al., 2013). The most notable differences between these zones are in the distribution of granites of the two voluminous Mesoproterozoic supersuites — the Wankanki and Pitjantjatjara supersuites (Figure 4.3) — and in detrital zircon age distribution patterns in Mesoproterozoic paragneisses (Figures 4.4 and 4.5).

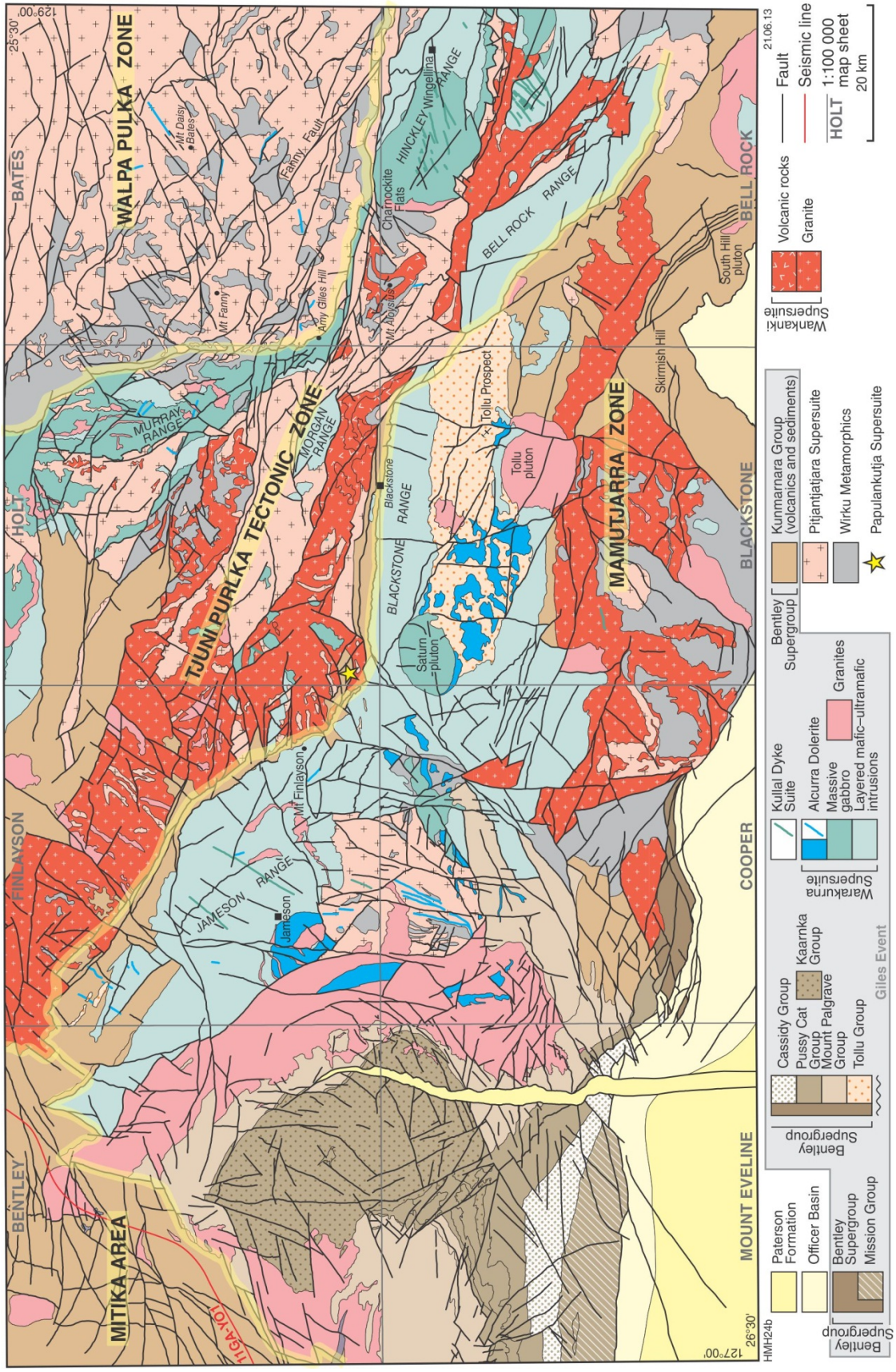

Figure 4.2 *Interpreted bedrock geology of the west Musgrave Province.*

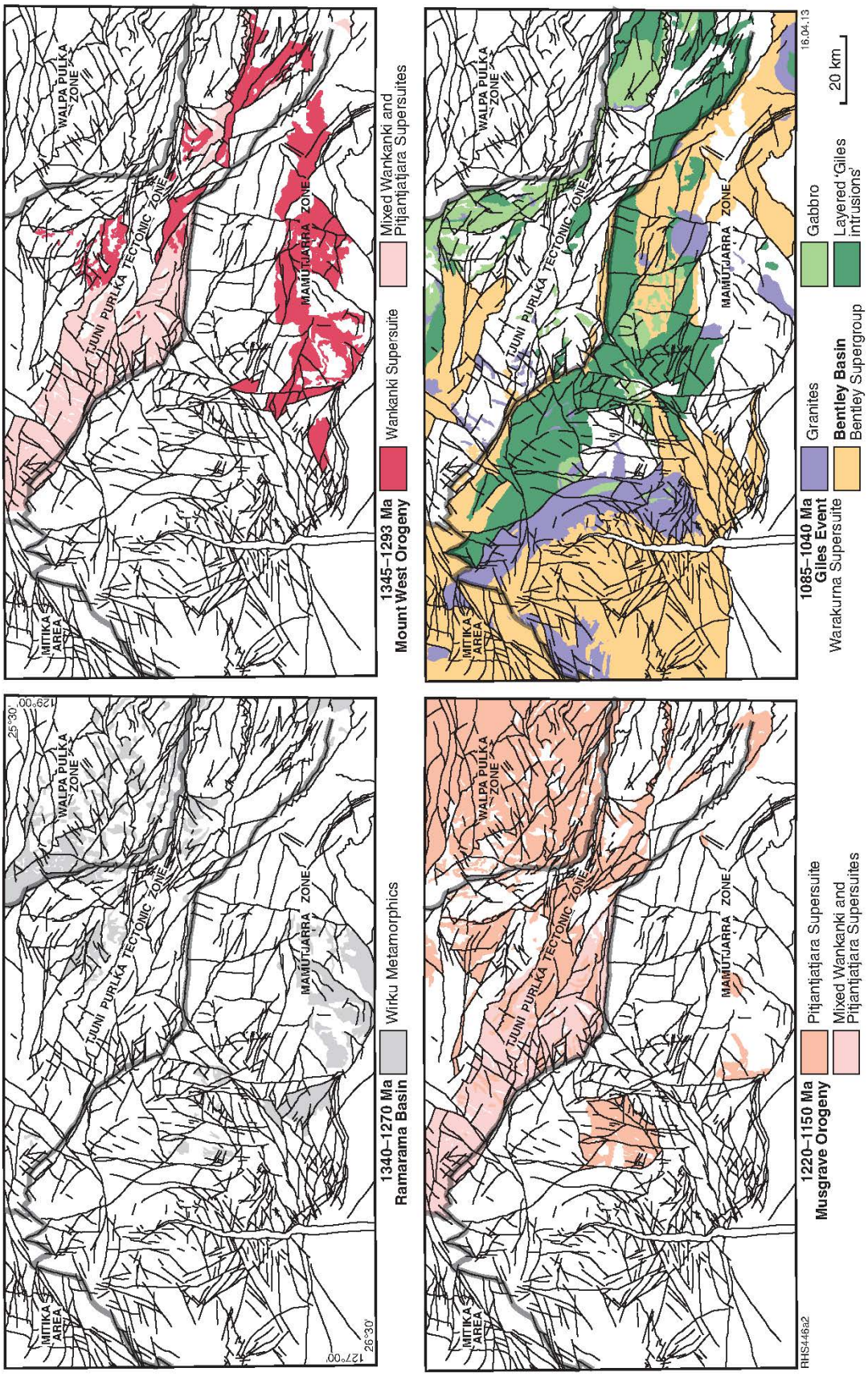

Figure 4.3 *Interpreted bedrock geology maps of the west Musgrave Province showing outcrop distribution for rocks of specific age groups.*

The **Tjuni Purlka Tectonic Zone** is a broad northwest-trending zone (Figure 4.2) of multigenerational (c. 1220 Ma, 1075 Ma, and 550 Ma) shearing. The extent and intensity of northwest-trending shearing in this zone exceeds that of neighbouring zones, and the observation that a compositionally unique suite of schlieric leucogranites (the Tjuni Purlka suite of the Pitjantjatjara Supersuite; Smithies et al., 2010) related to the Musgrave Orogeny is totally restricted to this zone, suggests that it is a synmagmatic zone of deformation throughout that period. The boundaries of the Tjuni Purlka Tectonic Zone were also the locus for mafic and felsic magmatism during the 1085–1040 Ma Giles Event (Figures 4.2 and 4.3). During the early stages of the Giles Event, giant layered troctolite–gabbronorite–gabbro intrusions (Giles intrusions) were emplaced along the southwestern edge of the zone. A thick zone of syntectonic and co-mingled gabbro and granite follows the northeastern edge of the Tjuni Purlka Tectonic Zone (Figures 4.2 and 4.3). The effects of the Petermann Orogeny in this zone are most intense to the northeast, near the contact with the Walpa Pulka Zone, and decrease towards the southwest.

The **Walpa Pulka Zone** to the north (Figure 4.2) is a deep-crustal domain dominated by 1220–1150 Ma high-potassium granite plutons of the Pitjantjatjara Supersuite, emplaced during the Musgrave Orogeny. The zone contains high-pressure metamorphic assemblages preserved by rapid exhumation along easterly- and northwesterly-trending mylonites and migmatitic shear zones related to the Petermann Orogeny (Scrimgeour and Close, 1999; Camacho et al., 1997; Raimondo et al., 2009, 2010). The **Mamutjarra Zone**, south of the Tjuni Purlka Tectonic Zone, is dominated by c. 1345 Ma to c. 1293 Ma calc-alkaline granites of the Wankanki Supersuite, formed during the Mount West Orogeny (Figures 4.2 and 4.3). The effects of the Petermann Orogeny in this zone are minimal. The **Mitika area** to the northwest of the Mamutjarra Zone is dominated by rocks of the Kunmarnara Group (Bentley Supergroup). Further to the northeast, the **Wannarn area** consists of Kunmarnara Group interleaved with felsic basement, including granulite facies metagranites of the Pitjantjatjara Supersuite (Musgrave Orogeny). The Mitika and Wannarn areas have low-density, low-susceptibility crust and are interpreted to overly a shallowly south-dipping Woodroffe Thrust (Aitken et al., 2012).

Lithological subdivisions of the west Musgrave Province

Supersuites

Outcrop in the Musgrave Province is dominated by rocks of granitic protolith. All Mesoproterozoic metagranitic components of the west Musgrave Province are now assigned to four supersuites, largely on the basis of SHRIMP U–Pb zircon geochronology. These supersuites are the c. 1400 Ma Papulankutja Supersuite, formed during a hitherto un-named event; the Wankanki Supersuite, formed during the c. 1345 Ma to c. 1293 Ma Mount West Orogeny; the Pitjantjatjara Supersuite, formed during the 1220–1150 Ma Musgrave Orogeny and the Warakurna Supersuite, formed during the c. 1085 Ma to c. 1040 Ma Giles Event.

Basins and Supergroups

The oldest outcropping supracrustal gneissic rocks are assigned to the Wirku Metamorphics and are found in the Walpa Pulka, Tjuni Purlka and Mamutjarra Zones of the west Musgrave Province. The basin into which the Wirku Metamorphics protoliths were deposited is referred to as the Ramarama Basin (Figure 4.3; Evins et al., 2012). As the sedimentary protoliths to the Wirku Metamorphics were intruded by Mesoproterozoic granites of the Wankanki Supersuite, the depositional age range for the

sedimentary protoliths to the Wirku Metamorphics can be constrained between the minimum age range of the Wankanki Supersuite and the age of the youngest detrital zircon component within the paragneisses, and lies between 1340 Ma and 1293 Ma (Smithies et al., 2009; Evins et al., 2012).

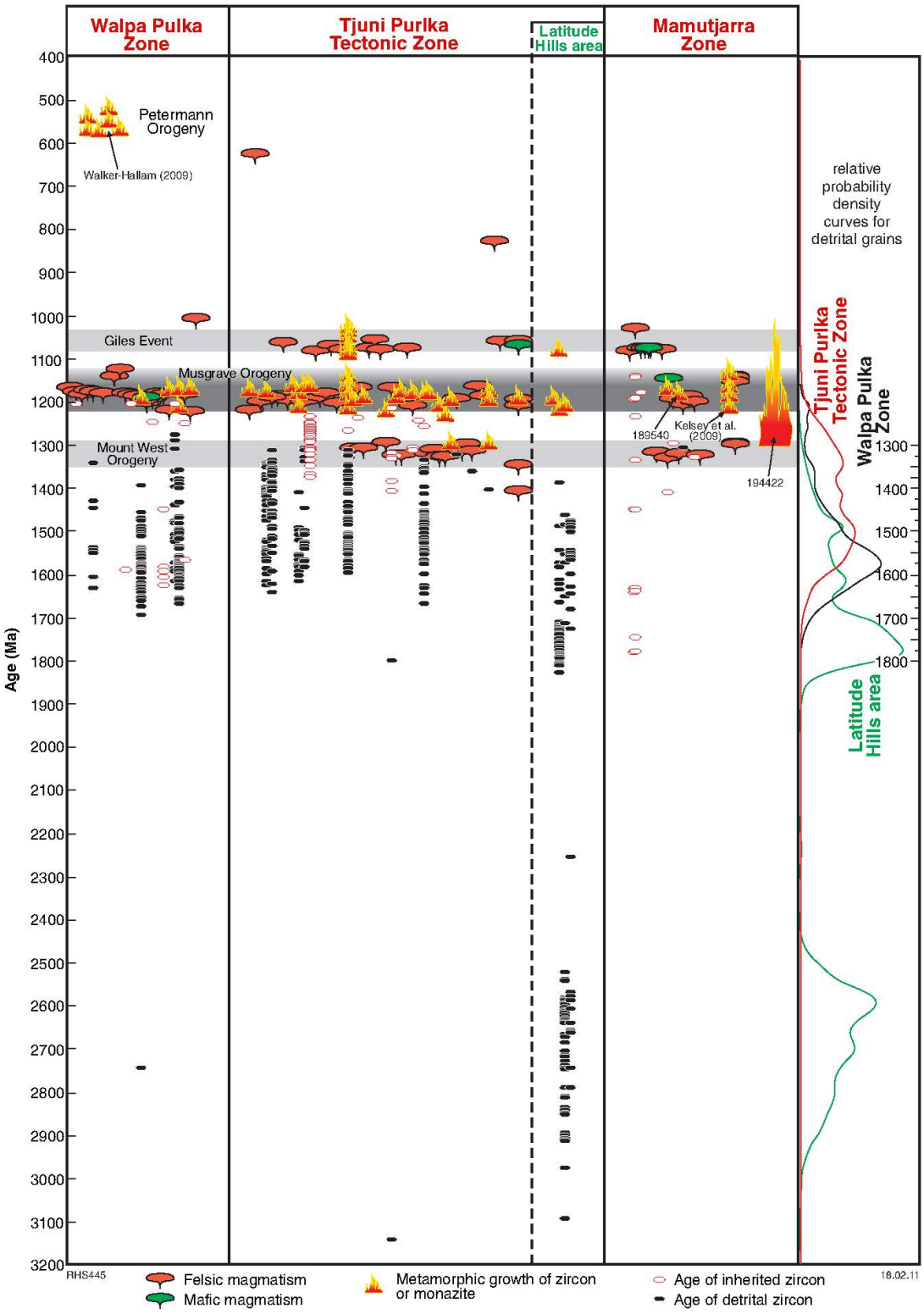

Figure 4.4 *Time-space plot of SHRIMP U–Pb zircon ages obtained from the west Musgrave Province (data from GSWA's online geochronology database <http://www.dmp.wa.gov.au/geochron>).*

Volcanic components of the Warakurna Supersuite are grouped into the Bentley Supergroup, which also includes volcaniclastic and sedimentary rocks. The outcrop extent of the Bentley Supergroup defines the preserved extent of the Bentley Basin (Figure 4.6). In Western Australia, this basin can be subdivided into at least two sub-basins — the Talbot Sub-basin, in the area west of the Jameson Community, and the smaller Blackstone Sub-basin, in the area south of the Blackstone Community. In the area to the north and east of Warakurna and continuing into the Northern Territory, supracrustal rocks of the Tjauwata Group also form part of the Bentley Supergroup.

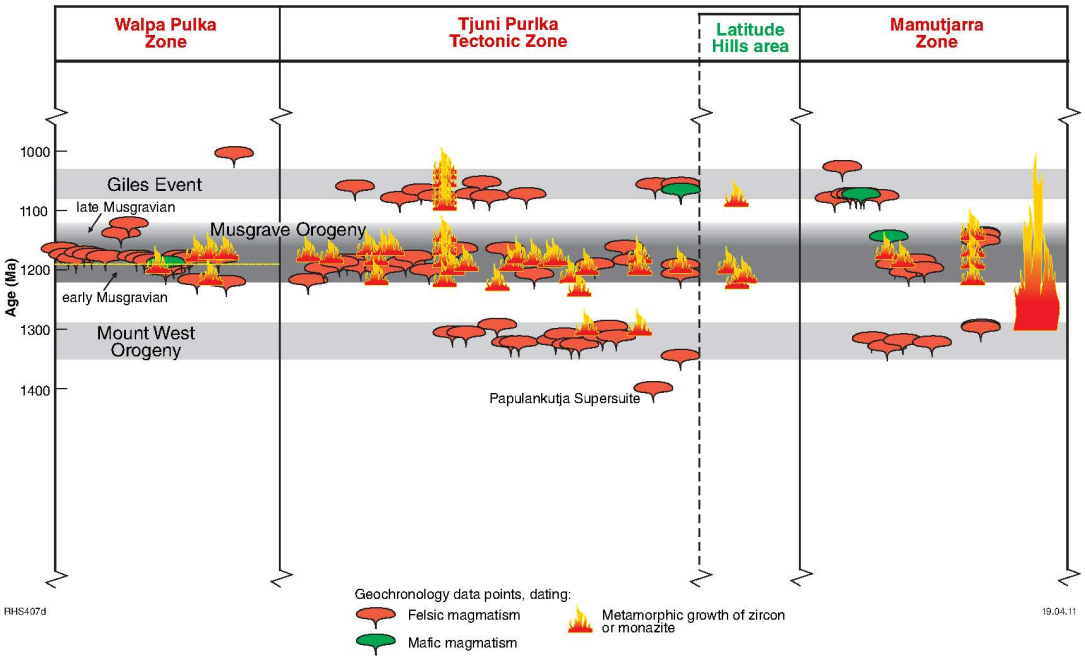

Figure 4.5 *Detailed time-space plot of SHRIMP U–Pb zircon ages obtained from the west Musgrave region, covering the period between c. 1400 Ma and 1000 Ma (data from GSWA's online geochronology database, <http://www.dmp.wa.gov.au/geochron>).*

Detailed geology and geological history of the west Musgrave Province

In the context of the Proterozoic geological evolution of central and southern Australia, the nature and tectonic setting of Mesoproterozoic events in the Musgrave Province are poorly constrained. A coincidence of intrusive and metamorphic ages provides a late Mesoproterozoic link between this province and the Albany–Fraser Orogen, which lies along the southern and southeastern margins of the West Australian Craton (e.g. Myers et al., 1996; White et al., 1999; Fitzsimons, 2003; Spaggiari et al., 2009). At some stage in its evolution, the Musgrave Province also likely formed the southeastern part of the Paterson Orogen (Figure 4.1), a 2000 km long Paleoproterozoic to Neoproterozoic belt in western and central Australia that connects to the Musgrave Province under Phanerozoic cover, via a prominent gravity-high known as the Anketell Regional Gravity Ridge (Fraser, 1976).

Regional surveys of the Musgrave Province have established a broad lithological framework (Daniels, 1974; Glikson et al., 1996; Edgoose et al., 2004). However, insight into the wider evolutionary context has hinged on only a few studies (e.g. Gray, 1971; Maboko, 1988; Camacho, 1997; White, 1997; Scrimgeour and Close, 1999; Scrimgeour et al., 2005; Wade et al., 2006, 2008; Aitken and Betts, 2008; Aitken et al., 2009).

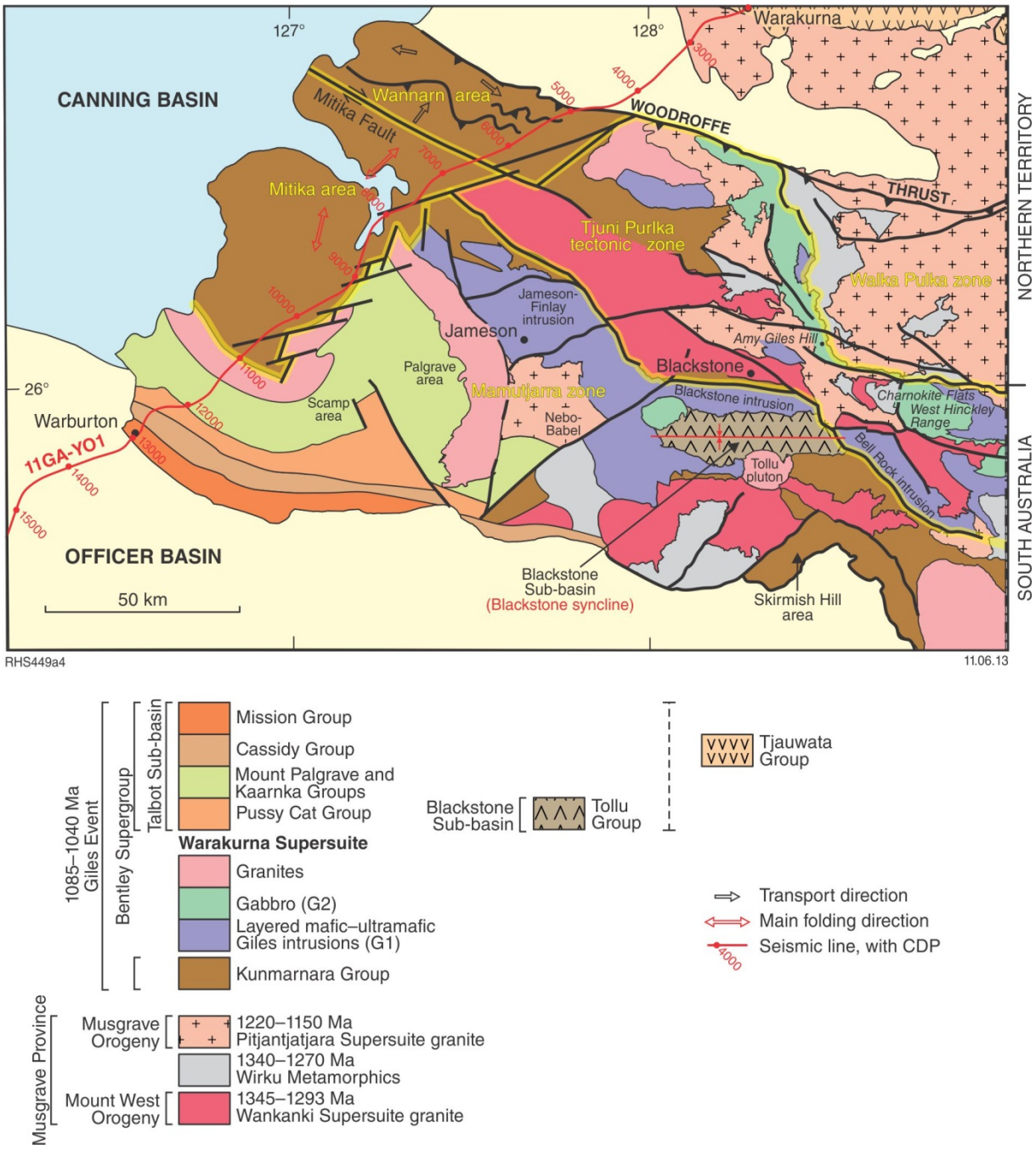

Figure 4.6 *Regional geology of the west Musgrave Province and Bentley Basin.*

Basement rocks

A recent study of Hf isotopes in zircons from magmatic and sedimentary rocks throughout the Musgrave Province (Kirkland et al., 2012) indicates that the unexposed basement to the region is dominated by two major juvenile crust-formation events - one at 1600–1550 Ma and a possibly more significant event at 1950–1900 Ma. Although no c. 1900 Ma juvenile rocks or crystals are known from the province, radiogenic addition into the crust at this time is required to account for consistent Nd and Hf evolution patterns which show no indication of mixing processes (Kirkland et al., 2012).

Clear evidence for exposed crust formed before c. 1400 Ma is yet to be found in the west Musgrave Province. In the South Australian section of the Musgrave Province, all rocks metamorphosed during the Musgrave Orogeny, including the Mesoproterozoic granite suites and the basement through which they intruded, were initially grouped into the Birksgate Complex (Major and Conor, 1993). The basement component was thought to have included orthogneiss as well as banded paragneiss derived mainly from volcanic, volcaniclastic, and sedimentary rocks, all formed or deposited between c. 1600 Ma and 1550 Ma (Gray, 1971, 1978; Gray and Compston, 1978; Maboko et al., 1991; Major and Conor, 1993; Camacho and Fanning, 1995; Edgoose et al., 2004). However, recent work has shown that much of what was previously regarded as exposed basement in the west Musgrave Province actually comprises supracrustal packages (now mainly paragneiss) deposited between c. 1340 Ma and 1270 Ma (Evins et al., 2012). These are referred to as the Wirku Metamorphics (Howard et al., 2007; Evins et al., 2009; Smithies et al., 2009).

Recent SHRIMP U–Pb zircon dating from an area between the communities of Blackstone and Jameson, has suggested the presence of isolated remnants of c. 1400 Ma crust (Kirkland et al., 2012). The original extent of this crust cannot be inferred from the isolated outcrops that remain, but the rocks are referred to here as the Papulankutja Supersuite.

The c. 1400 Ma Papulankutja Supersuite

In a small region to the south of Mount Scott, in the southwestern part of HOLT (shown by a yellow star on Figure 4.2), recent geochronological studies on a small outcrop of felsic gneiss have identified an orthogneiss with protolith ages significantly older than the maximum depositional age of protoliths to the Wirku Metamorphics. One sample from this region — a moderately foliated, K-feldspar porphyritic, orthopyroxene–clinopyroxene–biotite granodiorite to monzogranite, metamorphosed at or near granulite-facies conditions (GSWA 194764) — contains a population of 19 (out of 20) euhedral oscillatory zoned zircons that yielded a date of 1402 ± 4 Ma (Kirkland et al., 2011a). A single zircon rim yielded a date of 1316 ± 8 Ma (1σ), equivalent to the crystallisation age of the Wankanki Supersuite of the Mount West Orogeny.

The mineralogy and geochemistry of limited samples of granodiorites and monzogranites from this area are indistinguishable from that of calc-alkaline granites belonging to the Wankanki Supersuite. Dated samples of the Wankanki Supersuite typically do not contain significant proportions of inherited zircons, and much of the recorded inheritance is of zircons with crystallisation ages that fall within the interval of the Mount West Orogeny itself (Evins et al., 2012). This presumably indicates that most intrusions of the Wankanki Supersuite were emplaced into only slightly older rocks. The granodiorites and monzogranites from the area south of Mount Scott have intruded paragneisses with a dominant detrital component of c. 1400 Ma zircons, but include detrital age components as old as c. 1550 Ma (GSWA 187195, Kirkland et al., 2010a). If these metagranites belong to the geochemically similar Wankanki Supersuite, they must have selectively inherited only the c. 1400 Ma detrital component from the country rock. A more likely explanation is that the c. 1400 Ma zircon component reflects the true crystallisation age of the granodiorites and monzogranites. If this interpretation is correct, then this metagranite sample represents outcrop of hitherto unrecognised igneous basement rocks significantly older than the Wankanki Supersuite of the 1345–1293 Ma Mount West Orogeny. Therefore, we have tentatively assigned the granodiorites and monzogranites from the area south of Mount Scott to the Papulankutja Supersuite (a new name derived from the Aboriginal name for the nearby Blackstone Community).

A garnetiferous diatexite, locally with rafts of psammitic gneiss, outcrops approximately 10 km to the north of Mount Scott. Dating of the psammitic gneiss (GSWA 194767, Kirkland et al., in prep.) yielded a

major detrital zircon age component of 1404 ± 15 Ma. Likewise, two samples of the host diatexite (GSWA 187195, Kirkland et al., 2010a; GSWA 194768, Kirkland et al., in prep.) yielded dominant zircon age components of c. 1409 Ma and c. 1402 Ma respectively. In all three cases, a significantly smaller component of younger zircons (mainly rims), dated at 1313 ± 15 Ma (GSWA 194767), 1298 ± 26 Ma (GSWA 187195, one zircon), and 1311 ± 21 Ma (GSWA 194768), can either be interpreted as a detrital component that constrains a maximum depositional age of the protolith, or the result of local partial melting (incipient migmatisation) during the Mount West Orogeny. If the former is correct, the psammite and diatexite belong to the Wirku Metamorphics, the sedimentary protoliths for which were deposited between c. 1340 Ma and 1270 Ma (Evins et al., 2012). However, rocks of the Wirku Metamorphics do not typically contain a significant 1400 Ma detrital age component. Because zircons of this age overwhelmingly dominate the samples from near Mount Scott, the alternative suggestion — that the protoliths to these rocks contain a major volcanic component deposited at c. 1400 Ma, likely related to the Papulankutja Supersuite — is favoured here. The c. 1300 Ma age component in these rocks is thus attributed to metamorphic regrowth of zircon during the Mount West Orogeny.

To the south of Mount Scott, in the southwestern part of HOLT (Tjuni Purlka Tectonic Zone), a fine-grained, unfoliated leucogranitic dyke cuts foliated granodiorites and monzogranites of the c. 1400 Ma Papulankutja Supersuite (Figure 4.7). The leucogranitic dyke has an igneous crystallisation age of 1318 ± 9 Ma (GSWA 194765, Kirkland et al., in prep.) and belongs to the Wankanki Supersuite. The c. 1318 Ma date also represents the minimum age for deformation of the host granodiorites and monzogranites, whereas the c. 1400 Ma zircon age component from the Papulankutja Supersuite represents a maximum age constraint on that deformation, irrespective of how that date is interpreted. This represents the first clear temporal constraint on deformation events either associated with, or older than, the Mount West Orogeny — at some time between c. 1400 Ma and 1318 Ma.

RHS451 19.04.11

Figure 4.7 *Outcrop photograph showing the contact between a foliated granite (yellow dashed line depicts foliation) of the Papulankutja Supersuite and an unfoliated leucogranite (margin shown by red line) of the Wankanki Supersuite (southwestern HOLT).*

The 1345–1293 Ma Mount West Orogeny

Migmatitic gneisses with protolith ages between c. 1330 Ma and c. 1300 Ma were identified by Gray (1971), who also noted that these rocks appeared to be restricted to the south of the Mann and Hinckley Faults. Gray (1978) further suggested that the gneissic rocks were metamorphosed volcanic rocks; however, gradational contacts with foliated porphyritic monzogranites of equivalent age (Sun

et al., 1996; White, 1997; White et al., 1999; Howard et al., 2007) suggest that many of these rocks were intrusive. The results of subsequent regional mapping in the west Musgrave Province (Howard et al., 2007; Smithies et al., 2009; Evins et al., 2009) and of geochronological data (Figures 4.4 and 4.5) show that intrusive igneous rocks of this age form a significant component within the Tjuni Purlka Tectonic Zone, and represent the most voluminous pre- c. 1100 Ma magmatic component to the Mamutjarra Zone (Figures 4.2 and 4.3). Howard et al. (2007) grouped these rocks into the Wankanki Supersuite and termed the crustal event that produced them the Mount West Orogeny. The crystallisation age range of the supersuite is from c. 1345 Ma to c. 1293 Ma (White et al., 1999; Kirkland et al., 2008; GSWA 194393, Kirkland et al., 2010b), with most ages lying within a narrow interval between c. 1326 Ma and c. 1312 Ma (Figures 4.4 and 4.5).

Wirku Metamorphics and the Ramarama Basin

Banded gneiss, mainly preserved as rafts in granite, occurs in all three zones of the west Musgrave Province and is assigned to the Wirku Metamorphics (Figures 4.2 and 4.3). Based on locally continuous layering, the presence of pelitic, arkosic, and near-orthoquartzitic interlayers (Figure 4.8), and on complex zircon age spectra, this gneiss is interpreted to have protoliths of sedimentary and lesser volcaniclastic and volcanic origin (e.g. Evins et al., 2012). Detailed analysis of detrital zircon age patterns from a large number of samples of the Wirku Metamorphics, collected throughout the west Musgrave Province (Evins et al., 2012), indicates that the protoliths to these supracrustal rocks were deposited between c. 1340 Ma and c. 1270 Ma. Because sedimentary deposition overlapped in space and time with magmatism related to the c. 1345 Ma to c. 1293 Ma Wankanki Supersuite, the Wirku Metamorphics can also be regarded as a supracrustal (depositional) component of the Mount West Orogeny. Volcanic units of the Wankanki Supersuite (see below) are interlayered with, contributed detritus to, and are thus a component of, the Wirku Metamorphics in both the Mamutjarra Zone and the Tjuni Purlka Tectonic Zone. However, no volcanic or intrusive rocks of this age are known from the Walpa Pulka Zone (BATES). The basin into which the protoliths to the Wirku Metamorphics were deposited is referred to as the Ramarama Basin (Figure 4.3; Evins et al., 2012).

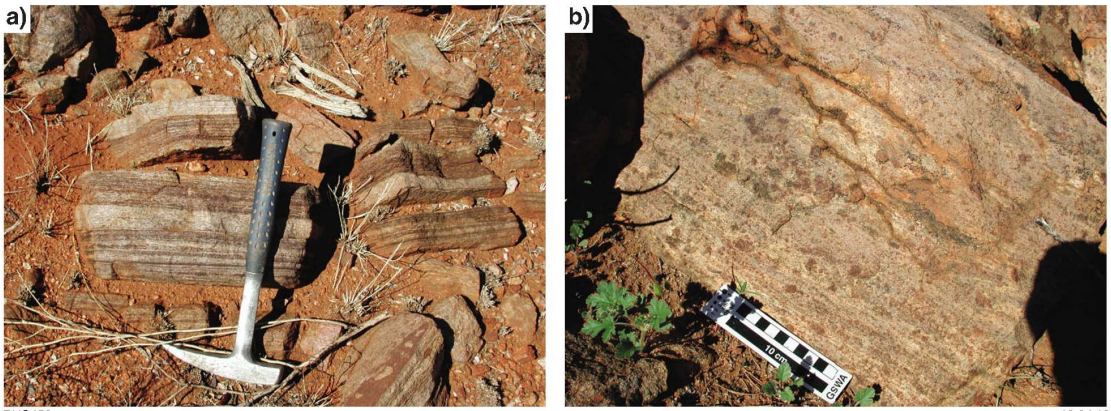

Figure 4.8 *Outcrop photographs of the Wirku Metamorphics: a) laminated arkosic metasandstone (southern HOLT); b) pelitic (garnet-sillimanite-hercynite-cordierite) gneiss (Latitude Hills area – BELL ROCK).*

Detrital zircon age spectra from the Wirku Metamorphics reveal distinct age trends for the Walpa Pulka, Tjuni Purlka Tectonic, and Mamutjarra Zones. Wirku Metamorphics of the Walpa Pulka Zone contain a main 1650 Ma to 1530 Ma detrital zircon age component dominated by c. 1570 Ma zircons. More varied and slightly more pelitic lithologies in the Tjuni Purlka Tectonic Zone contain a main 1580

Ma to 1450 Ma detrital zircon age component dominated by c. 1520 Ma zircons, and with significant c. 1370 Ma and c. 1320 Ma age components sourced from the Wankanki Supersuite. In the western portion of the Tjuni Purlka Tectonic Zone (Prostenthera Hill – Mount Scott area of HOLT), the Wirku Metamorphics are possibly exposed at a higher stratigraphic level, and are dominated by c. 1500 Ma to 1400 Ma detrital zircons. Samples from the Mamutjarra Zone are characterised by zircons derived from younger c. 1345 Ma to c. 1293 Ma Wankanki Supersuite magmatism, and by zircons older than c. 1410 Ma. Wirku Metamorphics from the Latitude Hills area in the southeast part of the Tjuni Purlka Tectonic Zone (BELL ROCK) yield unique detrital spectra with two main Proterozoic detrital zircon components at c. 1560 Ma to c. 1400 Ma and c. 1820 Ma to c. 1700 Ma, as well as an Archean component as old as c. 3200 Ma. Zircons in the Wirku Metamorphics of the Cohn Hill – Mount Blythe area (COOPER) in the far southwest of the Mamutjarra Zone are variably to completely reset by later high-grade metamorphism and deformation, and yield no detrital zircon ages (Evins et al., 2012).

In the Mamutjarra Zone, rare, laminated, orthopyroxene-bearing granulites to the south of the Cavenagh Range are geochemically similar to granites of the Wankanki Supersuite, and are interpreted as representing the volcanic or volcaniclastic equivalents of these granites (Smithies et al., 2009). These units with magmatic protoliths belong to the Wankanki Supersuite. They are also interleaved (?interbedded) with minor garnet and garnet–hercynite pelitic gneiss, and are a component of the Wirku Metamorphics, and thus the Ramarama Basin. Geochemically similar sequences of laminated, fine- to medium-grained, orthopyroxene-bearing felsic granulites also occur in the Tjuni Purlka Tectonic Zone (on HOLT) to the north of the Blackstone Range, where they are also interlayered with other clastic paragneisses of the Wirku Metamorphics, including pelitic units. Dating of zircons from these orthopyroxene-bearing felsic granulites gives a maximum depositional age of 1310 ± 7 Ma (GSWA 184150, Kirkland et al., 2011c) in the Tjuni Purlka Tectonic Zone north of the Blackstone Range, and a magmatic age of 1324 ± 7 Ma (GSWA 180867, Kirkland et al., 2009a) in the Mamutjarra Zone.

The indication that the Wirku Metamorphics and Wankanki Supersuite, in both the Tjuni Purlka Tectonic Zone north of the Blackstone Range and in the southwestern part of the Mamutjarra Zone, contain rocks of volcanic origin, suggests that these areas represent a slightly higher crustal level than in the Tjuni Purlka Tectonic Zone to the north of the Latitude Hills area (BELL ROCK), where only the intrusive rocks of the Wankanki Supersuite are exposed. Some samples of the Wirku Metamorphics from the Walpa Pulka Zone (BATES) show detrital zircon age patterns that reflect a very minor contribution from sources equivalent in age to rocks of the Wankanki Supersuite (Smithies et al., 2009; Evins et al., 2012), and may reflect a sporadic volcano-sedimentary contribution from distal Wankanki Supersuite felsic volcanism. The dominance of medium-grained and quartz-rich lithologies, the absence of abundant pelitic units, and the distribution of the Wirku Metamorphics, led Evins et al. (2012) to suggest that the protoliths to these rocks were deposited in the proximal regions of submarine fans.

The Wankanki Supersuite

Granites of the Wankanki Supersuite are typically strongly deformed and have been metamorphosed up to granulite facies (Figure 4.9). Migmatisation in the most leucocratic granites of the Wankanki Supersuite is locally conspicuous (Figure 4.9). In lower strain zones, the granites are typically porphyritic granodiorites and monzogranites, containing up to 15% (?primary) clinopyroxene and orthopyroxene, and late (?retrograde) hornblende.

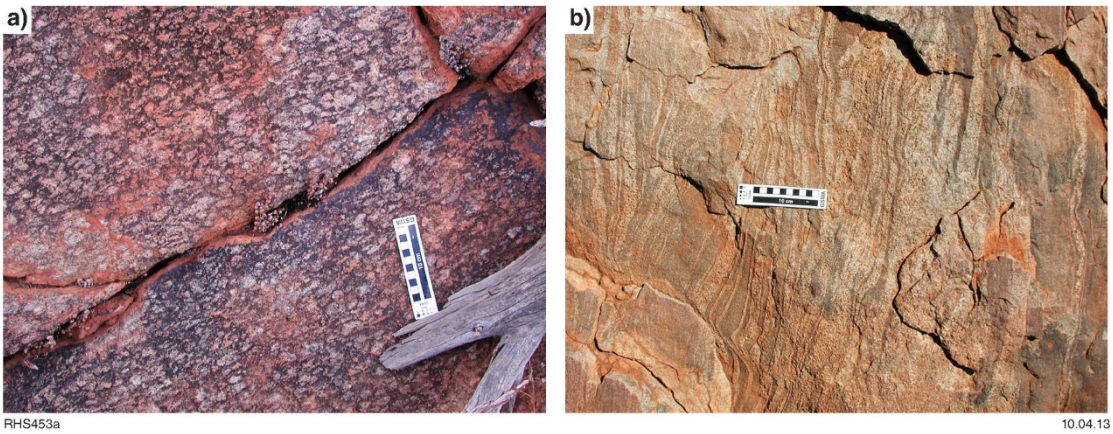

Figure 4.9 *Outcrop photographs of granite and gneiss of the Wankanki Supersuite a) weakly foliated porphyritic monzogranite; b) leucosome-rich gneiss.*

The granites are metaluminous, calc-alkaline, I-type rocks. On tectonic discrimination diagrams (e.g. Pearce et al., 1984), they consistently fall within the field for volcanic-arc granites, and in this respect they differ from all other granites in the west Musgrave Province. For both neodymium- and hafnium-isotope data, calculated T_{DM} model ages (DM= depleted mantle) for the Wankanki Supersuite lie between c. 2000 Ma and c. 1900 Ma, up to 700 Myr older than the crystallisation age (Figure 4.10; Smithies et al., 2010). This suggests a source component with considerable (>700 Myr) crustal residence time. If these rocks are indeed arc-related, then these isotope data suggest a continental-, rather than oceanic- or island-arc.

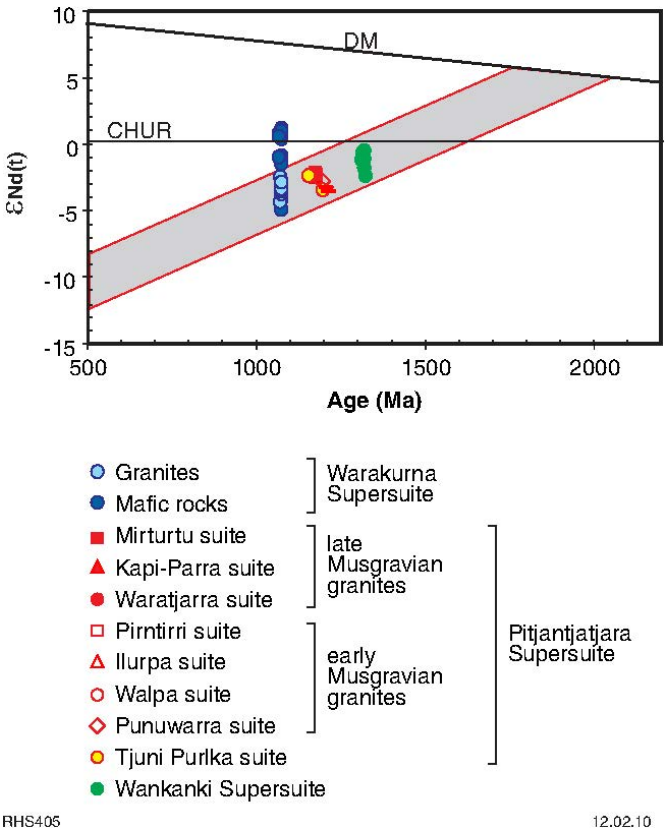

Figure 4.10 *εNd evolution diagram for rocks of the Wankanki, Pitjantjatjara and Warakurna Supersuites.*

The Wankanki Supersuite may reflect the final stage in the Proterozoic amalgamation (at least by lateral accretion) of central Australia (Giles et al., 2004; Betts and Giles, 2006; Smithies et al., 2010), ending before the main onset of the Musgrave Orogeny, with a collisional event that produced regional northeast-trending folds. Several studies suggest that the evolution of the Albany–Fraser Orogen to the southwest involved the convergence, collision, and suturing of the West Australian Craton with the southern Mawson Craton, along a southeast-dipping subduction zone between c. 1345 Ma and c. 1290 Ma (e.g. Clark et al., 2000; Bodorkos and Clark, 2004; Cawood and Korsch, 2008). For the Wankanki Supersuite, subduction-like geochemistry and moderately juvenile isotope compositions (Figure 4.10) favour a subduction setting. However, a south-dipping slab, as proposed for the Albany–Fraser Orogen, is difficult to accommodate with the Mount West Orogeny if, as suggested by neodymium- and hafnium-isotope compositions, granites in both the Wankanki Supersuite and the Pitjantjatjara Supersuite share a common crustal source component (Smithies et al., 2010, 2011). If the Wankanki granites are arc-related, then a north-dipping slab is required. In this scenario, the Tjuni Purlka Tectonic Zone may have been initiated during the Mount West Orogeny as an incipient backarc rift. Indeed, a recent reinterpretation of the tectonic evolution of the Albany–Fraser Orogen also favours subduction, with a northwest-dipping slab, during the event (Stage 1) temporally equivalent to the Mount West Orogeny (Kirkland et al., 2011d).

Unnamed and undated deformation events

In the southwestern part of the Mamutjarra Zone (BLACKSTONE and COOPER), in the area around, and immediately east and southeast of, Borrows Hill, the gneissosity developed in rocks of the Wirku Metamorphics and the Wankanki Supersuite is folded about kilometre-scale folds with a northeast-trending axial plane. Granite of the Pitjantjatjara Supersuite locally forms thin, northeast-trending dykes (mostly too small to show at map scale), axial planar to these large-scale folds, and which cut the gneissosity (Figure 4.11). Two of these granites have been dated: GSWA 184146, with a crystallisation age of 1201 ± 6 Ma (Kirkland et al., 2009b), and GSWA 185610, with a crystallisation age of 1199 ± 5 Ma (Kirkland et al., 2009c). These are the oldest manifestations of the Pitjantjatjara Supersuite in this region. The granite dykes do not show an axial-planar fabric, suggesting that the folding predates intrusion of granites into axial planar fractures, and occurred prior to c. 1201 Ma. These granites (Mamut suite of Smithies et al., 2010) have compositions that are very highly depleted in ytterbium and other heavy rare-earth elements compared with all other granites of the Pitjantjatjara Supersuite. An exception is the granites of the Pirntirri suite, from the Tjuni Purlka Tectonic Zone (Smithies et al., 2010), which, like those of the Mamut suite, are the oldest local manifestation of the Pitjantjatjara Supersuite. Two samples from the Pirntirri suite yielded crystallisation ages of 1217 ± 12 Ma (GSWA 187166, Kirkland et al., in prep.) and 1205 ± 6 Ma (GSWA 187274, Kirkland et al., 2009d).

In both regions, all younger granites of the Pitjantjatjara Supersuite are ytterbium-enriched, and Smithies et al. (2010, 2011) relates this to a change from a garnet-present to a garnet-free crustal source region, most likely reflecting removal, or significant thinning, of the lower crust from c. 1220 Ma (beneath the Walpa Pulka Zone) to c. 1200 Ma (beneath the Mamutjarra Zone). The presence of unfoliated ytterbium-depleted granites cutting regional folds indicates that the crustal thinning event beneath the Mamutjarra Zone was either synchronous with the latest stages of, or post-dated, the pre-c. 1201 Ma compressional deformation described above. However, the timing of the pre- c. 1201 Ma compressional deformation with respect to the thinning event beneath the Walpa Pulka Zone remains unclear. The interpretation preferred here is that this sequence of events reflects large-scale northwest–southeast compression followed by crustal thinning, between the end of the Mount West Orogeny and the beginning of the Musgrave Orogeny. Even if this is the case, it is highly likely that this

is an oversimplification of pre- Musgrave Orogeny events. In the Mount Aloysius region (BELL ROCK) for example, layering within rocks of the Wirku Metamorphics shows evidence for at least two phases of folding prior to the intrusion of granites related to the early stages of the Musgrave Orogeny.

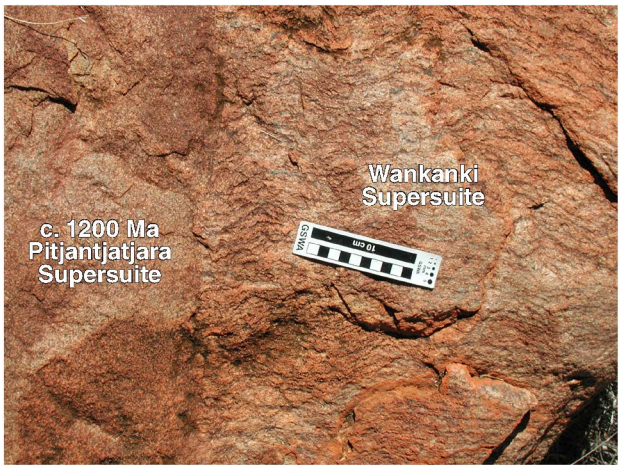

Figure 4.11 *Outcrop photograph of the contact between an unfoliated northeast-trending granite dyke of the Pitjantjatjara Supersuite, and a strongly foliated gneissic granite of the Wankanki Supersuite.*

The 1220–1150 Ma Musgrave Orogeny and the Pitjantjatjara Supersuite

The dominant northwest structural trend of the west Musgrave Province reflects a crustal architecture established during or before the Musgrave Orogeny, what was subsequently locally modified and reactivated during the Musgrave Orogeny, Giles Event, and Petermann Orogeny. The Musgrave Orogeny is the oldest orogenic event to have clearly affected all areas of the west Musgrave Province, and involved intense deformation and widespread granulite-facies crustal reworking. Edgoose et al. (2004) placed the orogeny between c. 1200 Ma and c. 1160 Ma, and grouped syn- to post-tectonic granite magmas into the Pitjantjatjara Supersuite. Geochronological studies during the west Musgrave Province mapping project have extended this range from c. 1220 Ma to c. 1120 Ma (Figures 4.4 and 4.5; e.g. Kirkland et al., 2010b).

Most rocks of the Pitjantjatjara Supersuite have been metamorphosed under granulite-facies conditions, in some cases as a result of thermal events late in the Musgrave Orogeny, but also during the 1085–1040 Ma Giles Event (Clarke et al., 1995b). In addition, parts of the region were deeply buried beneath Neoproterozoic sedimentary basins, and rapid, differential uplift of the Walpa Pulka Zone during the c. 580 Ma to c. 530 Ma Petermann Orogeny has exposed metamorphic assemblages reflecting pressures as high as 10 kbar to 14 kbar (Scrimgeour and Close, 1999). The metamorphosed granites of the Pitjantjatjara Supersuite range from statically recrystallised and unfoliated, to strongly foliated and mylonitised (Figure 4.12). Whereas the primary mineralogy of these granites was essentially anhydrous (quartz, plagioclase, K-feldspar, orthopyroxene, clinopyroxene, biotite), retrograde recrystallisation is locally directly associated with foliation development, resulting in partial to near-complete alteration of pyroxene to hornblende, actinolite, and biotite.

A compilation of SHRIMP U–Pb dates on zircons from >100 samples (see Smithies et al., 2010) includes ages interpreted to reflect crystallisation of granite magmas, as well as ages interpreted to reflect growth during metamorphism. The oldest Musgravian granite identified so far is dated at

1219 ± 12 Ma (GSWA 174737, Bodorkos et al., 2008). The youngest granite is dated at 1149 ± 10 Ma (GSWA 194376, Kirkland et al., 2010c).

There is a broad northeast to southwest trend in the crystallisation ages of Pitjantjatjara Supersuite granites. However, only Musgravian granites younger than c. 1190 Ma occur to the northeast of the Fanny Fault. To the southwest of the Fanny Fault, crystallisation ages decrease from c. 1220 Ma in the northeast to c. 1155 Ma in the southwest (Mamutjarra Zone). This trend in crystallisation age reflects a migration of the locus of melting, the locus of intrusion, or both.

There is also a clear antithetic relationship in the relative geographical distribution of granites of the Pitjantjatjara and Wankanki Supersuites (Figure 4.3), with granites of the Pitjantjatjara Supersuite dominating in the northeast (to the total exclusion of granites of the Wankanki Supersuite in the Walpa Pulka Zone) and granites of the Wankanki Supersuite dominating in the southwest.

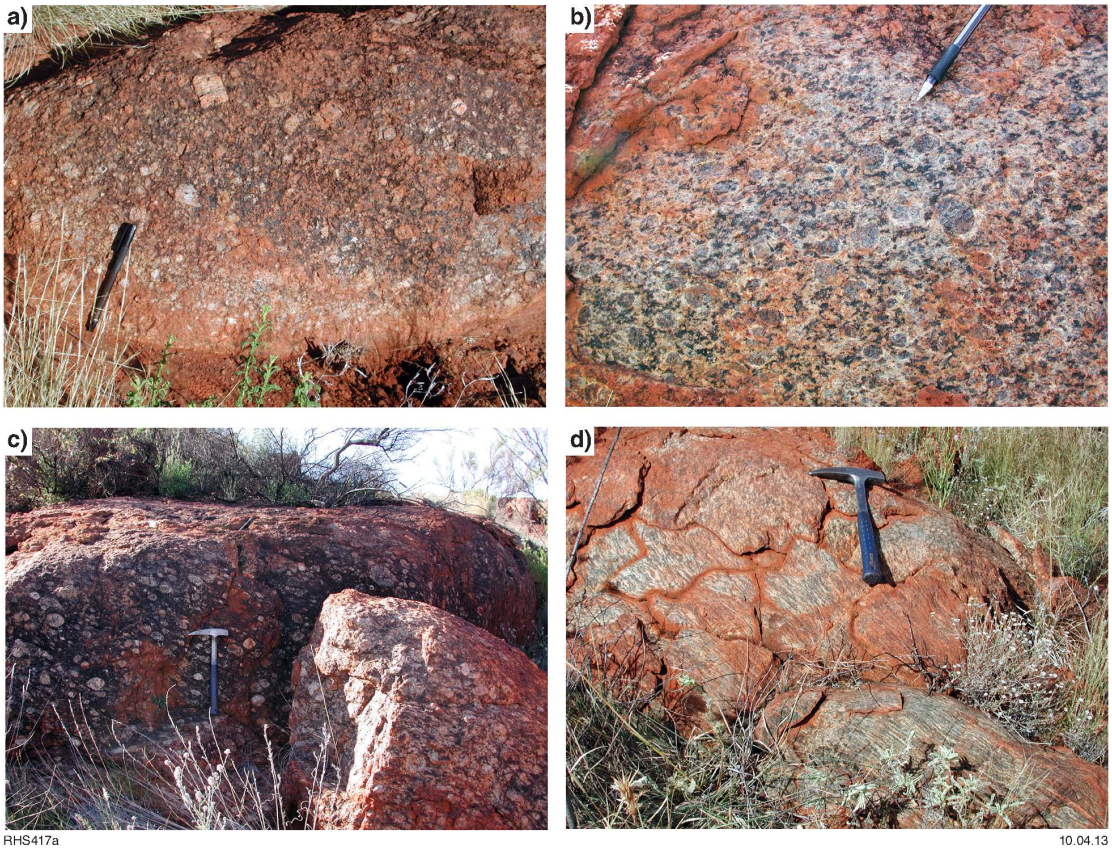

Figure 4.12 *Various textural manifestations of the Pitjantjatjara Supersuite: a) massive and seriate textured; b) massive, with large rapakivi-textured feldspar; c) weakly foliated, with large rapakivi-textured feldspar; d) mylonitic.*

Metamorphic conditions during the Musgrave Orogeny

In the Walpa Pulka Zone, metamorphic assemblages in the pelitic gneisses intruded by granites of the Pitjantjatjara Supersuite have been overprinted by high-pressure granulite assemblages and this region was exhumed during the Petermann Orogeny. However, pelitic rocks located sufficiently south of areas significantly affected by Petermann Orogeny metamorphism (e.g. Mamutjarra Zone and much of the southwestern portion of the Tjuni Purlka Tectonic Zone) preserve mineral assemblages that

reflect pressure–temperature (P–T) conditions achieved during the Musgrave Orogeny (e.g. King, 2009; Kelsey et al., 2009). In the southeastern parts of the Tjuni Purlka Tectonic Zone and west of the Mamutjarra Zone, King (2009) and Kelsey et al. (2009; also D. Kelsey, written comm., 2010) established that metapelites with the coarse-grained peak mineral assemblage of garnet–sillimanite–spinel–quartz equilibrated at conditions of ≥1000°C and 7–8 kbar at several stages between 1220 and 1150 Ma. Such conditions reflect ultra-high temperature (UHT) metamorphism, the most thermally extreme type of crustal metamorphism, characterised by temperatures >900°C (Harley, 1998; Kelsey et al., 2004; Kelsey, 2008) and an average geothermal gradient >20°C/km (Brown, 2007). In the case of the west Musgrave Province, the P–T estimates define an apparent average geothermal gradient in excess of 40°C/km.

Patterns of lead diffusion in dated zircon crystals also indicate that UHT metamorphic conditions occurred at the present level of exposure during several events throughout the Musgrave Orogeny, at least until c. 1119 ± 7 Ma (Kirkland et al., 2010d; Kelsey et al., 2009; Smithies et al., 2010).

This ~100 m.y. history of UHT metamorphism, including more or less continuous high-temperature charnockitic magmatism, chronicles an extremely unusual tectonothermal regime, almost certainly involving extensive crust–mantle interaction.

Tectonic setting of the Musgrave Orogeny

There is debate over the timing of final amalgamation of the North, South, and West Australian cratons (e.g. Li, 2000; Giles et al., 2004; Betts and Giles, 2006; Wade et al., 2006, 2008; Cawood and Korsch, 2008), although most models of Australian continental amalgamation have the major cratonic components in place by at least c. 1290 Ma (e.g. Cawood and Korsch, 2008). This means that during the Musgrave Orogeny, a large portion (possibly as much as 60 000 km^2) of central Australia, overlying the point where the cratonic elements of the continent join, was subjected to unusually high heat flow for up to 100 million years.

Taylor et al. (2010) reviewed various models proposed to explain regional episodes of low- to medium-pressure, high-temperature metamorphism, typically with isobaric cooling paths, similar to that prevailing during the Musgrave Orogeny. Common to these models is a substantial amount of advective mantle heat, and significant crustal thinning and extension. Currie and Hyndmann (2006) and Kelsey (2008) suggested that one possible setting for UHT metamorphism is in the thin, weak crust of back-arc basins, and Brown (2006) noted that many Ediacaran–Cambrian-age UHT belts resemble inverted and thickened back-arc basins.

Although a compressional regime may have existed locally, or at some stages, during the Musgrave Orogeny (e.g. Aitken and Betts, 2008), the evidence from the west Musgrave Province is that the major northeasterly folding pre-dates the main stage of the Musgrave Orogeny, that the onset of UHT metamorphism coincided with significant thinning of the lower crust, and that this thin crust was sustained throughout the orogeny. The Musgrave Orogeny appears more compatible with an intracratonic extensional regime (e.g. Wade et al., 2006, 2008), in terms of both sustained UHT conditions and granite geochemistry.

The 1085–1040 Ma Giles Event, Warakurna Supersuite and Ngaanyatjarra Rift

Regional tectonic overview

The volcanic rocks of the Bentley Supergroup (Figure 4.6) formed during the Mesoproterozoic Giles Event. Mafic magmatic elements of this event, known collectively as the Warakurna Supersuite, are recognised in outcrop as dolerite dykes and sills across approximately 1.5 million km2 of central and Western Australia (Figure 4.13). This craton-scale mafic magmatism appears to be restricted in age to c. 1078–1073 Ma, providing a basis for grouping the igneous rocks into a Large Igneous Province – the Warakurna Large Igneous Province (Wingate et al., 2004; Morris and Pirajno, 2005). In the Musgrave region, and in the area around Bloods Range (Tjauwata Group), in the Northern Territory (Figure 4.2), extensive intrusion and extrusion of voluminous mafic magmas also occurred at c. 1075 Ma. However, in these regions, it was contemporaneous with felsic magmatism and voluminous mafic and felsic magmatism occurred, more or less continuously, for at least 10 Ma before and 35 Ma after the craton-scale c. 1075 Ma event. Thus, the Warakurna Large Igneous Province should be regarded simply as a component of the Giles Event, rather than the expression of it, and the Warakurna Supersuite is the magmatic expression of the entire c. 1085 Ma to 1040 Ma magmatic history of the Giles Event. In the west Musgrave Province, the Warakurna Supersuite incorporates more than 10 geochemically and chronologically distinct phases of mafic magmatism and 25 phases of felsic magmatism.

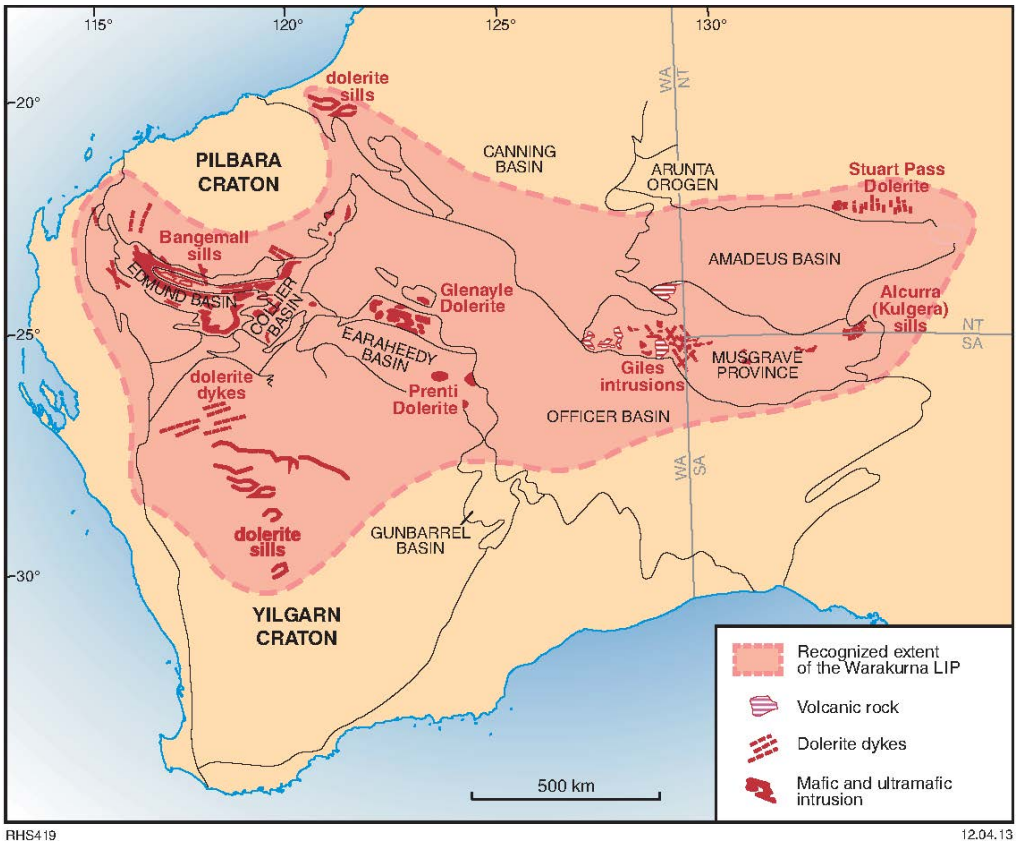

Figure 4.13 *Map of central and western Australia showing the regional extent of extrusive and intrusive rocks attributed to the Warakurna Large Igneous Province (modified from Wingate et al., 2004).*

The Giles Event has been interpreted as the result of a single mantle plume (Wingate et al., 2004; Morris and Pirajno, 2005; Godel et al., 2011), but the c. 45 Ma (minimum) duration of mantle-derived igneous activity suggests the event reflects a more complex geodynamic setting. According to Evins et al. (2010), the magmatic and structural history of the Giles Event in the Musgrave region chronicles the formation and evolution of a long-lived, failed intracontinental rift which they refer to as the Ngaanyatjarra Rift.

The Bentley Basin (Figure 4.6) represents the extent of the volcano-sedimentary fill of the Ngaanyatjarra Rift. These volcano-sedimentary rocks (including siliciclastic and minor calcareous sediments) form the Bentley Supergroup, which includes the Tjauwata Group in the Bloods Range area of the Northern Territory (e.g. Edgoose et al., 2004). In the west Musgrave Province, the Bentley Basin can be subdivided into at least two rhyolite-dominated sub-basins (Figure 4.14); the larger Talbot Sub-basin, in the area west of the Jameson Community, and the smaller Blackstone Sub-basin, in the area south of the Blackstone Community. A third, poorly defined sub-basin, the Finlayson Sub-basin, lies to the north of Blackstone and Jameson Communities. In addition, recent mapping has now identified the basal components of the Bentley Supergroup — the Kunmarnara Group — overlying the northern parts of the west Musgrave Province (Mitika area, Figure 4.6), possibly linking the Talbot Sub-basin and the Bloods Range area of southern Northern Territory and the immediately adjacent parts of Western Australia as a single continuous depositional basin. To the east, components of the Kunmarnara Group are exposed at Skirmish Hill (Figure 4.6), and are interpreted to extend into the westernmost parts of South Australia. Based on these occurrences, the minimum original extent of the Bentley Basin was approximately 50,000 km^2.

Geological history of the Ngaanyatjarra Rift

Kunmarnara Group

In the Musgrave region, the earliest preserved lithological manifestation of the Giles Event was deposition of a succession of quartz sandstones, pebbly sandstones and conglomerates (MacDougall Formation), basalts (Mummawarrawarra Basalt), and minor felsic volcanic rocks, forming the Kunmarnara Group (Figure 4.6). The equivalent units of the Tjauwata Group include the Karukali Quartzite and the Mount Harris Basalt (Edgoose et al., 2004). These are the basal units of the Bentley Supergroup (Howard et al., 2011a; Evins et al., 2010) and have been interpreted to represent the basal succession to the Ngaanyatjarra Rift (Evins et al., 2010). There are no direct maximum age constraints on deposition, other than the minimum age constraint on high-grade metamorphism related to the Musgrave Orogeny, at c. 1120 Ma. Minimum depositional age constraints are based on the crystallisation ages of the oldest igneous rocks to intrude the Kunmarnara Group - c. 1090 Ma in the Bloods Range (Edgoose et al., 2004) and c. 1078 Ma in the west Musgrave Province (Sun et al., 1996; Howard et al., 2011b).

Giles layered ultramafic-mafic intrusions (G1)

The next recognisable event was emplacement of the layered mafic-ultramafic Giles intrusions (G1). These dominate outcrop in the Musgrave region, forming the elevated west-northwest-trending spine, and were intruded mainly along, or near, the bounding faults separating the various major lithotectonic zones of the Musgrave Province basement (Figure 4.6). Troctolite, gabbronorite, and gabbro dominate. Ultramafic units also occur, but are cumulate rocks related to mafic, rather than ultramafic, magmas. The layered bodies (Figure 4.15) reach a maximum cumulative thickness of ~10 km in the Jameson area, and the present outcrop extent clearly understates the original size of some intrusions.

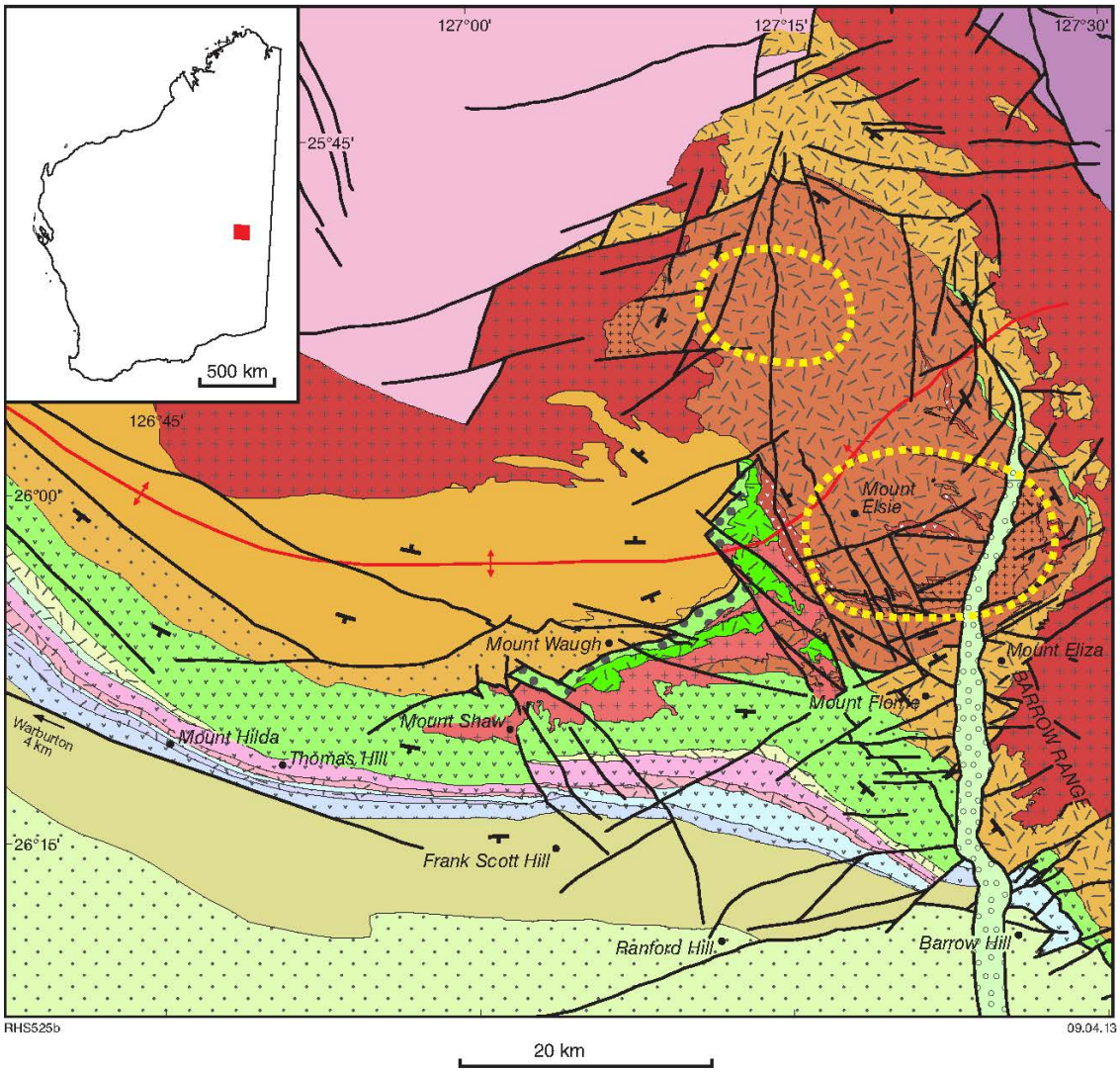

Figure 4.14 *Interpreted bedrock geology of the Talbot Sub-basin.*

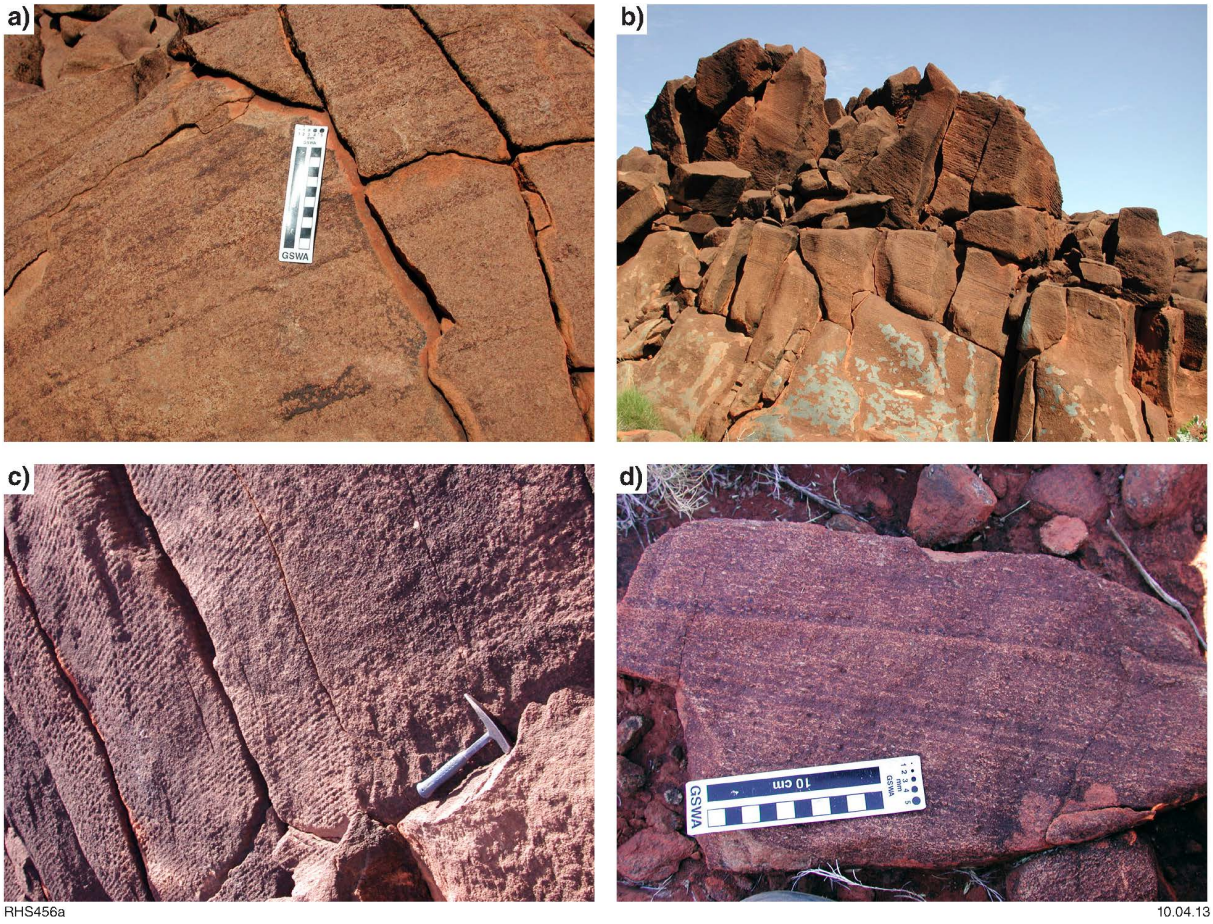

Figure 4.15 *Outcrop photographs showing various types of compositional and mineralogical layering within the Giles intrusions (G1): a) distinct mineralogical banding in gabbronorite (BELL ROCK intrusion – BELL ROCK); b) fine-scale banding overlying more massive layers in olivine gabbronorite (northeast HOLT); c) close-up of fine-scale banding in olivine gabbronorite (northeast HOLT); d) irregular mineralogical layering in olivine gabbronorite (Cavenagh intrusion – BLACKSTONE).*

It is very likely that the major troctolitic Bell Rock, Blackstone, and Jameson–Finlay Giles intrusions are tectonically dislocated parts of a single intrusion. If this is the case, then this intrusion could have originally been greater than 170 km long, 25 km wide, and up to 10 km thick, making it one of the largest known mafic magma chambers on Earth. Preserved county-rock inclusions and contacts indicate that the Giles intrusions in the west Musgrave region were emplaced at the stratigraphic level of the Mummawarrawarra Basalt (Kunmarnara Group). The low metamorphic grade (greenschist facies) of the basalts indicates an upper crustal and extensional environment for intrusion. Constraints on the crystallisation age of the Giles intrusions are the minimum depositional age of the Kunmarnara Group and a direct U–Pb zircon age of 1076 ± 4 Ma (Kirkland et al., 2011b) on a layered Giles intrusion gabbro (GSWA 194762).

To the north of the Jameson and Blackstone G1 intrusions, remnants of Kunmarnara Group are preserved (Figure 4.6), unconformably overlying high-grade basement rocks of the Wirku Metamorphics and the Wankanki and Pitjantjatjara Supersuites. These remnants of the Kunmarnara Group form the poorly defined Finlayson Sub-basin of the Bentley Basin. Immediately northeast of the Jameson G1 intrusion, andesite and dacite overlie Mummawarrawarra Basalt. Reconstructions indicate a northeast-up sense of movement along the northern margins of the Jameson–Blackstone–Bell Rock G1 intrusion (Evins et al., 2010), and so this andesitic and dacitic volcanism represents a lower stratigraphic level

than the emplacement level of the G1 intrusions, pre-dates the Smoke Hill Volcanics in the Blackstone Sub-basin, and likely also forms a component of the Kunmarnara Group itself.

Massive gabbro and leucogranite (G2)

Primarily in the eastern part of the west Musgrave region (Figure 4.6), massive gabbro (G2) cuts the layered Giles intrusions and typically shows abundant and widespread evidence of co-mingling with leucogranitic magmas (Figure 4.16). The leucogranite intruded as dykes and also forms larger pluton-scale bodies in basement rocks (e.g. South Hill, Tollu pluton). The leucogranite typically included clinopyroxene-, hornblende-, and biotite-bearing, equigranular to porphyritic quartz syenites, syenogranites, and lesser monzogranites, and locally shows well-developed rapakivi textures. This bimodal magmatism was also accompanied by deformation (shearing and west-northwest folding adjacent to major shear zones) and age constraints on magmatism and deformation lie between 1078 ± 3 Ma and 1074 ± 3 Ma (Howard et al., 2011b). These age constraints are virtually identical to those for the layered Giles (G1) intrusions but where temporal field relationships can be established, G2 intrusions are always younger than G1.

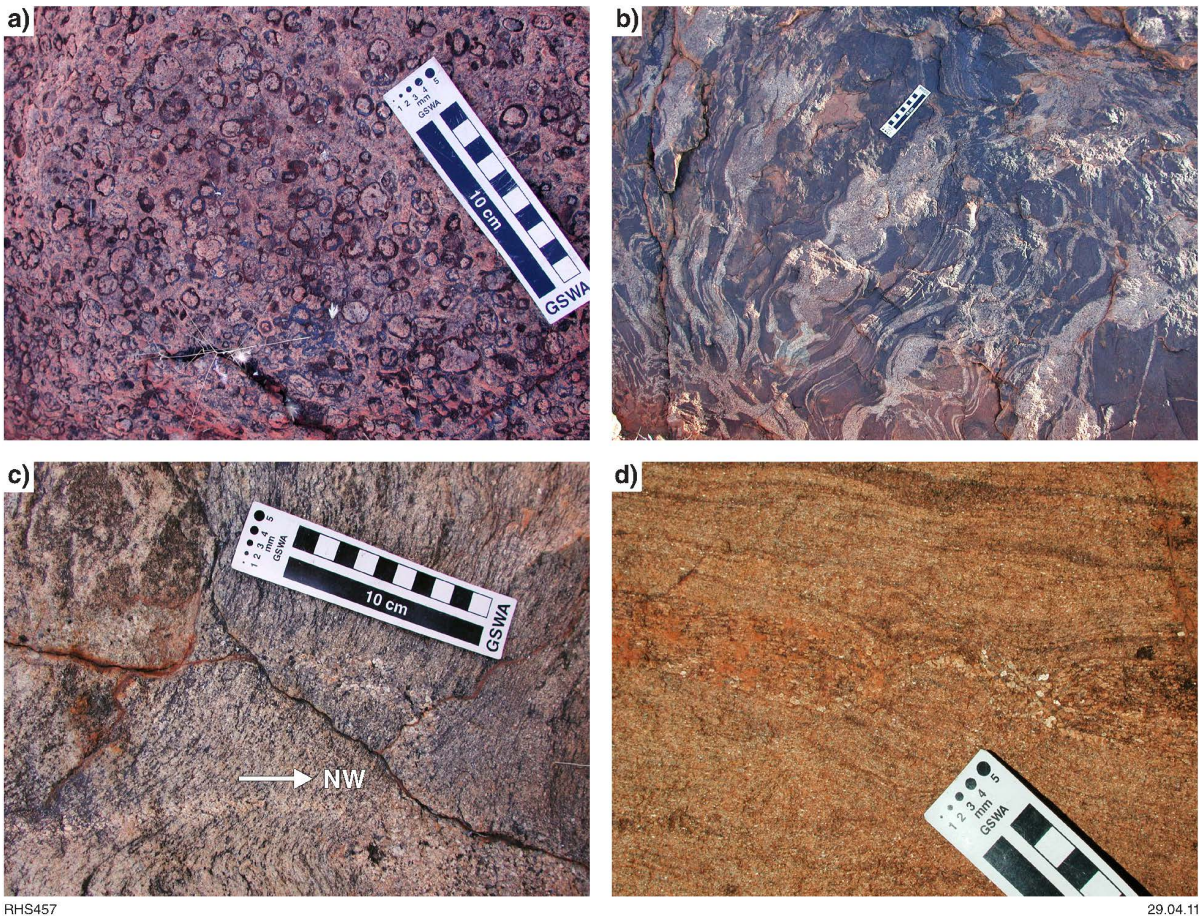

Figure 4.16 *Outcrop photographs showing general features associated with massive gabbro and leucogranite intrusions (G2) of the Warakurna Supersuite: a) rapakivi-textured leucogranite (northeast HOLT); b) ductile deformation associated with intrusion of partially to largely solidified gabbro by leucogranite magma (northern BELL ROCK); c) strongly foliated leucogranite cut by veins of leucogranite in fractures that are axial planar to northwest-trending folds (northern BELL ROCK); d) leucogranite migrated into boudin necks during syn-magmatic deformation (northern BELL ROCK).*

Tollu Group (Blackstone Sub-basin)

South of Blackstone community, in the Blackstone Sub-basin (Figure 4.6), rhyolites of the Smoke Hill Volcanics (Tollu Group) directly overlie the layered G1 Blackstone intrusion without an obvious intervening fault. Crystallisation, or depositional, ages of the rhyolites: 1071 ± 8 Ma (GSWA 191728, Coleman, 2009); 1073 ± 7 Ma (GSWA 191706, Coleman, 2009) and 1073 ± 8 Ma (GSWA 189561, Kirkland et al., in prep.) are within analytical error of the emplacement age range of the G1 and G2 intrusions, and rhyolite compositions strongly resemble those of leucogranites associated with G2 intrusions. This requires the extensive and rapid uplift, erosion and exhumation of the layered Giles G1 intrusions, immediately followed by felsic volcanism.

Evidence from U–Pb zircon dating (presented later) suggests that felsic volcanism in the Talbot Sub-basin commenced prior to emplacement of the layered Giles intrusions, possibly prior to c. 1080 Ma. However, the stratigraphically lower volcano-sedimentary rocks were also intruded by the syn-volcanic (and subvolcanic) Winburn Granite (Figure 4.14) and the preserved stratigraphic base now comprises younger rhyolites erupted at c. 1070 Ma. The Talbot Sub-basin possibly represents a silicic large igneous province in its own right, and it contains the Kaarnka caldera, or caldera cluster (Figure 4.14), related to the development of one or more supervolcanoes. The layered G1 Jameson intrusion is now in faulted contact with the volcano-sedimentary rocks of the Talbot Sub-basin and the Winburn Granite.

Alcurra Dolerite

A series of dolerite dykes in Western Australia are contemporaneous with, and compositionally similar to, the Alcurra Dolerite in the Northern Territory and have collectively been assigned to the Warakurna Large Igneous Province (Wingate et al., 2004). In the northern part of the west Musgrave Province, these dykes have a distinctive ophitic texture with pyroxene oikocrysts up to several centimetres in diameter, and are commonly oriented east-southeast. In the Jameson area, they form northeast-trending plagioclase-phyric dykes and to the north of Warburton they again trend to the east-southeast. In the Blackstone Sub-basin, iron-rich olivine gabbros, olivine norites, ferronorites, and ferrodiorites compositionally equivalent to Alcurra Dolerites (Howard et al., 2009), have intruded the Smoke Hill Volcanics. They also intruded along the margins of layered Giles intrusions, and locally host significant orthomagmatic nickel–copper mineralisation (Nebo–Babel; Seat, 2008; Figure 4.6). The gabbros have been dated at 1068 ± 4 Ma (Nebo–Babel; Seat, 2008) and 1067 ± 8 Ma (GSWA 194354; Kirkland et al., 2009e). In the Blackstone Sub-basin (Figure 4.6), the primitive (andesitic) end-members of the Hogarth Formation, which overly the Smoke Hill Volcanics, are also compositionally identical to dolerites and ferrogabbros of the Alcurra Dolerite and have an identical crystallisation age of 1068 ± 7 Ma (GSWA 185518; Kirkland et al., in prep.). These are the youngest rocks preserved in the Blackstone Sub-basin.

Basalt compositionally similar to the Alcurra Dolerite is interleaved with rhyolite throughout the lower and middle stratigraphic regions of the Talbot Sub-basin. It is mainly in the region of this sub-basin that the younger stratigraphic history of the Bentley Basin and of the Ngaanyatjarra Rift is preserved. The stratigraphy of this sub-basin was revised by Howard et al. (2011a) as a result of recent detailed mapping and the following geological and lithological descriptions are largely a result of that work.

Talbot Sub-basin

The Talbot Sub-basin contains the largest exposure of rocks of the Bentley Supergroup (Figure 4.6). These rocks show evidence for local weak, open, upright folding about east-southeast-trending axes

and an associated axial-planar fracture cleavage is locally strongly developed. Deformation is also locally intense in proximity to faults and shears, but apart from these occurrences, rocks of the Talbot Sub-basin are typically undeformed. Adjacent to the Winburn Granite, the metamorphic grade was high enough to coarsen rhyolites into a fine- to medium-grained granofelsic texture, and in the Scamp area (Figure 4.6), burial of lower stratigraphic levels resulted in lower amphibolite facies metamorphism. Elsewhere, the rocks are typically preserved at greenschist facies.

Our current stratigraphic interpretation of the Talbot Sub-basin does not recognise the Scamp caldera previously suggested by Daniels (1974) and requires modification to the extent of the postulated caldera in the Palgrave region (the Kaarnka caldera; Smithies et al., 2013). The preserved stratigraphic base of the Talbot Sub-basin is represented by the effusive and ignimbritic rocks of the Mount Palgrave Group and the overlying, dominantly ignimbritic rocks of the Kaarnka Group. Outcrop of the Kaarnka Group is almost entirely restricted to a discrete north-northwest-trending, oval basin, up to 27 km wide and 46 km long (Figure 4.14). Whereas this basin is interpreted here to define the extent of the Kaarnka caldera structure, this structure only partly corresponds to the caldera structure suggested by Daniels (1974). Rocks in the Scamp area are all assigned to the Mount Palgrave Group. Depositional layering within the Mount Palgrave Group generally dips shallowly (≤30º) between south (in the northern part of the sub-basin) and west (in the eastern part of the sub-basin), but is locally steeply (up to 85º) dipping adjacent to the Barrow Range anticline (see below), and elsewhere adjacent to the Winburn Granite. Nowhere is the stratigraphy overturned. The thickest preserved section of the Mount Palgrave Group is probably in the northeastern part of the Talbot Sub-basin, where up to 4500 m of volcanic stratigraphy is preserved.

In the southwestern parts of the Talbot Sub-basin, rocks of the Pussy Cat Group directly overlie the Mount Palgrave and Kaarnka Groups, and are in turn overlain by rocks of the Cassidy Group. Both the Pussy Cat and Kaarnka Groups comprise bimodal volcanic rocks and less common sedimentary units, that dip shallowly (≤30º) to the south and southwest, and form continuous packages that can be traced for over 100 km. The Cassidy Group, in particular, comprises four major mafic-felsic volcanic cycles (Figure 4.14) with a combined thickness of over 3400 m.

Both the size (extent and volume) and facies association of volcanic rocks within the Mount Palgrave, Kaarnka and Cassidy Groups (i.e. the lower Talbot Sub-basin stratigraphy) are very unusual. Many felsic volcanic units of these stratigraphic groups have volumes that reflect ‘super volcano’ class eruptions (≥450 km^3; e.g. Sparks et al., 2005). Magma compositions are water-poor but F-, alkali- and FeO-rich, and reflect very high eruptive temperatures (>900°C), as confirmed by Zr-saturation thermometry (Smithies et al., 2013). These high eruption temperatures are manifested in outcrop by very well developed and continuous flow-banding (in highly felsic rocks), including extensive evidence for rheomorphism, and high-temperature contact metamorphic assemblages in interflow sedimentary units. In terms of eruptive temperature, magma compositions and volcanic textures, the Talbot Sub-basin volcanic rocks show facies characteristics of large-scale Snake River (SR)-type volcanism described by Branney et al. (2008).

The Mission Group conformably overlies the Cassidy Group, and represents the youngest preserved stratigraphic interval of the Bentley Supergroup. It can be divided into a sedimentary lower part (Gamminah Conglomerate, Frank Scott Formation, and Lilian Formation), and an upper basalt-dominated part (Milesia Formation). No evidence of felsic volcanism has yet been found. The Mission Group is conformably to unconformably overlain by the Townsend Quartzite. Daniels (1974) reported a total thickness for the Mission Group of about 4000 m.

The thickest preserved continuous stratigraphic column of the Bentley Supergroup within the Talbot Sub-basin (taken in a north-south direction in the region of Mount Waugh) is approximately 12 km. However, the combined maximum stratigraphic thickness of individual units is estimated at about 18.6 km, although this is never achieved in any given region. Of this, basaltic magmas represent approximately 3.7 km, and felsic magmas represent approximately 9 km, giving a total preserved maximum thickness of igneous stratigraphy of approximately 12.7 km.

Along the exposed eastern and northern margins of the Talbot Sub-basin, various phases of the Winburn Granite either intrude, or are overlain by, generally west- to south-dipping rhyolitic lavas, and subvolcanic intrusive and pyroclastic rocks of the Mount Palgrave Group (Figure 4.14). Thus, the Winburn Granite forms a regionally extensive composite subvolcanic sheet close to the base of the Talbot Sub-basin. The exposed contact relationships between the granites and the volcanics indicate active uplift and erosion.

In the area around Barrow Range, there is a large west-trending (west-closing) anticline (Barrow Range anticline, Figure 4.14), with volcanic units of the Mount Palgrave Group younging away from a core of Winburn Granite. An intense west-trending (080–110º) fracture cleavage is locally developed throughout this region. Although there is likely a tectonic component to the development of the Barrow Range anticline, it is also possible that synmagmatic doming of the Winburn Granite played a major role. Approximately 6 km to the north of Mount Florrie, porphyritic microgranite with a crystallisation age of 1055 ± 10 Ma (GSWA 187054, Kirkland et al., in prep.) has intruded along a west-trending fracture, and possibly places a minimum age on the development of the fracture cleavage related to the anticline. Because the preserved stratigraphic base of the Mount Palgrave Group was deposited at c. 1070 Ma, doming or folding is potentially synvolcanic, or immediately post-volcanic. This is consistent with the observation that the volcanic rocks in the Mount Florrie region appear to contain a higher proportion of stratigraphically constrained tectonic breccia (rather than autoclastic breccia) than is typical elsewhere in the Mount Palgrave Group, and may have been deposited on the flanks of an active volcanic dome.

However, the steeply-dipping northeast-trending limb of the Barrow Range anticline lies along the northeastern margin of a c. 30 km wide northwest-trending fault zone, referred to here as the Barrow Range–Cavenagh corridor (Figure 4.6). Thus, development of the anticline can also be attributed to dextral and south-side-up movement along the northwestern margin of this structural corridor. The timing of faulting has not been established. Although units in the mid to upper stratigraphic parts of the Bentley Supersuite (Glyde Formation and above) in the southwestern extension of the Barrow Range–Cavenagh corridor may also have been displaced, they do not appear to have been affected to the same extent as the rocks in the Barrow Range anticline. On this basis, we suggest that at least a component of deformation within the structural corridor occurred prior to deposition of the upper part of the Bentley Supergroup.

The Ngaanyatjarra Rift

An intracontinental setting is indicated for the Musgrave Province for at least 150 m.y. prior to the Giles Event, and this is a setting in which the rocks have remained until the present day (Smithies et al., 2009; Evins et al., 2010). The sequence of events encompassed by the Giles Event describes a long-lived, failed intracontinental rift, which we refer to as the Ngaanyatjarra Rift. Rifting began with deposition of the Kunmarnara Group — a typical intracontinental rift sequence of basal conglomerates and sandstones, followed by basalt flows (the Mummawarrawarra Basalt). The Kunmarnara Group traces the rift-basin boundaries. The rift basin widens to 70 km in the west, where the Kunmarnara Group splits into a northern arm that trends northwest across the FINLAYSON map sheet, and a

southern arm that trends southwest across the COOPER sheet (Figure 4.2). The northern basin margin is defined by a major set of faults that can be traced west from the Blackstone Community, then northwest for a distance of over 100 km (Figure 4.2). The southern basin margin follows the southern limb of the regional Blackstone syncline, and continues southwest to Mount Blyth where its basal contact is undeformed and well exposed.

Following deposition of the Kunmarnara Group, giant, layered mafic–ultramafic Giles intrusions were emplaced into the Mummawarrawarra Basalt. Emplacement of these sills represents an addition of ~10 km of dense material to the upper crust. The lack of high-pressure and high-temperature assemblages at the bottom of these sills suggests that their emplacement was likely accommodated by inflation and roof uplift. These events occurred sometime between c. 1078 Ma and c. 1075 Ma; however, mutual contacts invariably show that the c. 1075 Ma massive gabbro and co-mingled leucogranite intruded fully crystallised Giles intrusions (Smithies et al., 2009). Therefore, immediately after emplacement of layered mafic–ultramafic Giles intrusions, c. 1075 Ma magmatism in the west Musgrave Province may have been characterised by mafic and felsic magmas focused along coeval, linear, shear zones (parallel to the Tjuni Purlka Tectonic Zone and the northern rift boundary). This magmatism was concomitant with macroscopic, upright folding in a transpressional setting — events indicative of basin inversion (Evins et al., 2010).

According to Evins et al. (2010), deformation ceased abruptly after intrusion of the massive gabbro and co-mingled leucogranite. Magmatic activity in the rift was sporadic thereafter, with at least four pulses of dominantly felsic magmatism alternating with ~10 m.y. long quiescent periods until approximately 1040 Ma.

The Ngaanyatjarra Rift is similar in many respects to the Mid-Continental Rift in North America (Evins et al., 2010). Each rifts was distant from a continental margin during its lifetime and failed to open into an ocean basin. Each has an episodic and complicated magmatic history that begins with basalt flows (1109–1107 Ma for the Mid-Continental Rift), followed by emplacement of large, layered mafic–ultramafic intrusions (the 1102–1094 Ma Duluth, Sonju Lake, and other intrusions in the Mid-Continental Rift), and a period of waning volcanism (1094–1086 Ma for the Mid-Continental Rift; Hanson et al., 2004). The first two stages in the Mid-Continental Rift were accompanied by voluminous felsic volcanism (Green and Fitz, 1993; Vervoort et al., 2007), producing similar lithologies to those found in the Ngaanyatjarra Rift. However, the Mid-Continental Rift differs from the Ngaanyatjarra Rift in several ways. Firstly, major magmatism in the Mid-Continental Rift spans about 25 m.y. as opposed to greater than 40 m.y. for the Ngaanyatjarra Rift. Secondly, the Mid-Continental Rift is dominated by mafic volcanic flows (flood basalts) rather than the intrusions seen in the west Musgrave Province, although this may simply reflect a deeper exposure level in the Ngaanyatjarra Rift. Thirdly, the main stage of felsic magmatism occurs much later in the evolution of the Ngaanyatjarra Rift than in the Mid-Continental Rift. Finally, in the Mid-Continental Rift, there is no evidence of a major synmagmatic deformation event.

Mafic dykes younger than the Giles Event

Kullal Dyke Suite (c. 1000 Ma)

Dykes belonging to the c. 1000 Ma Kullal Dyke Suite (Figure 4.2) are fine-grained olivine– and plagioclase–porphyritic dolerites. They are mostly northeast-trending, and are most common in the Michael Hills and Hinckley Range regions. They crosscut the igneous layering of the ≥1078 Ma Giles intrusions, and are crosscut by the c. 825 Ma Gairdner Dolerite. A poorly constrained Sm–Nd mineral isochron age of 1000 Ma was obtained for one of the dykes (S-S. Sun, unpublished data; Glikson et al., 1996).

Gairdner Dolerite (c. 825 Ma)

Intrusions related to the Gairdner Dolerite are mostly northwest- to north-trending and extend from the Gawler Craton and Stuart Shelf to the Musgrave Province. One dyke in Western Australia yielded a zircon U–Pb age of 824 ± 4 Ma (Glikson et al., 1996), similar to the baddeleyite U–Pb age of 827 ± 6 Ma for a Gairdner dyke on the Stuart Shelf (Wingate et al., 1998). Amata Dolerite dykes, which are confined to the east Musgrave Province, have been linked to the Gairdner Dolerite on the basis of similar chemistry and age (Glikson et al., 1996) — one Amata Dolerite dyke sample yielded an imprecise Sm–Nd age of 790 ± 40 Ma (Zhao et al., 1994). The Gairdner Dolerite crosscuts the Kullal Dyke Suite and layered Giles intrusions (e.g. the Hinckley Range intrusion and Michael Hills intrusion).

Unnamed dykes (c. 750 Ma)

The youngest mafic dykes to intrude the Musgrave Province are a suite of unnamed LREE-depleted dykes. Their orientation varies from east-northeast to northwest. They are medium-grained, massive, ophitic- to subophitic-textured metagabbros that are characterised by distinctive depletions in incompatible trace elements, and by high ε_{Nd} values. A three-point Sm–Nd age determination has yielded a 747 ± 48 Ma isochron (GSWA, unpublished data), suggesting that the rocks are either part of the c. 800 Ma magmatic event that produced the Gairdner Dolerite and Amata Dolerite of South Australia (Zhao et al., 1994), or a slightly younger suite, possibly contemporaneous with the 755 Ma Mundine Well Dolerite Suite of northwestern Australia (Wingate and Giddings, 2000).

Additional felsic magmatic events (c. 1000 Ma and c. 625 Ma)

In addition to the felsic magmatic events outlined above, at least two younger periods of felsic magmatism affected the west Musgrave Province. A thin, southwest-trending, undeformed garnet-bearing aplite dyke cuts granites formed during the Musgrave Orogeny immediately to the east of Mount Fanny, and has been dated at 995 ± 8 Ma (GSWA 183597, Kirkland et al., in prep.). This age is similar to a c. 1000 Ma Sm–Nd isochron age determined on an olivine-bearing Kullal dyke from the Musgrave Province (Glikson et al., 1996).

A series of undeformed tourmaline-bearing pegmatites intruded massive gabbro in the Murray Range, and have been dated at 625 ± 11 Ma (GSWA 187175, Kirkland et al., 2011e). This igneous age broadly corresponds to the 650–611 Ma magmatic event within the Telfer region of the Paterson Orogeny, in northwestern Western Australia (Rowins et al., 1997).

Although both of these two felsic magmatic events appear to be rather inconsequential volumetrically, the significance of the tectonothermal event to which they relate is difficult to determine. It is likely that extensive dehydration resulting from several previous tectonothermal events had exhausted the capacity of the crust to produce voluminous anatectic melts under most realistic conditions.

Petermann Orogeny

Structural and metamorphic aspects of the Petermann Orogeny have been the subject of intense study over the past 15 years. Camacho and Fanning (1995) and Camacho et al. (1997, 2001, 2009) focused mainly on the Davenport Shear Zone (Northern Territory) and the timing of deformation. Lambeck and Burgess (1992) proposed that the area between the Woodroffe Thrust and Mann Fault represents a flower structure. Recently, Raimondo et al. (2009, 2010) looked at the timing, metamorphism, and kinematics of the western portion of the Petermann Orogeny, and resolved apparently paradoxical shear-senses indicators. Scrimgeour and Close (1999) presented detailed work on the high-pressure assemblages associated with the core of the orogen.

Deformation during the Petermann Orogeny was focused along the northern margin of the Musgrave Province as east-trending shear zones that dissect the deep crust, and divide the province into two main domains characterised by different structural styles and metamorphic grades (Camacho, 1989; Major and Conor, 1993). The Mulga Park Zone north of the Woodroffe Thrust is characterised by amphibolite-facies metamorphism, and is structurally dominated by the Petermann Nappe Complex in the Northern Territory. The Fregon Zone between the Woodroffe Thrust and Mann Fault is considered the core of the Petermann Orogen. It is characterised by granulite-facies metamorphism and contains several important faults. From north to south these are the Woodroffe Thrust, Cockburn Shear Zone, Davenport Shear Zone, Mann Fault, Wingellina Fault, and Hinckley Fault (the latter three occurring in the west Musgrave Province). These shear zones were active over short time scales (up to 1.4 m.y.; Camacho et al., 2009). Of these shear zones, only the Woodroffe Thrust shows a reverse sense of movement.

Temperature and pressure estimates from rocks in the Fregon Zone reach 700–800°C and 13–14 kbar, indicating a depth in excess of 40 km (Scrimgeour and Close, 1999; Edgoose et al., 2004). Decompression from high pressures is evident in the same rocks, with distinctive garnet–clinopyroxene symplectites enclosing magmatic pyroxene and hornblende in low-strain zones, and dynamically recrystallised aggregates of clinopyroxene, garnet, hornblende, biotite, and ilmenite in high-strain zones. Plagioclase is typically recrystallised to kyanite and garnet throughout (Clarke and Powell, 1991; Scrimgeour and Close, 1999). Sm–Nd dating of garnet from the high-pressure assemblages described above confirms growth during the Petermann Orogeny (Camacho, 1997).

On BATES, mylonite zones parallel to, and only a few kilometres south of, the Woodroffe Thrust dip to the south and southwest and display normal shear sense. These normal kinematics dominate all the way south to the Mann Fault. Farther east, shear zones are thinner and contain only greenschist- to amphibolite-facies fabrics. Their lineations pitch closer to strike, and dextral kinematics have been interpreted (Camacho and McDougall, 2000). In the west Musgrave region, the Mann Fault has sinistrally displaced contaminated gabbros of the Hinckley Range (south of the fault) by 30 km to the west, where they are exposed (north of the fault) as the Murray Range, marking the northeastern edge of the Tjuni Purlka Tectonic Zone. These apparently divergent, strike-slip shear senses on either side of the Petermann orogenic core may represent escape tectonics akin to the strike-slip faults that frame the Himalayan foreland (Tapponnier et al., 1982; Replumaz and Tapponnier, 2003). Within the Tjuni Purlka Tectonic Zone, the continuation of the Mann Fault is lost into a series of northwest-trending splays, and the effects of the Petermann Orogeny decrease rapidly to the southwest. Very little evidence for Petermann-age deformation is present throughout the Mamutjarra Zone.

The 10 km wide mylonite between the Davenport Shear Zone and Mann Fault is more thoroughly recrystallised, and contains a higher percentage of leucosome generated along individual shear zones than to the north or south (Camacho, 1997; Scrimgeour and Close, 1999). The abrupt, typically <1 m thick, transition to these migmatitic zones highlights the localisation of their heat source, which is assumed to be shear heating (Camacho et al., 2001). Zircon interpreted to have crystallised within these leucosomes has been dated at 561 ± 11 Ma (Scrimgeour et al., 1999), providing the most reliable estimate of the age of the Petermann Orogeny. Similar zones of partial melting are found in mylonites in the west Musgrave Province, on BATES. Zircon from syn-deformational leucosomes in these mylonites has given an age of 570 ± 25 Ma (GSWA 155735, Walker-Hallam, 2009), indistinguishable from titanite crystallisation ages of c. 570 Ma from the same rocks (Raimondo et al., 2009).

The Fregon Zone core of the Petermann Orogeny has been interpreted as a crustal-scale, dextral transpressive system, cored by a pop-up wedge exhumed by channel flow (Lambeck and Burgess, 1992; Camacho and McDougall, 2000; Raimondo et al., 2009, 2010). North-directed transport was

accommodated by the Woodroffe Thrust, and south-directed overthrusting was concentrated along the Mann Fault and wider Davenport–Cockburn Shear Zone, which forms the core of the exhumed wedge.

Geological interpretation of the northeastern part of seismic line 11GA-YO1

Introduction

The YOM seismic line (Figure 4.17) crosses virtually perpendicular to the northwest-striking faulted contact of the Officer Basin and the Bentley Supergroup immediately to the southwest of Warburton at about CDP 13200 (Figure 4.6). To the northeast, the YOM seismic line crosses the northwest-striking bedding of the Bentley Supergroup up to about CDP 10500. This region shows well defined northwest-trending aeromagnetic trends that reflect bedding in the bimodal volcanic stratigraphy. The northeastern boundary of that region marks the northeastern limit of the Talbot Sub-basin. In this area Proterozoic outcrops to the north of the Talbot Sub-basin and up to the near-surface expression of the Mitika Fault at CDP 6500 belong to the Mitika area. These mainly consist of quartzofeldspathic gneiss and granofels, interbedded quartzite and quartz-muscovite schist and quartz-muscovite-garnet-kyanite schist. Detrital zircons from quartzite and granofelsic gneiss (GSWA 185414, 194806, 205194; Kirkland et al., in prep.) are dominated by crystallisation ages reflecting the Musgrave Orogeny and the age spectra closely resemble those found within outcrops of the MacDougall Formation at the base of the Kunmarnara Group (the lowest basal unit of the Bentley Supergroup; e.g. Evins et al., 2012).

In the Wannarn area, amygdaloidal basalt is compositionally indistinguishable from the Mummawarrawarra Basalt which forms the upper part of the Kunmarnara Group. The Mitika and Wannarn areas are interpreted to reflect exposed basement to the Talbot Sub-basin, which is thus interpreted to have originally continued to the north. Along the YOM seismic line, within both the Talbot Sub-basin (e.g. at around CDP 11400) and the southwestern part of the Mitika area (e.g. at around CDP 8500) fine- to medium-grained leucogranite is interpreted to form part of the Winburn granite, a subvolcanic composite granite intrusion directly linked to volcanism within the Talbot Sub-basin.

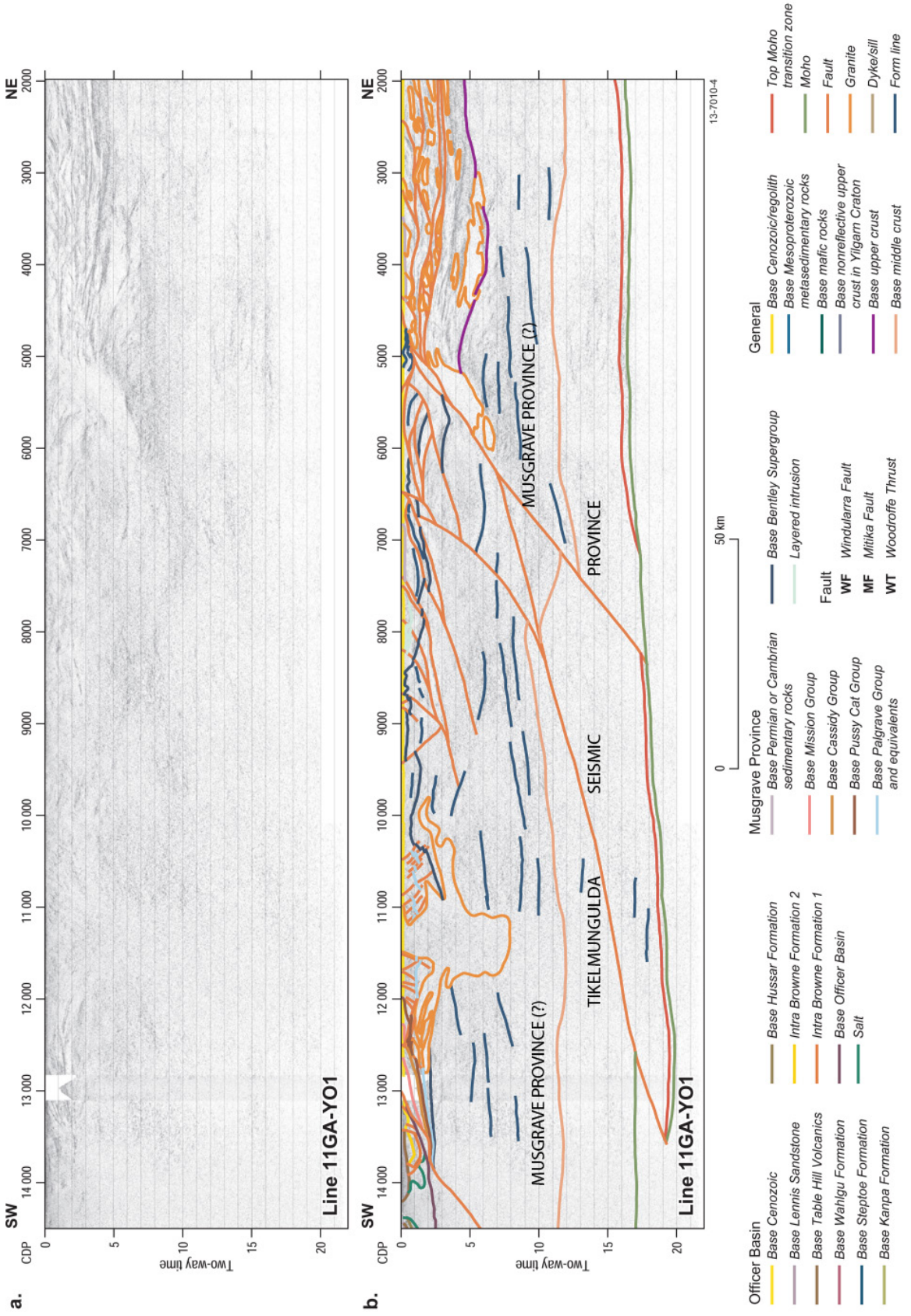

Figure 4.17 *Migrated seismic section for the northeastern half of the deep reflection line 11GA-YO1, showing both uninterpreted (a) and interpreted version (b).*

Due primarily to restrictions in accessing culturally sensitive regions, the location of the northeastern part of the YOM line was constrained to the road reserves along the Great Central Road. The orientation of the line was, nevertheless, optimal in some respects; at the southwestern end it was perpendicular both to the contact between the Officer Basin and the Bentley Supergroup and bedding within the well-exposed Bentley Supergroup itself, and at the northeastern end it was nearly perpendicular to the main Petermann Orogeny age structures.

In the intervening Mitika area (about CDP 10500 to about CDP 7400), however, the YOM line is parallel to the northeast-striking faulted contact between the Mitika area (to the northwest) and the Talbot Sub-basin, and (in the northeast) the northern part of the Tjuni Purlka Zone (including the western structural termination of the G1 Jameson intrusion). This fault is marked by a major change in both the aeromagnetic and gravity potential field data. The area to the southeast of the YOM line is typically characterised by a high gravity response and northwest-trending aeromagnetic trends, and corresponds to a domain with basement outcrop entirely consisting of rocks formed during the Giles Event (Talbot Sub-basin, including the Bentley Supergroup and Warakurna Supersuite). In contrast, the Mitika area immediately along, and to the northwest of, the YOM line is typically characterised by a low gravity response. In this area, aeromagnetic trends close to the line are to the northeast, but change abruptly to the northwest in areas further to the northwest. In addition, exposure of Proterozoic rocks form only sparse inliers in this area being otherwise covered by Cenozoic, Cretaceous and Permian deposits. As outlined above, geochronological data supports field interpretation that many of these basement inliers in the Mitika area are of metamorphosed rocks of the Kunmarnara Group. Nevertheless, it is currently unclear what constitutes basement to the Kunmarnara Group in this region. In other parts of the west Musgrave Province, the Kunmarnara Group unconformably overlies Mesoproterozoic rocks of the Musgrave Province (i.e. Pitjantjatjara Supersuite, Wankanki Supersuite, Wirku Metamorphics). The eastern part of the Mitika area, however, is up to 75 km to the west of the nearest exposed or inferred rocks of the Musgrave Province, and both gravity and magnetotelluric data show that the Palgrave region of the Talbot Sub-basin is separated from the eastern part of the west Musgrave Province by a crustal-scale structure (e.g. Aitken et al., 2013). Hence, there is no clear evidence that the Mitika area is underlain by Mesoproterozoic rocks of the Musgrave Province. For this reason, our interpretation that the mid-crustal region imaged in the YOM seismic section is indeed Musgrave Province remains tentative and is denoted ‘Musgrave Province (?)’.

Northeast of the Mitika area the YOM seismic line intersects several major west-northwest-trending structures identified in aeromagnetic images. These correspond with crustal-scale structures to the east related to north-directed thrusting during the Petermann Orogeny, including the Woodroffe Thrust (CDP 4500) and the Mitika Fault (CDP 6500). Northeast of the Woodroffe Thrust, basement geology is interpreted to be dominated by metagranites, although low reflective ovoidal areas are interpreted to represent subvolcanic intrusions belonging to the Warakurna Supersuite. The metagranites in the near surface part of the crust in this area of the YOM line are possibly amphibolite facies rocks of the Pitjantjatjara Supersuite (Musgrave Province) based on correlations with mapped regions to the east (e.g. Edgoose et al., 2004).

Korsch et al. (2013) identified six broad subdivisions of the crust within seismic section based on seismic character and on the presence of discrete, crustal-scale structures. These include the Officer Basin, the Manunda Basin, the Yamarna Terrane of the Yilgarn Craton, the Babool Seismic Province, the Musgrave Province(?) and the Tikelmungulda Seismic Province. The first four of these are described in detail by Korsch et al. (2013) and the remaining two are described here. In addition, rocks of the Bentley Supergroup (Bentley Basin) are described separately from, the Musgrave Province which is confined only to those rocks metamorphosed during the c. 1220–1150 Ma Musgrave

Orogeny. No rocks of the Musgrave Province [or Musgrave Province(?)] are exposed along or near the YOM seismic line, except perhaps in the Wannarn area (e.g. around CDP 6000 to 5000) where granites petrographically similar to those of the Pitjantjatjara Supersuite are tectonically interleaved with rocks of the Kunmarnara Group.

Exposed or near surface contacts

The northwest-trending faulted contact of the Officer Basin and the Bentley Supergroup is exposed immediately to the southwest of Warburton at about CDP 13200 (Figure 4.6). Korsch et al. (2013) named this contact the Winduldarra Fault and interpret it to be a moderately southwest-dipping crustal-scale feature that separates the Bentley Supergroup, Musgrave Province and Tikelmungulda Seismic Province to the northeast from the Officer Basin, Manunda Basin, Yamarna Terrane and Babool Seismic Province to the southwest. According to Korsch et al. (2013), the Winduldarra Fault was possibly the basin-bounding fault during extensional formation of the Officer Basin but was later reactivated as a reverse fault during contraction related to either the Petermann Orogeny or the late Cambrian Delamerian Orogeny.

The northeastern contact of the Talbot Sub-basin with rocks of the Kunmarnara Group (and the southwestern part of the Mitika area) at CDP 10500 is a northwest-dipping reverse fault, but to the southwest, beneath the Talbot Sub-basin, this contact is inferred to be conformable. Nevertheless, the basal unit of the Talbot Sub-basin (the Mount Palgrave Group) is never exposed in contact with the Kunmarnara Group.

Mohorovičić discontinuity (Moho)

Along the southwestern part of the YOM seismic line, beneath the Yilgarn Craton and Babool Seismic Province, the Moho is a reasonably well-defined, generally subhorizontal, feature at a depth of 15 s TWT (~45–46 km, Korsch et al., 2013; Figure 4.17). To the northeast of CDP 18200, the Moho becomes less distinct and progressively deeper until between about CDP 15000 and CDP 12600, where it flattens at a depth of 17 s TWT (~51 km). The Moho is, however, interpreted to be displaced along a southwest-dipping thrust (possibly the Woodroffe Thrust) at about CDP 12600, and to the southwest at CDP 13600, is at a depth of 19.3 s TWT (~58 km). The Moho is interpreted to reach a maximum depth of 19.7 s TWT (~59 km) at about CDP 13100, before shallowing to the northeast to a depth of 17 s TWT (~51 km) at CDP 6700. It is imaged between 16.3 and 17 s TWT (~51–49 km depth) for the remainder of the seismic line.

The interpretation that a thrust fault adds ~9 km depth to the Moho beneath the Musgrave region clearly implies shortening during the Petermann Orogeny. However, progressive deepening of the Moho begins well to the southwest (at around CDP 18200), adding 6 km depth to the Moho, prior to thrusting. It is possible that this thickening is related to mafic underplating associated with the Giles Event, which is consistent with the generally non-reflective seismic character of the lower crust in this region.

Bentley Supergroup (Bentley Basin)

The Bentley Supergroup has a moderately to highly reflective and distinctly layered seismic character. For the succession above the Kunmarnara Group, seismic layering matches the known or inferred orientation of depositional layering, and is most pronounced for the bimodal volcanic units of the Talbot Sub-basin and the felsic volcanic units in the area between the Woodroffe Thrust and

Warakurna. A slightly less reflective unit, underlying both regions and forming much of the upper crustal section in the Mitika area, is interpreted to represent the Kunmarnara Group.

In the area between the Woodroffe Thrust and Warakurna, and to a lesser extent within the Talbot Sub-basin, the seismic expression of the upper crust is augmented by numerous and voluminous layer parallel zones of seismically less- to non-reflective material, interpreted to be syn-volcanic granite sills or fossil magma chambers (see below). In the area between the Woodroffe Thrust and Warakurna emplacement of these sub-volcanic intrusions possibly relates to evolution of the Tjauwata Group during the Giles Event.

There is no evidence in the Talbot Sub-basin for structural repetition of units. Layers inferred to be subvolcanic sills and synvolcanic intrusions (see below) add significant thickness to the stratigraphy of the northeastern part of the sub-basin, but appear absent in the southwestern part. Here, depositional (volcanic and siliciclastic) stratigraphy reaches a thickness of 2.3 s TWT (~7 km at CDP 13000) of which the lower 0.4 s TWT (~1.2 km) is interpreted to belong to the Kunmarnara Group. At this point, the thickness of the uppermost stratigraphic unit (the Mission Group) is a minimum because it is truncated by the Winduldarra Fault. In addition, all depositional units appear to thicken to the northeast. Thus, at about CDP 12700, the total thickness of the bimodal volcanic succession (i.e. excluding the Kunmarnara and Mission Groups) is a minimum of 1.6 s TWT (~5 km).

Elsewhere within the Mitika area, from the northwestern margin of the Talbot Sub-basin to the interpreted plane of the Woodroffe Thrust approaches the surface, the base of the Bentley Supergroup is interpreted to generally lie at a depth of 2 s TWT (~6 km) or less, and around CDP 9100 and 6300 is only 0.5 s TWT (~1.5 km) deep. However, in a section between the Mitika Fault and the Woodroffe Thrust (i.e. between CDP 6300 and CDP 5400), the base of the Bentley Supergroup is at a depth of 3.0–3.5 s TWT (~9.0 to 10.5 km; see below).

Subvolcanic sills and synvolcanic intrusions

As noted above, in the area between the Woodroffe Thrust and Warakurna, and in the northeastern parts of the Talbot Sub-basin, the seismic expression of the layering in the upper crust, is augmented by bodies interpreted to be synvolcanic intrusions, subvolcanic sills, or fossil magma chambers. These bodies have a weakly- to non-reflective seismic character which strongly contrasts with the moderately to strongly reflective seismic character of their country rock. In the Woodroffe – Warakurna region, these bodies are interpreted to be up to 3 km thick and 30 km long in the plane of the seismic line. One very large granite body has been truncated along the hanging wall of the interpreted Woodroffe Thrust. The maximum depth of the granite bodies is ~6 s TWT (~18 km).

In and beneath the northeastern parts of the Talbot Sub-basin, subvolcanic sills and synvolcanic intrusions are interpreted to form a massive irregular body. This is defined in the seismic section as a zone where the distinctive layering of the Bentley Supergroup and (to a lesser extent) the distinctive seismic character of the underlying Musgrave Province(?) crust, breaks down into a weakly and randomly reflective zone. In the upper crustal region of the Bentley Supergroup, this body is generally conformable with layering and has a northeast-southwest extent of 60 km in the plane of the seismic section. However, between CDP 11500 and about CDP 11100, the body clearly truncates layering and extends from the surface, where it outcrops as part of the Winburn granite, to a depth of at least 8 s TWT (24 km) into the Musgrave Province(?) crust, where the basal contact is lost as a diffuse zone that merges in seismic character into country rock.

The Winburn granite is a large, composite, synvolcanic intrusion that underlies and intrudes the lowermost preserved rhyolitic unit of the Talbot Sub-basin, and outcrops extensively along the uplifted eastern and northern part of the sub-basin. Many phases of the granite can be matched geochemically with various rhyolitic units of the Talbot Sub-basin and so the suggestion (Smithies et al., in press) that the Winburn granite forms the intrusive equivalents of the volcanics and likely also forms part of the volcanic chamber system is probably well justified. The Talbot Sub-basin reflects a very large and long-lived magmatic system involving voluminous eruptions (including several super-volcano eruptions) over a period of more than 30 million years, with a minimum eruption volume (mafic and felsic) of 31,000 km^3 (Smithies et al., 2013). The lower crustal magma source was formed from melting of newly underplated mafic rock, and the resulting dacitic magmas were emplaced into an extensive mid- to upper crustal scale magma chamber system exposed at the surface as the Winburn granite. The seismically imaged granite body beneath the Talbot Sub-basin is interpreted to reflect part of this chamber system, where original country-rock components have been progressively excluded over the long duration of the system.

Musgrave Province(?)

The most likely interpretation of the seismically imaged mid crust [Musgrave Province(?)] is that it corresponds to Mesoproterozoic basement presently exposed in the eastern parts of the west Musgrave Province, formed before or during the Musgrave Orogeny. It extends from the unconformable contact with base of the Bentley Supergroup to the interpreted base of the middle crust at a depth generally between 11–12 s TWT (33–36 km). The lower surface is displaced along several south-dipping structures of Petermann Orogeny age, such as, the Woodroffe Thrust and the Mitika Fault. Along and near the YOM seismic line, rocks possibly belonging to the Musgrave Province(?) are exposed in thrust slices within the Mitika area, and are the main basement component to the northeast of the Woodroffe Thrust.

The seismic character of the Musgrave Province(?) is variable. Northeast of the Woodroffe Thrust, the upper part of the Musgrave Province(?), from the near surface to the base of the upper crust, is interpreted to consist of amphibolite facies metagranites with a moderately to strongly reflective character. However, below depths of about 4.2–6.2 s TWT (12.6–18.6 km), down to the base of the middle crust, Musgrave Province(?) crust in this region is only moderately reflective and relatively homogeneous, and very similar in character to Musgrave Province(?) crust imaged elsewhere to the southwest and the YOM seismic section. The interpreted presence of amphibolite facies upper Musgrave Province(?) crust to the northeast of the Woodroffe Thrust is consistent with Petermann Orogeny-age thrusting, and with exposure of amphibolite facies metagranites belonging to the Pottoyu Granite Suite of the Pitjantjatjara Supersuite (e.g. Scrimgeour et al., 1999) and the Mulga Park Zone of Camacho (1989) in the Northern Territory to the east.

Nevertheless, and as discussed above, it remains possible that the seismically imaged mid-crust does not represent the Musgrave Province at all, but is part of an exotic crustal block juxtaposed at some stage between the Musgrave Orogeny and the Giles Event.

Tikelmungulda Seismic Province

The Tikelmungulda Seismic Province is a seismically weakly- to non-reflective zone that extends below the Musgrave Province(?) crust (i.e. base of the middle crust) to the interpreted level of the Moho. It is relatively consistent in thickness between about 4.6 s and 6 s TWT (14 km to 18 km)

except where it is tectonically thickened through Petermann Orogeny-age thrusting. The interpretation of this zone is dependent upon the interpretation of the overlying Musgrave Province(?). If it is accepted that the Musgrave Province(?) corresponds to basement presently exposed in the eastern parts of the west Musgrave Province, then the most likely interpretation for the Tikelmungulda Seismic Province is that it is dominated by the products of at least two periods of mafic underplating. The first period contributed the large mantle-derived component required to induce regional and long lasting ultra-high-temperature metamorphism over 100 million years in the mid-crust and produce the voluminous and regionally-distributed granites of the Pitjantjatjara Supersuite during the Musgrave Orogeny. The second period of underplating was related to extensive mantle-derived magmatism during the Giles Event. A variation on this interpretation could take into account the systematic lithological variation observed in exposed Musgrave Province crust in the eastern part of the Musgrave Province. In that region, the relative abundance of Pitjantjatjara Supersuite granites and rocks of the Wirku Metamorphics decreased significantly to the west and southwest (Figure 4.3). It is the presence of these units that impose the requirements for regionally thin crust and ultra-high mid crustal temperatures during the Musgrave Orogeny. Hence, the decrease in their abundance towards the YOM line might suggest that the seismically-imaged Musgrave Province(?) is dominated by felsic units of the Wankanki Supersuite. The Tikelmungulda Seismic Province might then consist of a combination of mafic underplate and the older (?1950–1550 Ma) felsic basement units required by the isotopic compositions of all Mesoproterozoic crustal melts of the region. Alternatively, if the seismic Musgrave Province(?) is part of an exotic crustal block juxtaposed at some stage between the Musgrave Orogeny and the Giles Event, then the Tikelmungulda Seismic Province is likewise of unknown origin.

Detailed description of the Mitika–Wannarn–Warakurna areas

Section between CDP 6500 and CDP 9400: Mitika area

In the vicinity of the seismic line in the Mitika area, outcrops are dominated by interbedded quartzite, garnet-bearing micaceous quartzite, and quartzofeldspatic granofels interpreted from field relationships and detrital zircon age spectra to represent metamorphosed Kunmarnara Group. The depth to the base of the Bentley Supergroup in the Mitika area is interpreted to vary between 0.4 s TWT (~1.2 km) around CDP 9000 and 2.1 s TWT (~6.3 km) at CDP 7450. Between CDP 8210 and CDP 8680, the seismic section shows a low reflectivity sub-surface area that reaches a maximum depth of 0.9 s TWT (~1.8 km) at CDP 8300. Although this particular body is not exposed, it is interpreted as a Giles-age granite of the Warakurna Supersuite intruded into sedimentary rocks of the Kunmarnara Group. Between CDP 7600 and CDP 8210 at an approximate depth of 0.5 s (~1.5 km), strong sub-horizontal reflectors within the Bentley Supergroup are interpreted as the continuation of the Jameson G1 layered intrusion that outcrops to the southeast of the seismic line (Figure 4.6).

In the seismic section, the Mitika area is dominated by shallow southwest-dipping faults that extend through the Bentley Supergroup and into the underlying homogeneous and moderately reflective Musgrave Province(?). These faults show both normal and reverse apparent displacements. The set of steeply northeast and southwest-dipping faults, between CDP 9440 and CDP 8680, shows reverse sense of movement. However, their configuration resembles horst- and graben-structures that may have formed during the evolution of the Bentley Basin. Both the shallow- and steep-dipping sets of faults appear to have been reactivated into reverse faults, possibly during north-south shortening related to the Petermann Orogeny (Quentin de Gromard, in prep.). Not all normal movement has been re-equilibrated; as a result, similarly dipping neighbouring faults show opposite sense of movement. A good example of this occurs near CDP 7500 at a depth of around 2 s TWT (~6 km). Here, reverse

displacement of the base of the Bentley Supergroup occurs along a lower fault whereas the overlying fault shows normal displacement of the same boundary at around CDP 7750 at a depth of around 1.5 s TWT (~4.5 km).

The Bentley Supergroup in the Mitika area is characterised by apparent sub-horizontal reflectors. However, mapping of these rocks revealed strong folding; the regional structure consists of tight to isoclinal west verging folds with a very consistent shallow to moderately east-dipping bedding (S0) and bedding parallel foliation (S2//S0). These folds trend north-northeast away from the Mitika Fault and are rotated towards the northeast due to dextral shearing along the Mitika Fault (Figure 4.6; Quentin de Gromard, in prep.). The YOM seismic line follows exactly the same trends: north-northeast between CDP 9440 and CDP 8200 and northeast between CDP 8200 and CDP 6500. Therefore the subhorizontal reflectors do not represent the structures mapped in this region.

Along the YOM seismic line, the Kunmarnara Group is metamorphosed up to lower amphibolite facies into a garnet–muscovite quartzite corresponding to PT conditions of about 5 kbar and 550°C. However, just 5 km west of the seismic line, the same package was metamorphosed to upper amphibolite facies and preserve garnet and staurolite inclusions inside kyanite reflecting PT conditions of a minimum of 7 kbar and 650°C.

Section between CDP 4500 and CDP 6500: Wannarn area

The Wannarn area, bounded to the south by the Mitika Fault and to the north by the Woodroffe Thrust, consists of interlayered quartzofeldspatic paragneisses and quartzite, overlain by metamorphosed Mummawarrawarra Basalt. These are in tectonic contact with deformed and metamorphosed granites possibly of the Pitjantjatjara Supersuite. The presence of Mummawarrawarra Basalt directly overlying the metasedimentary unit confirms that the latter forms part of the Kunmarnara Group. We therefore interpret the strong sub-horizontal reflectors between CDP 6500 and CDP 6100 at about 0.5 s TWT (~1.5 km) to represent the base of the Bentley Supergroup. By extension, similar reflectors between CDP 6100 and CDP 5600 at a depth between 1.2 s TWT (~3.6 km) and 2 s TWT (~6 km) respectively, and CDP 6300 and CDP 5430 at a depth of about 3 s TWT (~9 km) with a maximum depth of 3.5 s TWT (~10.5 km), are also interpreted as the base of the Bentley Supergroup. The low reflective areas offsetting the reflectors of the base of the Bentley Supergroup are interpreted to represent slivers of the interpreted Pitjantjatjara Supersuite basement tectonically interleaved into the Bentley Supergroup.

The contacts between metasedimentary rocks of the Bentley Supergroup and the metamorphosed granites interpreted to be of the Pitjantjatjara Supersuite are always mylonitic. In the seismic section, the subhorizontal to shallow south-dipping faults correspond to the mylonitic contacts that bound slivers of the metagranite basement. This is consistent with field observation showing very consistent subhorizontal to shallow south-dipping mylonitic foliations, northeast-trending lineation and a general top to the northeast sense of shear along shallow south-dipping thrusts. A good example of this is shown at around CDP 6100; the base of the Bentley Supergroup is offset downward from 0.5 s TWT (~1.5 km) to 1.2 s TWT (~3.6 km) by a low reflective area interpreted to represent Pitjantjatjara Supersuite granite tectonically interleaved into the Bentley Supergroup. Thickening of the Bentley Supergroup in the Wannarn area is attributed to tectonic interleaving of interpreted Pitjantjatjara Supersuite granite into the Bentley Supergroup along shallow-dipping thrusts.

In the Wannarn area, Petermann Orogeny deformation resulted from a general dextral transpressive environment (Quentin de Gromard, in prep.). This produces the above-described northeast-directed thrusting and dextral strike slip motion along the Mitika Fault but also lateral extrusion of the northern half of the Wannarn area and folding of the Bentley Basin metasedimentary rocks against the rigid

Tjuni Purlka Zone of the Musgrave Province (Figure 4.6). The lateral extrusion is possibly accommodated along a steep fault that runs from CDP 5300 at a depth of 0.5 s TWT (~1.5 km) to CDP 7000 at a depth of 4.3 s TWT (~12.9 km) where it is more gently-dipping. Folding of the Bentley Supergroup against the Tjuni Purlka Zone is well imaged in the subsurface of the seismic section between CDP 5200 and CDP 4700 at an average depth of about 0.6 s TWT (~1.8 km).

Rocks in the Wannarn area commonly preserve evidence of high grade metamorphism (Quentin de Gromard, in prep.). Deformed garnetiferous feldspar porphyritic biotite granites interpreted to be of the Pitjantjatjara Supersuite commonly contain syn- to post-mylonite migmatites. The Mummawarrawarra Basalt contains widespread euhedral garnet porphyroblasts, relict biotite crystals and calcium rich andesine plagioclase (30-50% An), indicative of upper amphibolite to granulite facies metamorphism. Two kilometres northwest of CDP 6180, a garnet-bearing dolerite dyke, suggesting pressures in the range of 10 kbar, preserves high-grade reaction textures involving garnet-bearing coronas between plagioclase and pyroxene typical of retrograde reaction in the granulite facies. This suggests that the Wannarn area was buried to a minimum depth of 25 km and potentially up to 30 km before having been exhumed to its original level of deposition (i.e. Mummawarrawarra Basalt back at the surface) during the Petermann Orogeny.

Section between CDP 2000 and CDP 4500: Warakurna area

North of the Woodroffe Thrust and along the YOM seismic line, Proterozoic rocks are essentially covered by Cenozoic, Cretaceous and Permian sedimentary successions. Most of the understanding of the Warakurna area comes from the westward extrapolation of the work done in the Bloods Ranges by the Northern Territory Geological Survey (NTGS) at the border with Western Australia. The Woodroffe Thrust is commonly interpreted as the boundary between the granulite facies Fregon Zone to the south and the amphibolite facies Mulga Park Zone to the north. The Mulga Park Zone mainly consists of Pitjantjatjara Supersuite granites unconformably overlain by the volcano-sedimentary sequence of the Tjauwata Group, equivalent to the Bentley Supergroup. Therefore, our preferred interpretation is that the subsurface north of CDP 4500 represents an amphibolite facies Pitjantjatjara Supersuite basement unconformably overlain by Bentley Supergroup volcano-sedimentary succession. The numerous low reflective ovoidal areas are interpreted to represent sub-volcanic intrusions contemporaneous to the Bentley Supergroup volcanic succession.

The strong reflections of the upper crust in this area may represent the great contrast between layered volcano-sedimentary units and homogeneous sub-volcanic intrusions but they also might be a product of the localisation of intense shearing within Pitjantjatjara Supersuite granites. The numerous truncations between sets of reflection trends suggest tectonic repetitions. A good example of this is imaged between CDP 3850 and CDP 4600 at an approximate depth of 2 s TWT (~6 km) displaying a duplex structure. The similar structural position between the Warakurna area and the Bloods Range area of Northern Territory suggests that the structures imaged at depth in the YOM seismic line north of the Woodroffe Thrust correspond to the Petermann Nappe Complex mapped in the Northern Territory. The base of the strongly reflective upper crust at an average depth of about 5.5 s TWT (~16.5 km) most probably represents the boundary between a strongly deformed upper crust and a less deformed and more homogeneous middle crust. This implies that this boundary is a decollement layer that potentially corresponds of the westward extension of the Piltardi Detachment Zone that crops out in the Bloods Range in Northern Territory.

Acknowledgements

This paper forms part of a collaborative project between Geoscience Australia and the Geological Survey of Western Australia (GSWA). The work that GSWA carries out in the Musgrave region forms part of an ongoing collaborative project between GSWA and the Ngaanyatjarra Council. We thank the following for their contributions to the project: Jenny Maher, for project management during the planning, acquisition and processing phase of the seismic data; and Narelle Neumann and Tristan Kemp for project management during the interpretation phase of the project. H. Howard, R. Quentin de Gromard, H. Smithies, C. Kirkland, K. Gessner and M. Wingate publish with the permission of the Executive Director of the Geological Survey of Western Australia.

References

Aitken, A.R.A., and Betts, P.G., 2008. High-resolution aeromagnetic data over central Australia assist Grenville-era (1300–1100 Ma) Rodinia reconstructions. *Geophysical Research Letters*, 35, L01306, doi: 10.1029/2007GL031563.

Aitken, A.R.A., Betts, P.G., Weinberg, R.F., and Gray, D., 2009. Constrained modelling of the crustal architecture of the Musgrave Province in central Australia: evidence for lithospheric strengthening due to crust–mantle boundary uplift. *Journal of Geophysical Research B: Solid Earth*, 114, B12405, doi:10.1029/2008JB006194.

Aitken, A.R.A., Smithies, R.H., Dentith, M.C., Joly, A., Evans, S., and Howard, H.M., 2012. Magmatism-dominated intracontinental rifting in the Mesoproterozoic: The Ngaanyatjarra Rift, central Australia. *Gondwana Research*, doi.org/10.1016/j.gr.2012.10.003.

Aitken A., Dentith M.C., Evans S., Gallardo L., Joly A., Thiel S., Smithies R.H., and Tyler I.M., 2013. Imaging crustal structure in the west Musgrave Province from magnetotelluric and potential field data. *Geological Survey of Western Australia, Report* 114.

Betts, P.G., and Giles, D., 2006. The 1800–1100 Ma tectonic evolution of Australia. *Precambrian Research*, 144, 92–125.

Bodorkos, S., and Clark, D.J., 2004. Evolution of a crustal-scale transpressive shear zone in the Albany Fraser Orogen, SW Australia: 2. Tectonic history of the Coramup Gneiss and a kinematic framework for Mesoproterozoic collision of the West Australian and Mawson cratons. *Journal of Metamorphic Geology*, 22, 713–731.

Bodorkos, S., Wingate, M.T.D., and Kirkland, C.L., 2008. 174737: foliated metamonzogranite, Mount Fanny; Geochronology Record 718. *Geological Survey of Western Australia*, 5p.

Branney, M.J., Bonnichsen, B., Andrews, G.D.M., Ellis, B., Barry, T.L., and McCurry, M., 2008. 'Snake River (SR)-type' volcanism at the Yellowstone hotspot track: distinctive products from unusual, high-temperature silicic super-eruptions. *Bulletin of Volcanology*, 70, 293–314.

Brown, M., 2006. Duality of thermal regimes is the distinctive characteristic of plate tectonics since the Neoarchean. *Geology*, 34, 961–964.

Brown, M., 2007. Metamorphic conditions in orogenic belts: a record of secular change. *International Geology Review*, 49, 193–234.

Camacho, A., 1989. The Woodroffe Thrust, eastern Musgrave Block, NT: A problem of large scale melting during thrusting. *Geological Society of Australia, Abstracts* 24, 14–15.

Camacho, A., 1997. An isotopic study of deep-crustal orogenic processes: Musgrave Block, central Australia: The Australian National University, Canberra, Australian Capital Territory, PhD thesis (unpublished).

Camacho, A., and Fanning, C.M., 1995. Some isotopic constraints on the evolution of the granulite and upper amphibolite facies terranes in the eastern Musgrave Block, central Australia. *Precambrian Research*, 71, 155–172.

Camacho, A., and McDougall, I., 2000. Intracratonic, strike-slip partitioned transpression and the formation of eclogite facies rocks: an example from the Musgrave Block, central Australia. *Tectonics*, 19, 978–996.

Camacho, A., Compston, W., McCulloch, M., and McDougall, I., 1997. Timing and exhumation of eclogite facies shear zones, Musgrave Block, central Australia. *Journal of Metamorphic Geology*, 15, 735–751.

Camacho, A., McDougall, I., Armstrong, R., and Braun, J., 2001. Evidence for shear heating, Musgrave Block, central Australia. *Journal of Structural Geology*, 23, 1007–1013.

Camacho, A., Yang, P., and Frederiksen, A., 2009. Constraints from diffusion profiles on the duration of high-strain deformation in thickened crust. *Geology*, 37, 755–758.

Cawood, P.A., and Korsch, R.J., 2008. Assembling Australia: Proterozoic building of a continent. *Precambrian Research*, 166, 1–38.

Clark, D.J., Hensen, B.J., and Kinny, P.D., 2000. Geochronological constraints for a two-stage history of the Albany–Fraser Orogen, Western Australia. *Precambrian Research*, 102, 155–183.

Clarke, G.L., and Powell, R., 1991. Decompressional coronas and symplectites in granulites of the Musgrave Complex, central Australia. *Journal of Metamorphic Geology*, 9, 441–450.

Clarke, G.L., Sun, S-S., and White, R.W., 1995a. Grenville age belts and associated older terranes in Australia and Antarctica. *AGSO Journal of Australian Geology and Geophysics*, 16, 25–39.

Clarke, G.L., Buick, I.S., Glikson, A.Y., and Stewart, A.J., 1995b. Structural and pressure–temperature evolution of host rocks of the Giles Complex, western Musgrave Block, central Australia: evidence for multiple high-pressure events. *AGSO Journal of Australian Geology and Geophysics*, 16, 127–146.

Coleman, P., 2009. Intracontinental orogenesis in the heart of Australia: structure, provenance and tectonic significance of the Bentley Supergroup, western Musgrave Block, Western Australia. *Geological Survey of Western Australia, Record* 2009/23, 50p.

Currie, C.A., and Hyndman, R.D., 2006. The thermal structure of subduction zone back arcs. *Journal of Geophysical Research*, 111, B08404, doi:10.1029/2005JB004024.

Daniels, J.L., 1974. The geology of the Blackstone region, Western Australia. *Geological Survey of Western Australia, Bulletin* 123, 257p.

Edgoose, C.J., Scrimgeour, I.R., and Close, D.F., 2004. Geology of the Musgrave Block, Northern Territory. *Northern Territory Geological Survey, Report* 15, 48p.

Evins, P.M., Smithies, R.H., Howard, H.M., and Maier, W.D., 2009. Holt, WA Sheet 4546. *Geological Survey of Western Australia, 1:100 000 Geological Series*.

Evins, P.M., Smithies, R.H., Howard, H.M., Kirkland, C.L., Wingate, M.T.D., and Bodorkos, S., 2010. Redefining the Giles Event within the setting of the 1120–1020 Ma Ngaanyatjarra Rift, west Musgrave Province, central Australia. *Geological Survey of Western Australia, Record* 2010/6, 36p.

Evins, P.M., Kirkland, C.L., Wingate, M.T.D., Smithies, R.H., Howard, H.M., and Bodorkos, S., 2012. Provenance of the 1340–1270 Ma Ramarama Basin in the west Musgrave Province, central Australia. *Geological Survey of Western Australia, Report* 116, 39p.

Fitzsimons, I.C.W., 2003. Proterozoic basement provinces of southern and southwestern Australia and their correlation with Antarctica. *Geological Society, London, Special Publications*, 206, 93–130.

Fraser, A.R., 1976. Gravity provinces and their nomenclature. *BMR Journal of Australian Geology and Geophysics*, 1, 350–352.

Giles, D., Betts, P.G., and Lister, G.S., 2004. 1.8–1.5-Ga links between the North and South Australian Cratons and the Early–Middle Proterozoic configuration of Australia. *Tectonophysics*, 380, 27–41.

Glikson, A.Y., Stewart, A.T., Ballhaus, G.L., Clarke, G.L., Feeken, E.H.T., Level, J.H., Sheraton, J.W., and Sun, S-S., 1996. Geology of the western Musgrave Block, central Australia, with reference to the mafic–ultramafic Giles Complex. *Australian Geological Survey Organisation, Bulletin* 239, 206p.

Godel, B., Seat, Z., Maier, W.D., and Barnes, S-J., 2011. The Nebo-Babel Ni-Cu-PGE Sulfide Deposit (West Musgrave Block, Australia): Part 2- Constraints on Parental Magma and Processes, with Implications for Mineral Exploration. *Economic Geology*, 106, 557–584

Gray, C.M., 1971. Strontium isotope studies on granulites: Australian National University, Canberra, Australian Capital Territory, PhD thesis (unpublished), 242p.

Gray, C.M., 1978. Geochronology of granulite-facies gneisses in the western Musgrave Block, central Australia. *Geological Society of Australia Journal*, 25, 403–414.

Gray, C.M., and Compston, W., 1978. A Rb–Sr chronology of the metamorphism and prehistory of central Australian granulites. *Geochimica et Cosmochimica Acta*, 42, 1735–1748.

Green, J.C., and Fitz, T.J., 1993. Extensive felsic lavas and rheoignimbrites in the Keweenawan Midcontinent Rift plateau volcanics, Minnesota: petrographic and field recognition. *Journal of Volcanology and Geothermal Research*, 54, 177–196.

Hanson, R.E., Crowley, J.L., Bowring, S.A., Ramezani, J., Gose, W.A., Dalziel, I.W.D., Pancake, J.A., Seidel, E.K., Blenkinsop, T.G., and Mukwakwami, J., 2004. Coeval large-scale magmatism in the Kalahari and Laurentian cratons during Rodinia assembly. *Science*, 304, 1126-1129.

Harley, S.L., 1998. On the occurrence and characterization of ultrahigh-temperature crustal metamorphism. In: Treloar, P.J. and O'Brien, P.J. (editors), What drives metamorphism and metamorphic relations? *Geological Society, London, Special Publication*, 81–107.

Howard, H.M., Smithies, R.H., Pirajno, F., and Skwarnecki, M.S., 2007. Bell Rock, WA Sheet 4645. *Geological Survey of Western Australia, 1:100 000 Geological Series*.

Howard, H.M., Smithies, R.H., Kirkland, C.L., Evins, P.M., and Wingate, M.T.D., 2009. Age and geochemistry of the Alcurra Suite in the west Musgrave Province and implications for orthomagmatic Ni–Cu–PGE mineralization during the Giles Event. *Geological Survey of Western Australia, Record* 2009/16, 16p.

Howard, H.M., Werner, M., Smithies, R.H., Kirkland, C.L., Kelsey, D.L., Hand, M., Collins, A., Pirajno, F., Wingate, M.T.D., Maier, W.D., and Raimondo, T., 2011a. The geology of the west Musgrave Province and the Bentley Supergroup - a field guide. *Geological Survey of Western Australia Record* 2011/4, 119p.

Howard, H.M., Smithies, R.H., Werner, M., Kirkland, C.L., and Wingate, M.T.D., 2011b. Geochemical characteristics of the Alcurra Dolerite (Giles Event) and its extrusive equivalents in the Bentley Supergroup. In: GSWA 2011 extended abstracts: promoting the prospectivity of Western Australia. *Geological Survey of Western Australia, Record* 2011/2, 27–30.

Kelsey, D.E., 2008. On ultrahigh-temperature crustal metamorphism. *Gondwana Research*, 13, 1–29.

Kelsey, D.E., White, R.W., Powell, R., and Holland, T.J.B., 2004. Calculated phase equilibria in K_2O–FeO–MgO–Al_2O_3–SiO_2–H_2O for sapphirine–quartz-bearing mineral assemblages. *Journal of Metamorphic Geology*, 22, 559–578.

Kelsey, D.E., Hand, M., Evins, P., Clark, C., and Smithies, H., 2009. High temperature, high geothermal gradient metamorphism in the Musgrave Province, central Australia; potential constraints on tectonic setting. In: *Specialist Group in Geochemistry, Mineralogy and Petrology, Geological Society of Australia*; Kangaroo Island 2009 conference, Kangaroo Island, South Australia, 8–13 November, 2009, 28p.

King, R.J., 2009. Using calculated pseudosections in the system NCKFMASHTO and SHRIMP II U–Pb zircon dating to constrain the metamorphic evolution of paragneisses in the Latitude Hills, west Musgrave Province, Western Australia. *Geological Survey of Western Australia, Record* 2009/15, 67p.

Kirkland, C.L., Wingate, M.T.D., and Bodorkos, S., 2008. 183496: orthogneiss, Mount West; Geochronology Record 747. *Geological Survey of Western Australia*, 5p.

Kirkland, C.L., Wingate, M.T.D., Evins, P.M., and Smithies, R.H., 2009a. 180867: quartz monzonite, Mount Holt; Geochronology Record 838. *Geological Survey of Western Australia*, 5p.

Kirkland, C.L., Wingate, M.T.D., Bodorkos, S., and Smithies, R.H., 2009b. 184146: syenogranite, Borrows Hill; Geochronology Record 823. *Geological Survey of Western Australia*, 4p.

Kirkland, C.L., Bodorkos, S., Wingate, M.T.D., and Smithies, R.H., 2009c. 185610: coarse-grained leucogranite, Borrows Hill; Geochronology Record 794. *Geological Survey of Western Australia*, 4p.

Kirkland, C.L., Wingate, M.T.D., Bodorkos, S., and Smithies, R.H., 2009d. 187274: porphyritic granite, Murray Range; Geochronology Record 825. *Geological Survey of Western Australia*, 4p.

Kirkland, C.L., Wingate, M.T.D., Evins, P.M., Howard, H.M., and Smithies, R.H., 2009e. 194354: gabbro, north of Jameson Range; Geochronology Record 799. *Geological Survey of Western Australia*, 4p.

Kirkland, C.L., Wingate, M.T.D., and Smithies, R.H., 2010a. 187195: leucogranitic gneiss, Mount Scott; Geochronology Record 912. *Geological Survey of Western Australia*, 4p.

Kirkland, C.L., Wingate, M.T.D., and Evins, P.M., 2010b. 194393: granitic gneiss, Ngaturn; Geochronology Record 920. *Geological Survey of Western Australia*, 4p.

Kirkland, C.L., Wingate, M.T.D., and Evins, P.M., 2010c. 194376: norite dyke, Minnie Hill; Geochronology Record 921. *Geological Survey of Western Australia*, 4p.

Kirkland, C.L., Wingate, M.T.D., and Smithies, R.H., 2010d. 194422: quartzite, Cohn Hill; Geochronology Record 864. *Geological Survey of Western Australia*, 5p.

Kirkland, C.L., Wingate, M.T.D., and Smithies, R.H., 2011a. 194764: monzogranite, Mount Scott; Geochronology Record 965. *Geological Survey of Western Australia*, 4p.

Kirkland, C.L., Wingate, M.T.D., and Smithies, R.H., 2011b. 194762: leucogabbro, Mount Finlayson; Geochronology Record 966. *Geological Survey of Western Australia*, 4p.

Kirkland, C.L., Wingate, M.T.D., Bodorkos, S., and Smithies, R.H., 2011c. 184150: metasandstone, Kampurarr Pirti; Geochronology Record 940. *Geological Survey of Western Australia*, 5p.

Kirkland, C.L., Spaggiari, C.V., Pawley, M.J., Wingate, M.T.D., Smithies, R.H., Howard, H.M., Tyler, I.M., Belousova, E.A., and Poujol, M., 2011d. On the edge: U–Pb, Lu–Hf, and Sm–Nd data suggests reworking of the Yilgarn Craton margin during formation of the Albany–Fraser Orogen. *Precambrian Research*, 187, 223–247.

Kirkland, C.L., Wingate, M.T.D., and Smithies, R.H., 2011e. 187175: muscovite–tourmaline pegmatite, Morgan Range; Geochronology Record 936. *Geological Survey of Western Australia*, 4p.

Kirkland, C.L., Smithies, R.H., Woodhouse, E., Howard, H.M., Wingate, M.T.D., Belousova, E.A., Cliff, J.B., Murphy, R.C., and Spagiari, C.V., 2012. A multi-isotopic approach to the crustal evolution of the west Musgrave Province, central Australia. *Geological Survey of Western Australia, Report* 115, 47p.

Korsch, R.J., Blewett, R.S., Pawley, M.J., Carr, L.K., Hocking, R.M., Neumann, N.L., Smithies, R.H, Quentin de Gromard, R., Howard, H.M., Kennett, B.L.N., Aitken, A.R.A., Holzschuh, J., Duan, J., Goodwin, J.A., Jones, T., Gessner, K., and Gorczyk, W., 2013. Geological setting and interpretation of the southwest half of deep seismic reflection line 11GA-YO1: Yamarna Terrane of the Yilgarn Craton and the western Officer Basin. In: Neumann, N.L. (editor), *Yilgarn Craton–Officer Basin–Musgrave Province (YOM) Seismic and MT Workshop*. Geoscience Australia Record 2013/28, 24–50.

Lambeck, K., and Burgess, G., 1992. Deep crustal structure of the Musgrave Block, central Australia: results from teleseismic travel–time anomalies. *Australian Journal of Earth Sciences*, 39, 1–20.

Li, Z-X., 2000. Palaeomagnetic evidence for unification of the North and West Australian Cratons by ca. 1.7Ga: new results from the Kimberley Basin of northwestern Australia. *Geophysical Journal International*, 142, 173–180.

Maboko, M.A.H., 1988. Metamorphic and geochronological evolution in the Musgrave Ranges, central Australia: Australian National University, Canberra, Australian Capital Territory, PhD thesis (unpublished).

Maboko, M.A.H., McDougall, I., Zeitler, P.K., and Fitzgerald, J.D., 1991. Discordant ^{40}Ar–^{39}Ar ages from the Musgrave Ranges, central Australia: implications for the significance of hornblende ^{40}Ar–^{39}Ar spectra. *Chemical Geology*, 86, 139–160.

Major, R.B., and Conor, C.H.H., 1993. Musgrave Block. In: Drexel, J.F., Preiss, W.V. and Parker, A.J. (editors), The Geology of South Australia. *Geological Survey of South Australia, Bulletin* 54, 156–167.

Morris, P.A., and Pirajno, F., 2005. Geology, geochemistry, and mineralization potential of Mesoproterozoic sill complexes of the Bangemall Supergroup, Western Australia. *Geological Survey of Western Australia, Report* 99, 75p.

Myers, J.S., Shaw, R.D., and Tyler, I.M., 1996. Tectonic evolution of Proterozoic Australia. *Tectonics*, 16, 1431–1446.

Pearce, J.A., Harris, N.B.W., and Tindle, A.G., 1984. Trace element discrimination diagrams for the tectonic interpretation of granitic rocks. *Journal of Petrology*, 25, 956–983.

Quentin de Gromard, R., Kirkland, C.L., Wingate, M.T.D., Smithies, R.H., and Howard, H.M., in prep. Structural and metamorphic evolution of the Mitika–Wannarn area, west Musgrave Province, central Australia. *Geological Survey of Western Australia, Record*.

Raimondo, T., Collins, A.S., Hand, M., Walker-Hallam, A., Smithies, R.H., Evins, P.M., and Howard, H.M., 2009. Ediacaran intracontinental channel flow. *Geology*, 37, 291–294.

Raimondo, T., Collins, A.S., Hand, M., Walker-Hallam, A., Smithies, R.H., Evins, P.M., and Howard, H.M., 2010. The anatomy of a deep intracontinental orogeny. *Tectonics*, 29, TC4024, doi:10.1029/2009TC002504.

Replumaz, A., and Tapponnier, P., 2003. Reconstruction of the deformed collision zone between India and Asia by backward motion of lithospheric blocks. *Journal of Geophysical Research,* 108 (6), 2285.

Rowins, S.M., Groves, D.I., McNaughton, N.J., Palmer, M.R., and Eldridge, C.S., 1997. A reinterpretation of the role of granitoids in the genesis of Neoproterozoic gold mineralisation in the Telfer Dome, Western Australia. *Economic Geology*, 92, 133–160.

Scrimgeour, I.R., and Close, D.F., 1999. Regional high pressure metamorphism during intracratonic deformation: the Petermann Orogeny, central Australia. *Journal of Metamorphic Geology*, 17, 557–572.

Scrimgeour, I., Close, D.F., and Edgoose, C.J., 1999. Petermann Ranges, Northern Territory (2nd edition). *Northern Territory Geological Survey, 1:250 000 geological map series explanatory notes* SG52-07, 59p.

Scrimgeour, I.R., Kinny, P.D., Close, D.F., and Edgoose C.J., 2005. High-T granulites and polymetamorphism in the southern Arunta Region, central Australia: evidence for a 1.64 Ga accretionary event. *Precambrian Research*, 142, 1–27.

Seat, Z., 2008. Geology, petrology, mineral and whole-rock chemistry, stable and radiogenic isotope systematics and Ni–Cu–PGE mineralisation of the Nebo–Babel intrusion, west Musgrave, Western Australia: University of Western Australia, Perth, Western Australia, PhD thesis (unpublished).

Smithies, R.H., Howard, H.M., Evins, P.M., Kirkland, C.L., Bodorkos, S. and Wingate, M.T.D., 2009. West Musgrave Complex — new geological insights from recent mapping, geochronology, and geochemical studies. *Geological Survey of Western Australia, Record* 2008/19, 20p.

Smithies, R.H., Howard, H.M., Evins, P.M., Kirkland, C.L., Kelsey, D.E., Hand, M., Wingate, M.T.D., Collins, A.S., Belousova, E., and Allchurch, S., 2010. Geochemistry, geochronology, and petrogenesis of Mesoproterozoic felsic rocks in the western Musgrave Province of central Australia, and implication for the Mesoproterozoic tectonic evolution of the region. *Geological Survey of Western Australia, Report* 106, 73p.

Smithies, R.H., Howard, H.M., Evins, P.M., Kirkland, C.L., Kelsey, D.E., Hand, M., Wingate, M.T.D., Collins, A.S., and Belousova, E., 2011. Mesoproterozoic high temperature granite magmatism, crust–mantle interaction and the intracontinental evolution of the Musgrave Province. *Journal of Petrology*, 52, 931–958.

Smithies, R.H., Howard, H.M., Kirkland, C.L., Werner, M., Medlin, C.C., Wingate, M.T.D., and Cliff, J.B., 2013. Geochemical evolution of rhyolites of the Talbot Sub-basin and associated felsic units of the Warakurna Supersuite. *Geological Survey of Western Australia, Report* 118.

Spaggiari, C.V., Bodorkos, S., Barquero-Molina, M., and Tyler, I.M., 2009. Interpreted bedrock geology of the South Yilgarn and central Albany–Fraser Orogen, Western Australia. *Geological Survey of Western Australia, Record* 2009/10, 84p.

Sparks, R.S.F., Self, S., and working Group, 2005. Super-eruptions: global effects and future threats. Report, Geological Society of London Working Group (2nd Edition), Geological Society, London, 24p.

Sun, S-S., Sheraton, J.W., Glikson, A.Y., and Stewart, A.J., 1996. A major magmatic event during 1050–1080 Ma in central Australia, and an emplacement age for the Giles Complex. *AGSO Journal of Australian Geology and Geophysics*, 24, 13–15.

Tapponnier, P., Peltzer, G., Le Dain, A.Y., Armijo, R., Cobbold, P., 1982. Propagating extrusion tectonics in Asia; new insights from simple experiments with plasticine. *Geology*, 10, 611–616.

Taylor, J., Stevens, G., Armstrong, R., and Kisters, A.F.M., 2010. Granulite facies anatexis in the Ancient Gneiss Complex, Swaziland, at 2.73 Ga: mid-crustal metamorphic evidence for mantle heating of the Kaapvaal craton during Ventersdorp magmatism. *Precambrian Research*, 177, 88–102.

Vervoort, J.D., Wirth, K., Kennedy, B., Sandland, T., and Harpp, K.S., 2007. The magmatic evolution of the Midcontinent rift: new geochronologic and geochemical evidence from felsic magmatism. *Precambrian Research*, 157, 235–268

Wade, B.P., Barovich, K., Hand, M., Scrimgeour, I.R., and Close, D.F., 2006. Evidence for early Mesoproterozoic arc magmatism in the Musgrave Block, central Australia: implications for Proterozoic crustal growth and tectonic reconstructions of Australia. *Journal of Geology*, 114, 43–63.

Wade, B.P., Kelsey, D.E., Hand, M., and Barovich, K.M., 2008. The Musgrave Province: stitching north, west and south Australia. *Precambrian Research*, 166, 370–386.

Walker-Hallam, A., 2009. Complex strain in mylonites from the western Musgraves, north of the Mann Fault, Western Australia. *Geological Survey of Western Australia, Record* 2009/14, 33p.

White, R.W., 1997. The pressure–temperature evolution of a granulite facies terrain, western Musgrave Block, central Australia. Macquarie University, Sydney, New South Wales, PhD thesis (unpublished), 256p.

White, R.W., Clarke, G.L., and Nelson, D.R., 1999. SHRIMP U–Pb zircon dating of Grenville-age events in the western part of the Musgrave Block, central Australia. *Journal of Metamorphic Geology*, 17, 465–481.

Wingate, M.T.D., and Giddings, J.W., 2000. Age and palaeomagnetism of the Mundine Well dyke swarm, Western Australia: implications for an Australia–Laurentia connection at 755 Ma. *Precambrian Research*, 100, 335–357.

Wingate, M.T.D., Campbell, I.H., Compston, W., and Gibson, G.M., 1998. Ion microprobe U–Pb ages for Neoproterozoic basaltic magmatism in south-central Australia and implications for the breakup of Rodinia. *Precambrian Research*, 87, 135–159.

Wingate, M.T.D., Pirajno, F., and Morris, P.A., 2004. Warakurna large igneous province: a new Mesoproterozoic large igneous province in west-central Australia. *Geology*, 32, 105–108.

Zhao, J-X., McCulloch, M.T., and Korsch, R.J., 1994. Characterisation of a plume-related ~800 Ma magmatic event and its implications for basin formation in central-southern Australia. *Earth and Planetary Science Letters*, 121, 349–367.

5 Geophysical investigation and 3D geological model of the Yilgarn Craton–Officer Basin–Musgrave Province region

J. Goodwin, T. Jones, T. Brennan and M. Nicoll

Minerals and Natural Hazards Division, Geoscience Australia, GPO Box 378, Canberra, ACT 2601.

james.goodwin@ga.gov.au

Introduction

To complement the interpretation of the Yilgarn Craton–Officer Basin–Musgrave Province (11GA-YO1) seismic survey, a geophysical study of the gravity and magnetic data surrounding the seismic line was undertaken. Primarily this involved the interpretation of gravity and magnetic data grids and forward modelling of sections both along the 11GA-YO1 seismic line and sub-parallel to it.

In combination with this, a 3D geological model was constructed with a focus on the whole-crust scale architecture of the region between the northeast Yilgarn Craton and west Musgrave Province. The purpose of this study was to extend the 11GA-YO1 seismic interpretation into 3D space and understand the regional scale geology. The 3D geological model presented here incorporates multidisciplinary datasets and integrates them into a single environment. The 3D architectures defined across the study area are derived from seismic, gravity, magnetic, surface geology and drill hole datasets. The extent of the 3D geological model is shown in Figure 5.1.

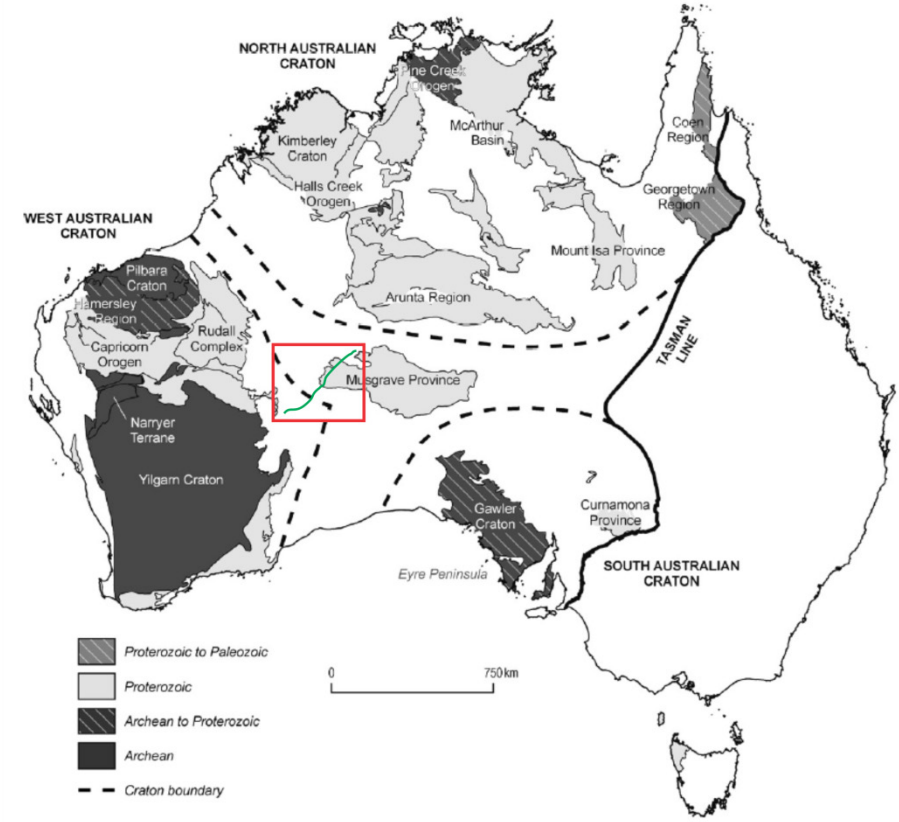

Figure 5.1 *Location of the 11GA-YO1 seismic line with respect to major geological provinces within Australia. Green line - 11GA-YO1 seismic line, red box - study area.*

Input data

The following outlines the data used in the geophysical investigation and in the construction of the 3D geological model.

Gravity

The study area has a basic gravity station coverage of 11 km spacing with more detailed 2.5 km spacing across the Musgrave Province and variably spaced transects covering the Officer Basin (Figure 5.2).

During this study, the Isostatic Residual Gravity Anomaly Map of Nakamura et al. (2011) was used for the interpretation of gravity anomalies as it highlights a greater level of contrast in the data by removing long-wavelength anomalies (Figure 5.3). Forward modelling along the 11GA-YO1 seismic line utilised the 400 m station spacing Bouguer gravity data collected along the 11GA-YO1 seismic transect. For all other gravity studies the Bouguer Gravity Anomaly Map of Australia, Fourth Edition (Bacchin et al., 2008) was used. Both the Bouguer and Isostatic Residual Gravity Anomaly maps are gridded using a variable sample density gridding method with a nominal cell resolution of 800 m. Gravity data is available from the Geophysical Archive Data Delivery System (www.geoscience.gov.au/gadds).

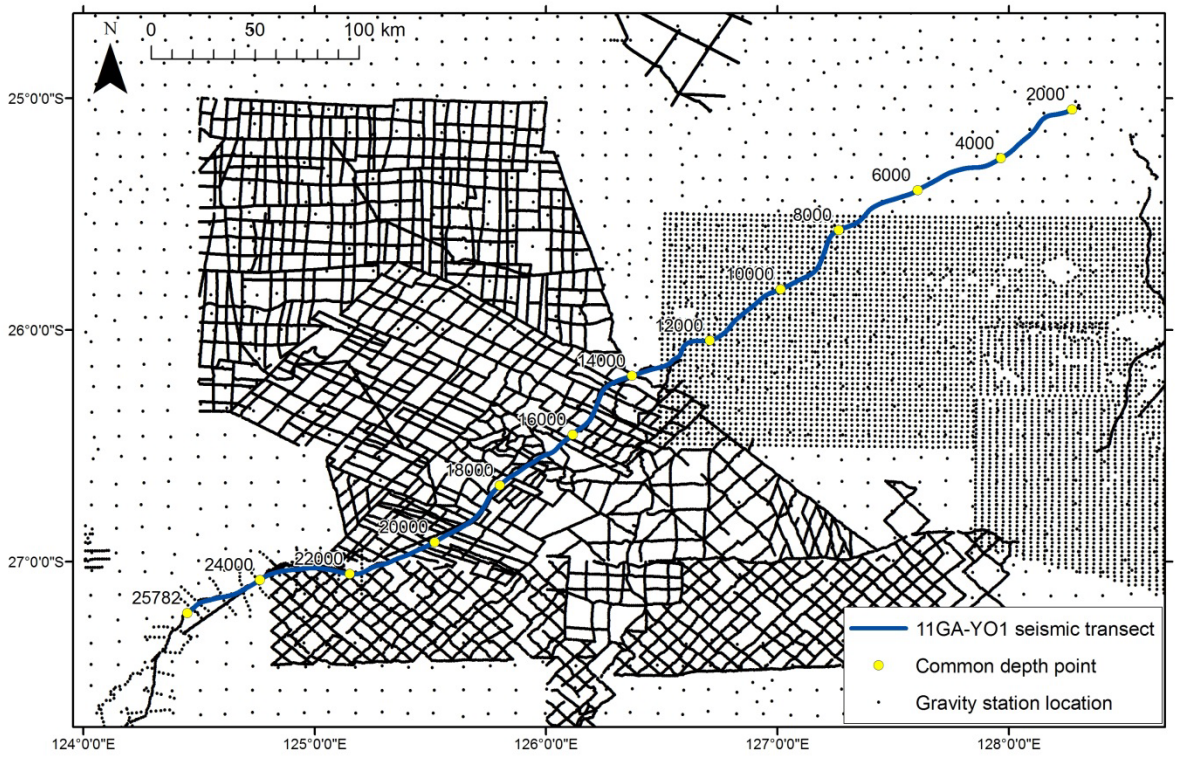

Figure 5.2 *Station spacing of gravity data in the area surrounding the 11GA-YO1 seismic line.*

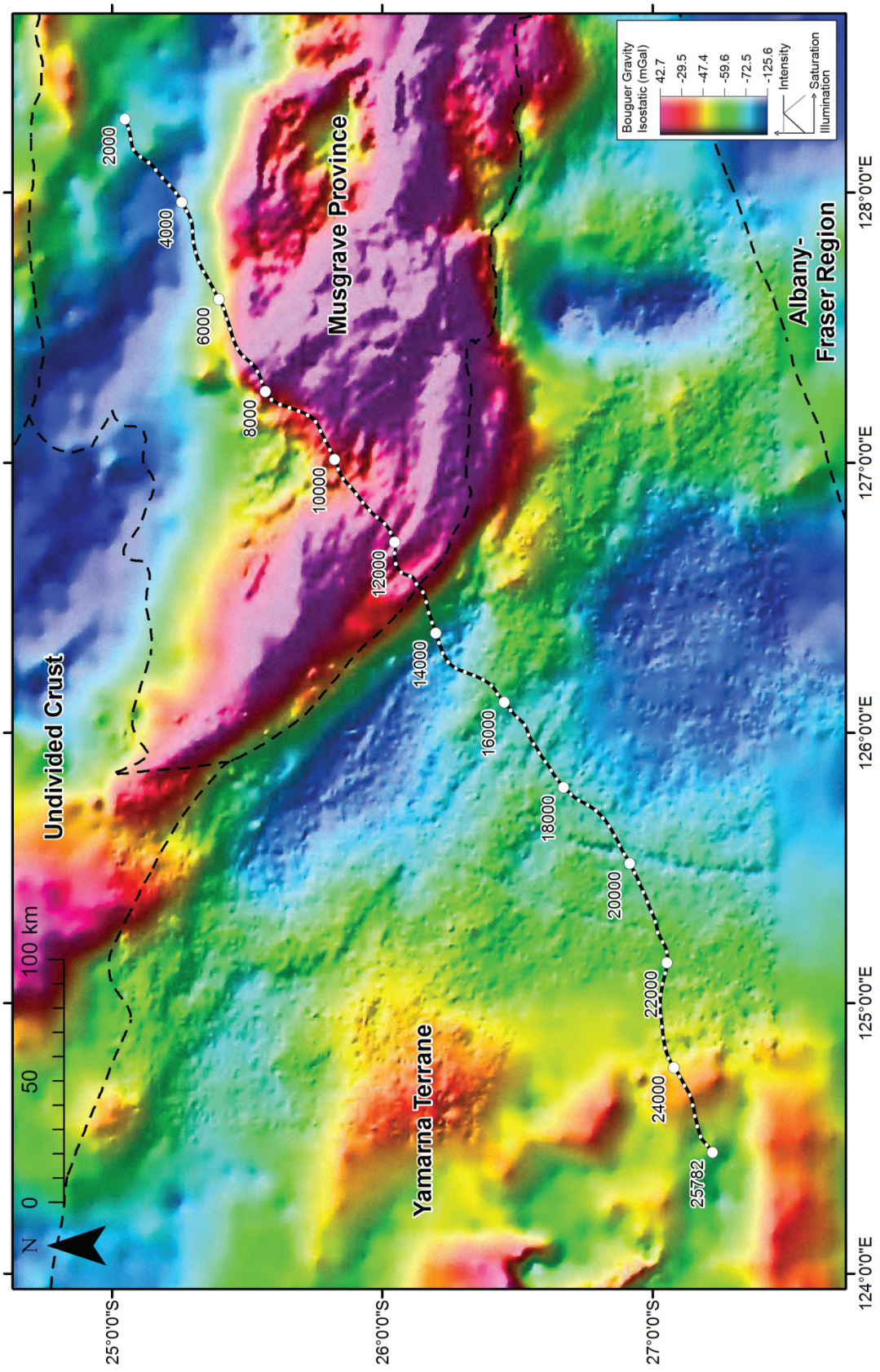

Figure 5.3 *Isostatic residual gravity anomaly grid (Nakamura et al., 2011) of the study area, with dashed lines representing the major province boundaries.*

Magnetics

Magnetic intensity data used in this study was extracted from the Magnetic Anomaly Map of Australia, Fifth Edition (Milligan et al., 2010) and is available from the Geophysical Archive Data Delivery System (www.geoscience.gov.au/gadds). The majority of the data within the area of interest is of a high quality with a flight line spacing of 300–500 m. Poorer quality data exists to the north and southeast, ranging from 1500–3000 m spacing (Figure 5.4). The Magnetic Anomaly Map of Australia was generated by grid merging the individual survey grids with a nominal cell resolution of 80 m. An image of this grid is shown in Figure 5.5. A variable reduction to the pole was applied to the data using Intrepid 4.5 software.

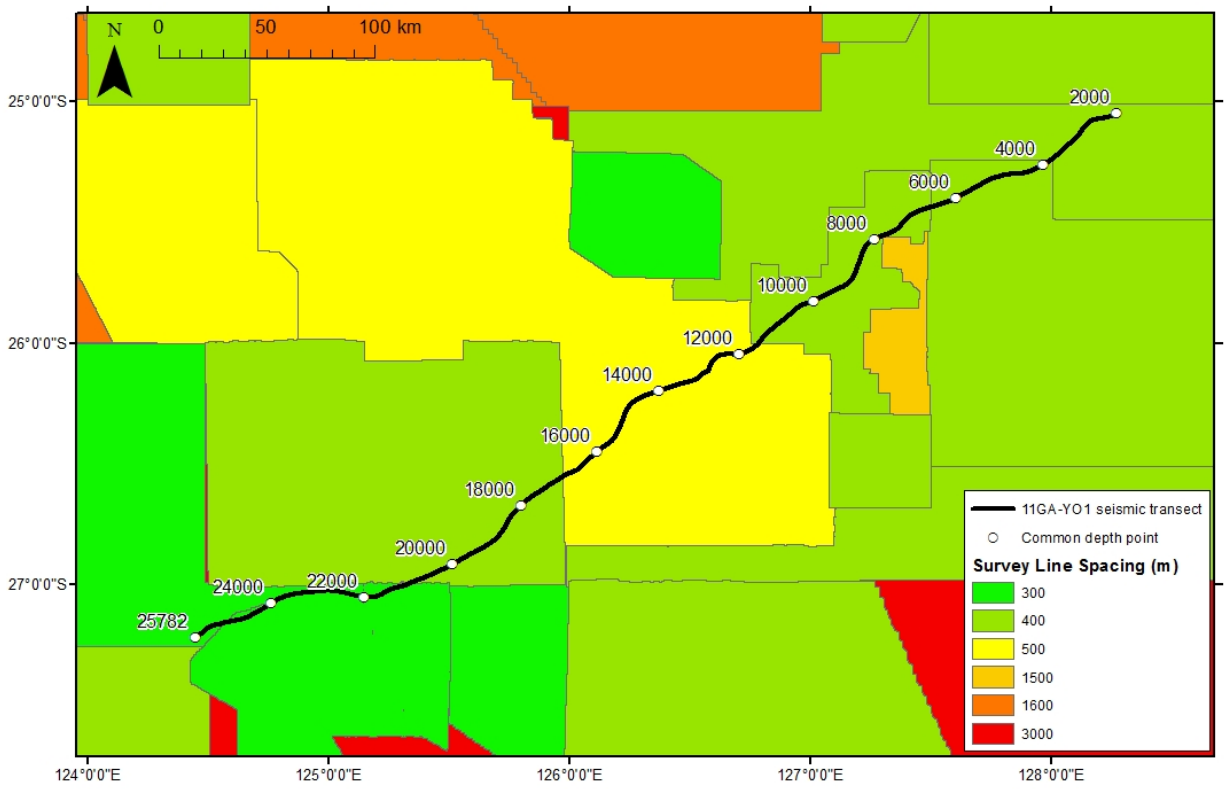

Figure 5.4 *Aeromagnetic survey coverage surrounding the 11GA-YO1 seismic line.*

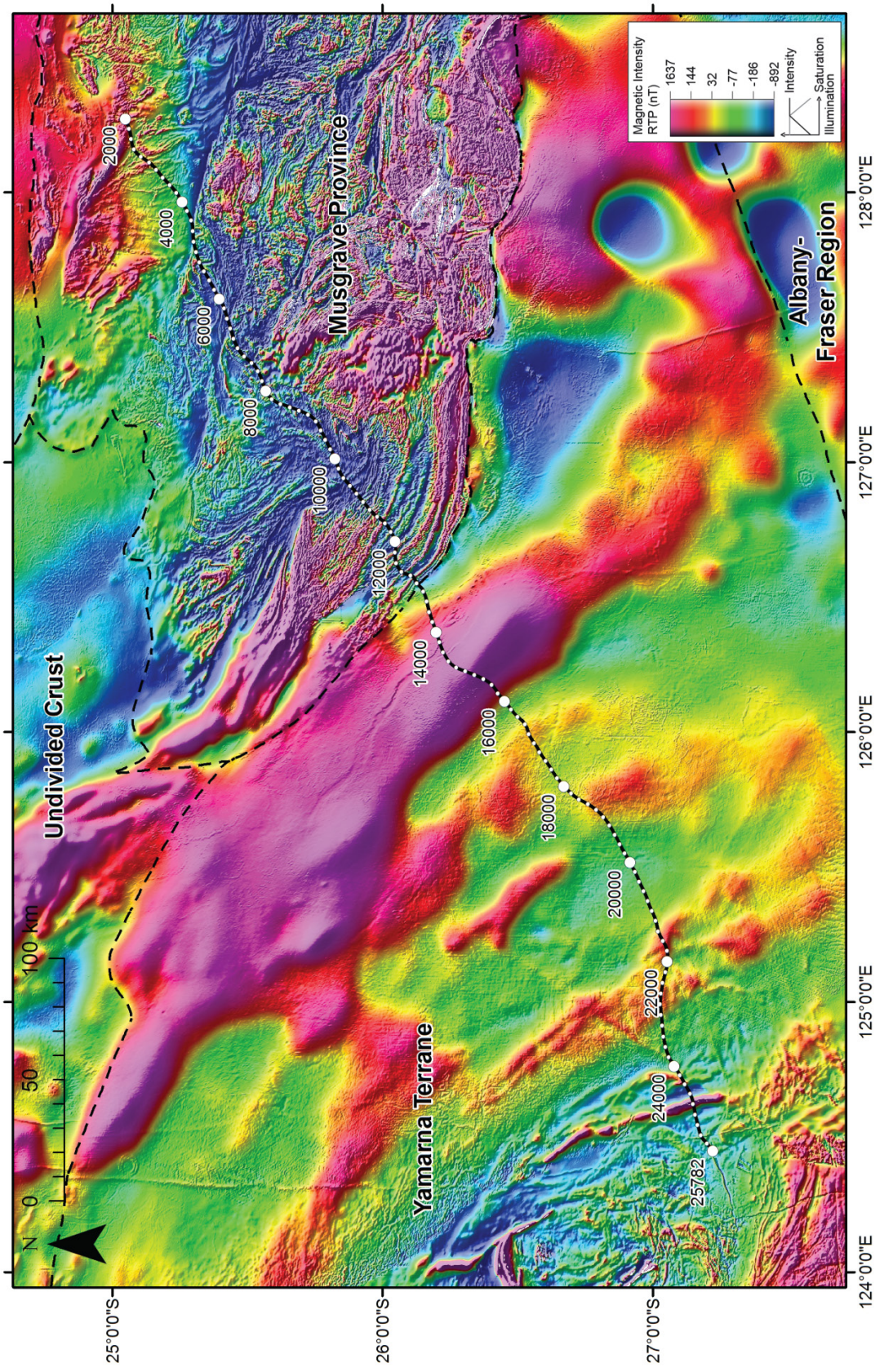

Figure 5.5 *Total magnetic intensity grid (reduced to the pole) of the study area, with dashed lines representing the major province boundaries.*

Seismic interpretation

The seismic reflection data used in this study comes from the 11GA-YO1 deep-seismic reflection survey and also from industry-collected shallow-seismic reflection data acquired during the 1980s (locations shown in Figure 5.6).

The interpretation of the 11GA-YO1 seismic data used in this study is derived from Korsch et al. (2013) and Howard et al. (2013). This seismic transect consists of 484 km of deep-crustal (22 second two-way travel time) seismic reflection data and was collected as a collaborative project between Geoscience Australia and the Geological Survey of Western Australia (GSWA). The seismic data provides an insight into the structures associated with the western Officer Basin, west Musgrave Province, northeast Yilgarn Craton and the Mohorovičić discontinuity (Moho). The 11GA-YO1 seismic interpretation was the primary constraint used in forward modelling and in the construction of 3D architectures in the geological model.

The interpretations from shallow-seismic reflection data were made by GSWA and consist of 4268 km of 2D data also reprocessed by GSWA (via contractor Western Geco) in 2002, and 2165 km of data reprocessed by Japan National Oil Corporation in 1996. The original data were acquired by Shell in 1980–82 (4628 km), News Corporation in 1983–84 (1132 km), and Swan Resources in 1981 (106 km). Together the shallow-seismic datasets make up a low-density regional grid with a line spacing ranging from 2.5–40 km (Figure 5.6). The data quality is highly variable and only provided useful information down to the base of the Officer Basin. Many of the complicated structural features within the Officer Basin, such as minor faults and salt intrusions have not been included in the forward or 3D models for simplicity.

Solid geology

The solid geology map utilised for this study was compiled by Schofield et al. (2013, in prep) and drew extensively on published 1:250 000 regional geological maps and analysis of aeromagnetic data (Figure 5.6). Gravity, drill hole, and geochronological data were also used during the interpretation.

This solid geology map aims to represent the major pre-Neoproterozoic lithologies and regional scale faulting. The study region contains varying degrees of geological complexity. This is a direct function of the amount of geology exposed at the surface rather than a reflection of the actual lithological complexity. As a result, there are two distinct subregions within the study area; an undifferentiated basement terrain beneath the Officer Basin; and a number of structurally complex, near-surface lithologies within the Musgrave Province.

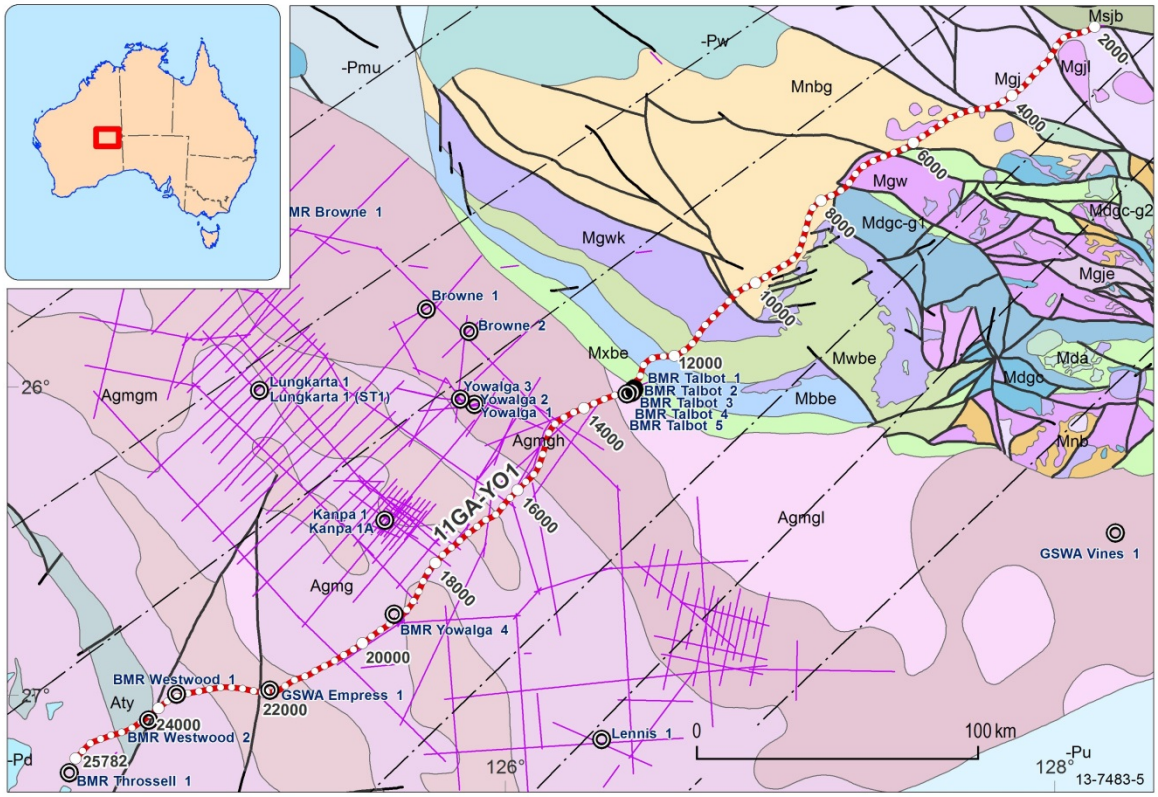

Figure 5.6 *Solid geology map of the area surrounding the 11GA-YO1 seismic line. The extent of this image corresponds with the extent of the 3D geological model (Lambert conformal conic projection GDA94). Also shown is the location of industry-collected seismic data, drill holes and forward models.*

Drill holes

Drill hole data was used in conjunction with the seismic data to constrain the thickness of the Officer Basin throughout the study area. The following drill holes were used in this study (locations shown in Figure 5.6):

- BMR Browne 1
- Browne 1 and 2
- Yowalga 1, 2, and 3
- BMR Yowalga 4
- GSWA Vines 1
- BMR Talbot 1, 2, 3, 4 and 5
- Lungkarta 1, 1 (ST1)
- Kanpa 1 and 1A
- GSWA Empress 1A
- BMR Westwood 1 and 2
- BMR Throssell 1
- Lennis 1

AusMoho

The AusMoho 2012 model provides an estimate of the depth to the Mohorovičić discontinuity (referred to here as the Moho) across Australia based on seismological estimates (Salmon et al., 2012). In particular, AusMoho is derived from onshore and offshore seismic refraction experiments, receiver function techniques and picks from more than 10500 km of full-crustal seismic reflection profiles. In the study area, however, the only constraint on the depth to the Moho comes from the 11GA-YO1 seismic line. This means that while AusMoho still provides our best estimate of the depth to Moho, our confidence in this estimate either side of the seismic line is significantly lower.

Geophysical studies

The following section describes the techniques used to investigate the gravity and magnetic data.

Interpretation of gravity and magnetic data grids

A broad-wavelength gravity high is observed between CDP 6000 to 12800 on the 11GA-YO1 seismic line and lies within the Musgrave Province (Figure 5.3). This contrasts with the sediments of the Officer Basin, which cross the seismic line from CDP 12800 to the end (CDP 25782), where a broad-wavelength gravity low is observed.

The Musgrave Province also correlates with a large number of short-wavelength magnetic anomalies with a stippled/mottled texture, typical of volcanic rocks (Figure 5.5). A smooth texture is seen from CDP 12800, where the sediments of the Officer Basin are interpreted to be ~7 km thick, to ~CDP 22000, where the sediments are interpreted to be ~2 km in thickness (Korsch et al., 2013).

The Yamarna Terrane of the Yilgarn Craton is interpreted to extend below the Officer Basin (Korsch et al., 2013) and correlates with a series of magnetic anomalies that trend northwest-southeast (Figure 5.5).

CDP 2000 to 8000

Towards the northeast section of the 11GA-YO1 seismic line the bimodal volcanics of the Tjauwata Group correlate with a stippled texture in the magnetic data (Figure 5.7). This stippled texture overprints a number of contact aureoles from plutons (Figure 5.7). These plutons are interpreted to be Giles Event granites intruding into the Pitjantjatjara Supersuite. Together these anomalies define a distinct geophysical terrane that is separated from a terrane to the south by the Woodroffe Thrust at CDP 4500 (Figure 5.7b).

South of the Woodroffe Thrust, magnetic anomalies highlight an intensely folded region that correlates with the Kunmarnara Group (Figure 5.7). These anomalies are truncated and offset by the Mitika Fault and highlight a dextral sense of movement across this fault.

In the gravity data (Figure 5.7c), two gravity ridges are highlighted which correlate with outcrops of Giles Suite gabbros and mafic/ultramafic intrusions. In particular, they suggest that the Giles Suite extends towards the seismic line between CDP 7000 to 8000.

CDP 8000 to 16000

The Kunmarnara Group is interpreted to extend south to ~CDP 10400 where the continuous and linear nature of weakly to moderately magnetic anomalies suggest it is being dragged into a regional shear zone (Figure 5.8b).

Thicker successions of the Bentley Supergroup interpreted in the seismic data (Howard et al., 2013) correlate with gravity highs, while thinner sections, such as where the Kunmarnara Group is exposed, correlate with relatively low amplitude gravity anomalies (Figure 5.8c).

At CDP 12800 the Windularra Fault separates the Musgrave Province from the Officer Basin. Across this fault, a transition into a smoother magnetic texture and a regional gravity low are seen (Figure 5.8). A broad-wavelength magnetic high, up to 1000 nT, extends from CDP 12800 to 16000 (Figure 5.8b). The smooth nature of this anomaly and its broad wavelength suggest that the source causing it lies below the sedimentary rocks of the Officer Basin.

Overprinting this magnetic high is a distinct depression that correlates well with the near surface expression of an interpreted salt diapir in the seismic data (Korsch et al., 2013). In profile, it is clear that where the salt is reaching the surface a ~40 nT depression occurs in the magnetic data (Figure 5.9). Salt diapirs are buoyancy driven and can pierce through overlying strata, truncating them as they rise. The Table Hill Volcanics (a basalt layer within the Officer Basin) is deformed in this way and creates a distinct gravity peak at -79 mGal as it curves upwards towards the surface (Figure 5.9). The regional gravity data also highlights a broad gravity low that matches well with the extent of this salt diapir at depth (Figure 5.8c).

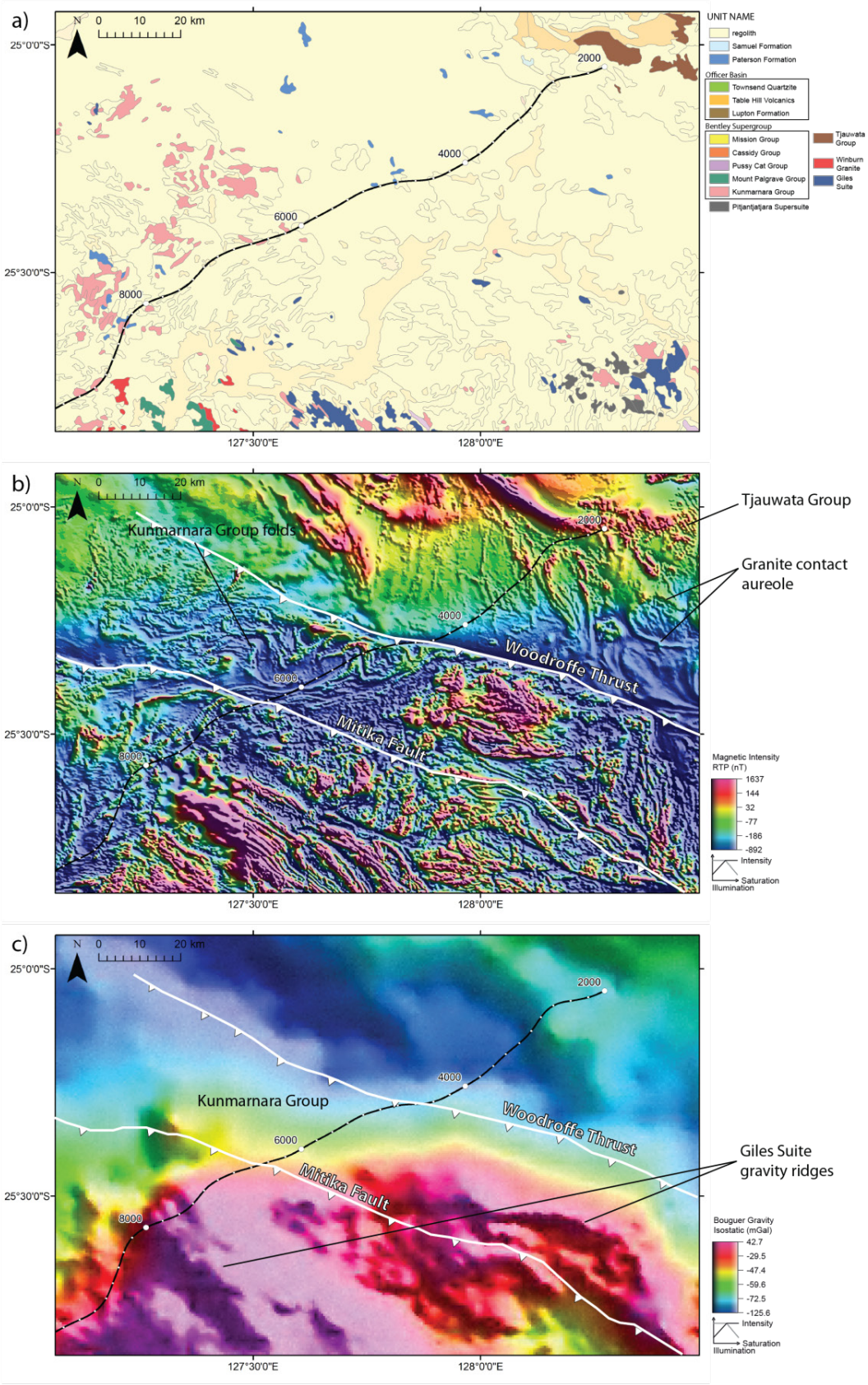

Figure 5.7 *CDP 2000 to 8000 of seismic line 11GA-YO1 on a) 1:1 million surface geology map, b) total magnetic intensity RTP grid and c) isostatic residual Bouguer gravity grid.*

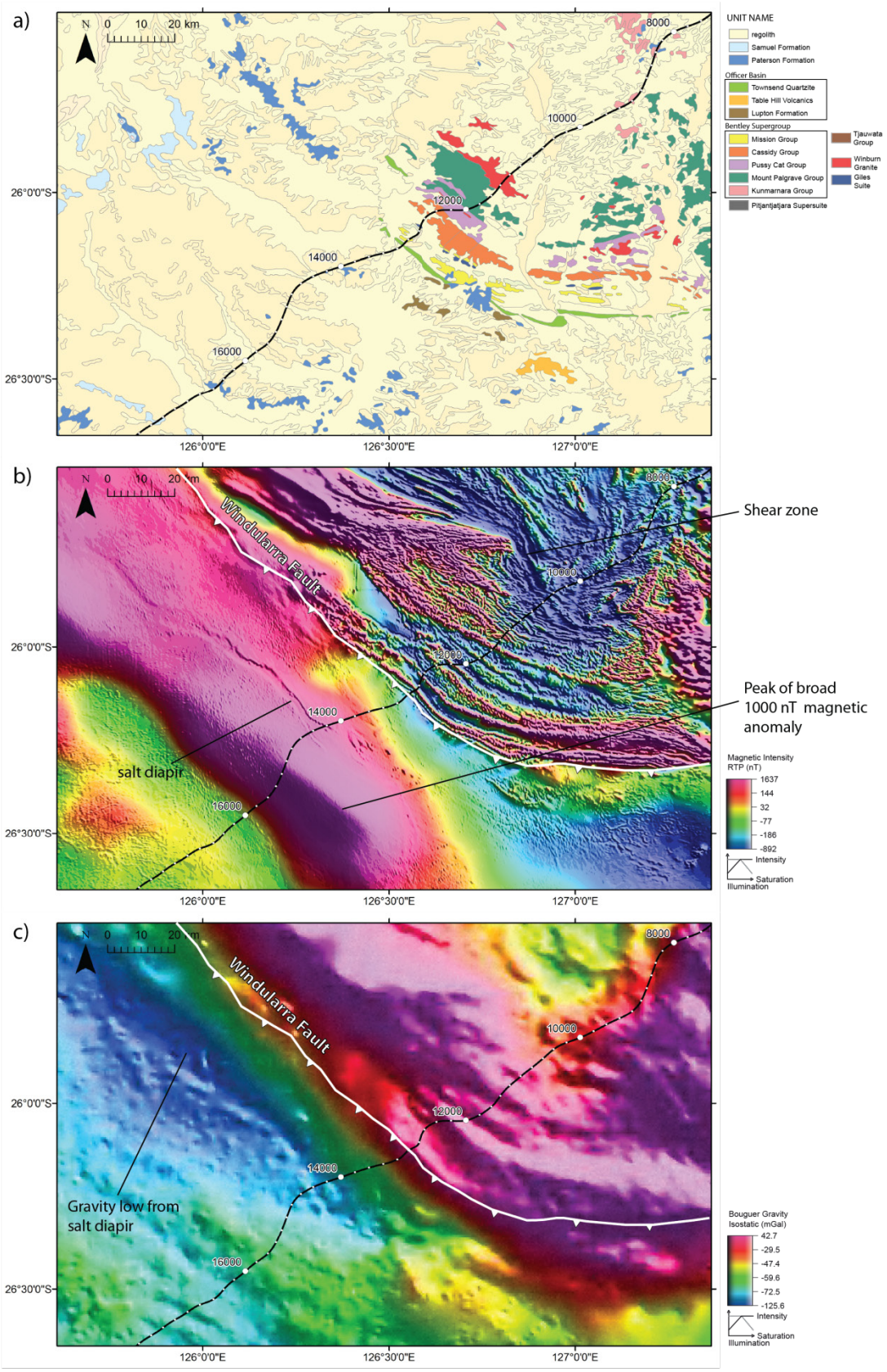

Figure 5.8 *CDP 8000 to 16000 of seismic line 11GA-YO1 on a) 1:1 million surface geology map, b) total magnetic intensity RTP grid and c) isostatic residual Bouguer gravity grid.*

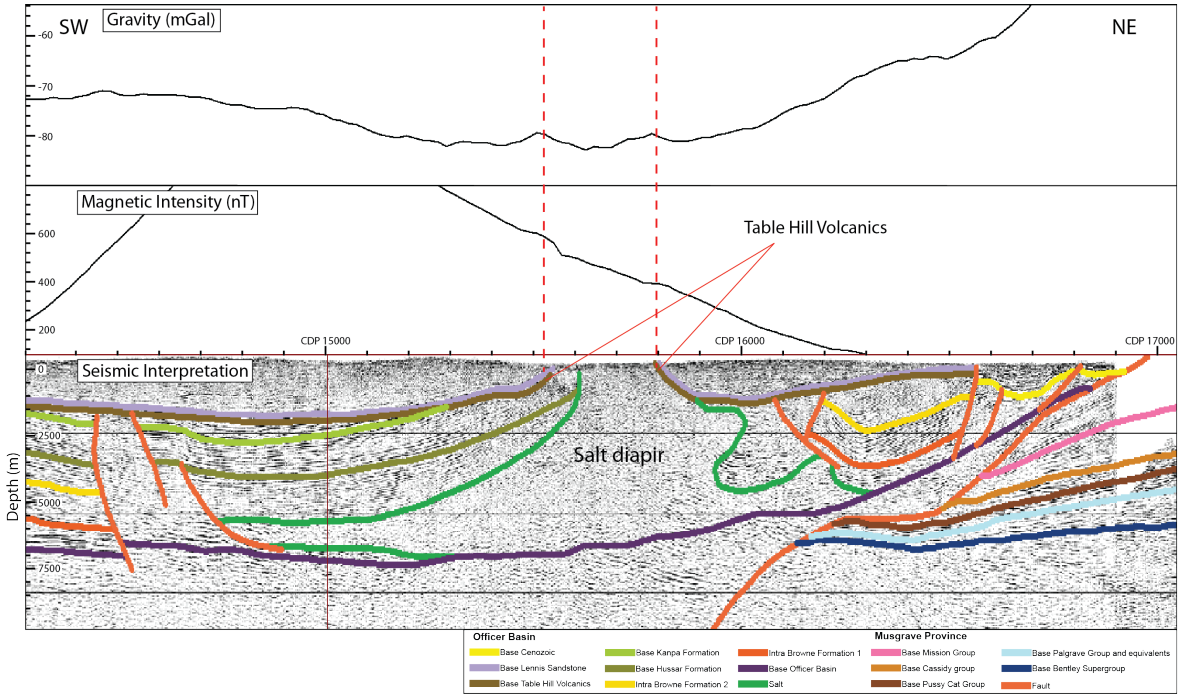

Figure 5.9 *Gravity and magnetic profile over the 11GA-YO1 seismic line highlighting anomalies associated with an interpreted salt diapir. Dashed red lines highlight gravity peaks associated with the Table Hill Volcanics (basalt) as well as highlighting the magnetic depression between them.*

CDP 16000 to 25782

In this section of the line, surface geology outcrops are limited and only reveal information on the Officer Basin and overlying sediments (Figure 5.10a). The gravity and magnetic data, however, reveals information on units underlying the Officer Basin (Figure 5.10b and 5.10c). In particular, a short-wavelength magnetic high reaching ~2000 nT stands out as a unique feature that crosses the line at ~CDP 25000. Based on its intensity and distribution this anomaly appears to be related to a hook shaped feature to the northwest that lies within Greatland Gold's Ernest Giles Project area (Figure 5.10b).

Greatland Gold have intersected structurally-altered banded iron formation and mafic rock in drill holes at the Ernest Giles Ranges in the Yamarna Terrane of the Yilgarn Craton (Greatland Gold, 2010). These areas of banded iron formation and mafic rock appear in the data as both gravity and magnetic highs. Using these and other distinguishing characteristics (such as the style, shape and distribution of the anomalies) similar units are interpreted to lie below the Officer Basin between CDP 24000 and CDP 25000 and have been incorporated into the seismic interpretation (Korsch et al., 2013).

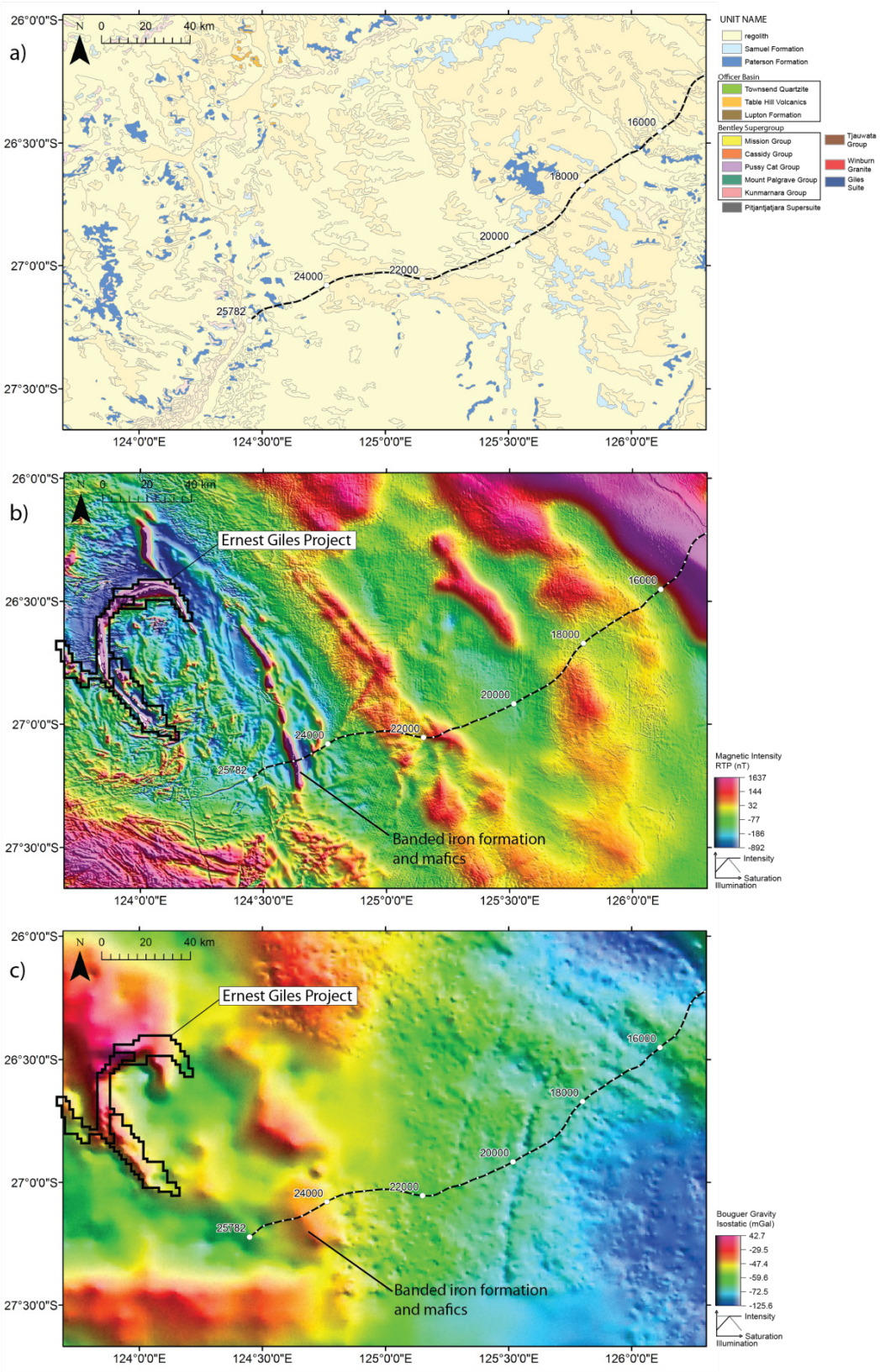

Figure 5.10 *CDP 16000 to 25782 of seismic line 11GA-YO1 on a) 1:1 million surface geology map, b) total magnetic intensity RTP grid and c) isostatic residual Bouguer gravity grid. The thick black outline indicates the area occupied by Greatland Gold for the Ernest Giles Project.*

Multiscale edge detection

Multiscale edge detection is a technique for highlighting areas of contrast in potential-field data (Archibald et al., 1999). The areas of contrast are represented as edges and are generated across a range of levels of upward continuation. When viewed together, the edges indicate where contacts with contrasting properties are occurring in the subsurface geology. Discontinuities or interfaces where contrasting rock materials occur may include faults, unconformities or intrusive contacts.

Multiscale edges were generated using Intrepid software (v4.5) with the multiscale edge detection function. For both the gravity and magnetic grids, 10 upward continuation levels were specified, with each level varying by a factor of 1.4, using the Canny points calculation method. A variable reduction to the pole (RTP) was applied to the magnetic grid before undergoing multiscale edge detection. Features in the multiscale edges were delineated following Archibald et al. (1999) and Holden et al. (2000), who infer that higher continuation levels correspond to features at relatively greater depths, and that the orientation of the multiscale edges relate to the orientation of the contact.

Gravity multiscale edges

Two major contacts are defined by multiscale edges associated with the Musgrave Province (Figure 5.11). The first is a northwest-southeast trending multiscale edge that marks the northern most extent of the gravity high within the Musgrave Province. Multiscale edges from low levels of upward continuation cross the seismic transect at ~CDP 5400 and higher levels cross the seismic transect at ~CDP 7000 (Figure 5.11). Together these edges define a south- to southwest-dipping contact that matches with the interpreted dip direction of the Woodroffe Thrust seen in the 11GA-YO1 seismic interpretation.

The second major contact coincides with the southwest margin of the Musgrave Province where a south- to southwest-dipping contact is observed (Figure 5.11). This contact coincides with the known dip direction of the Windularra Fault which separates the bimodal volcanics of the Bentley Supergroup from the sediments of the Officer Basin.

Between CDP 21400 and CDP 22800 a north-south trending set of edges define an east-dipping contact (Figure 5.11). One possibility is that these edges are related to the Mesoproterozoic Manunda Basin, interpreted by Korsch et al. (2013), which thickens towards the east beneath the Officer Basin.

Magnetic multiscale edges

The most distinctive magnetic multiscale edges are defined by the broad-wavelength magnetic high that crosses the seismic line from ~CDP 12800 to 16000 (Figure 5.12). Both a southwest-dipping contact and a northeast-dipping contact are evident in the multiscale edges and suggest that the body causing the magnetic high trends towards the northwest. This follows the general trend of the geology seen throughout much of the Yamarna Terrane.

The Windularra Fault is also highlighted by multiscale edges that indicate a southwest-dipping contact. This contrast is due to the low magnetic susceptibility of the Officer Basin sediments being faulted against the bimodal volcanics of the Bentley Supergroup.

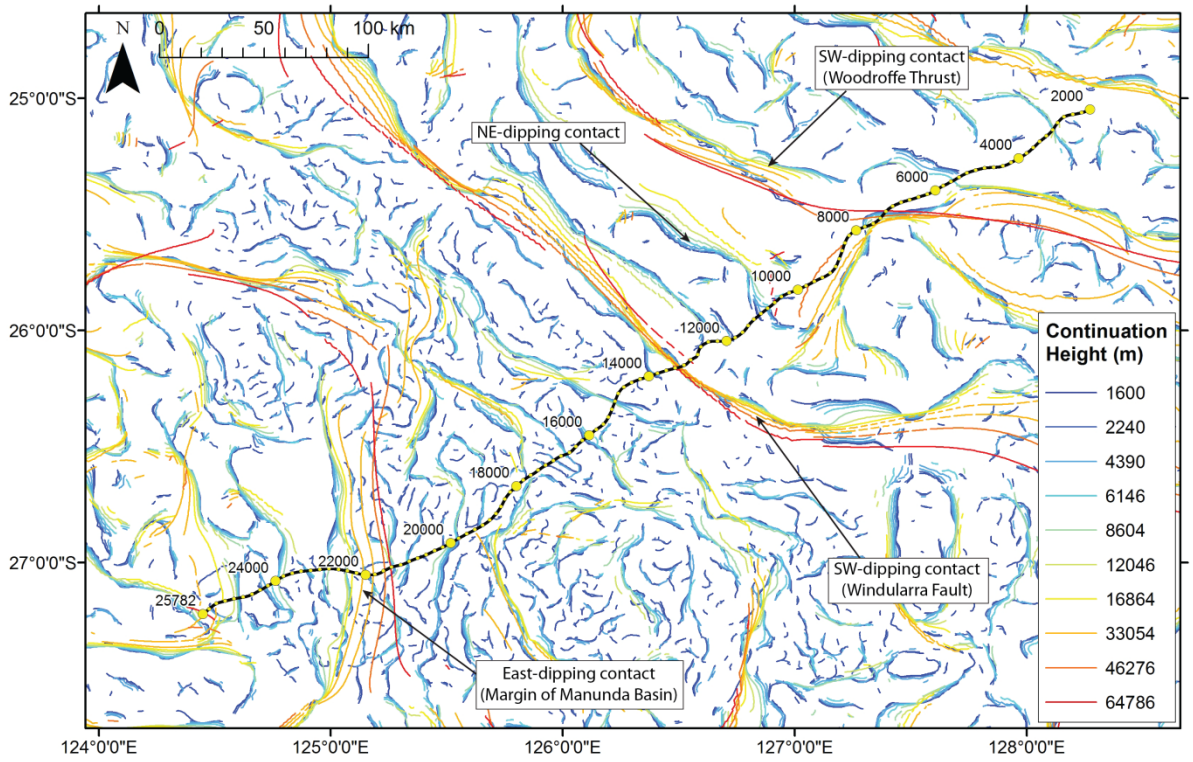

Figure 5.11 *Multiscale edges derived from gravity data.*

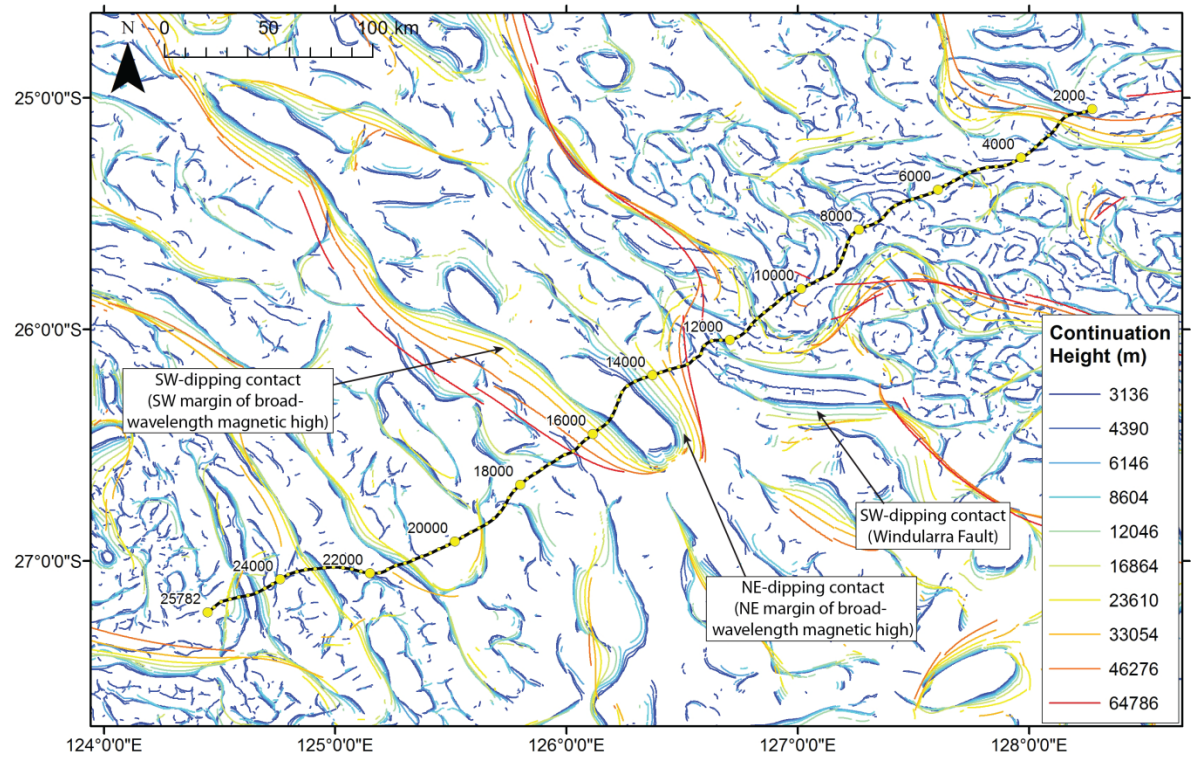

Figure 5.12 *Multiscale edges derived from magnetic data.*

Forward modelling

Forward modelling was used for two purposes:

1. To test the validity of the geometries in the 11GA-YO1 seismic line interpretation with respect to gravity and magnetic data, and,
2. To extend the seismic interpretation into 3D space by forward modelling sections sub-parallel to the 11GA-YO1 seismic section (locations shown in Figure 5.6).

The forward modelling described here refers to the process of attributing density or magnetic susceptibility to bodies and calculating their gravity or magnetic response respectively. The calculated response is then compared to the observed data, where a good fit between the two indicates that the modelled bodies are geophysically valid.

Gravity and magnetic data were extracted along the 11GA-YO1 seismic line as well as along sub-parallel sections using the dataset resampler tool in Intrepid v4.5. Forward models were then created using ModelVision v11.0 software, extending from 600 m above the datum (sea level) to 65400 m below. To approximate the three-dimensional geometries of the interpreted bodies they were extended into three-dimensional space by extending their strike length to a distance large enough, perpendicular to the section, to avoided edge effects. The scales shown on the forward models (Figures 5.13, 14, and 15) are in kilometres, and assume that one second of two-way travel time (TWT) is equal to three kilometres depth (based on an average crustal velocity of 6000 m/s).

In this study, the observed gravity data was the main dataset used to constrain the forward modelling. Magnetic data across the region are dominated by short wavelength anomalies and relate to near-surface features that generally bear little relation to the crustal-scale interpretations made in this study. Only magnetic anomalies interpreted to be associated with greenstone belts were modelled.

Forward modelling of potential-field data is inherently non-unique. Although it is possible to generate a model that is consistent with both the seismic interpretation and the observed potential-field data, this represents only a single plausible interpretation. Further investigation of the model space (including the addition of further geological constraints) should be undertaken to improve the confidence of these interpretations.

Forward models of the 11GA-YO1 seismic line

The geometries used in the forward modelling of seismic line 11GA-YO1 were generated using the seismic reflection interpretations by Korsch et al. (2013) and Howard et al. (2013). A progression of forward models is shown in Figure 5.13 to highlight the effect of the geology on the modelled gravity profile.

The simplest model consists of two layers; the crust and upper mantle (Figure 5.13a). The crust is modelled with a density of 2.83 g/cm^3 to represent continental crust (Christensen and Mooney, 1995) and a density of 3.31 g/cm^3 is used to model the upper mantle (Poudjom Djomani et al., 2001). This model shows the effect of the Moho on the gravity profile where a regional low, reaching -120 mGal, occurs across the Musgrave Province due to the thickened crust in this region.

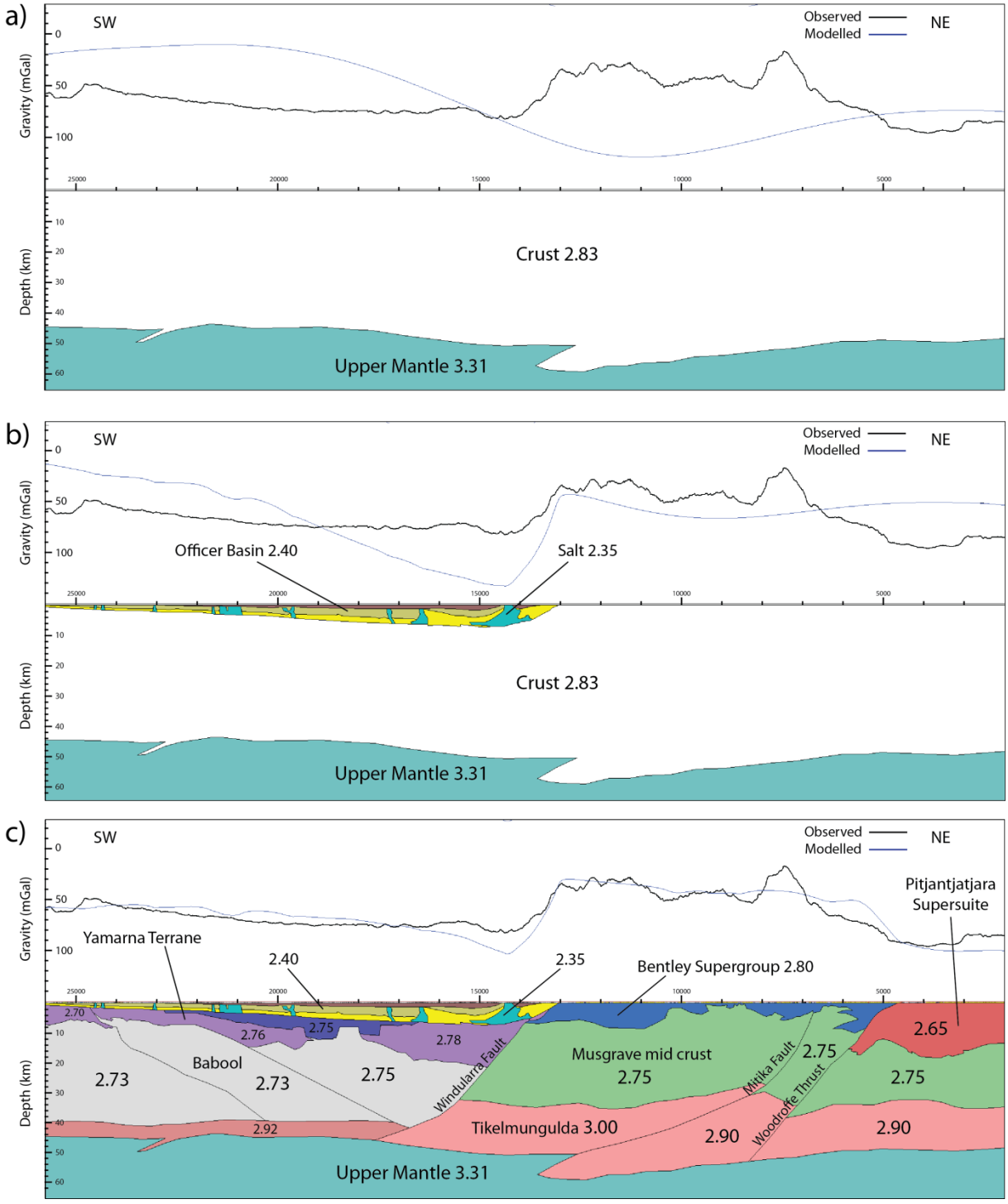

Figure 5.13 *Forward models along seismic line 11GA-YO1 with densities displayed as g/cm^3. Three models are presented: a) a two layer model highlighting the effect of the Moho, b) a two layer model with the addition of the Officer Basin, and c) a 3 layer crust with the Officer Basin included.*

When the low density sedimentary rocks of the Officer Basin are included in the model with a density of 2.40 g/cm^3 (Emerson, 1990; Telford et al., 1990), a large contrast with the surrounding rock types is created between CDP 13000-14000 (Figure 5.13b). Within the Officer Basin a number of salt intrusions interpreted by Korsch et al. (2013) are included and are modelled with slightly lower densities (2.35 g/cm^3) that could represent halite or gypsum (Emerson, 1990; Telford et al., 1990).

The third model consists of a 3 layer crust that also includes the Officer Basin (Figure 5.13c). The rock types at mid to lower crustal levels are not known so estimated values for these rocks are derived from Rudnick and Fountain (1995) and Christensen and Mooney (1995). A combination of the Bentley Supergroup with a density of 2.80 g/cm^3 (to represent bi-modal volcanics with minor sediments) and a relatively shallow lower crust beneath the Musgrave Province (the Tikelmungulda Seismic Province), create a regional gravity high across the Musgrave Province. This contrasts with the Pitjantjatjara Supersuite towards the northeast and the Officer Basin to the southwest which create broad-wavelength gravity lows (Figure 5.13c).

Once the broad scale structures are accounted for further detail can be added to the forward models. Three forward models are shown in Figure 5.14, which incorporate further detail and highlight areas of inconsistency between the seismic interpretation and the gravity data.

Figure 5.14a shows the gravity response of bodies with geometries derived from Korsch et al. (2013) and Howard et al. (2013). In this model the Winburn Granite is modelled with a representative value for granite of 2.64 g/cm^3 (Telford et al. 1990). This density causes a large gravity low within the Musgrave Province, which does not match the observed data (Figure 5.14a).

Figure 5.14b shows an alternative model where the Winburn Granite is divided into sections which progress from low densities at the surface to denser units at the base. This was done to reflect a fractionated magma chamber where felsic units are separated from more mafic units. A closer fit to the observed data is achieved with this change to the Winburn Granite.

Also included in this model are Giles Suite gabbros and mafic/ultramafic intrusions between CDP 7000 to 8000 (Figure 5.13b). A density of 3.00 g/cm^3 is used to account for the gravity high, reaching -17 mGal, in this region.

A body causing a 1000 nT magnetic high between CDP 12800 and 16000 is suggested to lie below the sedimentary rocks of the Officer Basin based on its broad-wavelength and smooth texture (Figure 5.8b). This suggests it lies within the Yamarna Terrane, which is interpreted by Korsch et al. (2013) to extend as far northeast as the Windularra Fault beneath the Officer Basin (Figure 5.13b). A ~1 km thick, northeast-dipping slab has been included in the model with a density of 3.20 g/cm^3 and a magnetic susceptibility of 1 SI between CDP 14000 to 15500 in an attempt to account for this broad-wavelength magnetic high (Figure 5.13b). These physical properties are consistent with banded iron formation (BIF) and mafics. These lithologies have been identified in other locations within the Yamarna terrane (Greatland Gold, 2010).

Figure 5.14c shows the second alternative to the 11GA-YO1 interpretation where the Winburn Granite is reduced to a 0.3–1 km deep body. With this reduction the fit of the modelled to the observed gravity anomalies is improved. Overall, thicker sections of the Bentley Supergroup correlate with gravity highs across the Musgrave Province. Giles Suite gabbros and mafic/ultramafic intrusions are also included in areas where extra density is required near the surface to account for gravity anomalies throughout the Bentley Supergroup. Shorter wavelength gravity peaks within the Bentley Supergroup correlate with basaltic units that crop out at the surface, such as those within the Mission and Cassidy groups.

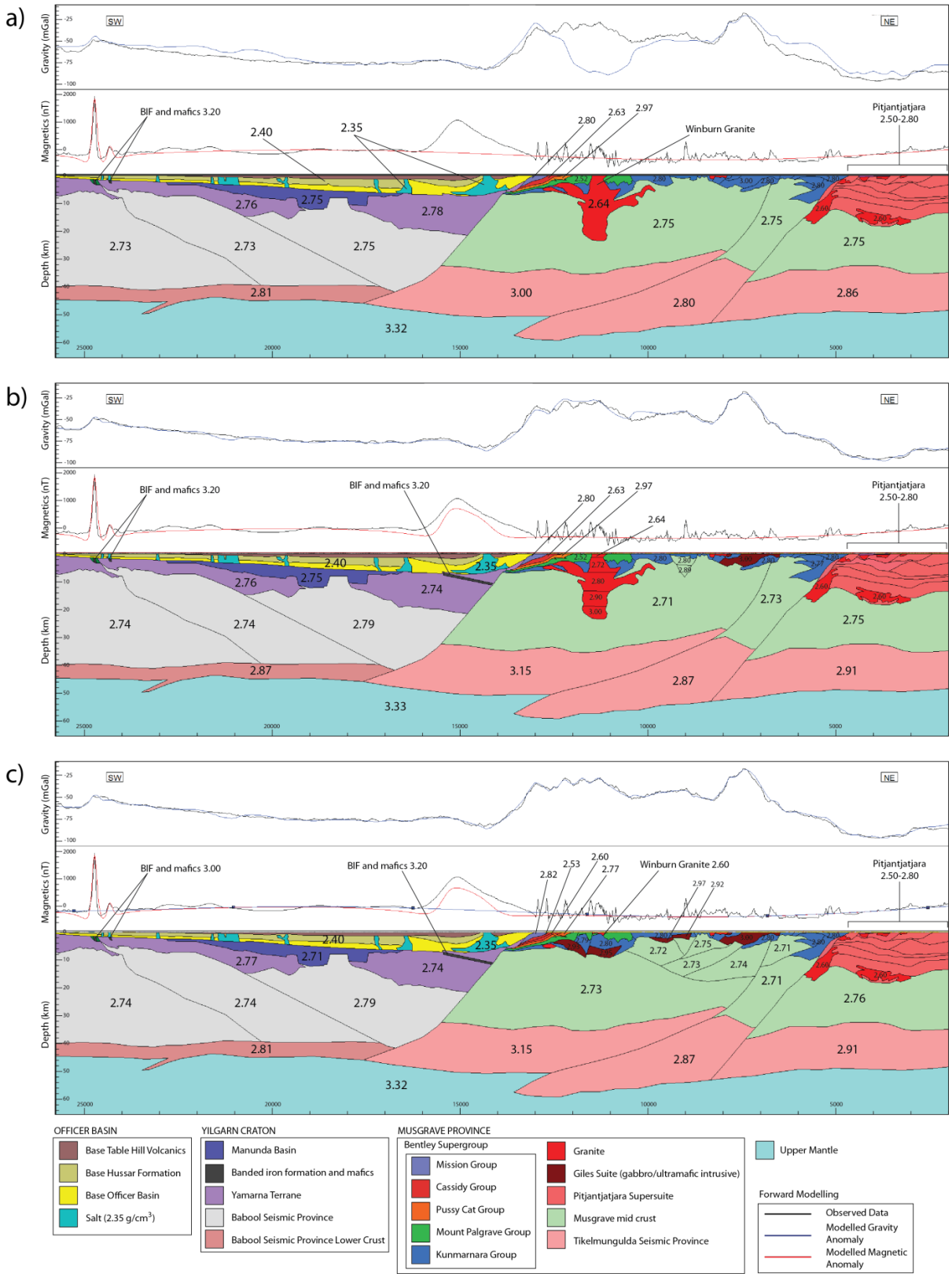

Figure 5.14 *Forward models along seismic line 11GA-YO1 with densities displayed as g/cm^3. Three models are presented: a) geometries as per Korsch et al. (2013) and Howard et al. (2013), b) the Winburn Granite divided into felsic layers near the surface and mafic layers at depth, and c) the Winburn Granite retained as a smaller near-surface intrusion.*

Korsch et al. (2013) has interpreted several zones within the Officer Basin as salt due to the lack of reflectivity in the seismic data. However, Holzschuh et al. (2013) suggests that some of these zones of low reflectivity may be due to other near surface Cretaceous and Permian sedimentary units such as the Paterson Formation, which may cause reflected energy penetration problems. In terms of the gravity response of these salt intrusions, the modelled profile shows that several depressions are caused by the modelled salt within the Officer Basin between CDP 16000 to 25000. These depressions do not match the observed gravity data and are not supported by it (Figure 5.15).

Additional forward models across the study area

To provide a framework to build the 3D geological model, several forward models (Figure 5.15) using gravity and magnetics data were generated to constrain the geometries of rock units away from the 11GA-YO1 seismic interpretation (the location of these sections is shown in Figure 5.6). Each forward model represents a cross section of the Earth from the surface through to the upper mantle (~ 66 km depth in total) and was constructed using the methodology outlined above. These forward models were built with a higher level of detail in the upper crust than has been incorporated into the 3D geological model. These upper crustal layers were not included in the 3D model due to the timing constraints of the project.

Although seismic data provides a constraint on the architecture beneath the seismic line, determining valid geometries away from the line required an iterative process. The first step was making an approximation of the architecture for the entire study area based on solid geology and potential field multiscale edges, keeping deviation from the seismic interpreted architecture to a minimum. These geometries were tested by forward modelling the gravity response for a series of geological cross sections that adequately covered the study region. Where a misfit occurred between the modelled response and the observed gravity field, the geometries were updated to reduce the misfit. An attempt was made to use the simplest architecture possible to explain the data.

Figures 5.15b and 5.15c both show a vertically elongate prism (coloured red), which is a simplified geometry for the Winburn Granite. This granite is interpreted by Howard et al. (2013) to be a large, composite, syn-volcanic intrusion, and in these models it is assigned a density value of 2.85 g/cm^3. Although this is not a realistic gravity value for granite, it was modelled with this value to match the observed gravity.

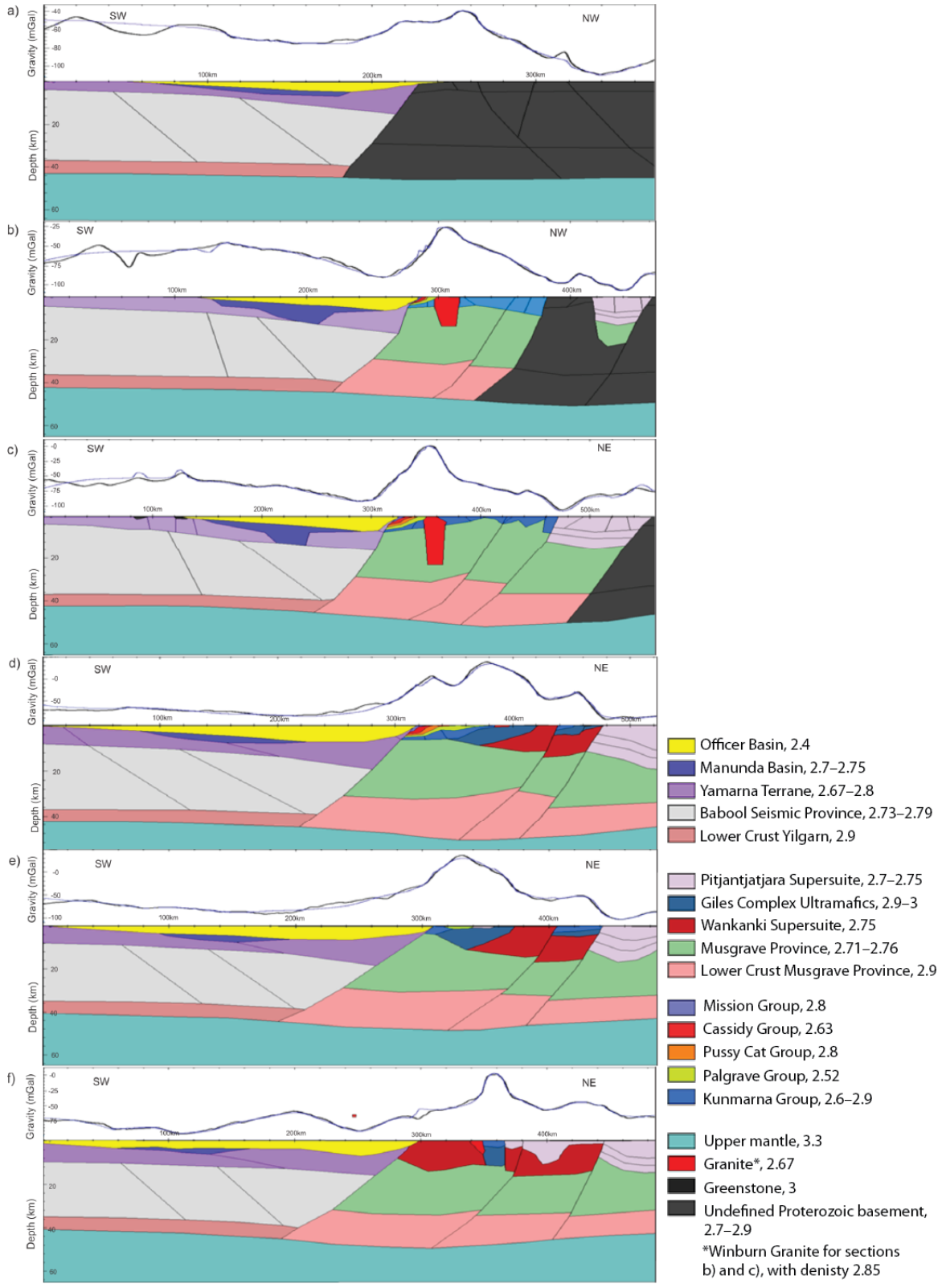

Figure 5.15 *Forward models of sections sub-parallel to the 11GA-YO1seismic line. These sections were used to constrain the 3D mode away from seismic line. The observed (black line) and calculated (blue line) gravity responses are displayed above each profile. Location of cross sections is shown in Figure 5.6, section (a) is the northwest most line and section (f) is the southeast most line. Legend is given with unit names and density values in g/cm^3.*

3D geological model

Introduction

One of the aims of this project was to compile all the available data for the Yilgarn Craton–Officer Basin–Musgrave Province (YOM) region into 3D space so that a series of volumes that represent the 3D architecture for the study area could be produced. At the surface, these volumes were constrained by solid geology interpretations. At depth, they were constrained using the 11GA-YO1 seismic interpretation and forward models. Linking the geometries and timing constraints between each cross-section was an iterative process, where by the validity of the 2D interpretation was tested in 3D space. Where geometries along the cross sections failed to link together in 3D space they were updated in 2D to reflect the necessary changes and retested against potential field data through forward modelling. The updated cross sections where then reimported into 3D space for further interpretation. This process was repeated until an internally consistent interpretation was achievable in 3D space that agreed with all the available constraints.

Conflict between the 3D model and the seismic interpretation

The final 3D model was built around a preliminary interpretation of the 11GA-YO1 seismic data. As a result, there are some inconsistencies between the YOM 3D model and the 11GA-YO1 seismic interpretation, especially associated with the interpretation of the Woodroffe Thrust and the Mitika Fault. The preliminary interpretation (Figure 5.16a) shows both the Woodroffe Thrust and Mitika Fault as steep, south-dipping faults, where both meet the Moho and the Mitika Fault offsets it. The final interpretation (Figure 5.16b) shows the Mitika Fault as a steep, south-dipping fault that on-laps a shallow, south-dipping Woodroffe Thrust. Additionally, a fault splays off the Woodroffe Thrust and meets the Moho directly beneath CDP 8200.

Data limitations

The different datasets used in this study have a large variation in coverage. The seismic data provided the most significant control with depth for the whole of crust architecture. Gravity and magnetics data have good regional coverage and were used extensively in conjunction with a solid geology map to extrapolate interpretations made in two dimensions on the seismic reflection line. Consequently, these data provided important spatial constraints to the 3D interpretations for the region. However, gravity and magnetic datasets inherently provide no unique solution for characterising source depth and, therefore, are most helpful when used in conjunction with the seismic interpretation as a starting model for the subsurface architecture. Drill hole data, while providing a hard constraint on lithology, has extremely poor regional coverage and depth extent, providing constrains for the Officer Basin only. These data could only be used as a guide to determine the maximum depth extent of the Officer Basin. Industry-collected seismic data provided the best coverage for determining the depth of the Officer Basin, but contained little information on the basement below. The crust-mantle boundary is constrained throughout the model space using the AusMoho surface (Salmon et al., 2012), which is reliant on both active and passive seismic techniques. Unfortunately, AusMoho is poorly constrained in the study region as the YOM seismic traverse is the primary constraint on it. Thus, the reliability of this surface diminishes with distance away from the seismic traverse.

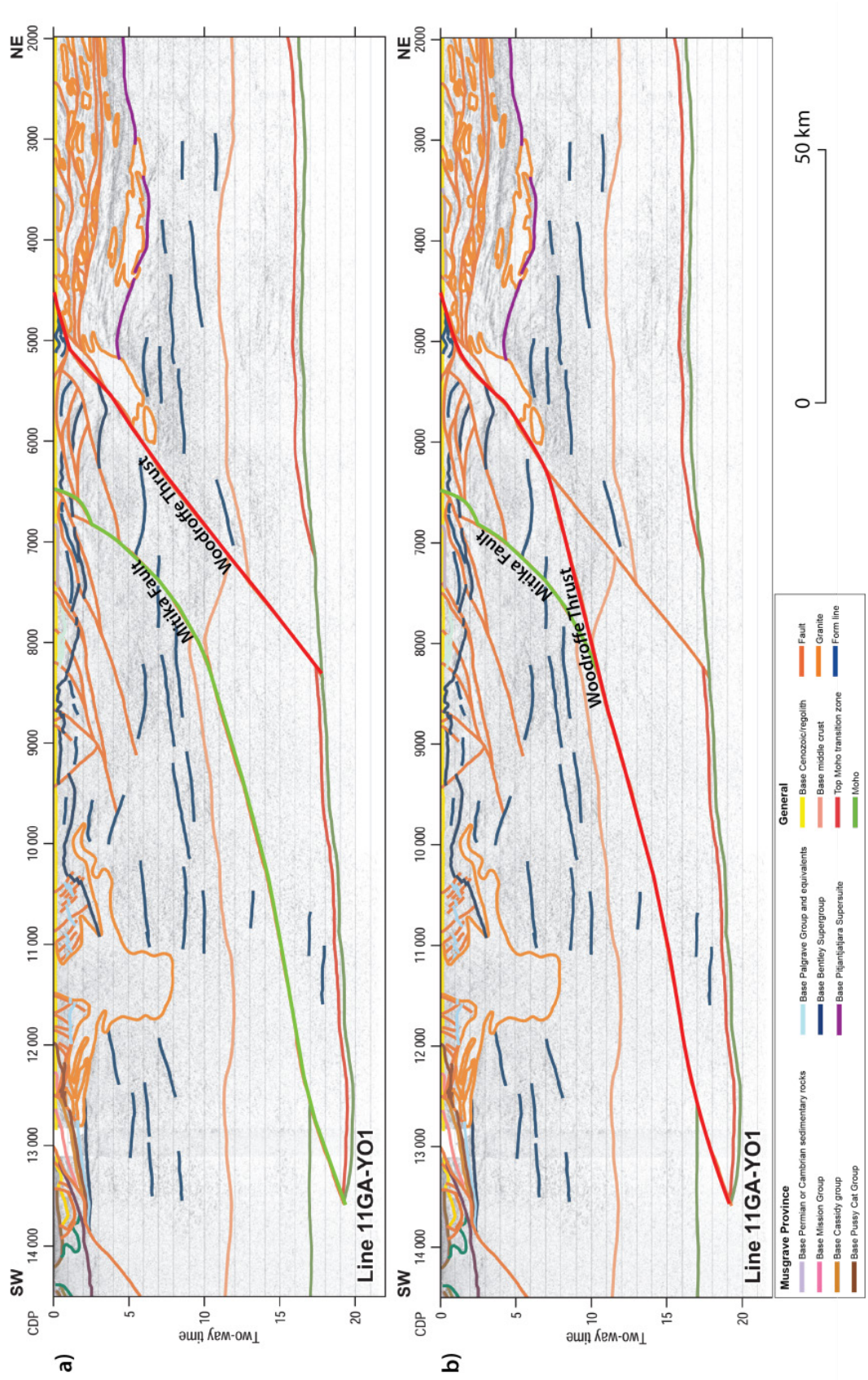

Figure 5.16 *Northeast end of YOM seismic line, annotated with preliminary interpretation (a) and final interpretation (b).*

Building the 3D architecture and description of major divisions

The 3D model is made up of a series of volumes representing provinces and lithological units. These volumes are separated by surfaces which represent major crustal faults, shear zones, unconformities, intermediate layers and the crust-mantle boundary. The surfaces are shown in Figure 5.17 and were constructed first in order to define the structural relationship between each geological division. There are four major divisions in the 3D model:

- Yilgarn Craton,
- Musgrave Province,
- Officer Basin, and,
- Upper mantle.

Each of these divisions are discussed in this section and are represented as volumes.

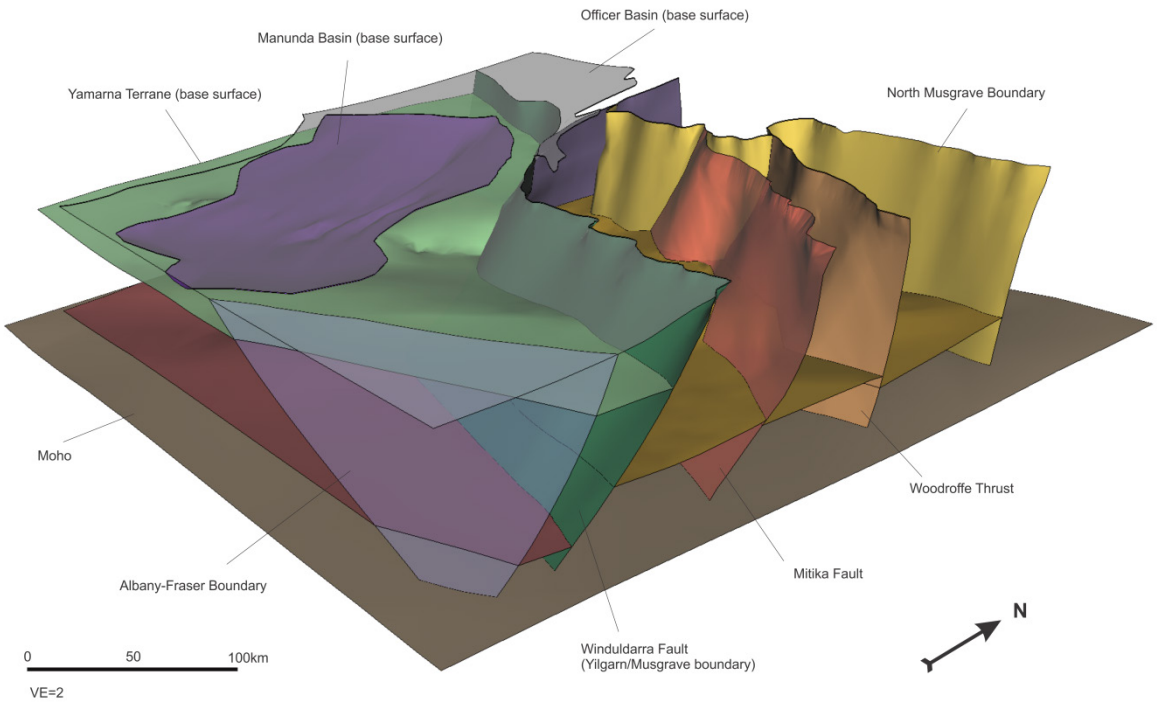

Figure 5.17 *Surfaces delineating the crustal-scale architecture in the Yilgarn Craton–Officer Basin–Musgrave Province model. These surfaces were used to constrain the geological volumes.*

Yilgarn Craton

The Yilgarn Craton is characterised by several northeast-dipping faults (along the plane of the seismic line) that lap onto the middle to lower crust boundary. Within the Yilgarn Craton model (Figure 5.18), the lower crust is interpreted to be a thin (5–7 km) basal layer. A seismically distinct upper zone of the Yilgarn Craton was identified on the seismic line and is defined by Korsch et al. (2013) as “non-reflective Yilgarn”. This is interpreted as the Yamarna Terrane that is exposed at the surface south west of the study area. The boundary between this zone and the mid-crust varies between depths of 7

km in the southwest down to 20 km in the northeast. Within the study region, the Officer Basin and the Mesoproterozoic metasedimentary rocks form an unconformable surface with the Yilgarn Craton.

One of the key aims of this study was to delineate the boundary between the Yilgarn Craton and the Musgrave Province, with the new seismic reflection data providing a constraint on the crustal architecture and geodynamic evolution of the region. The seismic interpretation indicates a southeast-dipping fabric across this boundary that strikes northwest to southeast at the surface. This southeast dip direction is in agreement with multi-scale edge detection data and is further supported by the gravity forward modelling over the two crustal blocks.

With the exception of known greenstone belts in the south western corner of the study region, the gravity field revealed little variation within the Yilgarn Craton, with the signal mostly being dominated by the overlying Officer Basin.

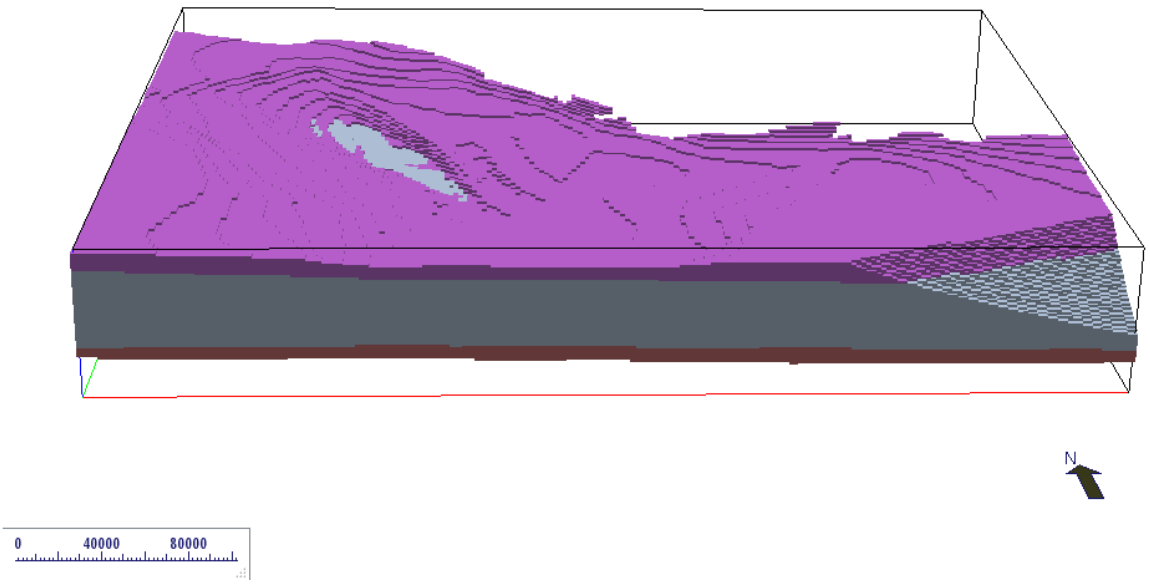

Figure 5.18 *3D model of Yilgarn Craton within the study area, including lower crust (red), the Babool Seismic Province (grey) and the Yamarna Terrane (purple).*

Musgrave Province

The Musgrave Province is characterised by a three layer crust. For the purpose of the 3D model, only two layers were built, a lower crust (called the Tikelmungulda Seismic Province) and an undivided Musgrave Province middle to lower crust (Figure 5.19). Upper crustal layers were built into forward models, but unfortunately were not extended into a full 3D interpretation due to time constraints on the project.

The boundary of the middle to lower crust varies between 35 km and 40 km in depth and is offset by the Woodroffe Thrust. The Woodroffe Thrust is a major, crustal-scale thrust that extends across the entire Musgrave Province. In the study region, it marks the boundary between the Bentley Supergroup and Pitjantjatjara Supersuite at the surface and dips to the southwest, terminating at the Moho, but not offsetting it. The southwest dip of the Woodroffe Thrust was distinguishable in the seismic data and

supported by the gravity forward modelling. The Tikelmungulda Seismic Province varies between 15 km and 25 km in thickness and is significantly thicker than the lower crust interpreted for the Yilgarn Craton.

The Mitika Fault is another crustal scale fault identified in the 11GA-YO1 seismic data that is included in the 3D model. It dips steeply to the south and offsets the Moho beneath the Musgrave Province.

The magnetic data over the Musgrave Province is dominated by short wavelengths, likely related to features at the near surface, and can be used to distinguish some lithological boundaries. However, gravity data was of greater use in defining the broader architecture of the Musgrave Province.

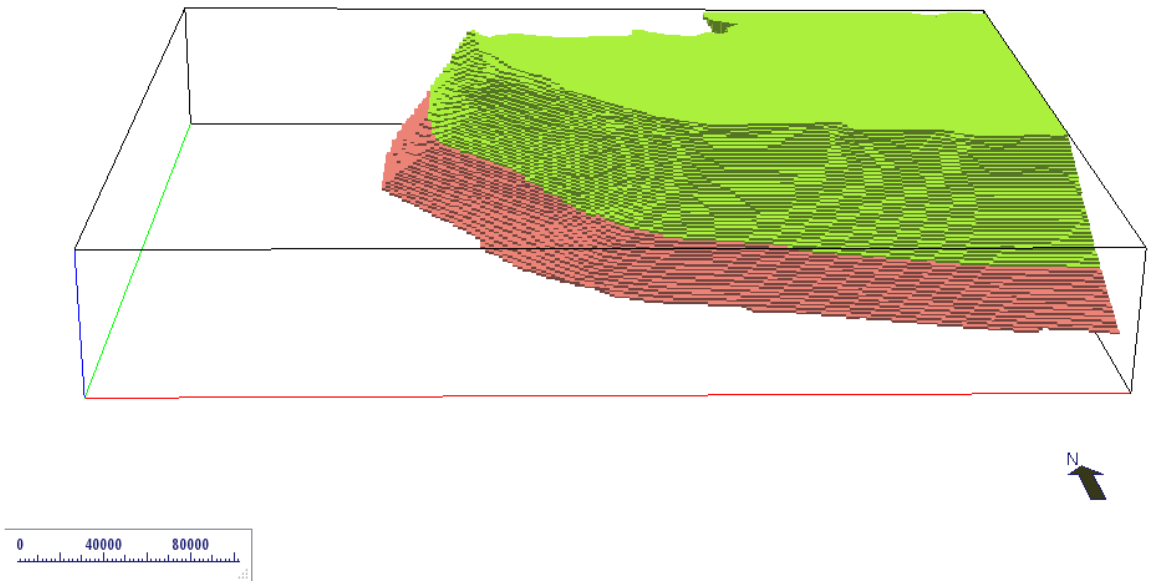

Figure 5.19 *3D model for the extent of the Musgrave Province within the study area, divided into a middle to lower crust (green), and the lower crust or Tikelmungulda Seismic Province (pink).*

Officer Basin

Within the study area, the Officer Basin trends northwest-southeast (Figure 5.20). The north-eastern margin is bounded by a thrust fault, separating it from the Musgrave Province, and represents the deepest (~6 km) part of the basin. This margin is defined by a large negative Bouguer anomaly, characteristic of other intracratonic basins of central Australia (such as the Amadeus and Ngalia basins). The southwest margin of the Officer Basin onlaps the Yamarna Terrane of the Yilgarn Craton, which outcrops southwest of the seismic line. Several faults and salt domes have been identified within the Officer Basin as part of a more detailed interpretation (Korsch et al., 2013) which are not included in the 3D model.

Away from the 11GA-YO1 seismic reflection line, the Officer Basin is the only section of the 3D model that is constrained by industry-collected shallow seismic reflection data. The coverage of industry seismic lines is sufficient over the study region so that a confident depth to basement could be provided (Figure 5.6). Gravity forward modelling indicates that the regional trend over the Officer Basin dominates the observed gravity signal. Magnetotelluric (MT) data described by Duan et al. (2013) showed the basin as a highly conductive layer, the spatial extent of which correlates with that defined by the seismic interpretations.

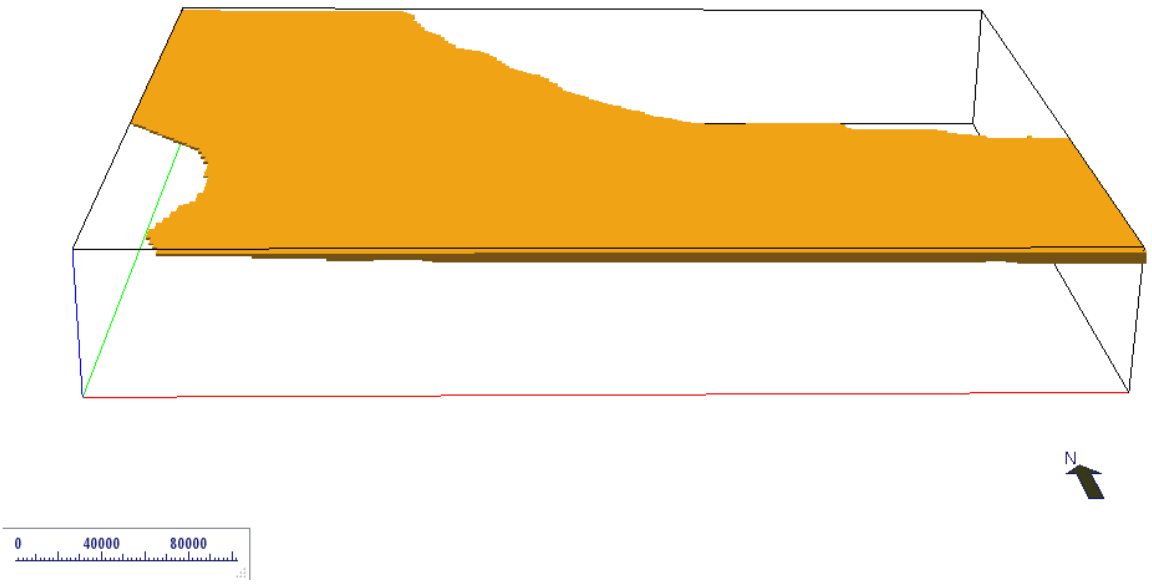

Figure 5.20 *3D model of the Officer Basin within the study area (orange).*

Crust-mantle boundary

The 3D model is a whole crustal scale model that includes a portion of upper mantle down to 65400 m (Figure 5.21). In order to accurately apply forward modelling techniques to the entire crust, the crust-mantle boundary must be considered; here this boundary is taken to be the Moho. The Moho is strongly reflective and well defined across most of the seismic line. Beneath the Yilgarn Craton the Moho remains relatively flat resulting in a crustal thickness of approximately 45 km. The crust thickens to a depth of ~50 km beneath the Musgrave Province. Within the Musgrave Province, a large crustal scale thrust fault is interpreted to dip to the southwest, offsetting the Moho by 6 km. The thickest section of Musgravian crust approaches 60 km directly beneath the interpreted Officer Basin–Musgrave Province boundary at the surface and thins to ~47 km at the northeast end of the line.

Across the rest of the study area this boundary was constrained using the AusMoho surface (Salmon et al., 2012). This surface is deepest (60 km) directly beneath the seismic line at around CDP 12000. Away from this point, the surface pulls up to ~45 km throughout most of the model space but is based on sparse extrapolated data derived from a gridding routine.

While the MT data provides information down to ~100 km (Duan et al. 2013), there is no discernible conductivity contrast across the crust-mantle boundary in this study region. The regional response of the observed gravity data provides no unique solution to crustal thickness but indicates that the overall trend seen in the AusMoho surface is a valid model.

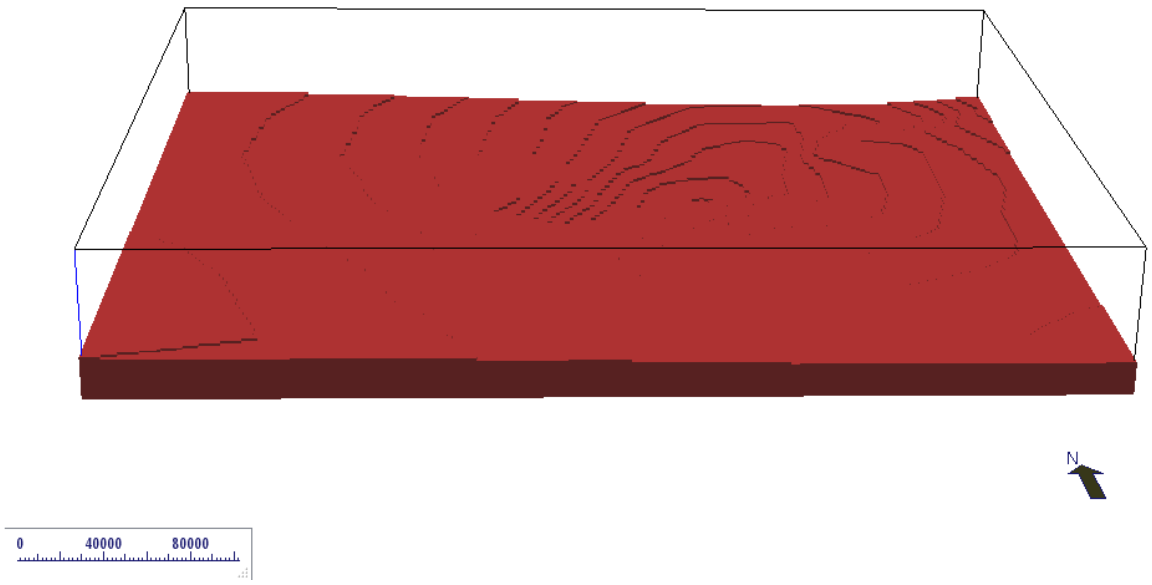

Figure 5.21 *3D model of the upper mantle (red). The upper surface of this volume represents the crust-mantle boundary; interpreted here to be the Moho.*

Description of minor divisions

There are several minor divisions within the 3D model that were not a focus of the study but are significant geological features nonetheless. They are:

- Manunda Basin (Figure 5.22),
- Albany-Fraser Province (Figure 5.23), and,
- Unnamed Proterozoic basement (undivided; Figure 5.24).

Manunda Basin

The Officer Basin unconformably overlies the Manunda Basin. The units within the Manunda Basin are interpreted to be Mesoproterozoic metasedimentary rocks as described from drill hole samples (Korsch et al., 2013). The basin itself is seismically characterised by a set of high amplitude sub-horizontal reflectors, cut by steeply-dipping faults. The basin is observed in the gravity data, producing a slight positive high in the signal, tapering off towards the interpreted basin edges.

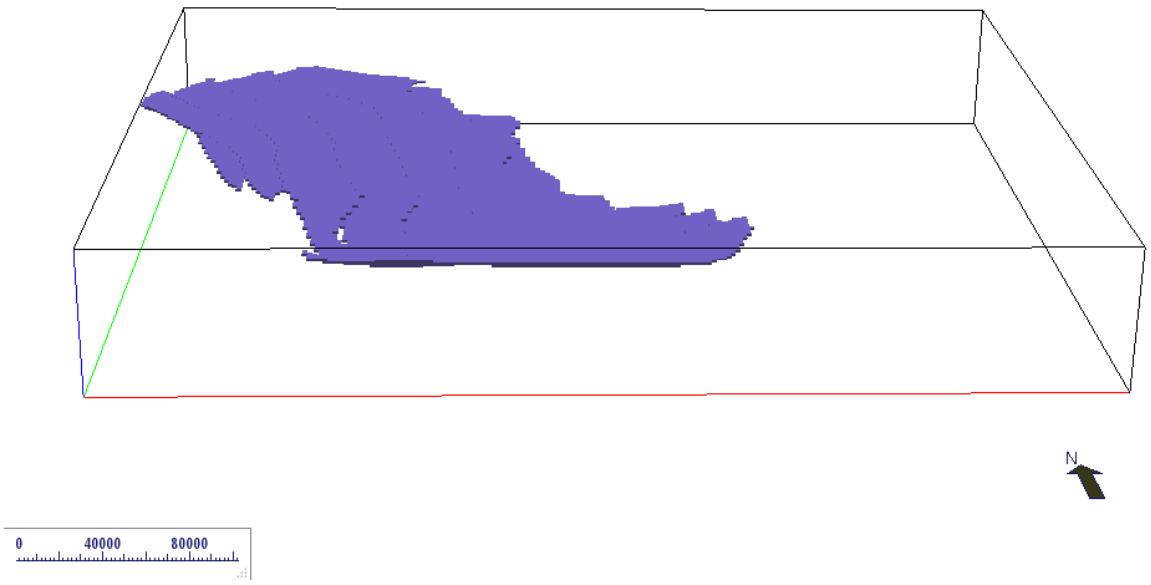

Figure 5.22 *3D model for the extent of the Manunda Basin within the study area (dark purple).*

Albany-Fraser Province

The small volume presented below represents an edge of the Albany-Fraser Province that cuts through a corner of the model area. The geometry of this boundary is not well constrained; however, Kirkland et al. (2011) suggest a pre-Albany-Fraser Orogeny dip direction of east-southeast for the Yilgarn Craton, with the present day boundary the result of significant reworking during Mesoproterozoic deformation. In this model, we have assumed an east-southeast dip direction for the present day boundary.

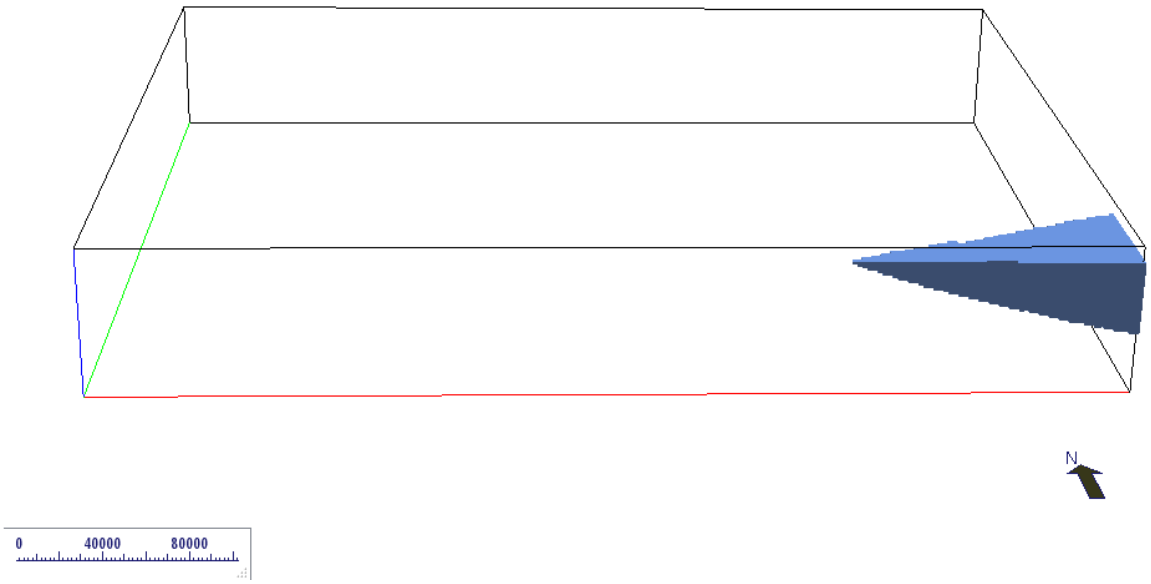

Figure 5.23 *3D model for the extent of the Albany-Fraser Province within the study area (light blue).*

Undefined Proterozoic basement

There are volumes within the model that have been interpreted to be Proterozoic basement but have been left undefined due to a lack of information. These volumes exist beneath the large intracratonic basins; the Officer Basin, the Canning Basin and the Amadeus Basin. Both the Canning Basin and Amadeus Basin extend within the model area as a thin veneer and were not included in the 3D model.

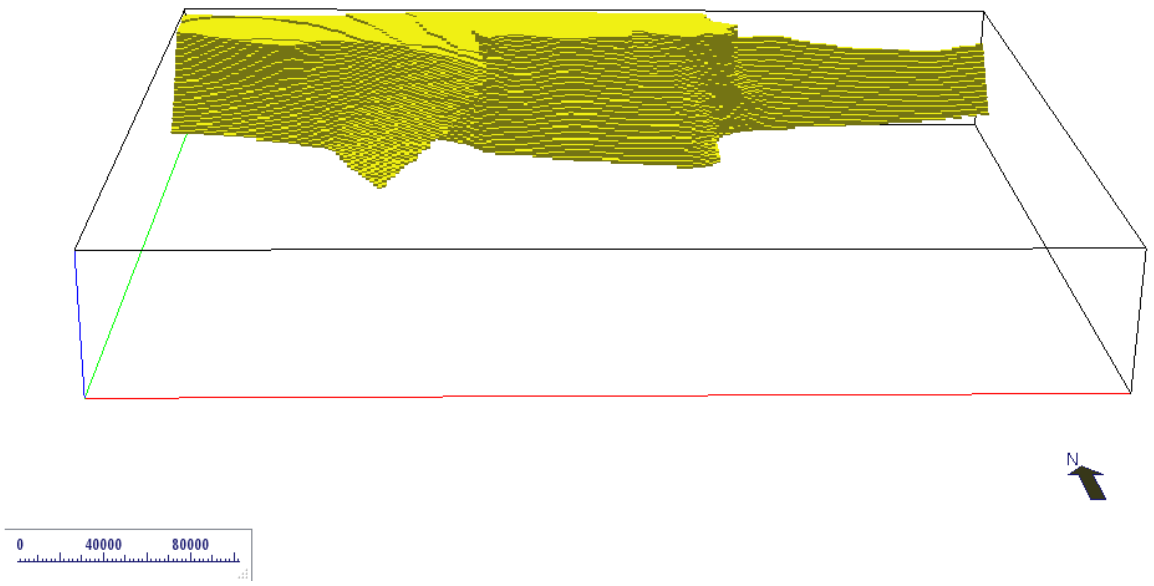

Figure 5.24 *3D model of the undivided Proterozoic basement within the study area (yellow).*

Full 3D model

The full 3D model is presented below and includes numerous intermediate layers (Figure 5.25). While this report details various aspects of each volume generated for the 3D model, it is recommended that the reader access the model in an interaction medium so its full scope can be understood and utilised in future investigations. The model will be available from www.ga.gov.au.

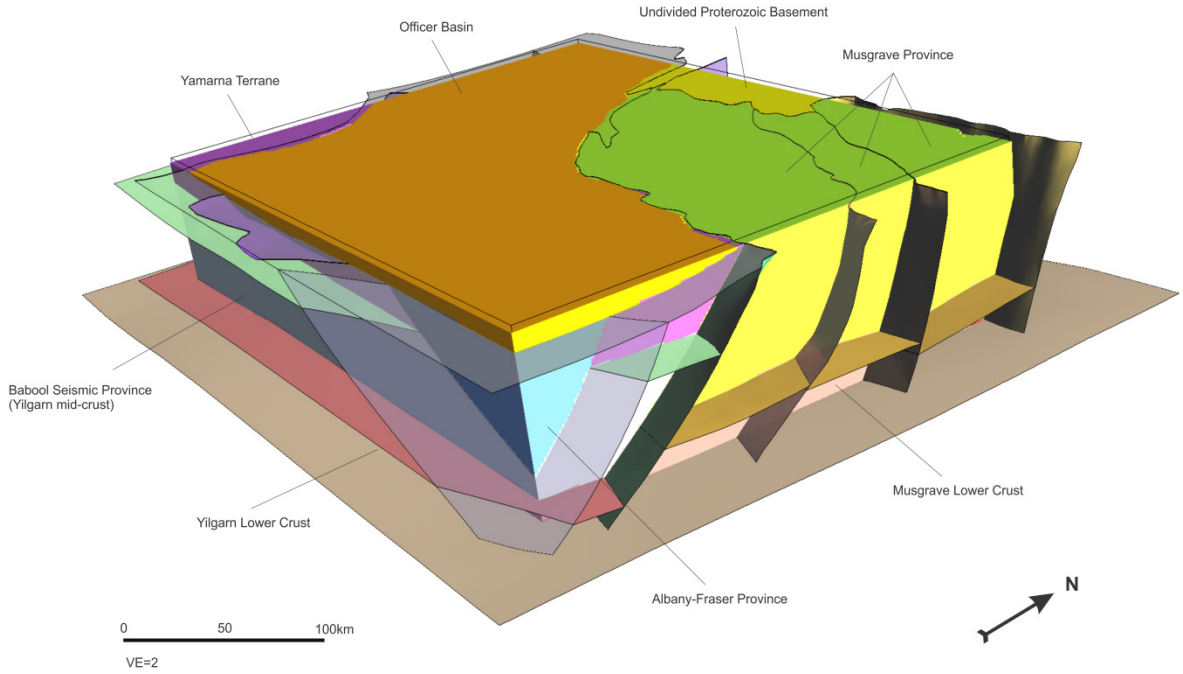

Figure 5.25 *3D model of the Yilgarn Craton–Officer Basin–Musgrave Province showing braod scale structural interpretations (surfaces) and major divisions (volumes).*

Concluding remarks

Forward modelling of gravity data has allowed interpretations of the 11GA-YO1 seismic data to be tested, and these insights used to extrapolate this interpretation, including areas under significant cover, into 3D space. Other data such as solid geology and multiscale edge detection maps also provide valuable input into the character of fault structures and lithological boundaries.

Forward modelling of gravity data has revealed that the geometry of the Winburn Granite interpreted in the 11GA-YO1 seismic line is not plausible with a magma chamber reaching 24 km depth. The best fit to the observed gravity data is achieved when the Winburn Granite is modelled as a body extending to a maximum of 1 km depth. Similarly, various sections of the Officer Basin interpreted to be intruded by salt between CDP 16000 and 25000 are not supported by the gravity data.

The resulting 3D model is a georeferenced, closed volume that is consistent with the geological interpretations derived from each of the input datasets. This represents a geological framework to be tested and understood within the context of geodynamic models for the region. The 3D architecture provides a valuable regional dataset that can be used for future studies relating to mineral systems and the geodynamic evolution of this region.

Acknowledgements

Russell Korsch, Narelle Neumann, Richard Blewett, Ron Hackney, Richard Chopping, Geoff Fraser, Richard Lane and Anthony Schofield from Geoscience Australia are thanked for their insight and assistance with completing this work. Tony Meixner and Carina Kemp from Geoscience Australia are also thanked for reviewing this report.

References

Archibald, N., Cow, P., and Boschetti, F., 1999. Multiscale edge analysis of potential field data. *Exploration Geophysics*, 30, 38–44.

Bacchin, M., Milligan, P.R., Wynne, P., and Tracey, R., 2008. Gravity Anomaly Map of the Australian Region (Fourth Edition) Geoscience Australia, Canberra.

Christensen, N.I., and Mooney, W.D., 1995. Seismic velocity structure and composition of the continental crust: A global view. *Journal of Geophysical Research: Solid Earth (1978–2012)*, 100, 9761–9788.

Duan, J., Milligan, P.R., and Fomin, T., 2013. Electrical resistivity distribution from magnetotelluric data in the Yilgarn Craton, western Officer Basin and western Musgrave Province. In: Neumann, N.L. (editor), *Yilgarn Craton–Officer Basin–Musgrave Province (YOM) Seismic and MT Workshop*. Geoscience Australia Record 2013/28, 9–23.

Emerson, D., 1990. Notes on mass properties of rocks: density, porosity, permeability. *Exploration Geophysics*, 21, 209–216.

Greatland-Gold, 2010. Proof of concept in initial drilling at Ernest Giles, A new large greenstone sequence discovered in the Eastern Goldfields of Western Australia. Greatland Gold Exploration Update, 10 November 2010: http://www.greatlandgold.com/pdfs/20101110%20Exploration%20Update.pdf.

Holden, D.J., Archibald, N.J., Boschetti, F., and Jessell, M.W., 2000. Inferring geological structures using wavelet-based multiscale edge analysis and forward models. *Exploration Geophysics*, 31, 617–621.

Holzschuh, J., 2013. 11GA-YO1 Yilgarn Craton–Officer Basin–Musgrave Province Seismic Survey – Acquisition and Processing. In: Neumann, N.L. (editor), *Yilgarn Craton–Officer Basin–Musgrave Province (YOM) Seismic and MT Workshop*. Geoscience Australia Record 2013/28, 1–8.

Howard, H.M., Quentin de Gromard, R., Smithies, R.H., Kirkland, C.L., Korsch, R.J., Aitken, A.R.A., Gessner, K., Wingate, M.T.D., Blewett, R.S., Holzschuh, J., Kennett, B.L.N., Duan, J., Goodwin, J.A., Jones, T., Neumann, N.L., and Gorczyk , W., 2013. Geological setting and interpretation of the northeastern half of deep seismic reflection line 11GA-YO1: west Musgrave Province and the Bentley Supergroup. In: Neumann, N.L. (editor), *Yilgarn Craton–Officer Basin–Musgrave Province (YOM) Seismic and MT Workshop*. Geoscience Australia Record 2013/28, 51–95.

Kirkland, C.L., Spaggiari, C.V., Pawley, M.J., Wingate, M.T.D., Smithies, R.H., Howard, H.M., Tyler, I.M., Belousova, E.A. and Poujol, M., 2011. On the edge: U–Pb, Lu–Hf, and Sm–Nd data suggests reworking of the Yilgarn craton margin during formation of the Albany-Fraser Orogen. *Precambrian Research*, 187, 223–247.

Korsch, R.J., Blewett, R.S., Pawley, M.J., Carr, L.K., Hocking, R.M., Neumann, N.L., Smithies, R.H, Quentin de Gromard, R., Howard, H.M., Kennett, B.L.N., Aitken, A.R.A., Holzschuh, J., Duan, J., Goodwin, J.A., Jones, T., Gessner, K., and Gorczyk, W., 2013. Geological setting and interpretation of the southwest half of deep seismic reflection line 11GA-YO1: Yamarna Terrane of the Yilgarn Craton and the western Officer Basin. In: Neumann, N.L. (editor), *Yilgarn Craton–Officer Basin–Musgrave Province (YOM) Seismic and MT Workshop*. Geoscience Australia Record 2013/28, 24–50.

Milligan, P.R., Franklin, R., Minty, B.R.S., Richardson, L.M., and Percival, P.J., 2010. Magnetic Anomaly Map of Australia (Fifth Edition). Geoscience Australia, Canberra.

Nakamura, A., Bacchin, M., Milligan, P.R., Wynne, P. and Tracey, R., 2011. Isostatic Residual Gravity Anomaly Map of Onshore Australia, scale 1:5 000 000. Geoscience Australia, Canberra.

Poudjom Djomani, Y.H., O'Reilly, S.Y., Griffin, W. and Morgan, P., 2001. The density structure of subcontinental lithosphere through time. *Earth and Planetary Science Letters*, 184, 605–621.

Rudnick, R.L. and Fountain, D.M., 1995. Nature and composition of the continental crust: a lower crustal perspective. *Reviews of Geophysics*, 33, 267–309.

Salmon, M., Kennett, B.L.N., Stern, T. and Aitken, A.R.A., 2012. The Moho in Australia and New Zealand. Tectonophysics, http://dx.doi.org/10.1016/j.tecto.2012.07.009.

Schofield, A., Fraser, G., Neumann, N., Huston, D., Goodwin, J.A. and Jones, T., 2013. Solid Geology Map of Central Australia. Geoscience Australia Record, *in prep*.

Telford, W.M., Geldart, L.P. and Sheriff, R.E., 1990. Applied Geophysics, 1. Cambridge University Press.

6 Four-dimensional architecture of the west Musgrave Province

A.R.A. Aitken[1], A. Joly[1], R. H. Smithies[2], H.M. Howard[2], S. Evans[3], M. C. Dentith[1], I.Tyler[2]

[1] Centre for Exploration Targeting, School of Earth and Environment, The University of Western Australia, 35 Stirling Highway, Crawley, WA 6009.
[2] Geological Survey of Western Australia, Department of Mines and Petroleum, 100 Plain Street, East Perth, WA 6004.
[3] Moombarriga Geoscience, 32 Townshend Road, Subiaco, WA 6008.

alan.aitken@uwa.edu.au

Introduction

Here we review recent work in the west Musgrave Province that characterises the 4-dimensional architecture of the province. This work was undertaken by the Centre for Exploration Targeting and was funded by the Geological Survey of Western Australia (GSWA) as part of the Royalties for Regions Exploration Incentive Scheme. The overall aim of this work is to better understand the crustal architecture and structural evolution of the west Musgrave Province and, through doing so foster effective exploration targeting in this challenging greenfields region. It is important to note that the work was completed late in 2011, and so represents a predominantly pre-seismic view of crustal architecture within the region.

The west Musgrave Province

The west Musgrave Province preserves a mostly Mesoproterozoic to Cambrian evolution, including several major events (Smithies et al., 2009a). Events prior to the ca. 1345 Ma to 1293 Ma Mount West Orogeny are somewhat cryptic, and are not obviously preserved as regional scale architectural elements, and so we exclude these from the analysis. The west Musgrave Province has been divided into several tectonic zones, each with different character for the major events. These are the Mulga Park Zone; north of the Woodroffe Thrust, the Walpa Pulka Zone; characterised by high-pressure metamorphic rocks, the Tjuni-Purlka Zone, characterised by sheared and metamorphosed rocks, the Mamutjarra Zone, characterised by the upper crustal rocks of the Ngaanyatjarra Rift, and the Mitika area, characterised by relatively thin Bentley Supergroup cover over basement geophysically similar to the Mulga Park Zone. From south to north, the Yilgarn Craton–Officer Basin–Musgrave Province (YOM) seismic line traverses the southwestern Mamutjarra Zone, the Mitika area, and the Mulga Park Zone (Figure 6.1).

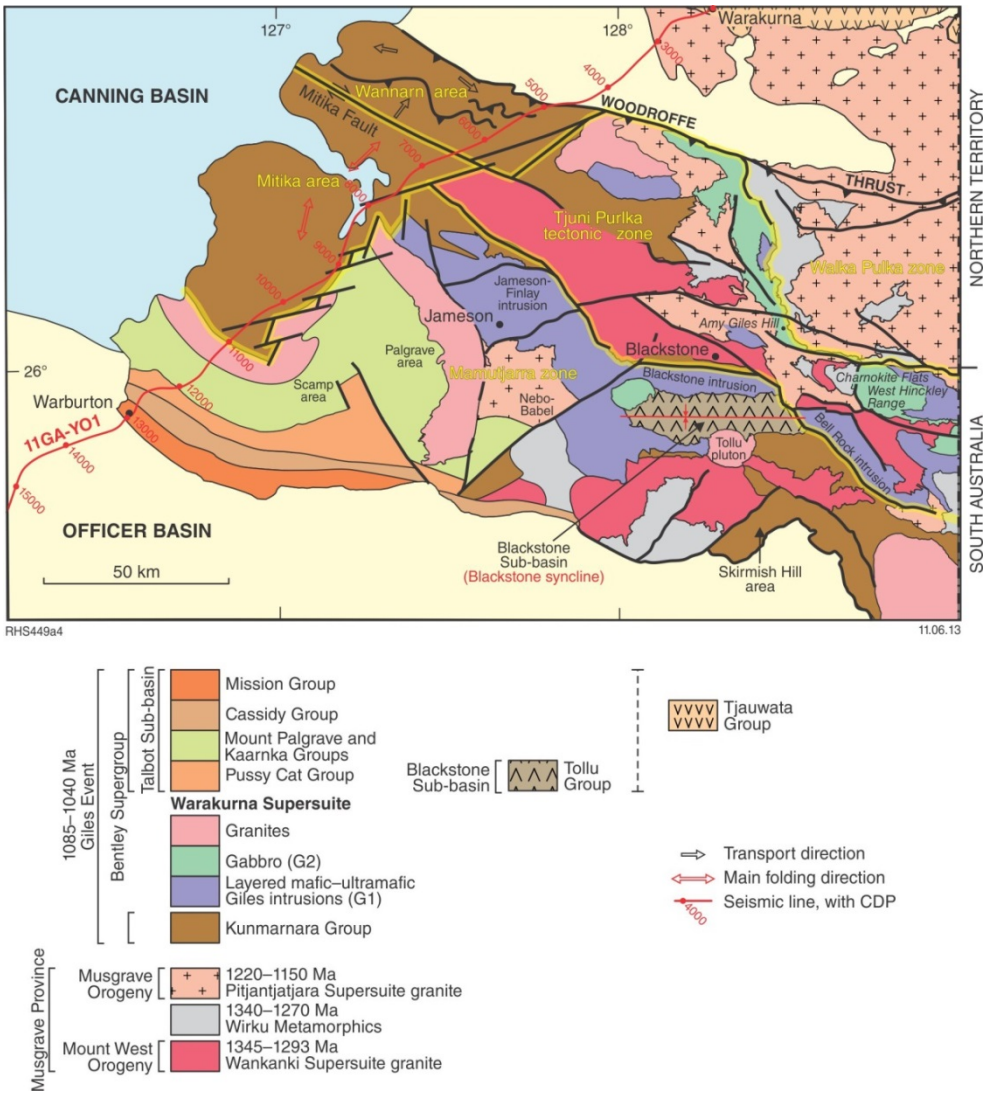

Figure 6.1 *Regional geological sketch of the west Musgrave Province (Modified by Smithies et al., 2009a from Glikson et al., 1996 and Edgoose et al., 2004).*

The Mount West Orogeny

The Mount West Orogeny is characterised by granitic magmatism of the Wankanki Supersuite and limited volcanism, as well as the deposition of the sedimentary rocks that make up the Wirku Metamorphics (Figure 6.1) (Howard et al., 2009a; Smithies et al., 2011). The granulite facies paragneisses of the Wirku Metamorphics contain several suites of rocks that may represent the metamorphosed and tectonically dissected remnants of an originally continuous sedimentary basin (Smithies et al., 2009a), the Ramarama Basin (Evins et al., 2012). The Wankanki Supersuite is characterised by porphyritic granodiorites and monzogranites, often with a significant mafic mineral component, including clinopyroxene, orthopyroxene and hornblende (Smithies et al., 2009a). Currently, U–Pb SHRIMP dating on these granites suggests magmatism extended from 1345 Ma to 1293 Ma.

The Musgrave Orogeny

The Musgrave Orogeny is defined by ultra-high temperature (UHT) metamorphism with widespread granitic magmatism (Pitjantjatjara Supersuite) and deformation of prior fabrics (Edgoose et al., 2004; Smithies et al., 2011). In the west Musgrave Province, the Pitjantjatjara Supersuite includes high-grade granitic gneisses and charnockites. Current U–Pb SHRIMP dating suggests magmatism extended from between ca. 1220 Ma to 1150 Ma, and may indicate several sub-groupings, although there is significant overlap between these (Smithies et al., 2009a; Smithies et al., 2011). Rocks of the Pitjantjatjara Supersuite are chemically distinct from the Wankanki Supersuite, and this chemistry suggests within-plate, A-type magmatism (Smithies et al., 2009a).

The Ngaanyatjarra Rift (NR)

The ca. 1085–1040 Ma Ngaanyatjarra Rift (NR) is a stunning example of a magmatism-dominated intraplate rifting event, which occurred along with the shorter lived, but more geographically extensive Warakurna LIP (Aitken et al., 2013; Evins et al., 2010). Magmatism during this rift was bimodal, and both intrusive and extrusive (Glikson et al., 1996), resulting in the voluminous mafic intrusions of the Giles Suite; widespread granitic intrusions; abundant Alcurra Dolerite Suite dykes and sills and the extensive bimodal volcanics of the Bentley Supergroup (Figure 6.1).

Recent work suggests that the Giles Suite intrusions can be separated into two main groups. The first (G1) includes the layered mafic-ultramafic intrusions that make up the main ranges of the west Musgrave Province. The age of these rocks is ill-constrained, but a minimum age of 1078 ± 3 Ma (U–Pb SHRIMP) is obtained from a leucogranite within the Bell Rock Intrusion (Sun et al., 1996). More recently, a sample of interpreted G1 layered leucogabbro at Mt Finlayson returned a U–Pb SHRIMP crystallisation age of 1076 ± 7 Ma (GSWA 194762).

The second group of intrusions (G2) includes massive gabbros that intrude into the G1 rocks. G2 rocks are characterised by fine- to medium-grained, leuco-to-mesocratic gabbro and gabbronorite (Evins et al., 2010). Characteristically, they also contain granitic material, interpreted to represent mingling of co-existing gabbroic and leucogranitic melts during emplacement (Evins et al., 2010).

Granitic rocks associated with the NR are widespread throughout the west Musgrave Province. Current radiometric dating (U–Pb SHRIMP) suggests granitic magmatism extending from 1078 Ma to at least 1065 Ma (Howard et al., 2011).

The Alcurra Dolerite Suite is a suite of mafic intrusions that are geochemically and compositionally distinct from the Giles Suite (Howard et al., 2009b). Most of these intrusions are relatively small dykes and sills, however some larger intrusions exist (e.g. the Saturn gabbro) and most basalt units within the Talbot Sub-basin are also included. This suite of rocks includes several mineralised examples, including the Nebo-Babel deposit, and Halleys prospect. Current radiometric dating suggests that Alcurra Dolerite Suite magmatism occurred between ca. 1072 Ma and ca. 1067 Ma (Evins et al., 2010; Howard et al., 2009b; Seat et al., 2007).

Rocks of the Bentley Supergroup are present throughout the south and west of the west Musgrave Province, and dominate outcrop in the western Mamutjarra Zone. These rocks make up a thick sequence of volcanic, volcaniclastic and sedimentary rocks (Evins et al., 2010; Howard et al., 2011; Smithies et al., 2009a). This sequence of rocks includes a widespread pre-Giles Complex lower sequence, the Kurnmarnara Group. The upper Bentley Supergroup comprises several groups,

deposited in at least two distinct sub-basins. The Tollu Group is a remnant of a presumably larger Blackstone Sub-basin (Smithies et al., 2009b). The western Talbot Sub-basin preserves most of the stratigraphy including the Mount Palgrave, Pussy Cat, Cassidy and Mission groups.

Post-NR tectonics

Subsequent to the NR, a prolonged period of sedimentation was interrupted by several intraplate orogenic events, including the ca. 600–520 Ma Petermann Orogeny and the ca. 450–350 Ma Alice Springs Orogeny. Recent studies suggest that the Petermann Orogeny event is characterized by three contrasting styles of deformation. In the Mulga Park Zone of the Northern Territory, deformation is characterized by low-angle thrust faulting and nappe-style folding that involves both granitic basement and the overlying cover sequences (Edgoose et al., 2004; Flottmann et al., 2005). Within the Walpa Pulka Zone ductile upwards flow of lower crustal material is identified along low-angle structures (Raimondo et al., 2010). Finally, transpressional shearing on high-angle crustal-scale shear zones, that divide regions exhibiting little deformation is identified (Aitken et al., 2009b). Within South Australia, this last style of deformation involves significant vertical offset of the lower-crust and crust-mantle boundaries, as imaged in the GOMA seismic reflection transect (Aitken et al., 2009b; Korsch and Kositcin, 2010; Lambeck and Burgess, 1992).

The Alice Springs Orogeny is most intense to the north, in the Arunta Province and Amadeus Basin, however, two major structures have been identified in the west Musgrave Province that are associated with this event. Seismic data within South Australia indicate that early Paleozoic strata within the Officer Basin have been monoclinally upturned as a result of thrust faulting at the southern margin of the Musgrave Province (Lindsay and Leven, 1996). The second structure considered to be active during the Alice Springs Orogeny aged is the Lasseter–Mundrabilla shear zone, which may have accommodated the strain differential between shortening to the east and extension to the west (Braun et al., 1991).

Methods

Aeromagnetic structural interpretation

This study used domain-based structural interpretation of aeromagnetic data (e.g. Aitken and Betts, 2009) to glean a better understanding of the large-scale structural architecture and tectonic evolution of the region (Figure 6.2). Structures in this interpretation were defined primarily by their expression in reduced to pole aeromagnetic data. The interpretation drew upon several sources of geological constraint, including 1:100 000 scale maps in the central-eastern part of the study area supplemented by 1:250 000 scale maps elsewhere. The WAROX database of structural measurements was used to provide structural constraint on the strike, dip and type of foliations, and trend and plunge of fold axes.

Domains were structurally interpreted on an individual basis, using a method akin to form-surface mapping in structural geology. A key aim was to define magnetic form-lines for early structures. Later generations of structure could then be inferred from the deformation of these. From this mapping, a local sequence of deformation events was identified within each domain. These were linked into the stratigraphy on the basis of local overprinting relationships with mapped geology. Finally, cross-domain correlations can be drawn to provide an integrated regional evolution. The criteria for correlation included, in order of importance: stratigraphic position; shared overprinting relationships with other events; structural style; and orientation.

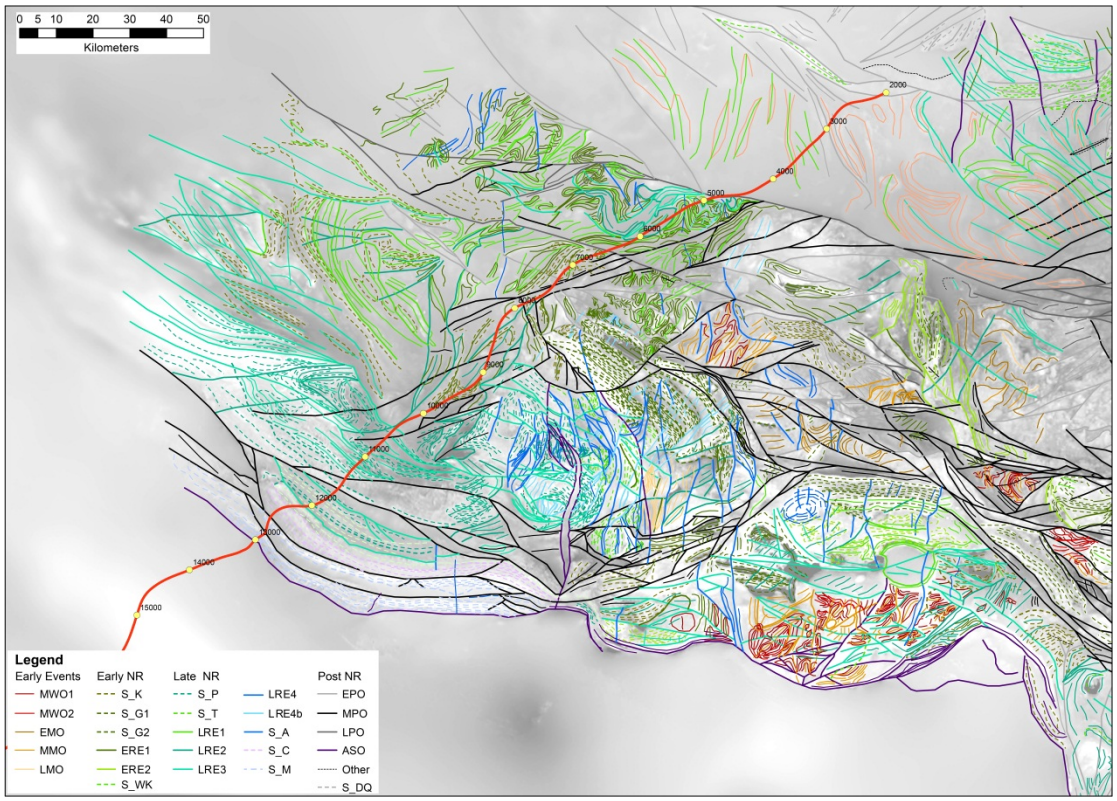

Figure 6.2 *Structural elements within the west Musgrave Province from the aeromagnetic interpretation, overlain on greyscale RTP magnetic data. The relevant portion of the YOM seismic line is annotated by CDP number. Detailed images of each event are available in Joly et al. (2013). Legend codes as follows: MWO1 and 2: Mount West Orogeny deformation events 1 and 2. EMO, MMO, LMO: early, middle and late Musgrave Orogeny deformation. S_K, S_G1, S_G2: layering in Kunmarnara Group, Giles Suite 1 and Giles Suite 2. ERE1 and 2: Early rift deformation event 1 and 2. S_Wk and S_A: syn-Warakurna granite and syn-Alcurra Dolerite Suite deformation. S_P, S_T, S_C and S_M: layering in the Mount Palgrave, Tollu, Cassidy and Mission Groups. LRE1 through 4: late rift events 1 through 4. S_DQ, Dean Quartzite layering; EPO, MPO,LPO: Early, mid and late Petermann Orogeny. ASO – Alice Springs Orogeny.*

Magnetic and Gravity Profile modelling

Forward modelling crustal structure with magnetic and gravity data is an effective and fairly robust method when applied using geological and petrophysical constraint. The method used here involves as a first step the construction of an interpreted geological cross section (Figure 6.3). Geological cross sections are constructed using the distribution of lithologies in mapped outcrop (where available) and interpreted geology elsewhere. Ultimately, the models generated using this method can be considered as geological models of crustal structure that satisfy both gravity and magnetic data. As such, they may include features that are not required by the geophysical data, but are supported by geological inference, and serve to illustrate the likely geological scenario. For example, thin layers are often continued to depths beyond their limit of sensitivity on the basis that they are part of a conformable package of rocks.

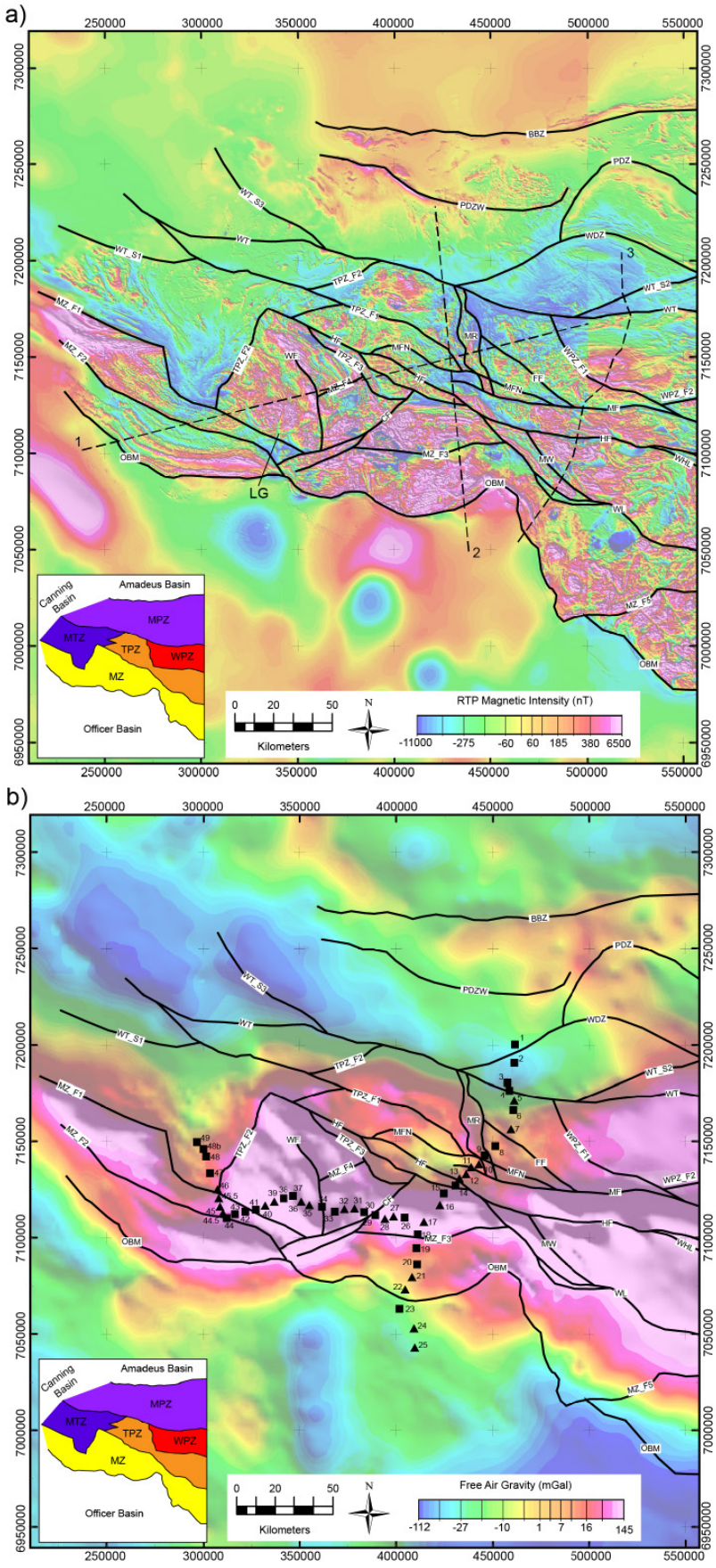
a)
b)
250000
300000
350000
400000
450000
500000
550000
7300000
7250000
7200000
7150000
7100000
7050000
7000000
6950000
BBZ
PDZ
PDZW
WDZ
WT_S3
WT_S1
WT
WT_S2
TPZ_F4
TPZ_F1
TPZ_F2
TPZ_F3
MZ_F1
MZ_F2
MZ_F3
MZ_F4
MZ_F5
WF
MFN
MR
HF
FF
WPZ_F1
WPZ_F2
MF
IF
MW
WHL
WL
OBM
LG
1
2
3
Amadeus Basin
Canning Basin
Officer Basin
MPZ
MTZ
TPZ
WPZ
MZ
0
20
50
Kilometers
N
RTP Magnetic Intensity (nT)
-11000
-275
-60
60
185
380
6500
Free Air Gravity (mGal)
-112
-27
-10
1
7
16
145

Figure 6.3 (Previous page) *Map of the west Musgrave Province showing a) Reduced-to-pole aeromagnetic data, major faults and shear zones, and the locations of gravity and magnetic forward modelling profiles (numbered) b) Free-air gravity data, faults and shear zones, and the locations of MT stations (numbered). Squares indicate sites occupied with ANSIR equipment, triangles indicate where Phoenix equipment was used. Named faults are denoted by: BBZ – Bloods Backthrust Zone, PDZ – Piltardi Detachment Zone; PDZW – Piltardi Detachment Zone West, WDZ – Wankari Detachment Zone, WT - Woodroffe Thrust, FF – Fanny Fault, MR – Murray Range, MF - Mann Fault, MFN - Mann Fault North HF - Hinckley Fault, WHL – Wintiginna-Hinckley Lineament, WL – Wintiginna Lineament, MW – Mount West Shear Zone, WF – Winburn Fault, CF – Cavenagh Fault, OBM – Officer Basin Margin. Unnamed faults are named according to their zone (MZ_F1, TPZ_F1 and so on), and splays are indicated by an S prefix (e.g. WT_S1). Inset shows the major tectonic zones of the west Musgrave Province, MZ – Mamutjarra Zone, TPZ – Tjuni Purlka Zone, WPZ – Walpa Pulka Zone, MTZ – Mitika Zone, MPZ - Mulga Park Zone.*

Profile 1 (Figure 6.4) crosses the west Musgrave Province from west to east, crossing all the main tectonic zones of the region, and some of the largest gravity and magnetic anomalies (Figure 6.3). This profile is targeted at understanding the thickness and geometry of the Bentley Supergroup and the Jameson Intrusion (G1), and understanding shear-zone architecture in the Tjuni Purlka and Walpa Pulka Zones.

Profile 2 (Figure 6.5) traverses the province from south to north, covering the Blackstone Syncline, the northern Tjuni Purlka Zone and basin structure and Petermann Orogeny deformation within the Tjauwata Group.

Profile 3 (Figure 6.6) traverses the south-east Tjuni Purlka Zone, the Walpa Pulka Zone and the Mulga Park Zone, with the aim of investigating the structuring of the Petermann Orogeny, which affected this area most strongly. Investigations in South Australia indicate the presence of significant crust-mantle boundary offsets accommodated on the major shear zones (Aitken et al., 2009a; 2009b; Korsch and Kositcin, 2010; Lambeck and Burgess, 1992) and it is important to determine if these continue into Western Australia.

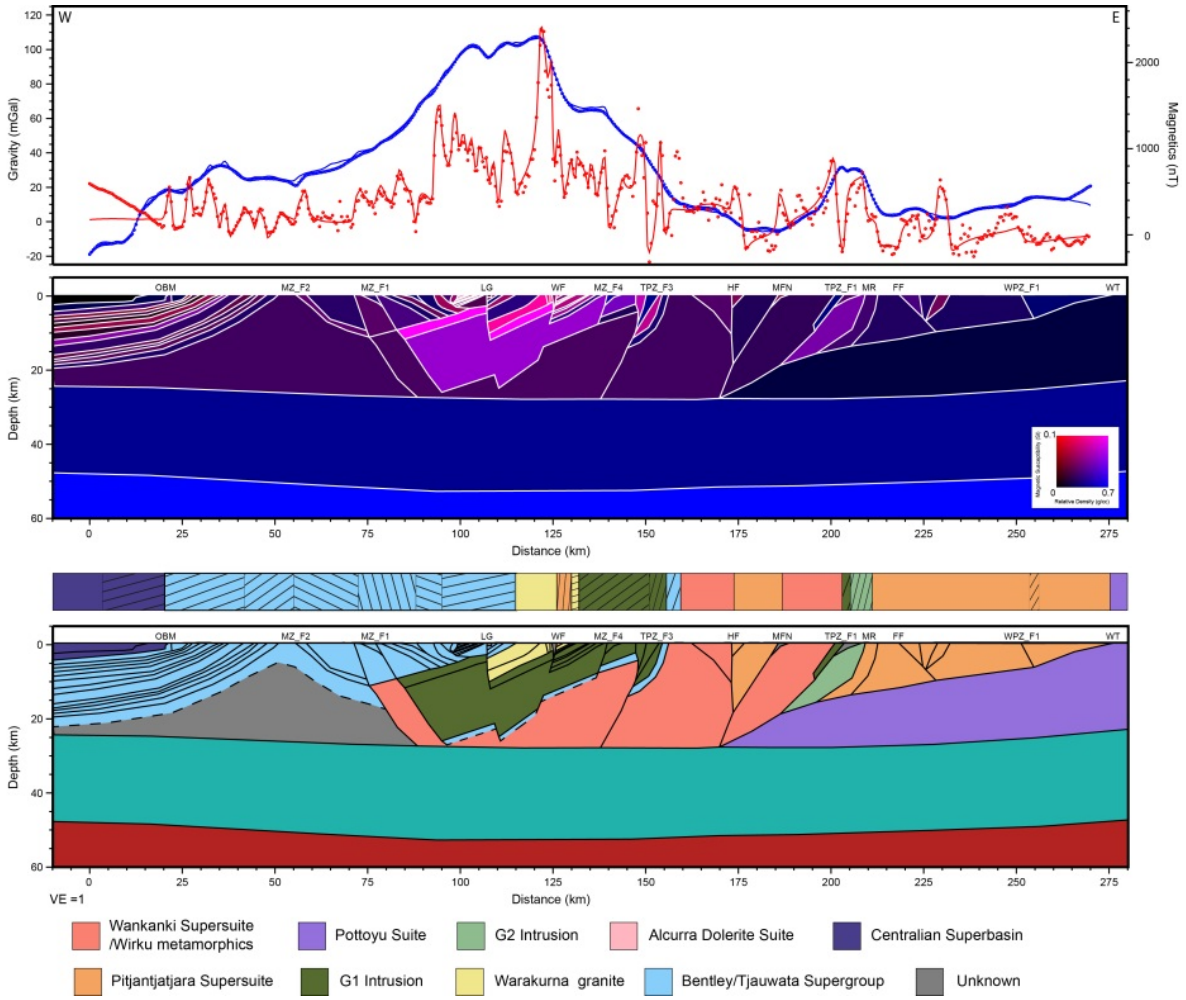

Figure 6.4 *Joint magnetic and gravity model of crustal structure along profile 1. Composite image shows magnetisation in red shades and density in blue shades, hence magenta colouring indicates dense, highly magnetised crust. The bar above the geological interpretation indicates the inferred near-surface geology (pre-modelling). Hashing indicates the apparent dips of structural observations from field mapping by the Geological Survey of Western Australia (GSWA). Broader hashing indicates primary structures (bedding, igneous layering) while finer hashing indicates secondary structures (cleavages, foliations etc.).*

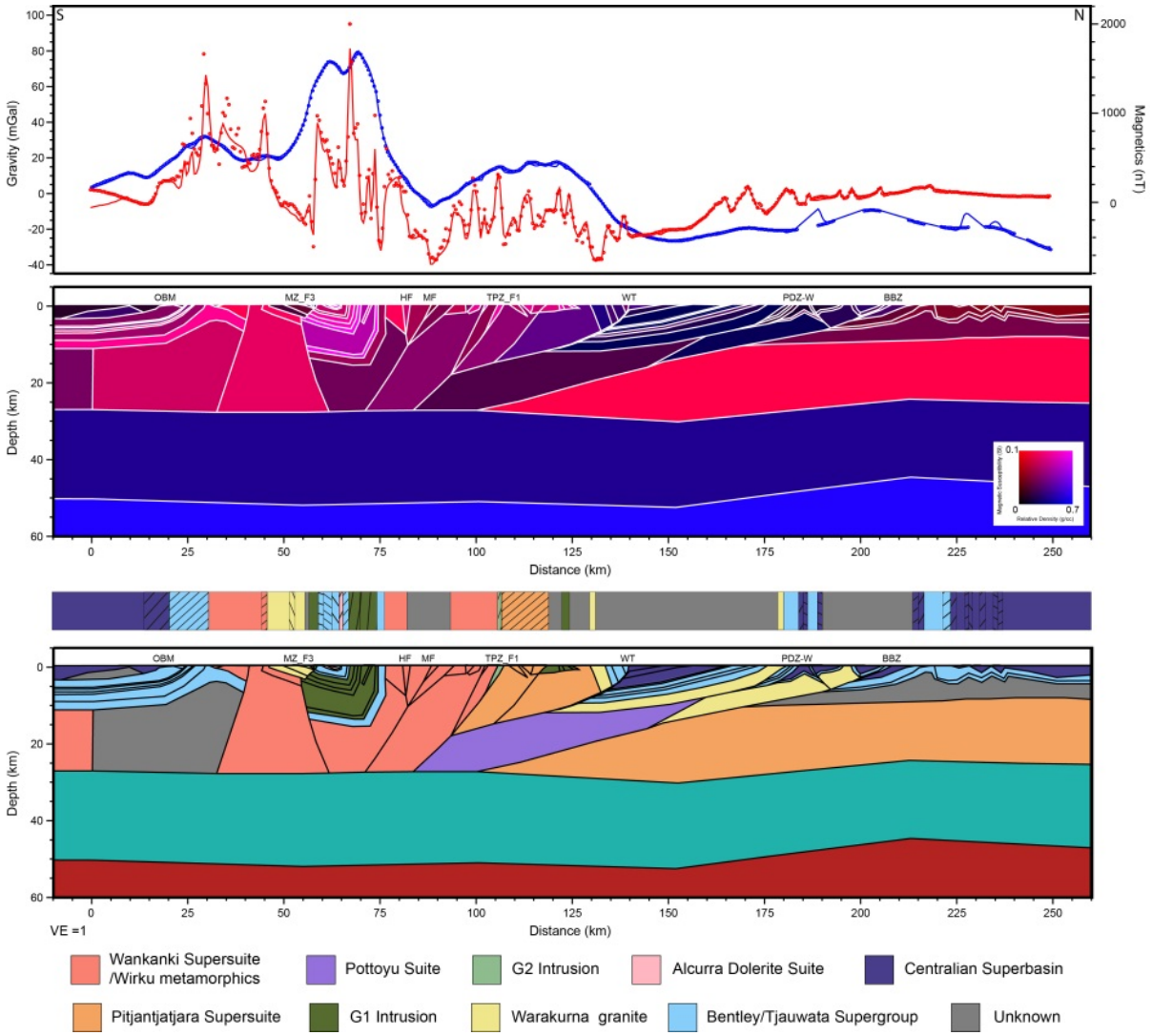

Figure 6.5 *Joint magnetic and gravity model of crustal structure along profile 2. Symbology is as shown in Figure 6.4.*

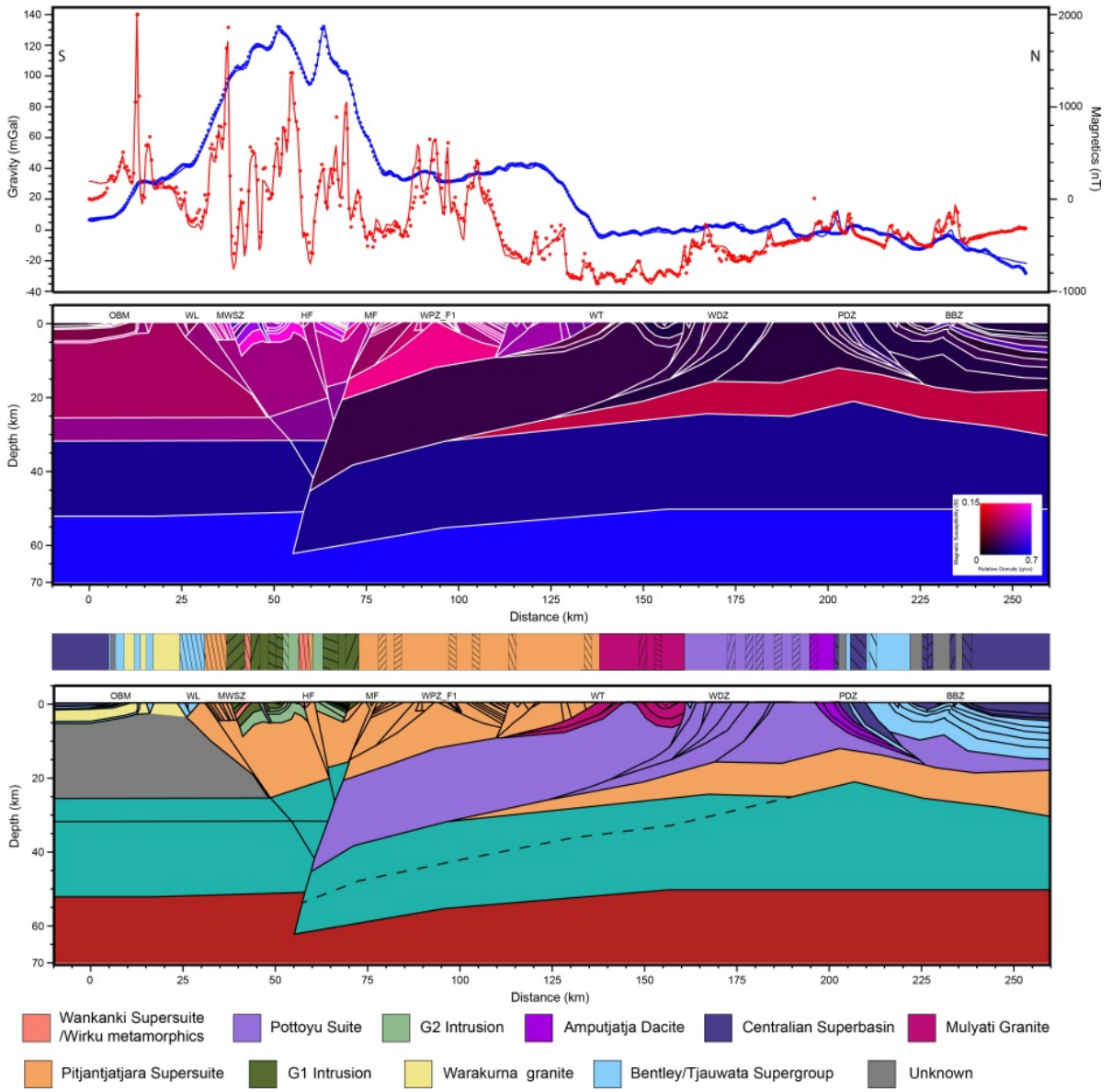

Figure 6.6 *Joint magnetic and gravity model of crustal structure along profile 3. Symbology is as shown in Figure 6.4. Dashed line indicates where inferred deep-crustal Pitjantjatjara Supersuite rocks, similar to those in the Walpa Pulka Zone, go below Curie depth.*

3D Magnetic and Gravity Inversions

A 3D model was constructed from the geological data, the forward model cross sections, and the magnetotelluric profiles. To construct the model we consider first the architecture of major faults and shear zones, and secondly, the nature of lithological boundaries within these fault-bounded blocks.

The major fault zones used for the model are generated using a simplified version of the fault maps presented in Joly et al. (2013) (Figure 6.2). These faults are separated into planar and listric geometries, based on their interpreted geometry in the upper-crust. These models suggest that a planar geometry is acceptable for the observed length of most faults south of the Woodroffe Thrust. The Woodroffe Thrust and the shear zones to its north typically have listric geometry (Edgoose et al., 2004).

Three dimensional gravity and magnetic inversions were undertaken using VPmg™ software (Fullagar et al., 2008). As a result of the inherent non-uniqueness in potential field inversions (e.g. Parker, 1994) changes in density and structure must be controlled during inversion to guide the inversion towards a realistic result. Hard constraints were imposed by fixing absolute maximum and minimum limits on properties based on the a priori lithological model distribution. Several styles of inversion were undertaken, including unconstrained least-squares (Magnetics and Gravity), lithologically constrained least squares (Magnetics and Gravity), lithologically constrained stochastic (Gravity) and combined property/geometry (Gravity).

We found that unconstrained least-squares magnetic inversions provided a reasonable image of regional structure, but that including lithological constraint provided sharper definition of known structures. For gravity, unconstrained inversions were useful only in imaging the degree of mass excess/deficit, and lithological constraints are necessary. Least squares and stochastic inversions differ appreciably in character due to the smooth vs chaotic tendencies of these approaches. Large-scale features are similar in both. In both styles, the initial model geometry provides a fit to the data with petrophysically acceptable density values. Combined density/property inversions demonstrated that even when permitted to change, the data were quite insensitive to geometry changes, and density changes are dominant.

For display purposes (Figure 6.7) we use the lithologically constrained models without any geometrical change.

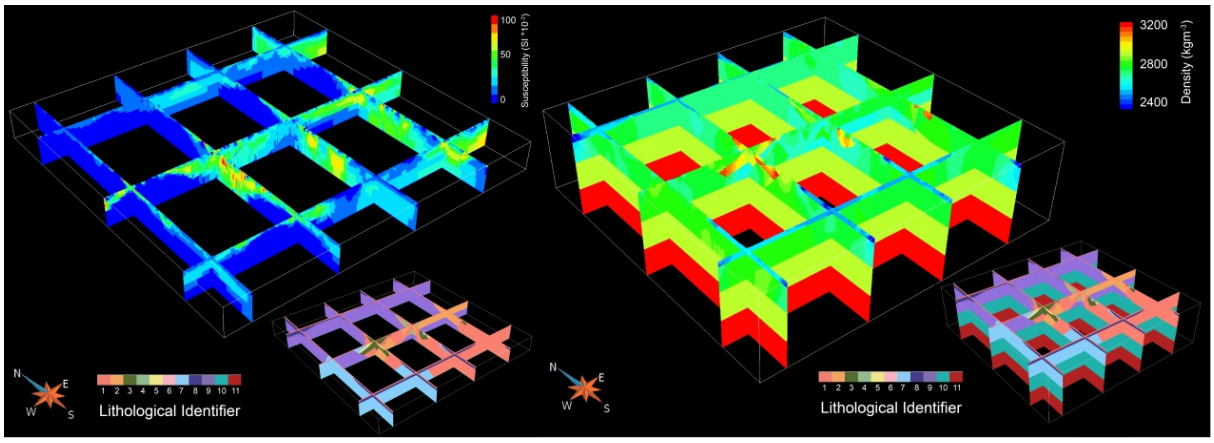

Figure 6.7 *3D fence diagrams for lithologically constrained least-squares magnetic and gravity inversions. Magnetic inversion is on the left, and gravity is on the right.*

Magnetotelluric Modelling

East–west and north–south magnetotelluric profiles also delineate the large scale geometry of the region. Figure 6.8 shows the final conductivity cross-sections in relation to the surface geology and the extent of major positive gravity features. Both cross-sections are notable for the very high resistivities of the lithosphere. The cause of the high resistivities is difficult to determine however, because of the poor understanding of controls on electrical properties in the deep crust and mantle. The high resistivity is indicative of a lack of conductive material, which in this context indicates a lack of conductive mineral species. The chemistry, especially iron content, of mineral species such as pyroxene and olivine, is thought to affect their electrical properties.

As is often seen in MT data in basement terrains, and is best developed on the north-south traverse, there are more conductive areas that comprise narrow linear zones and are probably due to the presence of more conductive mineral species in major fault zones. This includes the steeply-dipping Mann Fault (Figure 6.8). The maximum depth of such features is poorly constrained but most seem to terminate at roughly the seismically defined Moho depth. These features are a useful indicator of deep penetrating fault zones, which are important features in the prospectivity analyses described by Joly et al. (2013) due to the likelihood of their control on the movement of metal-bearing fluids.

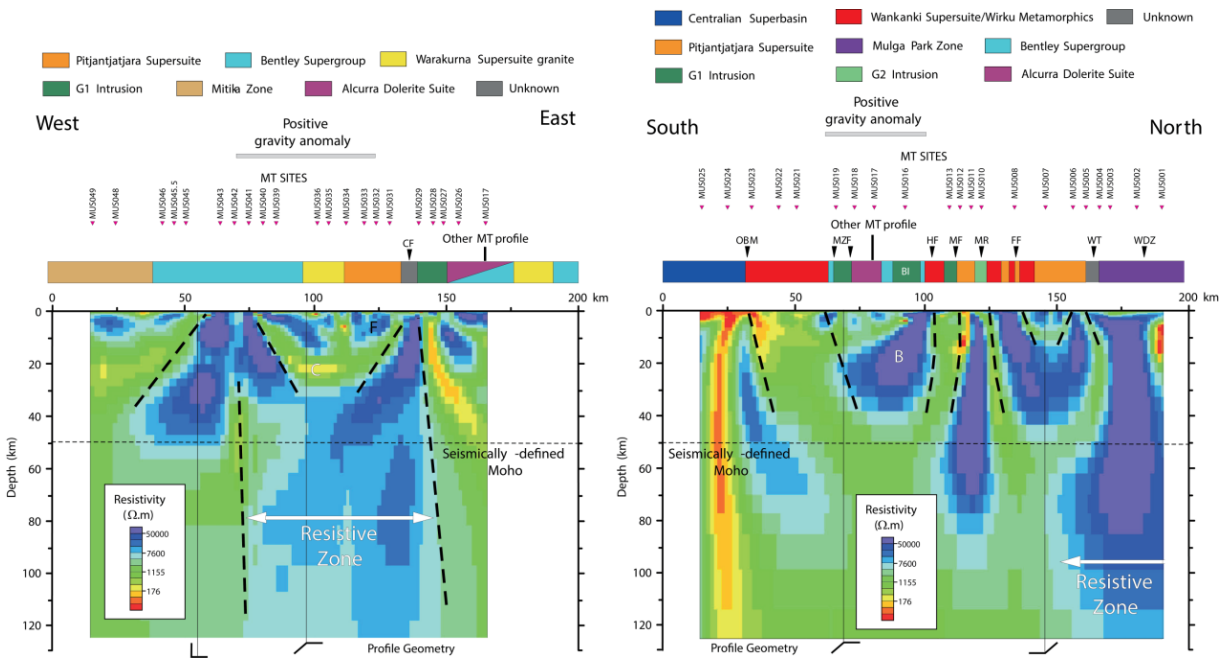

Figure 6.8 *East–west (a) and north–south (b) MT resistivity profiles.*

Tectonic architecture of the west Musgrave Province

The geophysical work described above has identified both the extent and evolution of the main events, and also their large-scale architecture. Typically, each major tectonic event involves several to many sub-events.

The Mount West Orogeny

This event is characterised by deformational fabrics in the Wankanki Supersuite and Wirku Metamorphics, that are overprinted by the Pitjantjatjara Supersuite. These events are recognised in several discrete regions and events may not be correlative between these. At Mount Aloysius the first event is defined by magnetic layering that correlates to layer-parallel gneissic banding in the Wirku Metamorphics and Wankanki Supersuite (Stewart, 1995). At Mount West, a similar fabric is observed with a dominant west-northwest orientation. An additional event, entailing west-oriented tight folding and faulting is observed at Mount West. Although it is likely that the Mount West Orogeny provided an architectural framework to be exploited during subsequent events, these structural observations cannot reliably inform interpretations of the larger scale tectonics.

The Musgrave Orogeny

This event is defined by structures that have an intimate relationship with ca. 1220 Ma to 1150 Ma Pitjantjatjara Supersuite granitoids, reflecting pre, syn and post magmatic deformation. Early-Musgrave Orogeny structures (EMO) are typically defined by contacts between Early Pitjantjatjara Supersuite rocks and basement gneiss. These early Musgravian structures are folded by a second Musgravian event which is defined by northeast-trending close folding. This folding is commonly intruded by later Pitjantjatjara Supersuite bodies which are unfolded.

At Cohn Hill, late-Musgravian deformation is defined by north-northeast-oriented tight folding and a north-northeast-trending shear zone which truncates these folds at a slight angle. Further late Musgravian structures may be resolved elsewhere but the ages of these fabrics are poorly constrained.

Large scale lithospheric architecture has been inferred from geochemical data from Pitjantjatjara Supersuite granites (Smithies et al., 2011). This model involves the ascent of the asthenosphere to the base of the crust (possibly partly facilitated by delamination of the lower crust and upper lithospheric mantle) to establish the long-lived ultra-high temperature (UHT) conditions of the Musgrave Orogeny (Smithies et al., 2011). Implicit in this model is that the lithospheric mantle was very thin and hot, if not almost absent during the Musgrave Orogeny.

The Ngaanyatjarra Rift

This rift event is fundamentally separated into the early-NR, which represents a dominantly magmatic phase during the emplacement of the Giles Suite, and the late-NR which represents a magmatic and deformational stage that post-dates the Giles Suite.

Early Rift Events

Early Rift Events are dominated by the emplacement of the Giles Suite into the lower-Bentley Supergroup. Two main deformation events are observed, corresponding with the emplacement of Giles Suite G1 and Giles Suite G2. The first is characterised by a magnetic fabric that corresponds to a metamorphic foliation developed in the Kunmarnara Group and near bedding-parallel deformation within Giles Complex intrusions. In both the Jameson and Blackstone intrusions, syn-magmatic deformation is common and igneous contacts often truncate layering. These relationships suggest that deformation likely reflects the influence of intrusion emplacement rather than tectonically-driven deformation.

The G1 layered intrusions are amongst the largest intrusions on Earth, totalling 36,000 km^3 in our 3D model. The distribution and structure of G1 intrusions indicates several key controls on their emplacement. Firstly, the intrusions are, by and large, parallel with layering in the Kunmarnara Group

suggesting that they were emplaced as lopoliths within the lower Bentley Supergroup. Gravity and magnetic modelling indicates that the major G1 intrusions of the Mamutjarra Zone (the Jameson Intrusion, the Cavenagh Intrusion and the Blackstone Intrusion, as well as the Bell Rock Intrusion) are connected at depth (Figure 6.9), and may have been emplaced as one enormous intrusion, with a total preserved volume of approximately 32,000 km^3. A near continuous layer of relatively low-density troctolite can be traced through these intrusions (Figure 6.9).

Although the geometry of this mega-intrusion is disrupted by post-emplacement faulting and folding, it is clear from the models that the Jameson and Blackstone intrusions are fault bounded to the south. The earlier Cavenagh Intrusion is present on both sides of this bounding fault and is significantly displaced across it. We suggest that, after the emplacement of the relatively thin and spatially restricted Cavenagh Intrusion, this structure became active during the emplacement of the Blackstone Intrusion, accommodating the addition of material to the crust. The Jameson Intrusion is also bounded to the west by a normal fault which likely accommodated the addition of material in a similar fashion. The location of the northern boundary of this mega-intrusion is not known, however, given the current geometries of the Jameson and Blackstone intrusions it is extremely likely that the intrusion originally continued above the currently exposed level for some distance.

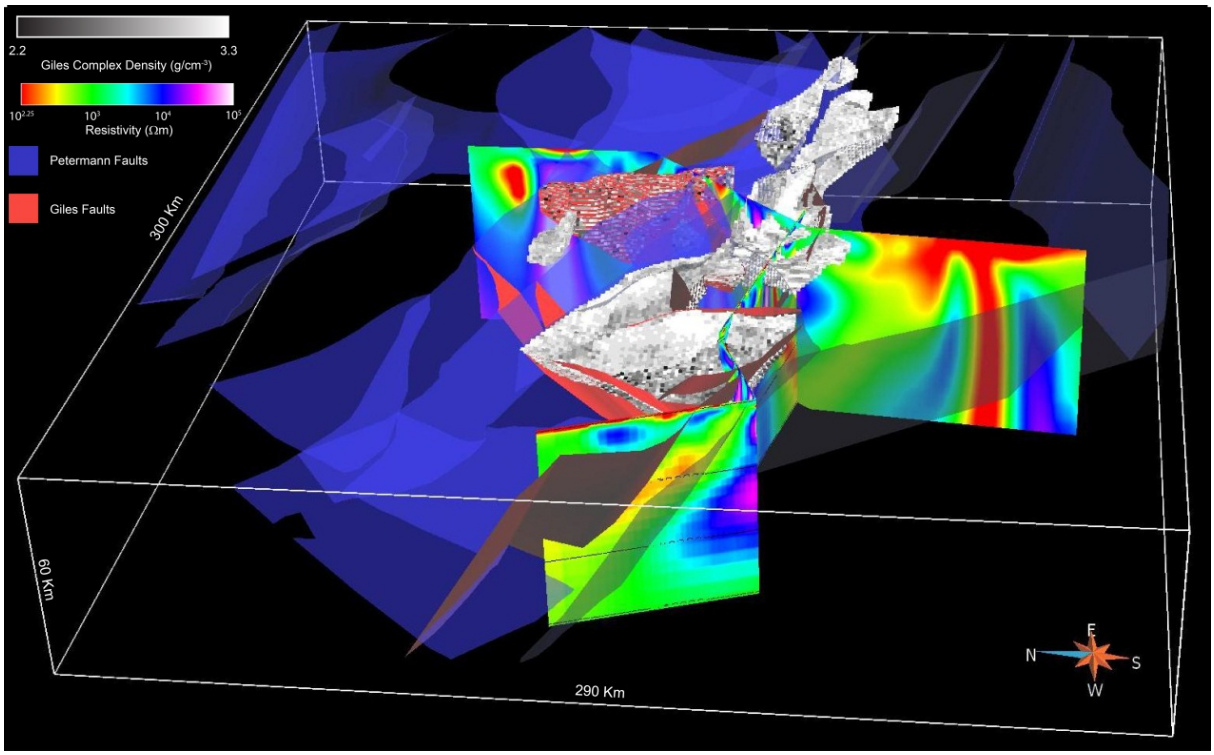

Figure 6.9 *3D view of the west Musgrave Province model showing the interpreted extent and geometry of Petermann Orogeny and Ngannyatjarra Rift Faults, the extent and density of the Giles Suite and the MT profiles.*

As a result of the Petermann Orogeny, the Tjuni Purlka Zone can be separated into northwest and southeast sections. Within the north-west Tjuni Purlka Zone, G1 rocks are relatively rare and disconnected in outcrop, however, forward modelling of gravity and magnetic data across this zone indicates that Giles Suite rocks are relatively extensive, but the intrusions are relatively thin (< 5 km) and are dissected by later structures. These likely represent the lower-levels of a relatively large intrusion. G1 and G2 intrusions within the southeast Tjuni Purlka Zone have been folded during late

NR deformation. The Michael Hills/Latitude Hills intrusion has also been tilted, such that the base of the intrusion slopes south at 12º. Maximum thickness (at the Mount West Fault) is ~10 km, and this reduces to ~6 km at the Hinckley Fault (Figure 6.6).

A significant component of the Giles Suite is made up of later stage massive gabbros (G2), especially in the Hinckley and Murray Range (7000 km^3). The Murray Range, represents a syn-magmatic shear zone, with emplacement of the gabbros under sinistral transpression (Evins et al., 2010). The Murray Range block dips to the west at a moderate angle. The emplacement of the Hinckley Gabbro was also accompanied by syn-magmatic deformation. Here, igneous layering from an early intrusive phase, including leucogranite layers and G1 material, is flattened along an east–west axis due to the intrusion of a later elliptical pluton that is much less deformed. Both these fabrics are folded around a north-northwest-trending axis that relates to an adjacent shear zone. The Murray Range and Hinckley gabbroic intrusions share many similarities, and were likely emplaced together, although they are now offset by ~30 km of sinistral offset on the Mann Fault (Evins et al., 2010).

Late Rift Events

The early rift events were followed by a brief period of relative quiescence, during which time the Giles Suite rocks were uplifted to the surface and partially eroded (Evins et al., 2010). The upper Bentley Supergroup was deposited upon this erosional surface. Although folded and faulted in places, the overall stratigraphy of the Bentley Supergroup is largely well preserved. Overall, this sequence dips shallowly to the south-west. Modelling suggests that the sequence comprises an approximately 15 km thick sequence from the base of the Mount Palgrave Group to the top of the Mission Group. This thickness estimate does not include the Kurnmarnara Group, the Tollu Group, the Scamp Formation or the Pussy Cat Group, for which thicknesses are not defined. These volcanic and subvolcanic rocks and the dykes and sills of the ca. 1068 Ma Alcurra Dolerite Suite provide stratigraphic control on the tectonic evolution of the late rift events.

There are several deformation events throughout this late rift stage. The first (LRE1) is characterised by large-scale folding of the Giles Suite 1 and 2 intrusions and the overlying Tollu Group. This event is best defined at the Blackstone Syncline where the Blackstone Intrusion is folded beneath the Tollu Group in a broad east-plunging syncline. The youngest unit involved in this folding is the Hogarth Formation, which has been dated at 1068 ± 7 Ma (GSWA, 2011), and a minimum age constraint on the folding is given by the 1072 ± 8 Ma Saturn gabbro pluton, which truncates the folding.

Late Rift Event 2 involves a series of NE-trending faults that are clustered around the Barrow Range–Cavenagh Corridor (Figure 6.1). Despite the fact that it was later reactivated, the Cavenagh Fault is interpreted to have been the main structure in this event, bounding one side of the Talbot Sub Basin. The steeply southeast-dipping fault that bounds the western edge of the Jameson Intrusion also bounds the western edge of the Mount Palgrave Group, suggesting reactivation during LRE2. LRE2 faults do not extend into the Cassidy Group, and one example is cut by a granite dated at 1065 ± 9 Ma (GSWA, 2011).

The third and fourth events (Late Rift Event 3 and Late Rift Event 4) consist of two fault sets that occurred very close together in time, although they both clearly post-date LRE2. LRE3 fault zones are ESE-trending, and most often show apparent dextral offset while LRE4 faults are usually north trending, and most often show sinistral offset. This conjugate geometry indicates a stress field with maximum horizontal stress oriented at 320°–140°. LRE4 faults post-date Nebo– Babel (1068 ± 4 Ma; Seat et al., 2011) but pre-date another Alcurra Dolerite Suite dyke set, dated at 1067 ± 8 Ma (Howard et al., 2009b).

Following LRE4, no major deformation is recognised that is correlated with the NR, although magmatism continued for some time, probably until at least 1040 Ma (Howard et al., 2011). This magmatism includes the Cassidy and Mission groups, which are essentially undeformed.

Post NR deformation

Following the NR, a series of deformation events have affected the west Musgrave Province. This includes the Petermann and Alice Springs orogenies, but also less regionally significant tectonic events, such as the ca. 750 Ma Areyonga movement. The lack of post 800 Ma magmatism in the province means that in the absence of direct dating it is hard to confidently ascribe structures to one event or another. Nevertheless, we have grouped structures into the main two events, based on the most regionally significant event that can be most confidently ascribed to these orogenies.

Petermann Orogeny (590–530 Ma)

The Petermann Orogeny is associated with numerous shear zones that dissect the prior architecture, commonly reactivating pre-existing structural trends. In the West Musgrave Region several stages are identified by their timing relative to the main network of crustal-scale shear zones.

Early Petermann Orogeny deformation is characterised by shear zones of varied orientations. West-southwest to southwest trending shear zones dominate in the Walpa Pulka and Tjuni Purlka zones. Raimondo et al. (2010) present a study that covers much of the Walpa Pulka Zone, and links the deformation here to southwest-directed lower crustal flow, with peak metamorphism at ca. 570 Ma. The Mulga Park Domains preserve significant early-Petermann deformation, whilst east-southeast trending structures dominate in the 590 Ma to 560 Ma Petermann Nappe Complex, the structure of which is comprehensively described in Edgoose et al. (2004) and Flottmann et al. (2005). The PDZ is terminated in Western Australia by a sinistral tear-fault, to the west of which Petermann Orogeny structures are characterised by less intense folding and ramp-flat thrust geometry, and so much less shortening is observed (c.f. Figures 5 and 6)

The mid-Petermann Orogeny event is characterised by an ESE trending array of anastomosing mylonite, ultramylonite and pseudotachylite zones, including several crustal scale examples (e.g. the 570–550 Ma Mann Fault). These are very prominent in the east of the Tjuni Purlka zone, where they define the bounds of high-pressure metamorphic domains exhumed during the Petermann Orogeny.

The density of Petermann Orogeny shear zones, and the continuity of earlier structures across them, indicates that the intensity of the Petermann Orogeny decreases to the west and south, leaving much of the region undeformed. Post NR offsets on the crustal scale faults varies from 22 km sinistral movement on the Mann Fault, down to just 4 km sinistral movement on the Cavenagh Fault.

The Woodroffe Thrust is the fundamental geological boundary of the Petermann Orogeny. In the West Musgrave Province this shear zone is characterised by a long, fairly linear east-southeast-trending lineament, with a number of splays. This fault network post-dates the main network of strike-slip shear zones, indicating late-Petermann activity. The Woodroffe Thrust does not crop out in Western Australia, but is well exposed further east, where radiometric ages of ~550–530 Ma are returned (Camacho et al., 1997; Camacho and Fanning, 1995; Maboko et al., 1992). The initial 3D model and forward models proposed a listric geometry for the Woodroffe Thrust merging into the Mann Fault at depth, however, magnetic inversion models suggested that a steeper and more planar geometry may be more appropriate for the upper crust. This latter geometry is consistent with the upper-crustal geometry imaged in the YOM seismic line.

Alice Springs Orogeny

Two post-Cambrian structure sets are identified that are consistent with deformation during the Alice Springs Orogeny. The first of these is characterised by south-directed thrust-faulting at the southern margin of the province. Seismic imaging in South Australia shows that south-directed thrusting of this margin has caused a monoclinal upturn of the Ordovician and Devonian sedimentary rocks of the Officer Basin (Lindsay and Leven, 1996). A similar margin geometry is not imaged in YOM, and the Winduldarra Fault clearly dips to the south. There is a change in the magnetic character of the margin from a sharp, faulted contact in the southern Mamutjarra Zone (Figure 5) to a more gradual transition in the Warburton region, perhaps reflecting differing behaviour either side of the Lasseter-Mundrabilla Shear Zone.

The post-NR expression of this structure is a 1–1.5 km deep north-trending graben characterised by smooth texture within the high-intensity responses of the Palgrave Group. The smooth texture is associated with a sandstone unit, which crops out near Mount Burt, and which was tentatively interpreted to be Permian-aged in 1st edition maps (BENTLEY SG52-5 and SCOTT SG52-9).

Summary

The magnetotelluric modeling, 2D potential-field forward modeling and 3D magnetic and gravity inversions indicate that crustal structure dominantly reflects the tectonics of the Ngaanyatjarra Rift and the Petermann Orogeny. The geometries of earlier events (Mount West Orogeny, Musgrave Orogeny) are recognized in places; however, at the crustal scale these have been comprehensively overprinted, and are not discussed here. The structure of the Alice Springs Orogeny is also important in places – most notably at the southern margin of the province, and in the vicinity of the Lasseter–Mundrabilla Shear Zone.

The structure of the Ngaanyatjarra Rift dominates the southwest of the area, which has been only moderately overprinted during subsequent events. Here we see the dominance initially, of the intrusion of the enormous mega-intrusions of the Giles Suite 1, and the less voluminous Giles Suite 2 and Warakurna Supersuite granites. Most of the deformation during this phase of the rift occurred through magmatic processes, or to accommodate the addition of the enormous intrusions into the upper crust. Subsequently, although magmatism remained the characteristic process of the NR, with the eruption of the Bentley Supergroup, some tectonically driven deformation took place, generating major fold events, basin-forming extension events, and widespread faulting. Overall, upper crustal shortening and extension are both somewhat limited, and the system is characterized by an enormous addition of magmatic material to the upper crust. The Tikelmungulda Seismic Province indicates that the lower crust was also subjected to the addition of an enormous amount of magmatic material as an underplate. Although this did not necessarily occur in a single event, nor during the NR (Howard et al., 2013; Korsch et al., 2013), for now we consider the NR the most likely source of the underplate. The remaining crust between the Tikelmungulda seismic province and the Bentley Supergroup is typically ca. 28 km thick along the YOM line. This compares with a likely pre-NR thickness of ca. 35 km (Smithies et al., 2011), suggesting a stretching factor in the pre-rift crust of ~1.25. This invites comparisons with the Midcontinent Rift, where a very thick and largely undeformed magmatic pile sits above thinned Archean crust (Hammer et al., 2010).

The Petermann Orogeny is prominent in the north and east and is characterized by three differing deformation styles. The Mulga Park Domain preserves low-angle thrust faulting and nappe style folding that involves both granitic basement and the overlying cover sequences (Edgoose et al., 2004;

Flottmann et al., 2005). This region has accommodated large amounts of shortening in the east, but much less to the west of a major tear-fault. High-pressure and temperature ductile deformation within the Walpa Pulka Zone is identified along low-angle structures (Raimondo et al., 2010). This region is exceptionally dense, but the structure of this flow-zone is not well imaged in the geophysical data. Finally, transpressional shearing on high-angle crustal-scale shear zones dominates the Tjuni Purlka Zone. Unlike in South Australia, a significant Moho offset is not clearly identified, although it is not inconsistent with the gravity field. The shear zones that bound the uplifted Moho in South Australia bound an area of tilted crust, that, with additional distance between them, would generate a similar Moho offset. Post NR strike-slip offsets on these crustal-scale fault zones can be as much as 22 km or as little as 4 km, and both dextral and sinistral offsets are observed.

Acknowledgements

The Musgrave MT survey was funded by the Exploration Incentives Scheme of the Western Australian Government. We acknowledge the support of AuScope for the ANSIR MT equipment, and Goran Boren for his assistance in the use of it. We thank GSWA field staff, Mario, Ray and Paul for their assistance in collecting the MT data, Chris Hocking for collecting the petrophysical data, and Mario Werner for his help understanding the geology of the west Musgrave Province.

References

Aitken, A.R.A., and Betts, P.G., 2009. Multi-scale integrated structural and aeromagnetic analysis to guide tectonic models: An example from the eastern Musgrave Province, Central Australia. *Tectonophysics*, 476, 418-435.

Aitken, A.R.A., Betts, P.G., Weinberg, R.F., and Gray, D., 2009a. Constrained potential field modelling of the crustal architecture of the Musgrave Province in central Australia: Evidence for lithospheric strengthening due to crust-mantle boundary uplift. *Journal of Geophysical Research B: Solid Earth* 114, B12405, doi:10.1029/2008JB006194.

Aitken, A.R.A., Betts, P.G., and Ailleres, L., 2009b. The architecture, kinematics, and lithospheric processes of a compressional intraplate orogen occurring under Gondwana assembly: The Petermann orogeny, central Australia. *Lithosphere* 1, 343–357.

Aitken, A.R.A., Smithies, R.H., Dentith, M.C., Joly, A., Evans, S., and Howard, H.M., 2013. Magmatism-dominated intracontinental rifting in the Mesoproterozoic: The Ngaanyatjarra Rift, central Australia. *Gondwana Research*, http://dx.doi.org/10.1016/j.gr.2012.10.003.

Braun, J., McQueen, H.W.S., and Etheridge, M.A., 1991. A fresh look at the late Palaeozoic Tectonic History of Western-central Australia. *Exploration Geophysics*, 22, 49–54.

Camacho, A., and Fanning, C.M., 1995. Some isotopic constraints on the evolution of the granulite and upper amphibolite facies terranes in the eastern Musgrave Block, central Australia. *Precambrian Research*, 71, 155–181.

Camacho, A., Compston, W., McCulloch, M., and McDougall, I., 1997. Timing and exhumation of eclogite facies shear zones, Musgrave Block, central Australia. *Journal of Metamorphic Geology*, 15, 735–751.

Edgoose, C.J., Scrimgeour, I.R., and Close, D.F., 2004. Geology of the Musgrave Block, Northern Territory. *Northern Territory Geological Survey*.

Evins, P.M., Smithies, R.H., Howard, H.M., Kirkland, C.L., Wingate, M.T.D., and Bodorkos, S., 2010. Devil in the detail; The 1150–1000Ma magmatic and structural evolution of the Ngaanyatjarra Rift, west Musgrave Province, Central Australia. *Precambrian Research*, 183, 572–588.

Evins, P.M., Kirkland, C.L., Wingate, M.T.D., Smithies, R.H., Howard, H.M., and Bodorkos, S., 2012. Provenance of the 1340–1270 Ma Ramarama Basin in the west Musgrave Province, central Australia. *Geological Survey of Western Australia, Report* 116, 39p.

Flottmann, T., Hand, M., Close, D., Edgoose, C., and Scrimgeour, I., 2005. Thrust tectonic styles of the intracratonic Alice Springs and Petermann orogenies, Central Australia. *AAPG Memoir*, 538–557.

Fullagar, P.K., Pears, G.A., and McMonnies, B., 2008. Constrained inversion of geologic surfaces - pushing the boundaries. The Leading Edge (Tulsa, OK) 27, 98–105.

Glikson, A.Y., Stewart, A.J., Ballhaus, C.G., Clarke, G.L., Feeken, E.H.J., Leven, J.H., Sheraton, J.W., and Sun, S.S., 1996. Geology of the western Musgrave Block, central Australia, with particular reference to the mafic-ultramafic Giles Complex. *AGSO Bulletin*, 239, 41–68.

GSWA, 2011. http://geodownloads.dmp.wa.gov.au/Downloads/Metadata_Statements/XML/Geochronology_2011.xml.

Hammer, P.T.C., Clowes, R.M., Cook, F.A., van der Velden, A.J., and Vasudevan, K., 2010. The Lithoprobe trans-continental lithospheric cross sections: Imaging the internal structure of the North American continent. *Canadian Journal of Earth Sciences,* 47, 821–857.

Howard, H.M., Smithies, R.H., Pirajno, F., and Skwarnecki, M.S., 2009a. Bell Rock, W.A. sheet 4645. 2nd Edition 1:100000 Geological Series. *Geological Survey of Western Australia*.

Howard, H.M., Smithies, R.H., Kirkland, C.L., Evins, P.M., and Wingate, M.T.D., 2009b. Age and geochemistry of the Alcurra Suite in the west Musgrave Province and implications for orthomagmatic Ni-Cu-PGE Mineralization during the Giles Event. *Geological Survey of Western Australia*.

Howard, H.M., Werner, M., Smithies, R.H., Evins, P.M., Kirkland, C.L., Kelsey, D.E., Hand, M., Collins, A.S., Pirajno, F., Wingate, M.T.D., Maier, W.D., and Raimondo, T., 2011. The geology of the west Musgrave Province and the Bentley Supergroup - a field guide. *Geological Survey of Western Australia*, 119p.

Howard, H.M., Quentin de Gromard, R., Smithies, R.H., Kirkland, C.L., Korsch, R.J., Aitken, A.R.A., Gessner, K., Wingate, M.T.D., Blewett, R.S., Holzschuh, J., Kennett, B.L.N., Duan, J., Goodwin, J.A., Jones, T., Neumann, N.L., and Gorczyk , W., 2013. Geological setting and interpretation of the northeastern half of deep seismic reflection line 11GA-YO1: west Musgrave Province and the Bentley Supergroup. In: Neumann, N.L. (editor), *Yilgarn Craton–Officer Basin–Musgrave Province (YOM) Seismic and MT Workshop*. Geoscience Australia Record 2013/28, 51–95.

Joly, A., Aitken, A.R.A., Dentith, M., Porwal, A.K., and Smithies, R.H., 2013. Mineral prospectivity analysis of the West Musgrave Province. *Geological Survey of Western Australia Report*.

Korsch, R.J., and Kositcin, N., 2010. GOMA (Gawler Craton–Officer Basin–Musgrave Province–Amadeus basin) Seismic and MT Workshop 2010. *Geoscience Australia Record* 2010/39, 162p.

Korsch, R.J., Blewett, R.S., Smithies, R.H., Quentin de Gromard, R., Howard, H.M., Pawley, M.J., Carr, L.K., Hocking, R.M., Neumann, N.L., Kennett, B.L.N., Aitken, A.R.A., Holzschuh, J., Duan, J., Goodwin, J.A., Jones, T., Gessner, K., and Gorczyk, W., 2013. Geodynamic implications of the Yilgarn Craton–Officer Basin–Musgrave Province (YOM) deep seismic reflection survey: part of a ~1800 km transect across Western Australia from the Pinjarra Orogen to the Musgrave Province. In: Neumann, N.L. (editor), *Yilgarn Craton–Officer Basin–Musgrave Province (YOM) Seismic and MT Workshop*. Geoscience Australia Record 2013/28, 169–197.

Lambeck, K., and Burgess, G., 1992. Deep crustal structure of the Musgrave Block, central Australia: results from teleseismic travel time anomalies. *Australian Journal of Earth Sciences*, 39, 1–19.

Lindsay, J.F., and Leven, J.H., 1996. Evolution of a Neoproterozoic to Palaeozoic intracratonic setting, Officer Basin, South Australia. *Basin Research*, 8, 403–424.

Maboko, M.A.H., McDougall, I., Zeitler, P.K., and Williams, I.S., 1992. Geochronological evidence for ~530–550 Ma juxtaposition of two Proterozoic metamorphic terranes in the Musgrave Ranges, central Australia. *Australian Journal of Earth Sciences*, 39, 457–471.

Parker, R.L., 1994. Geophysical inverse theory. Princeton University Press, Princeton N.J.

Raimondo, T., Collins, A.S., Hand, M., Walker-Hallam, A., Smithies, R.H., Evins, P.M., and Howard, H.M., 2010. The anatomy of a deep intracontinental orogen. *Tectonics*, 29, TC4024, doi:10.1029/2009TC002504.

Seat, Z., Beresford, S.W., Grguric, B.A., Waugh, R.S., Hronsky, J.M.A., Gee, M.A.M., Groves, D.I., and Mathison, C.I., 2007. Architecture and emplacement of the Nebo-Babel gabbronorite-hosted magmatic Ni-Cu-PGE sulphide deposit, West Musgrave, Western Australia. *Mineralium Deposita*, 42, 551–581.

Seat, Z., Mary Gee, M.A., Grguric, B.A., Beresford, S.W., and Grassineau, N.V., 2011. The Nebo-Babel Ni-Cu-PGE sulfide deposit (West Musgrave, Australia): Pt. 1. U/Pb zircon ages, whole-rock and mineral chemistry, and O-Sr-Nd isotope compositions of the intrusion, with constraints on petrogenesis. *Economic Geology*, 106, 527–556.

Smithies, R.H., Howard, H.M., Evins, P.M., Kirkland, C.L., Bodorkos, S., Wingate, M.T.D., 2009a. The west Musgrave Complex - new geological insights from recent mapping, geochronology, and geochemical studies. *Geological Survey of Western Australia Record* 2008/19, 20p.

Smithies, R.H., Howard, H.M., Maier, W.D., Evins, P.M., 2009b. Blackstone, WA Sheet 4545, 1:100000 Geological Series. *Geological Survey of Western Australia*.

Smithies, R.H., Howard, H.M., Evins, P.M., Kirkland, C.L., Kelsey, D.E., Hand, M., Wingate, M.T.D., Collins, A.S., and Belousova, E., 2011. High-temperature granite magmatism, crust-mantle interaction and the Mesoproterozoic intracontinental evolution of the Musgrave Province, Central Australia. *Journal of Petrology*, 52, 931–958.

Stewart, A.J., 1995. Resolution of conflicting structures and deformation history of the Mount Aloysius granulite massif, western Musgrave Block, central Australia. *AGSO Journal of Australian Geology and Geophysics*, 16, 91–105.

Sun, S.S., Sheraton, J.W., Glikson, A.Y., and Stewart, A.J., 1996. A major magmatic event during 1050–1080 Ma in central Australia, and an emplacement age for the Giles Complex. *AGSO Research Newsletter*, 24, 13–15.

7 Numerical modelling of the west Musgrave Province during Musgrave Orogeny

W. Gorczyk[1] and H. Smithies[2]

[1] Centre for Exploration Targeting, School of Earth and Environment, The University of Western Australia, 35 Stirling Highway, Crawley, WA 6009.
[2] Geological Survey of Western Australia, Department of Mines and Petroleum, 100 Plain Street, East Perth, WA 6004.

weronika.gorczyk@uwa.edu.au

Introduction

The west Musgrave Province is the Western Australian part of the Musgrave Province, which lies at the convergence of three major crustal blocks: the North, West and South Australian cratons. These cratons are interpreted to have amalgamated prior to c. 1290 Ma (e.g. Giles et al., 2004). The Musgrave Orogeny has been interpreted as an intra-continental orogeny (Wade et al., 2006, 2008) and has been dominated by ultra-high temperature (UHT) conditions, which have persisted from c. 1220 Ma to c. 1120 Ma. Granites of the Pitjantjatjara Supersuite dominate the west Musgrave Province and were emplaced at temperatures ≥1000°C from c. 1220 Ma to c. 1150 Ma. The onset of UHT metamorphism coincided with a change from low-Yb to voluminous high-Yb granite magmatism, reflecting a change to melting at lower pressures linked to a rapid decrease in crustal thickness. Pitjantjatjara magmatism and UHT metamorphism are related to the same thermal anomaly but the metamorphism is not a direct result of granite magmatism. UHT metamorphic conditions of ≥1000°C at 7-8 kbar (i.e. ~25 km depth) reflect a very thin crust (including crustal lithosphere), with a maximum thickness of ~35 km throughout the duration of the Musgrave Orogeny. The geochemical and isotopic homogeneity of the granites over a scale of >15 000 km^2 reflects a similarly homogeneous source. This source included an old enriched felsic crustal component but also incorporated >50% mantle material (Smithies et al., 2011). Pulsed addition of mantle magma resulted in at least four distinct granite age peaks each with a corresponding metamorphic age peak that occurs ~10 Myr later.

The duration of UHT metamorphic conditions that characterises the Musgrave Orogeny is inconsistent with a mantle plume and hence other geodynamical models have been proposed. The Musgrave Province itself is rigidly fixed at the nexus of three thick cratonic masses (North, West and South Australia cratons). Therefore, this geotectonic position may have provided a foci for both asthenospheric upwelling and far-field stresses acting on relatively thin lithosphere, producing periodic (pulsed) tectonic instabilities under a regime of a more continuous supply of both heat and mantle-derived magma (Smithies et al., 2011).

A series of 2D numerical experiments have been performed to test different scenarios for the development of UHT conditions at the indicated crustal levels for an extended period of time (~100 Ma) in tectonic settings relevant to Musgrave Orogeny. The numerical results indicate that the most plausible process that introduces high temperatures >1000°C for over 50 Myr is mechanical removal of the mantle lithosphere by asymmetric delamination (Gorczyk et al., 2013).

Numerical method

The 2D petrological-thermomechanical model used in this work simulates intra-continental deformation on a lithospheric to upper mantle cross-section. The model is based on the I2VIS code (Gerya, 2010; Gerya and Yuen, 2003), which uses conservative finite differences and a non-diffusive marker-in-cell technique to simulate multiphase flow. The rheologies used in this study are visco-plastic. Stable mineral assemblages, as a function of pressure and temperature are computed based on thermodynamic data and Gibbs free energy minimization using the software *Perplex* (Connolly, 2005). Dehydration reactions and associated water release are computed based on the physicochemical conditions and the assumption of thermodynamic equilibrium (Gerya and Meilick, 2011; Gorczyk et al., 2007; Sizova et al., 2010). As the water transport model used here does not permit complete hydration of the peridotitic mantle, the mantle solidus is intermediate between the wet and dry peridotite solidi. To account for this behaviour we assume that the degree of both hydrous and dry melting is a linear function of pressure and temperature (i.e. Gerya and Yuen, 2003).

For a given pressure and rock composition, the volumetric degree of melting M_0 is:

$M_0 = 0$ when $T < T_{solidus}$,

$M_0 = (T - T_{solidus}) / (T_{liquidus} - T_{solidus})$ when $T_{solidus} < T < T_{liquidus}$,

$M_0 = 1$ when $T > T_{liquidus}$,

$T_{solidus}$ and $T_{liquidus}$ are solidus temperature and dry liquidus temperature (wet and dry solidi are used for the hydrated and dry mantle, respectively) at a given pressure and rock composition.

Although melt might accumulate and form large melt reservoirs, it is more likely that melt collects in channels or dykes and leaves the melting zone before reaching high melt fractions (Schmeling et al., 2008; Schmeling et al., 1999). Hence, melt exceeding a predefined melt threshold (i.e. Schmeling et al., 2008) of M_{max} = 4 % is extracted and only a non-extractable amount of melt M_{min} = 2 % remains at the source (Gerya and Meilick, 2011; Nikolaeva et al., 2008; Sizova et al., 2010). Markers track the amount of extracted melt during the evolution of an experiment.

The total amount of melt, M, for every marker takes into account the amount of previously extracted melt and is calculated as:

$M = M_0 - \Sigma_n M_{ext}$

$\Sigma_n M_{ext}$ is the total melt fraction extracted during the previous *n* extraction episodes. Rocks are considered refractory when the extracted melt fraction is larger than the standard one, when $\Sigma_n M_{ext} > M_0$. If the total amount of melt exceeds M_{max}, the melt fraction $M_{ext} = M - M_{min}$ is extracted and $\Sigma_n M_{ext}$ is updated.

Extracted melt is transmitted instantaneously to emplacement areas, as melt migrates faster than rocks deform (Elliott et al., 1997; Hawkesworth et al., 1997). Although the average and range of intrusive:extrusive (I:E) volume ratios for different petrotectonic settings may differ (ranging from 1:1 to 16:1), a ratio of 5:1 can be viewed as common to most magmatic systems considering the uncertainties (White et al., 2006).

All experiments have been performed in a spatial coordinate frame of 3000 km x 400 km, representing a continental to upper mantle cross-section (Figure 7.1A). The rectangular grid with 1221 x 201 nodal points is non-uniform and contains a (1600 km wide) high-resolution (1 km x 2 km) in the centre of the

domain while the rest of the model remains at a lower resolution (10 x 2 km). The continental crust is composed of 15 km thick felsic upper and 15 km thick intermediate lower crust. The subjacent asthenosphere and the upper mantle are composed of anhydrous peridotite and are defined by the given temperature profile.

The initial temperature field of the continental plate increases linearly from 0°C at the surface to 1344°C at the lithosphere-asthenosphere boundary. A thermal gradient of 0.5°C km^{-1} is used for the asthenospheric mantle. The depth of mantle lithosphere is defined thermally.

The thermally shallow zone (Figure 7.1A) represents the area of younger/deformed/amalgamated continental lithosphere trapped between two cratonic bodies.

An internally prescribed velocity field within the convergence condition region ensures horizontal compression between the two continental blocks. The convergence rate is symmetric; each side is pushed with the same constant velocity for 6 Ma. After 6 Ma, the convergence rate is set to zero and deformation is purely self-driven from then on.

Results

In the model presented in Figure 7.1, at the initial stage of compression, buckling of the thermally thinner lithosphere is observed, which results in development of a lithospheric scale thrust, as well as thickening of the crust in this area (Figure 7.1B), which may lead to melting of low-Yb granites. As compression proceeds, partial subduction of lithospheric mantle with a portion of the crust takes place.

After 10 Ma, far field compression ceases. This causes the termination of subduction of lithospheric mantle and detachment of the eclogitized subducted part the lithosphere. Following the detachment of subducted lithosphere, asthenospheric material upwells (in response to downwelling cold slab) in this area and leads to a rise in the temperature at the Moho as well as local extension (Figure 7.1C). As a consequence, decompression melting of the dry perioditic mantle and horizontal melt intrusion at crustal levels occurs (Figure 7.1D). A portion of the lower crust and underlying mantle lithosphere decouples from the upper part, then peels away, and finally detaches as the density of the subducting part increases during eclogitization of the sinking material. Extension in the remaining upper crust enables additional asthenospheric inflow of hot mantle material to shallow depths; this results in ultra-high temperatures at very shallow levels (800–1100°C at the base of the crust). Occurrence of such elevated temperatures (exceeding 1000ºC) promotes melting of different kinds of rocks. Due to localized input of hot material, rocks experience melting under different thermal conditions (although dominated by HT and UHT melting) – from the centre of the heat influx to its flanks. A large growing magma chamber forms, where magmas from multiple melting events mix and mingle, strongly affecting the petrological and geochemical evolution of the crust. For example, more than 30% of all magmatic rocks are remelted after decompression melting is initially triggered, despite the continued supply of new volcanic and plutonic rocks. The main melting event (Figure 7.1D–E) starts at 52 Ma (Figure 7.2) and lasts for 25 Myr, when decompression melting is introduced and fertile crustal material melts for the first time. Since high temperatures remain for over 50 Myr (52 -105 Ma), rocks are exposed to periodic remelting and freezing episodes. Crystallised rocks may sink into partially molten melt reservoirs and mobile melt may rise to upper levels where it solidifies before reaching densities high enough for foundering.

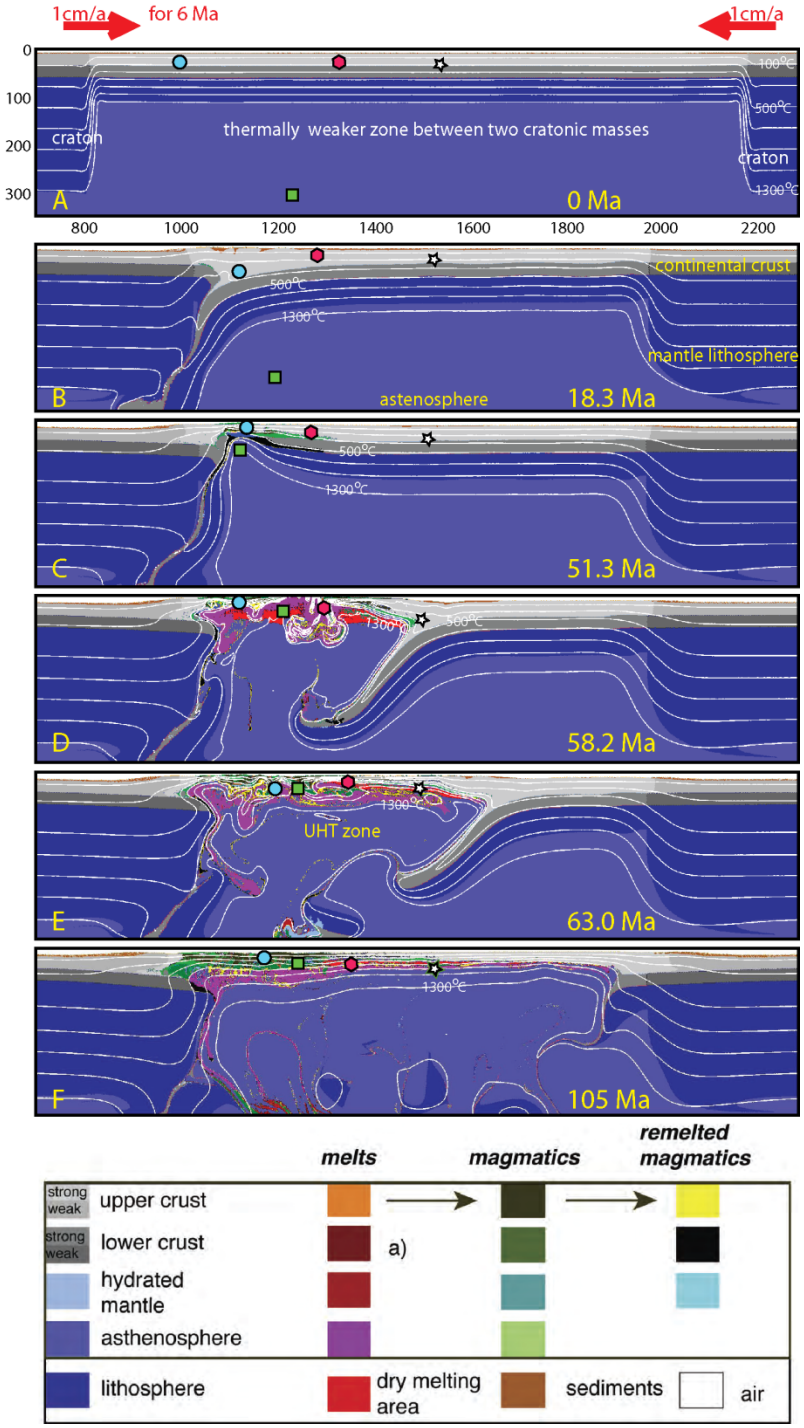

Figure 7.1 *Dynamic evolution of the lithosphere after 6 Ma of convergence at a rate of 2 cm/year. Detachment of dense lithosphere develops an asymmetric geometry and allows for hot inflow of asthenospheric material. Hence, decompression melting is triggered and results in ultra-high temperatures at shallow levels and multiple melting and remelting events of crustal- and mantle-derived rocks. Geometric figures represent traced markers, and their pressure-temperature histories are shown in Figure 7.3.*

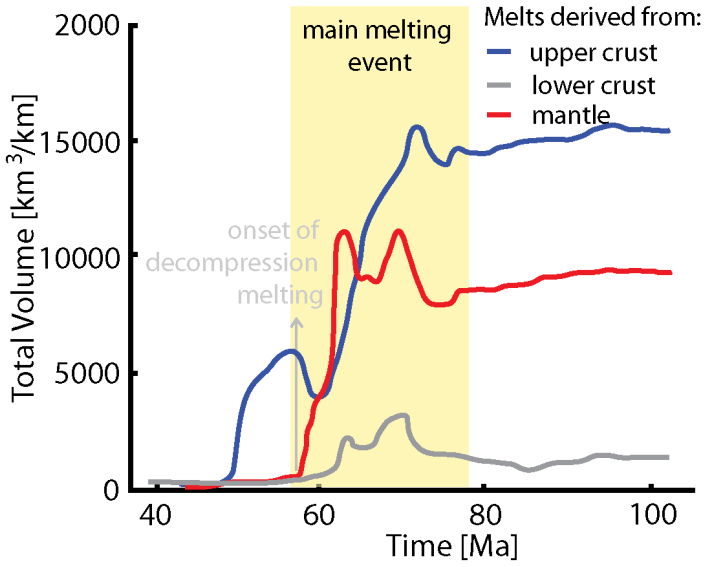

Figure 7.2 *Magmatic consequences of delamination event in terms of magmatic addition in km^3/km.*

However, after 73 Ma, decompression melting ceases and fertile source becomes exhausted. All subsequent melting events are related to remelting processes as temperatures remain high enough to allow for crustal anatexis. The spatial distribution of rocks caused by delamination and detachment is related to its tectonic evolution. Melting begins from a “central” point with the highest temperatures and extension, which leads to crustal thinning, and is dominated by mafic melts originating from the mantle. Farther to the sides of the initiation zone, the addition of the crustal material is observed and strong mixing and mingling of mafic and felsic material takes place. The melting zone is rimmed by a zone of thermally metamorphosed crustal rocks. Thermal equilibration follows, with new mantle lithosphere developing. The rocks in the melting zone mostly follow clockwise PT paths (Figure 7.3), with temperatures reaching 1200ºC. Further from the main melting zone, counter-clockwise PT paths occur and the thermal influence decreases.

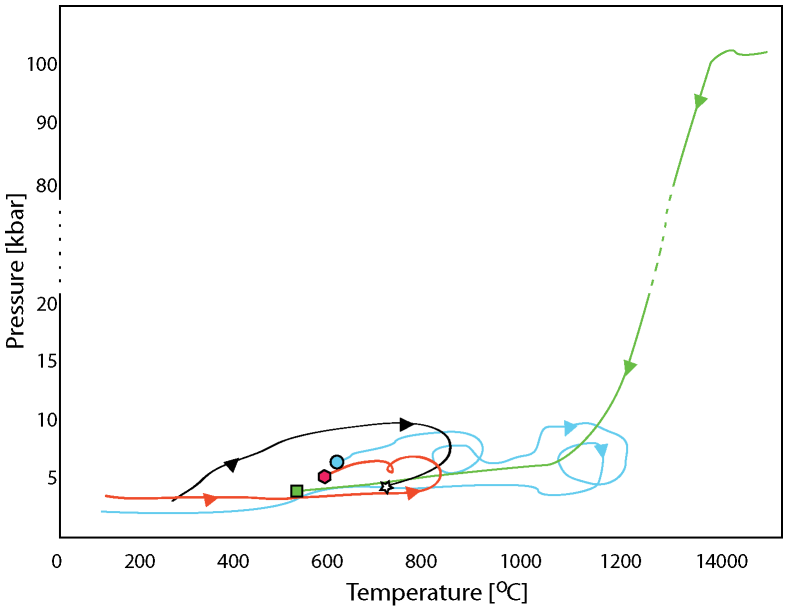

Figure 7.3 *The temperature-pressure evolution of markers represented as geometric figures in Figure 7.1.*

Conclusions

The reported UHT magmatism and high-grade temperature metamorphism event during the Musgrave Orogeny has lasted for ~100 Myr. The model presented in Figure 7.1 presents UHT melting event only for ~25 Myr. The time span of the Musgrave melting event extends the model melting time by 4 times. This discrepancy does not disqualify the process of asymmetric delamination of the mantle lithosphere as the leading process during the Musgrave Orogeny. In the models, the melting was extinguished with a lack of fertile melting sources. The prolonged influx of fresh asthenospheric material during the event may be related to 3-dimentionality of the process, and also due to small, not recorded extensional or compressional episodes caused by far field stress. In this regards, the pulsed nature of granite magmatism and of UHT metamorphism throughout the 100 Myr period of the orogeny provides a focus for future modelling.

Acknowledgments

This work was supported by the Australian Research Council Grant LP100200785. HS publishes with the permission of the Executive Director of the Geological Survey of Western Australia.

References

Connolly, J.A.D., 2005. Computation of phase equilibria by linear programming: a tool for geodynamic modeling and an application to subduction zone decarbonation. *Earth and Planetary Science Letters*, 236, 524–541.

Elliott, T., Plank, T., Zindler, A., White, W., and Bourdon, B., 1997. Element transport from slab to volcanic front at the Mariana arc. *Journal of Geophysical Research-Solid Earth*, 102(B7): 14991–15019.

Gerya, T., 2010. Introduction to Numerical Geodynamic Modelling. *Cambridge University Press*, 358p.

Gerya, T.V., and Meilick, F.I., 2011. Geodynamic regimes of subduction under an active margin: effects of rheological weakening by fluids and melts. *Journal of Metamorphic Geology*, 29, 7–31.

Gerya, T.V., and Yuen, D.A., 2003. Characteristics-based marker-in-cell method with conservative finite-differences schemes for modeling geological flows with strongly variable transport properties. *Physics of the Earth and Planetary Interiors*, 140, 293–318.

Giles, D., Betts, P.G., and Lister, G.S., 2004. 1.8–1.5-Ga links between the North and South Australian Cratons and the Early–Middle Proterozoic configuration of Australia. *Tectonophysics*, 380, 27–41.

Gorczyk, W., Gerya, T.V., Connolly, J.A.D., and Yuen, D.A., 2007. Growth and mixing dynamics of mantle wedge plumes. *Geology*, 35, 587–590.

Gorczyk, W., Hobbs, B., Gessner, K., and Gerya, T., 2013. Intracratonic geodynamics. *Gondwana Research,* (in press).

Hawkesworth, C.J., Turner, S.P., McDermott, F., Peate, D.W., and vanCalsteren, P., 1997. U–Th isotopes in arc magmas: Implications for element transfer from the subducted crust. *Science*, 276(5312), 551–555.

Nikolaeva, K., Gerya, T.V., and Connolly, J.A.D., 2008. Numerical modelling of crustal growth in intraoceanic volcanic arcs. *Physics of the Earth and Planetary Interiors*, 171, 336–356.

Schmeling, H., Babeyko, A.Y., Enns, A., Faccenna, C., Funiciello, F., Gerya, T., Golabek, G.J., Grigull, S., Kaus, B.J.P., Morra, G., Schmalholz, S.M., and van Hunen, J., 2008. A benchmark comparison of spontaneous subduction models-Towards a free surface. *Physics of the Earth and Planetary Interiors*, 171, 198–223.

Schmeling, H., Monz, R., and Rubie, D.C., 1999. The influence of olivine metastability on the dynamics of subduction. *Earth and Planetary Science Letters*, 165, 55–66.

Sizova, E., Gerya, T., Brown, M., and Perchuk, L.L., 2010. Subduction styles in the Precambrian: Insight from numerical experiments. *Lithos*, 116, 209–229.

Smithies, R.H., Howard, H.M., Evins, P.M., Kirkland, C.L., Kelsey, D.E., Hand, M., Wingate, M.T.D., Collins, A.S., and Belousova, E., 2011. High-Temperature Granite Magmatism, Crust-Mantle Interaction and the Mesoproterozoic Intracontinental Evolution of the Musgrave Province, Central Australia. *Journal of Petrology*, 52, 931–958.

Wade, B.P., Barovich, K.M., Hand, M., Scrimgeour, I.R., and Close, D.F., 2006. Evidence for early Mesoproterozoic arc magmatism in the Musgrave Block, central Australia: Implications for Proterozoic crustal growth and tectonic reconstructions of Australia. *Journal of Geology*, 114, 43–63.

Wade, B.P., Kelsey, D.E., Hand, M., and Barovich, K.M., 2008. The Musgrave Province: Stitching north, west and south Australia. *Precambrian Research*, 166, 370–386.

8 The nature of the lithosphere in the vicinity of the Yilgarn Craton–Officer Basin–Musgrave Province (11GA-YO1) seismic line

B.L.N. Kennett

Research School of Earth Sciences, The Australian National University, Canberra ACT 0200, Australia

Brian.Kennett@anu.edu.au

Introduction

In addition to the recent program of reflection profiling in western and central Australia, a broad range of seismological studies have been made using both man-made and natural sources. Up to the 1980s there was an extensive program of seismic refraction studies, which provided important information on crustal structure. Since 1992, the Australian National University has carried out deployments of portable broad-band seismic recorders across Australia. These instruments provide high-fidelity recording of ground motion and record both regional and distant earthquakes. In addition, the national seismic network operated by Geoscience Australia has been augmented in recent years, particularly for tsunami warning.

Figure 8.1 illustrates the coverage that has been achieved in the western part of central Australia. The very significant impact of the Yilgarn Craton–Officer Basin–Musgrave Province reflection line (11GA-YO1) on available information is immediately apparent. Previously in this remote area, there had just been two broadband seismic stations deployed in the SKIPPY reconnaissance survey of the entire continent from 1993–1996. These can be seen as the two blue diamonds under the track of the 11GA-YO1 line in Figure 8.1. Since that time extensive areas of Aboriginal freehold have been granted and land access has become more complex.

The seismograms from the portable and permanent seismic stations across the continent can be analysed to generate information on lithospheric structure beneath the Australian region, both in the crust and uppermost mantle, using a variety of styles of analysis (e.g. Kennett, 2003). The principal information from regional earthquakes comes from the analysis of the large amplitude surface waves which arrive late in the seismograms. These surface waves travel almost horizontally through the lithosphere and with a sufficient density of crossing paths can be used in a tomographic inversion to determine 3-D structure in the lithospheric mantle. Receiver based studies at individual stations exploit the conversions and reverberations following the onset of the P wave energy. From distant earthquakes information can be extracted about the structure in the crust and uppermost mantle, since the paths arriving at the stations are near vertical.

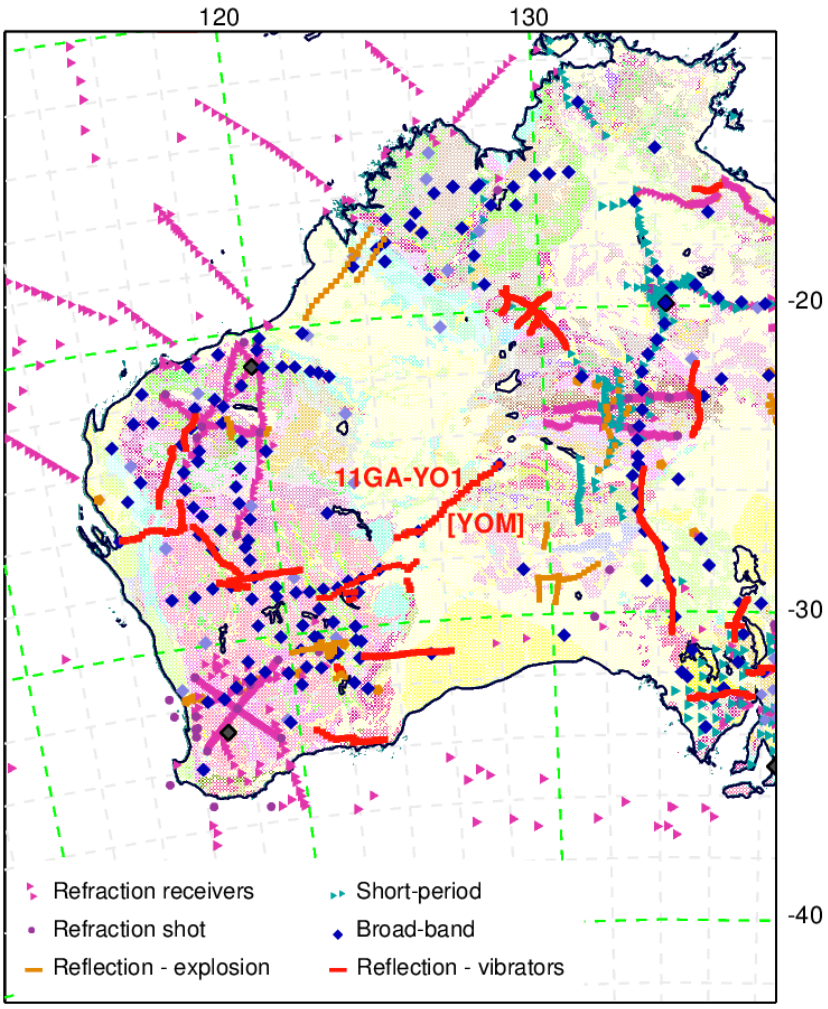

Figure 8.1 *Distribution of active seismic experiments and passive seismic recording across western and central Australia. Coverage is mostly sparse in the desert interior, with a few stations deployed during the SKIPPY reconnaissance survey of the continent from 1993–1996 using a limited number of stations deployed for 5–6 months at a time. Background generalised surface geology from Geoscience Australia.*

Additional information has begun to be extracted from the seismic noise field, through the stacked cross-correlation of signals at pairs of stations that provide an approximation to the signal expected for a source at one station recorded at the other location. This ambient noise tomography approach was pioneered in Australia by Saygin (2007) using the continuous data recordings at the portable stations in association with permanent seismic stations to link different experiments. The main signal comes from high frequency surface waves, which provide imaging of upper to middle crustal structure, and are particularly sensitive to the presence of sedimentary basins (Saygin and Kennett, 2010, 2012).

Recently a major synthesis of the available seismological constraints on lithospheric structure has been carried out to produce the Australian Seismological Reference Model (AuSREM). An overview of the AuSREM model is given in Kennett and Salmon (2012). A detailed description of the crustal component and its construction is presented in Salmon et al. (2013), with a comparable treatment for the mantle component in Kennett et al. (2013). The crustal and mantle components are linked through the Moho model constructed using all available information, including reflection picks (Kennett et al., 2011; Salmon et al., 2013).

We build on the results from the AuSREM model in this summary of lithospheric properties in the neighbourhood of the Yilgarn Craton–Officer Basin–Musgrave Province (YOM) reflection line. Though, as we shall see, the deeper part of the crustal structure is not well constrained through the area traversed by the reflection profile.

Crustal Structure

Receiver Function studies

A powerful method to extract information on crustal structure is the analysis of the conversions and reverberations immediately following the onset of the P wave for distant earthquakes using the receiver function technique. The two horizontal components of motion are combined to produce records with polarization along (radial) and perpendicular (tangential) to the great circle back to the source. The rotated components are then deconvolved using the vertical component of motion that represents dominantly P waves. In this way the influence of the source is largely eliminated and attention is focused on wave propagation processes close to the receiver. When there is little energy on the tangential receiver function 3-D structural variation is weak, and then an inversion may be made using a radial receiver function for an effective 1-D structure in the neighbourhood of the receiver (see e.g. Shibutani et al., 1996; Sambridge, 1999). Alternative approaches use stacking of receiver functions to emphasis features such as the conversion from the crust-mantle boundary and hence constrain the Moho depth. The move-out pattern of conversions and multiples from different source distances can be used to constrain the depth of seismic boundaries and Vp/Vs ratios (Zhu and Kanamori, 2000). It can also be advantageous to make a partial allowance for the influence of the free surface on the seismograms by a rotation of components in the vertical plane or a transformation (e.g. Reading et al., 2003a).

The first systematic treatment of receiver function results across Australia were made by Clitheroe et al. (2000a, 200b) with an emphasis on the thickness of the crust and also the base of sedimentary basins; just two of these stations lie in the zone near the YOM profile (Figure 8.1). A particular focus of portable broadband deployments since 2000 has been on Western Australia with a number of deployments that now provide good coverage of the Archean cratons and the Proterozoic Capricorn Orogen (Reading and Kennett, 2003; Reading et al., 2003b, 2007, 2012). However, the more remote area to the east has not been revisited since the 1990s.

AuSREM Crustal model

The results from receiver functions provide S wavespeed profiles in the immediate neighbourhood of the seismic stations, together with an estimate of the ratio between P and S wavespeeds. Refraction experiments provide P wavespeed along the line of stations with full crustal penetration only near the midpoints. The resulting model is illustrated in Figure 8.2 with depth slices at 10 km intervals starting at 5 km depth. The constraints from the ambient noise tomography are rather weak below 25 km, and so there are portions of the model without direct control. We have blanked out those regions that lie further than 200 km from a refraction or receiver function control point in Figure 8.2, notably in the Canning Basin at 35 km depth.

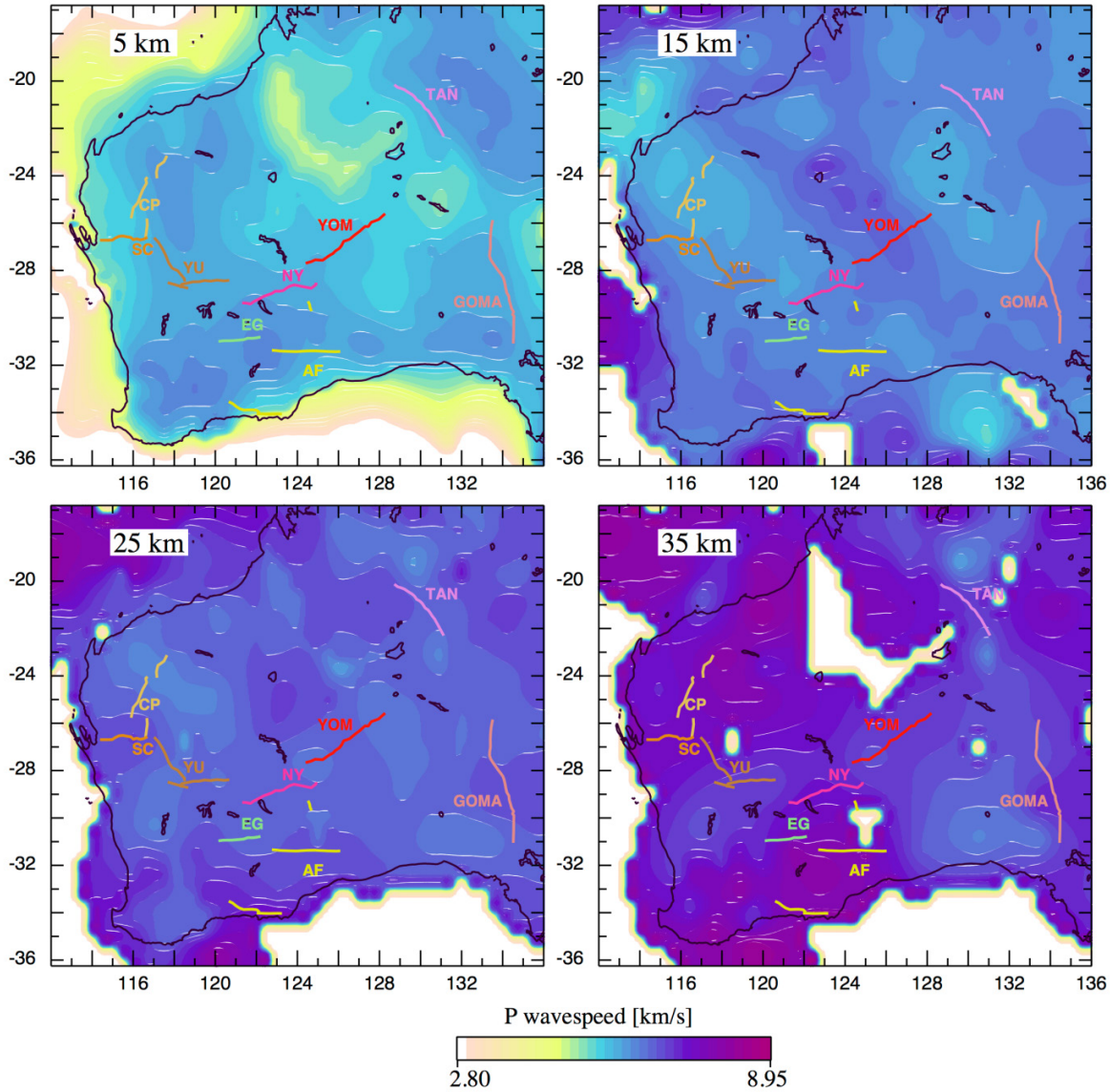

Figure 8.2 *Depth slices through the AuSREM crustal model for P wavespeed for the region around the YOM reflection line. The same wavespeed scale is used for all depths, since mantle speeds are encountered at 15 km off shore. Regions without direct control on wavespeed are blanked out at depth. In each panel the positions of recent seismic lines are indicated by coloured lines.*

At 5 km depth we see the influence of the deep sediments in the Canning Basin, principally from the ambient noise analysis, contrasting with the Proterozoic metasediments in the Capricorn Orogen. The transition to the Pinjarra Orogen is evident in slower P wavespeeds along the western coast of Western Australia at 5 km depth, but at greater depth there is very little contrast with the Yilgarn. The YOM line lies on a mild gradient of decreasing P wavespeed towards the northeast at 5 km depth, but the wavespeeds are comparatively fast at 15 km depth. The thinner crust in the Pilbara is reflected in the presence of mantle wavespeeds at 35 km depth, and rather high P wavespeeds are encountered in the southern Yilgarn, which recent reflection work suggests arises within the reflective crust and helps to explain a bimodal distribution of crustal thickness in this area from earlier studies, with estimates of crustal thickness varying from around 28 km to 40 km (e.g. Kennett et al., 2011). The transition from the Yilgarn Craton to the Musgrave Province along the YOM line lies within an area with modest variation in P wavespeed, even though there are distinct differences in the style of crustal reflectivity.

Crustal thickness

Kennett et al. (2011) assembled the full suite of available information on the depth to Moho across the continent by drawing on results from refraction experiments, receiver functions and Moho picks from the full suite of crustal reflection profiles across the continent. For refraction or receiver function studies the crust-mantle boundary is taken at the base of the transition to mantle seismic velocities (P wavespeeds above 7.9 km/s or shear wavespeeds above 4.4 km/s). On the reflection records, the Moho is taken at the base of the set of crustal reflectors and converted to depth using an average crustal velocity of 6 km/s.

The estimates of crustal thickness from Western Australia into the centre of the continent are summarized in Figure 8.3. There is a close correspondence in the estimates from the different techniques and station deployments even though the methods of analysis differ significantly, e.g., the profile of crust thickness in the northern Yilgarn from the receiver function studies is very similar to that seen on the reflection profile, and in consequence the receiver function results provide a check on the calibration of the time-depth conversion for the reflection results.

The YOM line has led to a significant revision of the pattern of crustal thickness in western central Australia. Not only does the YOM reflection profile provide the only dense coverage in a broad area, the Moho depth estimates taken at the base of crustal reflectivity require a significant thickening of the crust in the centre of the profile. The reflection results compare quite well with the Moho estimates from receiver functions at the two stations along the road. These two widely separated stations both suggested crustal thickness around 42–44 km, but there was no reason to guess that the crust might be 10 km thicker in between. The analysis by Aitken (2010) using gravity inversion to supplement the then available seismological estimates required significant crustal thickness (more than 40 km) through the area, but much thicker crust was not required to fit the gravity field.

A relatively smooth crustal thickness profile has been adopted for incorporation into a continent-wide synthesis, since steps are not easily incorporated into the interpolation for a single Moho surface. Nevertheless the reflection results are highly suggestive of an offset in the Moho of about 8 km, though the details of the transition across the zone of crustal thickening are difficult to extract from the rather weak reflectivity.

The background contour plot of the Moho in Figure 8.3 is taken from the continent wide synthesis of results, using all receiver functions and the refraction data from the compilation of Collins et al. (2003), with additional control from reflection experiments (Kennett et al., 2011; Salmon et al., 2013).

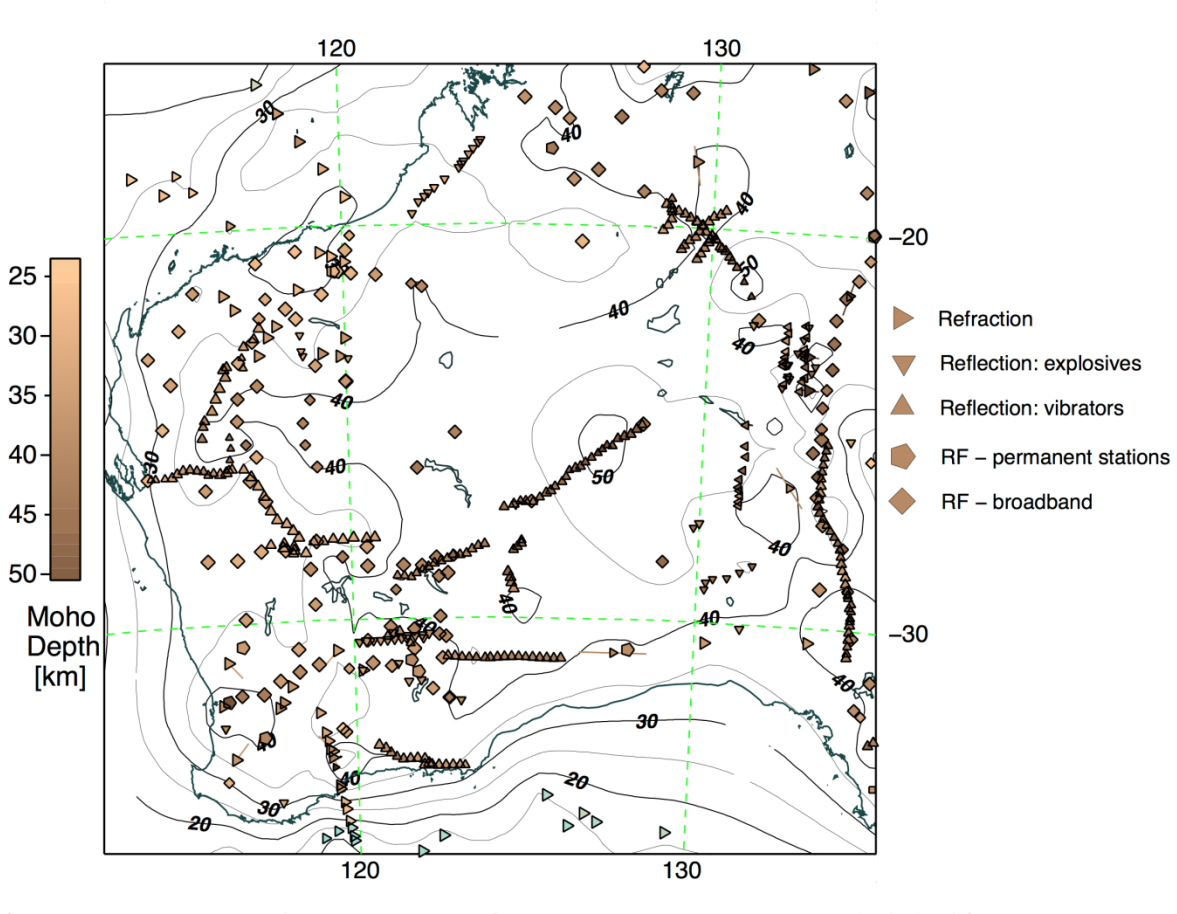

Figure 8.3 *Estimates of crustal thickness derived from the full range of available sources: refraction experiments (triangles) and receiver function studies (diamonds - broad-band stations, squares – short-period stations), less reliable results are indicated by smaller symbols. Moho estimates from reflection work are indicated by the dense lines of triangles. The contours of Moho depth are derived from a continent-wide synthesis (Salmon et al., 2013), and are strongly influenced by the results from the YOM line.*

Surface Wave tomography

The earthquake belts to the north of Australia along the Indonesian arc into New Guinea and to the east in the Tonga–Fiji zone provide frequent seismic events of suitable magnitude to be recorded well in Australia. There are less common events to the south along the mid-oceanic ridge between Australia and Antarctica, but these are important in providing additional directional control. A number of different techniques have been used to analyse the large amplitude surface waves that arrive late in the seismogram, and from the combinations of results from many paths, 3-D models of the seismic shear wavespeed distribution have been extracted (e.g. van der Hilst et al., 1998; Debayle and Kennett, 2000, 2003; Kennett et al., 2004a, 2004b; Fishwick et al., 2005, 2008; Yoshizawa and Kennett, 2004; Fichtner et al., 2009, 2010). Most of the methods rely on some approximations to wave propagation in three dimensions, but the work of Fitchtner et al. (2009, 2010) uses full seismogram calculations in a 3-D model. In consequence, the frequency range used is restricted to prevent excessive computational requirements. Fortunately the results with this sophisticated analysis indicate that the longer wavelength features obtained with the approximate methods are confirmed.

We can now have considerable confidence in the main structures in the lithosphere at a horizontal scale of about 200 km and a vertical resolution around 30 km. Figure 8.4 illustrates the shear wave

structure in western Australia using the AuSREM mantle model developed in a collaboration between the authors of a number of different studies (Yoshizawa and Kennett, 2004; Fishwick and Rawlinson, 2012; Fichtner et al., 2010). This new model benefits from the incorporation of more paths than in any individual study and includes the use of techniques that provide improved resolution at depth. The variations in seismic S wave velocity are displayed in terms of the absolute shear wavespeed at each depth, with the neutral colour chosen to represent typical continental values.

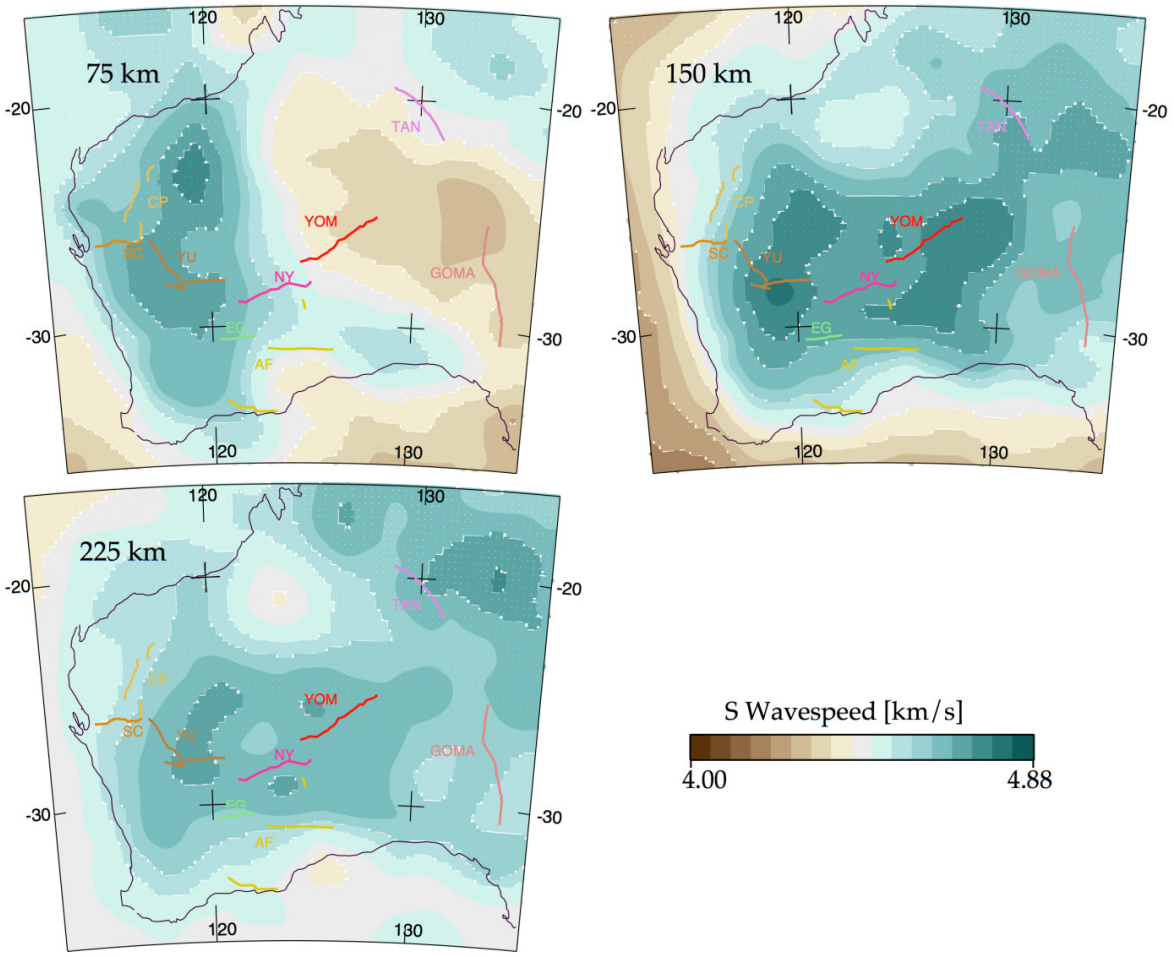

Figure 8.4 *Seismic shear-wavespeed structure in western to central Australia from the AuSREM mantle model, largely controlled by surface wave tomography. (a)–(c) Continental scale estimates of seismic wavespeed variation at 75, 150, and 225 km depth, inferred from the analysis of surface waves. In each panel the position of recent reflection seismic lines are indicated by coloured lines.*

Regions with faster S wavespeed than the continental reference are indicated by bluish tones, and zones with slower S wavespeed are shown in tones of brown in Figure 8.4. Reductions in seismic wavespeed are expected from the influence of increased temperature or the presence of volatiles. Faster wavespeeds are produced by cooler temperatures, but the very fast wavespeeds seen in Figure 8.4 are very difficult to produce by temperature alone and suggest the presence of chemical heterogeneity.

The mantle lithosphere below 100 km is marked by distinct fast seismic wavespeeds, but at about 75 km there is an indication of a reduction in wavespeeds (Figure 8.4a) in the east of Western Australia, that may be linked in part to the presence of thickened crust (Figure 8.3). The YOM reflection profile crosses into this lower wavespeed zone, yet at greater depth shear wavespeeds are

very fast. The area of lower S wavespeed is not associated with enhanced seismic attenuation as might be expected if the cause was a concentration of heat producing elements in the uppermost mantle, and its origin remains somewhat enigmatic.

At 75 km depth the Paterson Orogen is marked by very high seismic wavespeeds, and there is also a distinct rather fast patch in the northern Yilgarn Craton. There is no distinctive mantle feature associated with the Capricorn Orogen, though we note that at 225 km the Capricorn Orogen and Pilbara Craton show somewhat lower shear wavespeeds than in the Yilgarn Craton. The zone of very fast shear wavespeeds beneath the Yilgarn Craton extends towards central Australia under the area traversed by the YOM reflection line, and remains relatively fast even at 225 km depth. This zone of elevated wavespeeds is among the thickest seismic lithosphere on the Australian continent (Kennett and Salmon, 2012).

Discussion and Conclusions

The AuSREM model for lithospheric structure in the Australian region provides valuable controls on the 3-D variability of seismic wavespeed that can be helpful in the interpretation of other classes of information such as reflection seismic profiles. The crustal component of AuSREM builds on information from man-made and natural sources, using refraction experiments, near receiver studies using distant earthquakes and continent-wide tomography exploiting ambient seismic noise. In the uppermost mantle, surface wave tomography is the main source of information on 3-D S wavespeed variation, with the most reliable results available below 75 km depth. At shallower depth there is a strong influence from the crustal structure along the various paths and crustal structure can be mapped into the uppermost mantle – especially where the crust is thick.

The very distinct changes in styles of crustal reflectivity as one progresses from the Yilgarn Craton undercover to the Musgrave Province along the YOM reflection line, are not matched by comparable changes in P velocity, except for a modest gradient in the near surface. The reflection line itself has changed our perceptions of the way in which the crustal components interact, with a distinct crustal thickening that had not been anticipated from previous work.

The YOM reflection profile spans a significant gradient in shear wavespeed in the uppermost mantle (though this may be influenced by thickened crust above) with the slowest wavespeeds lying beneath the Musgrave Province. The estimates of mantle structure are affected by the nature of the crust and the reduction in wavespeeds may be influenced by thicker crust than assumed in the original analyses that were combined to create the AuSREM mantle model. At greater depth, the lithosphere beneath the YOM seismic line shows high wavespeeds characteristic of a cratonic environment, and extends to at least 225 km depth.

Acknowledgements

The deployments of portable broad-band stations across Australia have depended on the efforts of many people often working in trying circumstances. Particular thanks are due to John Grant, Steve Sirotjuk and Qi Li for their major role in maintaining equipment and logistics and to Armando Arciadiaco for field support and a critical role in data handling and organization. Receiver function results draw on the work of Drs Geoff Clitheroe, Anya Reading, Steve Revets, Erdinc Saygin, Michelle Salmon, and Elizabeth Vanacore. Special thanks go to Anya Reading for her systematic studies of seismic structure in Western Australia, which have been very significant in the construction of the crustal wavespeed distribution.

References

Aitken A.R.A., 2010. Moho geometry gravity inversion experiment (MoGGIE): a refined model of the Australian Moho and its tectonic and isostatic implications. *Earth and Planetary Science Letters*, 297, 71–83.

Clitheroe G., Gudmundsson O., and Kennett B.L.N., 2000a. The crustal thickness of Australia. *Journal of Geophysical Research*, 105, 13697–13713.

Clitheroe G., Gudmundsson O., and Kennett B.L.N., 2000b. Sedimentary and upper-crustal structure of Australia from receiver functions. *Australian Journal of Earth Sciences*, 47, 209–216.

Collins C.D.N., Drummond B.J., and Nicoll M.G., 2003. Crustal thickness patterns in the Australian continent. In: Müller, D. and Hillis, R. (editors), The Evolution and Dynamics of the Australian Plate. *Geological Society of Australia Special Publication 22 and Geological Society of America Special Paper* 372, 121–128.

Debayle E., and Kennett B.L.N., 2000. The Australian continental upper mantle - structure and deformation inferred from surface waves. *Journal of Geophysical Research*, 105, 25443–25540.

Debayle E., and Kennett B.L.N., 2003. Surface wave studies of the Australian region. In: Müller, D. and Hillis, R. (editors), The Evolution and Dynamics of the Australian Plate. *Geological Society of Australia Special Publication 22 and Geological Society of America Special Paper* 372, 25–40.

Fichtner A., Kennett B.L.N., Igel H., and Bunge H.-P., 2009. Full seismic waveform tomography for upper-mantle structure in the Australasian region using adjoint methods. *Geophysical Journal International*, 179, 1703–1725.

Fichtner A., Kennett B.L.N., Igel H., and Bunge H.-P., 2010. Full seismic waveform tomography for radially anisotropic structure: New insights into the past and present states of the Australasian upper mantle. *Earth and Planetary Science Letters*, 290, 270–280.

Fishwick S., Kennett B.L.N., and Reading A.M., 2005. Contrasts in lithospheric structure within the Australian Craton. *Earth and Planetary Science Letters*, 231, 163–176.

Fishwick S., Heintz M., Kennett B.L.N., Reading A.M., and Yoshizawa K., 2008. Steps in lithospheric thickness within eastern Australia, evidence from surface wave tomography. *Tectonics*, 27(4), TC0049, doi:10.129/2007TC002116.

Fishwick S., and Rawlinson N., 2012. 3-D structure of the Australian lithosphere from evolving seismic datasets. *Australian Journal of Earth Sciences*, 59, 809–826.

Kennett B.L.N., 2003. Seismic Structure in the mantle beneath Australia. In: Müller, D. and Hillis, R. (editors), The Evolution and Dynamics of the Australian Plate. *Geological Society of Australia Special Publication 22 and Geological Society of America Special Paper* 372, 7–23.

Kennett B.L.N., and Salmon M., 2012. AuSREM: Australian seismological reference model. *Australian Journal of Earth Sciences*, 59, 1091–1103.

Kennett B.L.N., Fishwick S., Reading A.M., and Rawlinson N., 2004a. Contrasts in mantle structure beneath Australia – relation to Tasman Lines? *Australian Journal of Earth Sciences*, 51, 563–569.

Kennett B.L.N., Fishwick S., and Heintz M., 2004b. Lithospheric structure in the Australian region - a synthesis of surface wave and body wave studies. *Exploration Geophysics*, 35, 258–266.

Kennett B.L.N., Salmon M., Saygin E., AusMoho working group, 2011. AusMoho: the variation in Moho depth across Australia. *Geophysical Journal International*, 187, 946–958

Kennett B.L.N., Fichtner A., Fishwick S., and Yoshizawa K., 2013. Australian Seismological Reference Model (AuSREM): mantle component. *Geophysical Journal International*, 192, 871–887.

Reading, A.M., and Kennett, B.L.N., 2003. Lithospheric structure of the Pilbara Craton, Capricorn Orogen and northern Yilgarn Craton, Western Australia, from teleseismic receiver functions. *Australian Journal of Earth Sciences*, 50, 439–445.

Reading A., Kennett B., and Sambridge M., 2003a. Improved inversion for seismic structure using transformed S-wavevector receiver functions: removing the effect of the free surface. *Geophysical Research Letters*, 30(19), 1981; doi: 10.1029/2003GL018090.

Reading, A.M., Kennett, B.L.N., and Dentith, M.C., 2003b. The seismic structure of the Yilgarn Craton, Western Australia. *Australian Journal of Earth Sciences*, 50, 427–438.

Reading, A.M., Kennett, B.L.N., and Goleby, B., 2007. New constraints on the seismic structure of West Australia: Evidence for terrane stabilization prior to the assembly of an ancient continent? *Geology*, 35, 379–379.

Reading A., Tkalčić H., Kennett B.L.N., Johnson S.P., and Sheppard S., 2012. Seismic structure of the crust and uppermost mantle of the Capricorn and Paterson Orogens and adjacent cratons, Western Australia, from passive seismic transects. *Precambrian Research*, 196, 295–308.

Salmon M., Kennett B.L.N., and Saygin E., 2013. Australian Seismological Reference Model (AuSREM): crustal component. *Geophysical Journal International*, 192, 190–206.

Sambridge M.S., 1999. Geophysical inversion with a neighbourhood algorithm – I. Searching a parameter space. *Geophysical Journal International*, 138, 479–494.

Saygin E., 2007. Seismic receiver and noise correlation based studies in Australia, Ph.D. Thesis, Australian National University.

Saygin E., and Kennett B.L.N., 2010. Ambient noise tomography for the Australian Continent. *Tectonophysics,* 481, 116–125, doi:10.106/j.tecto.2008.11.013.

Saygin E., and Kennett B.L.N., 2012. Crustal structure of Australia from ambient seismic noise tomography. *Journal of Geophysical Research,* 117, B01304; doi:10.1029/2011JB008403.

Shibutani T., Sambridge M., and Kennett B.L.N., 1996. Genetic algorithm inversion for receiver functions with application to crust and uppermost mantle structure beneath Eastern Australia. *Geophysical Research Letters*, 23, 1829–1832.

van der Hilst R.D., Kennett B.L.N. and Shibutani T., 1998. Upper mantle structure beneath Australia from portable array deployments. In: Braun, J., Dooley, J., Goleby, B., van der Hilst, R., and Klootwijk, C. (editors), The Structure and Evolution of the Australian Lithosphere. *Geodynamics Monograph 26, American Geophysical Union*, 39–58.

Yoshizawa K., and Kennett B.L.N., 2004. Multi-mode surface wave tomography for the Australian region using a 3-stage approach incorporating finite frequency effects. *Journal of Geophysical Research*, 109, B02310; doi: 10.129/2002JB002254.

Zhu L., and Kanamori H., 2000. Moho depth variation in southern California from teleseismic receiver functions. *Journal of Geophysical Research,* 105, 2969–2980.

9 Geodynamic implications of the Yilgarn Craton–Officer Basin–Musgrave Province (YOM) deep seismic reflection survey: part of a ~1800 km transect across Western Australia from the Pinjarra Orogen to the Musgrave Province

R.J. Korsch[1], R.S. Blewett[1], R.H. Smithies[2], R. Quentin de Gromard[2], H.M. Howard[2], M.J. Pawley[3], L.K. Carr[4], R.M. Hocking[2], N.L. Neumann[1], B.L.N. Kennett[5], A.R.A. Aitken[6], J. Holzschuh[1], J. Duan[1], J.A. Goodwin[1], T. Jones[1], K. Gessner[2] and W. Gorczyk[6]

[1] Minerals and Natural Hazards Division, Geoscience Australia, GPO Box 378, Canberra, ACT 2601
[2] Geological Survey of Western Australia, Department of Mines and Petroleum, 100 Plain Street, East Perth, WA 6004
[3] Geological Survey of South Australia, Department of Manufacturing, Innovation, Trade, Resources and Energy, Level 4, 101 Grenfell Street, Adelaide, SA 5000
[4] Energy Division, Geoscience Australia, GPO Box 378, Canberra, ACT 2601
[5] Research School of Earth Sciences, The Australian National University, Canberra. ACT 0200
[6] Centre for Exploration Targeting, School of Earth and Environment, The University of Western Australia, 35 Stirling Highway, Crawley, WA 6009

Russell.Korsch@ga.gov.au

Introduction

In May and June 2011, 484 line kilometres of vibroseis-source, deep seismic reflection, gravity and magnetotelluric (MT) data were acquired along a single, northeast-southwest oriented traverse (11GA-YO1), referred to here as the YOM (Yilgarn Craton–Officer Basin–Musgrave Province) seismic survey. The line started in the western part of the Mesoproterozoic Musgrave Province and crossed the Neoproterozoic-Phanerozoic western Officer Basin (Figures 9.1 to 9.4). The northeastern part of the Archean Yilgarn Craton lies beneath the western side of the Officer Basin. The survey was funded by Geoscience Australia (GA), as part of its Onshore Energy Security Program, and the Geological Survey of Western Australia, through the Western Australian Government's Royalties for Regions Exploration Incentive Scheme. Acquisition, processing and interpretation of the seismic and MT data were managed by Geoscience Australia.

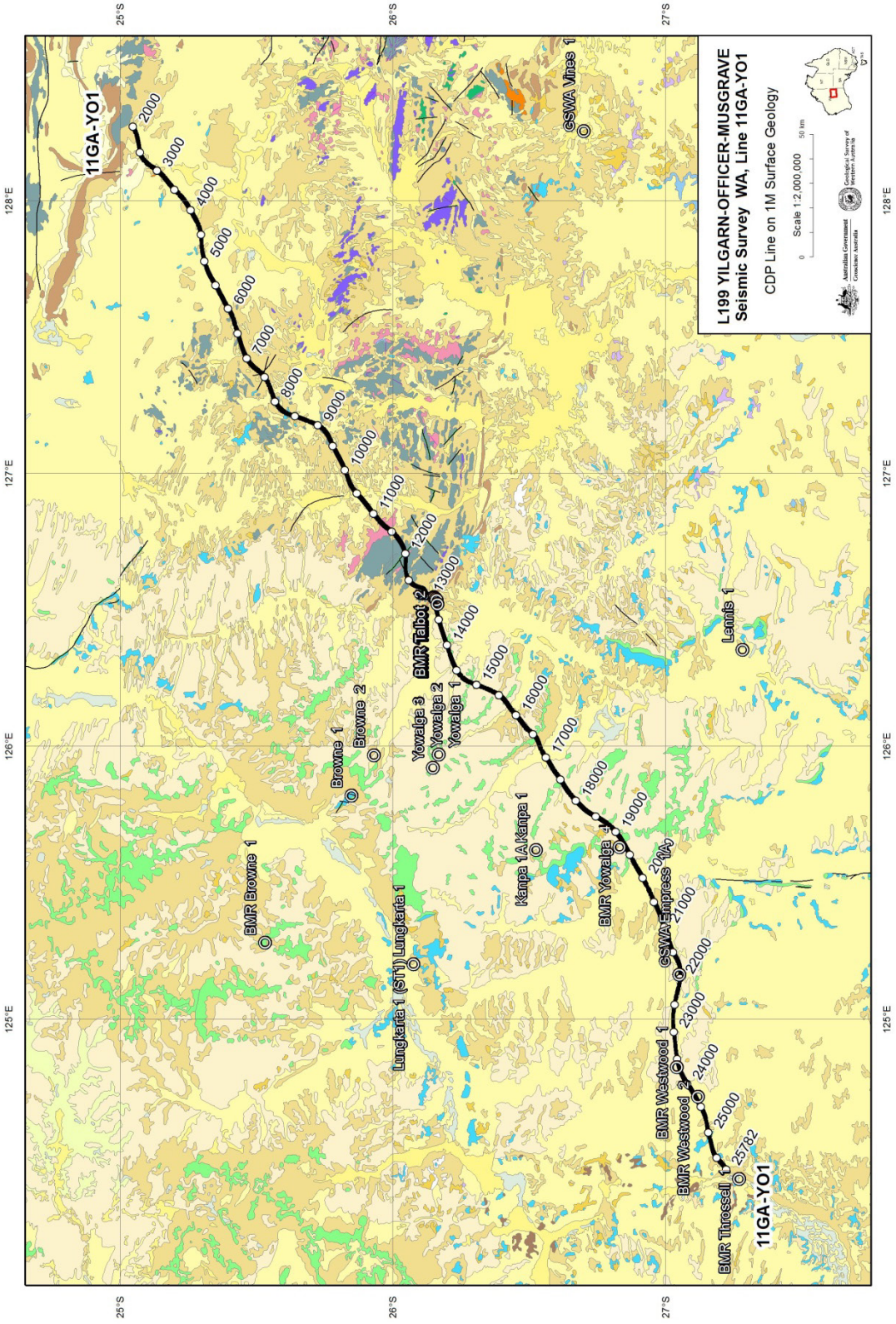

Figure 9.1 *Map showing the surface geology of the region covered by the YOM (11GA-YO1) seismic line, from the Yamarna Terrane in the northeastern Yilgarn Craton, across the western Officer Basin, to the west Musgrave Province. The surface geology is from the 1:1 000 000 scale geology map of Australia (Raymond, 2009, which also contains the legend). The seismic line has CDP stations labelled, and the locations of key drill holes are also shown.*

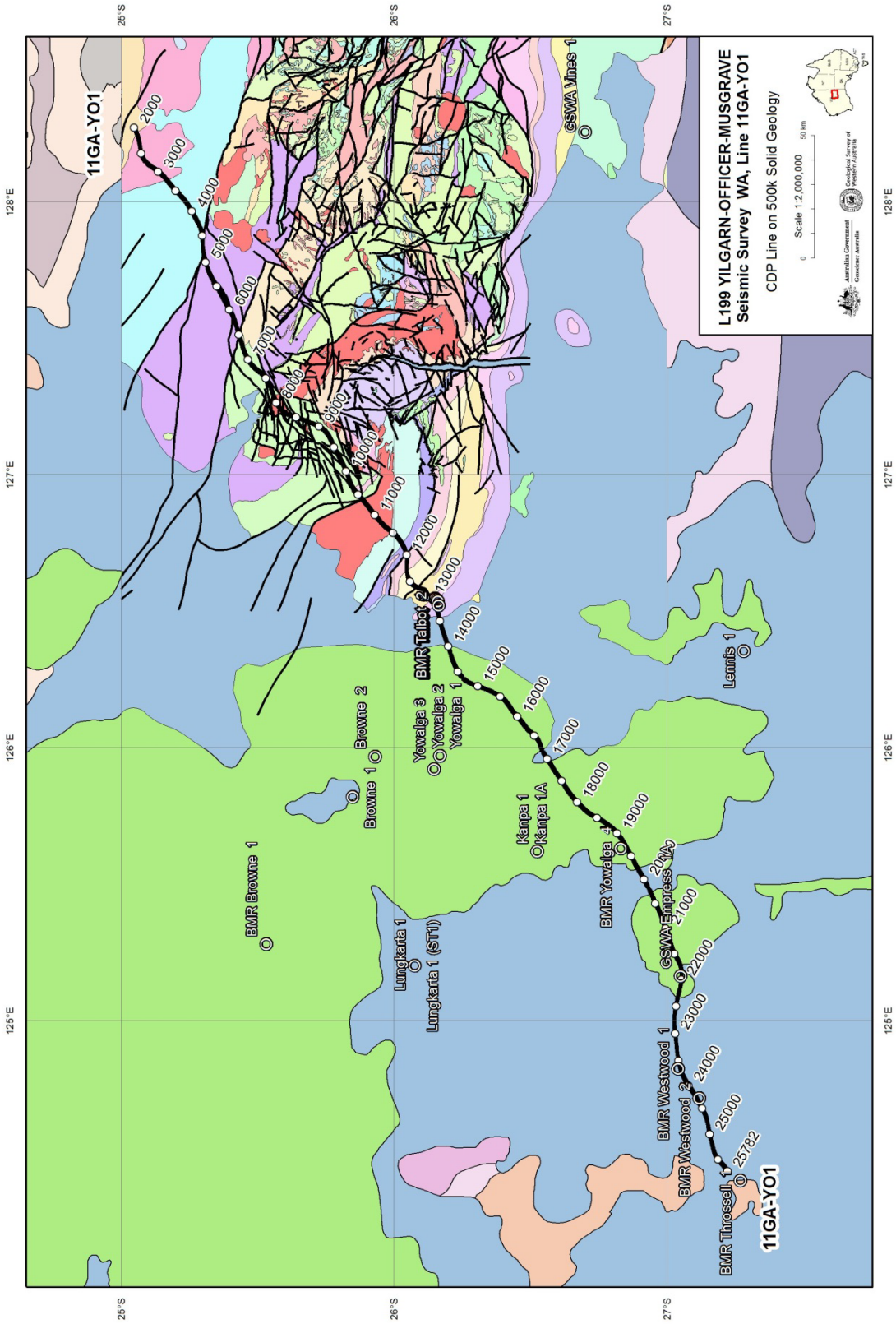

Figure 9.2 *Map showing the solid geology of the region covered by the YOM (11GA-YO1) seismic line, from the Yamarna Terrane in the northeastern Yilgarn Craton, across the western Officer Basin, to the west Musgrave Province. The solid geology is from the 1:500 000 scale solid geology map of Western Australia, which also contains the legend (Geological Survey of Western Australia, 2008; and unpublished data). The seismic line has CDP stations labelled, and the locations of key drill holes are also shown.*

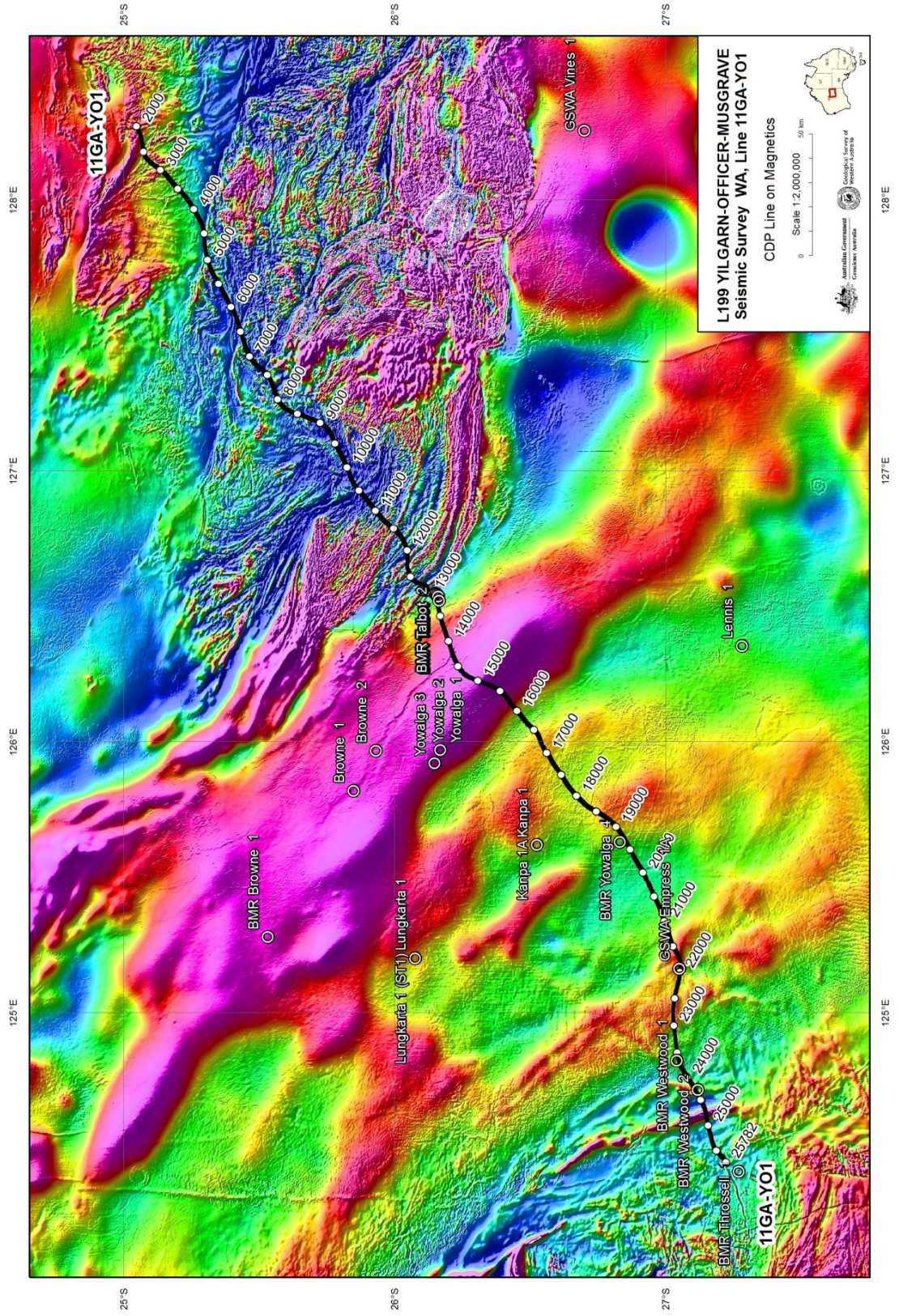

Figure 9.3 *Map showing regional aeromagnetic data for the region covered by the YOM (11GA-YO1) seismic line, from the Yamarna Terrane in the northeastern Yilgarn Craton, across the western Officer Basin, to the west Musgrave Province (extracted from Milligan et al., 2010). Warm colours are high magnetic intensities; cool colours are low magnetic intensities. The seismic line has CDP stations labelled, and the locations of key drill holes are also shown.*

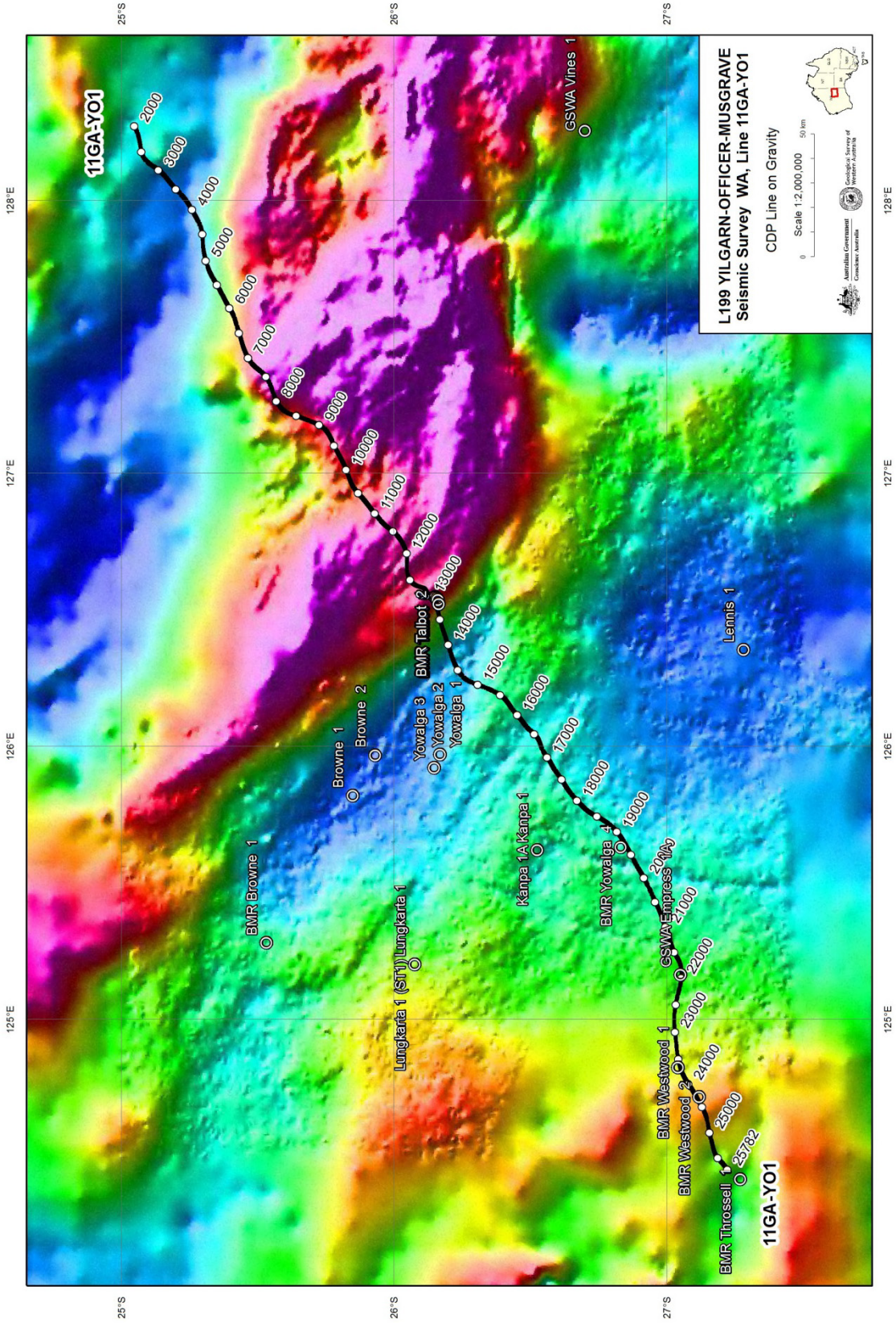

Figure 9.4 *Map showing a regional gravity image for the region covered by the YOM (11GA-YO1) seismic line, from the Yamarna Terrane in the northeastern Yilgarn Craton, across the western Officer Basin, to the west Musgrave Province (extracted from Bacchin et al., 2008). Warm colours are gravity highs, cool colours are gravity lows. The seismic line has CDP stations labelled, and the locations of key drill holes are also shown.*

The YOM seismic and MT survey was designed, in part, to evaluate:

1. the architecture of the western Officer Basin,
2. the potential of the western Officer Basin for structural and stratigraphic hydrocarbon traps, including the effects of the Neoproterozoic Petermann Orogeny, the late Cambrian Delamerian Orogeny, and the Late Ordovician to Carboniferous Alice Springs Orogeny,
3. the architecture and deep structure of the Archean Yamarna Terrane, in the northeast Yilgarn Craton, which is the easternmost terrane in the craton. It is largely hidden under younger cover and, thus, is the least well understood part of the Yilgarn Craton,
4. the architecture and deep structure of the Mesoproterozoic Musgrave Province [Note that Howard et al. (2013) use the term “Musgrave Province(?)” since the position of the YOM line, to the west of the Palgrave area, allows for the possibility that the region interpreted to be correlated with exposed Musgrave Province crust to the east is, in fact, exotic], and,
5. the relationship, in the subsurface beneath the western Officer Basin, between the Yamarna Terrane and the west Musgrave Province.

Companion papers in this volume present summaries of the geological evolution of the region and preliminary interpretations of the YOM seismic line (Korsch et al., 2013a; Howard et al., 2013), discussions of the potential field geophysics (Goodwin et al., 2013) and magnetotellurics (Duan et al., 2013). The approximate northeast–southwest orientation of the seismic line is essentially perpendicular to the major domains and structures in the region (Figures 9.2 to 9.4), and provides crustal-scale geometries which can be compared with existing geological interpretations. Overall, the crust in the vicinity of the seismic sections has variable reflectivity, with some parts of the section containing strong reflections, and other areas having very low reflectivity (Figure 9.5).

Here, we discuss some of the geodynamic implications which arise from interpretation of the new deep seismic reflection and MT data obtained during the YOM seismic survey. Of particular interest is the relationship, at a crustal scale, between the Yilgarn Craton and the Musgrave Province. For example, is there evidence for sutures between the terranes within the provinces, and is there evidence for a suture between the Yamarna Terrane and the west Musgrave Province? The current surveys build on the existing network of deep-crustal seismic surveys, and will improve the understanding of the crustal structure and geodynamics of Western Australia.

Moho

In the region of the YOM seismic survey, the crust below the Musgrave Province is thicker, by 5–15 km, than that below the Yilgarn Craton (Figure 9.5). The Mohorovičić discontinuity (Moho) has an undulating topography, varying in depth from about 14.8 s TWT (~44 km) at CDP 21500, beneath the Yilgarn Craton, to about 19.8 s TWT (~59 km) at about CDP 12500, beneath the Musgrave Province. The Moho is quite variable in seismic character. In places, for example at about CDP 19800, it is imaged as a relatively sharp discontinuity, at the base of strongly to moderately reflective packages, above nonreflective material which is interpreted as lithospheric mantle. In other places, however, the Moho is poorly imaged, and the transition from crust to mantle appears gradational, for example, in the centre of the line at about CDP 14600 (Figure 9.5).

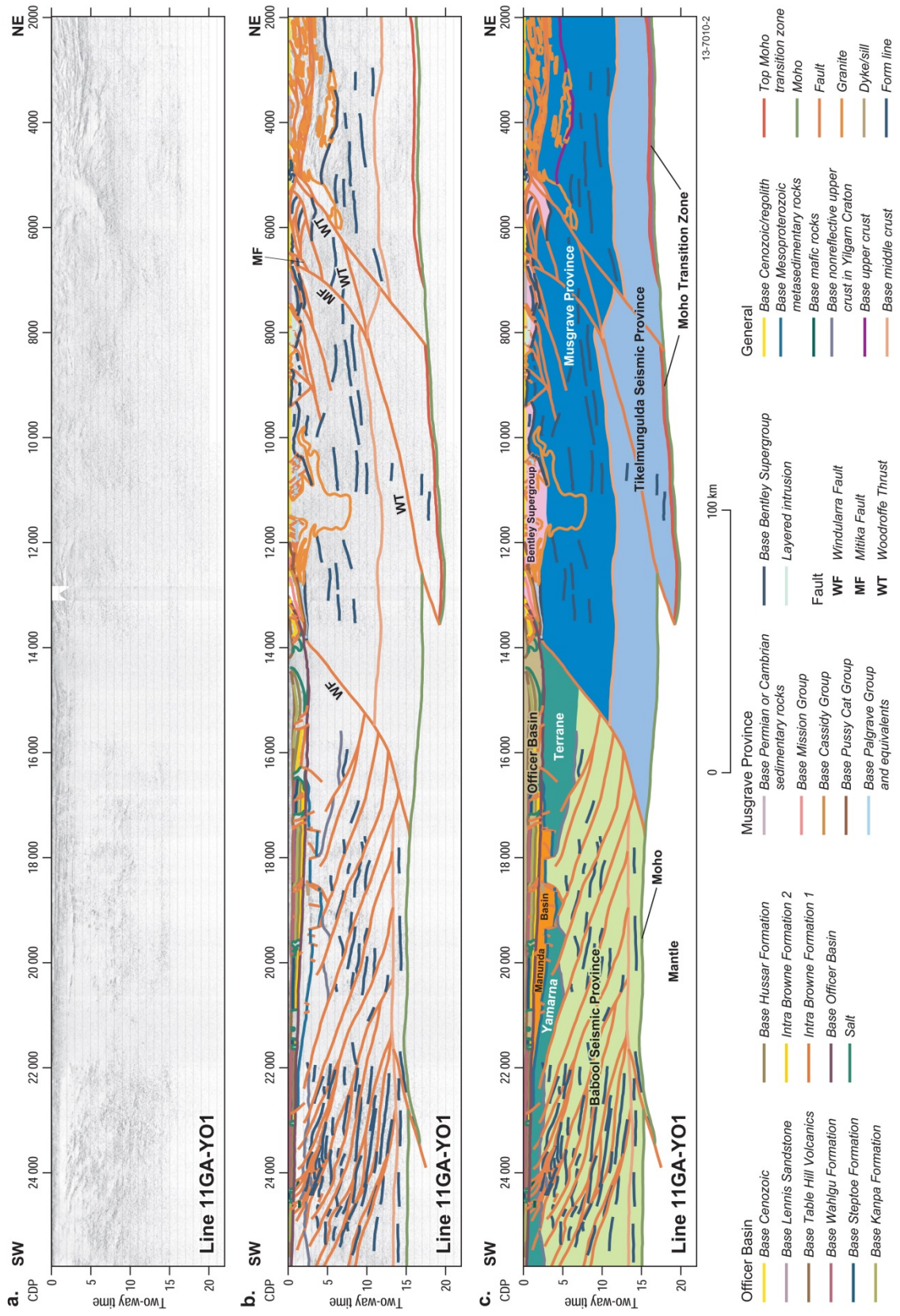

Figure 9.5 *Migrated seismic section for the seismic section 11GA-YO1, showing both (a) uninterpreted and (b) interpreted versions. Display is to 22 s TWT (~66 km) depth, and shows vertical scale equal to the horizontal scale, assuming a crustal velocity of 6000 ms^{-1}. Panel (c) shows the distribution of the basins and provinces along the YOM seismic line.*

Over the southwestern half of the YOM seismic survey, beneath the Yilgarn Craton, the Moho is essentially flat, at approximately 15 s TWT (~45 km) depth. Here, the Moho is mostly defined by the contrast between moderately reflective lower crust and mainly nonreflective upper mantle, but there is one area, centred on CDP 21200, where there is a lack of contrast between the lower crust and the upper mantle (Figure 9.5). Also, at about CDP 22800, the Moho appears to be displaced by a shallow, southwest-dipping fault, with strong reflections in the footwall being mapped to a depth of ~16.7 s TWT (~50 km) (Figure 9.5).

Several deep seismic reflection profiles across the Yilgarn Craton show that, with the exception of the Narryer Terrane, the Moho gradually deepens towards the east, from a depth of about 11 s TWT (~33 km) beneath the Youanmi Terrane (Korsch et al., 2013b), to about 12 s TWT (~36 km) under the Kalgoorlie Terrane (Drummond et al., 1993). It then deepens further, from about 13.5 s TWT (~40 km) under the Kurnalpi Terrane to about 15.5 s TWT (~46 km) under the western part of the Yamarna Terrane (Goleby et al., 2004).

Across the northeastern half of the YOM seismic survey, beneath the Musgrave Province, the Moho is generally much less distinctive than beneath the Yilgarn Craton, and is usually interpreted to be at the base of a weakly to moderately reflective package. The Moho dips gently to the southwest, from a depth of about 16.2 s TWT (~49 km), at the northern margin of the seismic section, to a depth of about 19.8 s TWT (~59 km), at about CDP 12500, beneath about the southern limit of the Musgrave Province, as mapped at the surface (Figure 9.5). In our interpretation, we map the Moho as being displaced by a low-angle fault, at about CDP 12550, with a vertical displacement of about 2.9 s TWT (~9 km) showing a thrust sense of movement. We have mapped this fault as cutting through the entire crust, the frontal splay of which is the Woodroffe Thrust at the surface (Figure 9.5). An alternative interpretation is that the Moho could ramp down smoothly, without displacement, from a depth of about 17 s TWT (~51 km), at about CDP 14200, to a depth of about 19.8 s TWT (~59 km), at about CDP 12500 (see Kennett, 2013).

The faulted character of the Moho near the southern margin of the Musgrave Province, and its gentle dip to the southwest, is in contrast to the Moho imaged on an older deep seismic reflection line across the boundary between the Musgrave Province and the Officer Basin in far western South Australia. There, it was interpreted to dip gently to the north, from a depth of about 43 km to about 48 km (Korsch et al., 1998; compare with a subhorizontal Moho at about 42 km depth inferred by Lindsay and Leven, 1996).

In the YOM seismic section, beneath the Musgrave Province, the Moho is best defined where there is a highly to moderately reflective crust–mantle transition zone, about 0.4–0.7 s TWT (~1–2 km) thick (Figure 9.5). The crust–mantle transition zone is not as persistent beneath the Musgrave Province as has been observed on deep seismic reflection lines elsewhere (e.g. North Queensland, Korsch et al., 2012; Canada, Hammer and Clowes, 1997; Clowes and Oueity, 2010), and it is not developed beneath the Yamarna Terrane in the YOM seismic line. This is in marked contrast to the moderately well-developed crust–mantle transition zone in deep seismic line 01AGS-NY1 under parts of the Kalgoorlie and Burtville terranes of the Yilgarn Craton to the west (Goleby et al., 2003), and the extremely well-developed crust–mantle transition zone imaged beneath the Youanmi Terrane of the Yilgarn Craton even farther west (Korsch et al., 2013b).

Crustal architecture

In the region of the YOM seismic section, the upper crust can be subdivided into several discrete provinces and basins, based principally on surface geological mapping, drill hole data, and the interpretation of potential-field data (Figure 9.5). These are the Yamarna Terrane of the Yilgarn Craton, the Officer and Manunda basins and the Musgrave Province (Figure 9.5). By comparison, the middle to lower crust appears to have a different seismic character, which is very different to that imaged in the upper crust immediately above it. Thus, we term the middle to lower crust beneath the Yamarna Terrane, the Babool Seismic Province (new name, after Babool Rockholes), and we term the lower crust below the Musgrave Province, the Tikelmungulda Seismic Province (new name, after Tikelmungulda Waterhole) (Figure 9.5). Following Korsch et al. (2010a), we use the term 'seismic province' to refer to a discrete volume of middle to lower crust, which cannot be traced to the surface, and whose crustal reflectivity is different to that of laterally or vertically adjoining provinces. All of the provinces, basins and seismic provinces can be distinguished by their seismic character (Korsch et al., 2013a; Howard et al., 2013) (Figure 9.5), and, to a lesser extent, by their electrical conductivity (Figure 9.6). The two middle to lower crustal seismic provinces interpreted in the YOM seismic line, for example, have very distinctive seismic characters, which are very different from each other (see below).

Southwestern half of the YOM seismic section

In the southwestern half of the YOM seismic section, five layers of crust can be seen (Figure 9.5):

1. The Officer Basin, consisting essentially of a gently-dipping layered succession, which thickens gradually towards the northeast,
2. The Manunda Basin, consisting of at least two graben, up to about 18 km wide, with thinner platforms extending to both sides, and containing at least three seismic stratigraphic sequences,
3. An upper crust, below the Officer and Manunda basins, which, in general, is only very weakly reflective, and varies in thickness from about 1.2 s TWT (~3–4 km) at about CDP 24000 to about 2.8 s TWT (~8 km) at about CDP 20750,
4. A strongly reflective middle crust, with reflections being planar or listric towards the northeast, and which sole onto the top of the lower crust. The middle crust is of variable thickness, ranging in thickness from about 8 s TWT (~24 km) at CDP 19600, to about 11.8 s TWT (~35 km) at about CDP 23950, and,
5. A relatively thin, moderately reflective lower crust, down to the Moho, but with predominantly subhorizontal reflections, ranging from about 1.3 s TWT (~4 km) at about CDP 21600 to about 2.2 s TWT (~7 km) at about CDP 17600. A highly reflective crust-mantle transition zone has not developed at the base of the lower crust, in contrast to one imaged on seismic line 01AGS-NY1 (Goleby et al., 2003) and on the Youanmi seismic lines (Korsch et al., 2013b).

In contrast to the Youanmi seismic lines (Korsch et al., 2013b), there are no obvious mafic sills intruding the crust, except for one intruding the upper succession in the Manunda Basin, at about CDP 18600, which could be related to the eruption of the late Cambrian Table Hill Volcanics, the Keene Basalt intersected in the GSWA Lancer 1 drill hole, or the Warakurna Large Igneous Province.

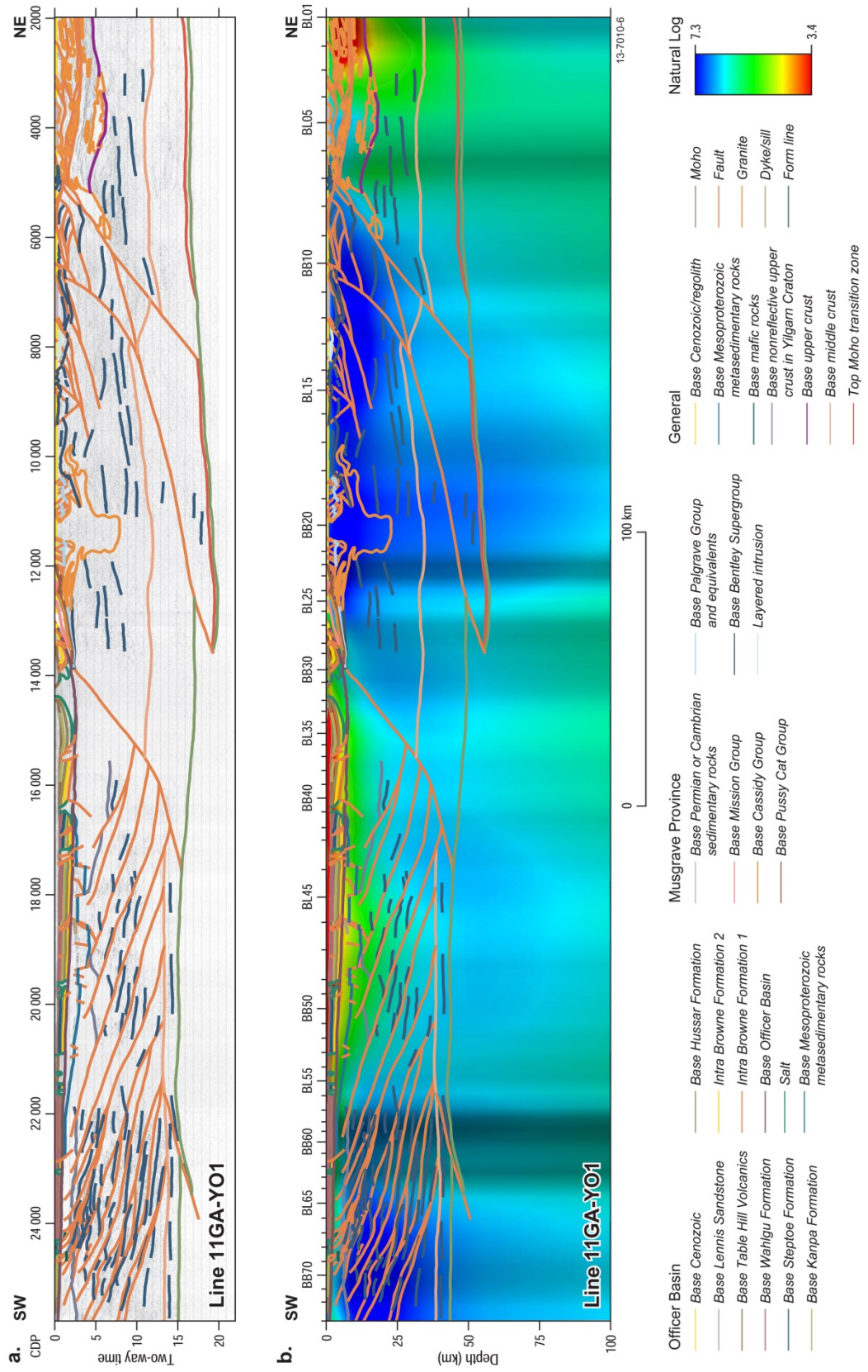

Figure 9.6 *Seismic interpretation (a) and magnetotelluric conductivity model (b) to a depth of 100 km, covering the YOM seismic traverse (see details in Duan et al., 2013). The display shows the vertical scale equal to the horizontal scale. Simplified line work from the interpretation of the seismic section in (a) is overlain on the MT model in (b). Locations of the MT recording stations are shown at the top of the section in (b).*

Yilgarn Craton

The Yilgarn Craton in Western Australia is a large (~1000 km by ~1000 km) Archean granite–greenstone terrain which forms a major part of the West Australian Craton, and represents well over one billion years of craton formation. The craton has been subdivided into several terranes (Cassidy et al., 2006; Pawley et al., 2012) (Figure 9.7), and consists of metamorphosed mafic and felsic volcanic and intrusive rocks, and metasedimentary units, intruded by granite and gneissic granite, all of which formed mainly between 3050 Ma and 2620 Ma (Cassidy et al., 2006). The Yamarna Terrane, which is the easternmost terrane in the Yilgarn Craton (Figure 9.7), contains greenstone belts which are younger than 2720 Ma, in contrast to all other terranes in the Yilgarn Craton (with the exception of the Kalgoorlie and Kurnalpi terranes) which contain older greenstone belts (Cassidy et al., 2006; Pawley et al., 2012). The YOM seismic line crossed only the eastern, non-exposed half of the Yamarna Terrane.

Because of the very distinctive change in the seismic character at the boundary between the upper and middle crust, we here confine the Yamarna Terrane (*sensu stricto*) to only the upper crust, which consists of the granite–greenstone units, and define its base as the contact between the relatively nonreflective upper crust and the package of strong reflections in the middle crust which have an apparent dip to the northeast. We combine the middle and lower crust into the Babool Seismic Province (see below).

In the YOM seismic section, the Yamarna Terrane, is only weakly reflective to nonreflective, with no distinct strong reflections, in contrast to the moderately reflective nature of the terrane imaged on seismic lines 01AGS-NY1 and 01AGS-NY3 (Goleby et al., 2003, 2004).

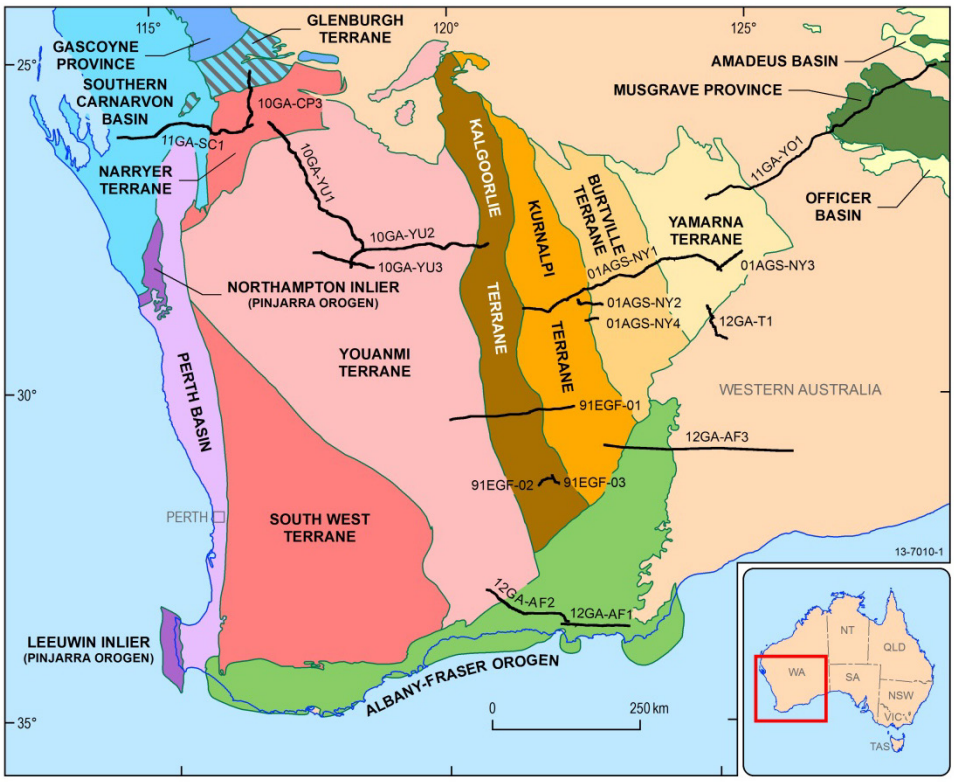

Figure 9.7 *Major tectonic subdivisions of the southern half of Western Australia, showing the locations of the major deep crustal seismic reflection lines.*

Babool Seismic Province

Below the Yamarna Terrane (*sensu stricto*), highly reflective middle and lower crust extends from the southwest margin of the YOM seismic section to about CDP 15700 (Figure 9.5). This zone is here named the Babool Seismic Province. The seismic province varies in thickness from about 11.7 s TWT (~35 km) at CDP 17600, to about 13.3 s TWT (~40 km) at about CDP 23950. As we have not been able to track these rocks to the surface, we have no direct constraints on their lithology or age. We are not able to demonstrate that this rock package forms part of the Yamarna Terrane, but with a different structural fabric. Hence, at this stage, we treat this seismic province as a discrete package of rocks which forms the current basement to the granite–greenstone rocks of the Yamarna Terrane.

Geochronological and isotopic data from the Yamarna Terrane are relatively sparse, with the few SHRIMP U–Pb zircon ages for greenstones and associated granites principally being in the range 2711 Ma to 2645 Ma (L.P. Black et al., 2002, unpublished data; Sircombe et al., 2007; Pawley et al., 2012). The Nd model ages for granites from the Yamarna Terrane suggest an average crustal age of 3000–2900 Ma (Champion and Cassidy, 2007, 2008). These model ages are supported by rare inherited zircons as old as 2940 Ma in felsic magmatic rocks from the Yamarna Terrane (L.P. Black et al., 2002, unpublished data; Sircombe et al., 2007). To date, only one rock in the Yamarna Terrane has an age older than 2711 Ma — the Ziggy Monzogranite, with a SHRIMP U–Pb zircon magmatic crystallisation age of 2832 ± 4 Ma (Pawley et al., 2012). Lu–Hf isotope data collected on this sample reveals a substantial juvenile input (εHf values are positive), and an average mantle extraction age of about 3200 Ma (Wyche et al., 2012). Lu–Hf isotope data collected on a dacite from the Toppin Hill Formation (SHRIMP magmatic crystallisation age of 2677 ± 7 Ma, with one inherited age of 2731 Ma; Pawley et al., 2012) also reveals a substantial juvenile input, and an average mantle extraction age of about 3000 Ma (Wyche et al., 2012). Thus, the Babool Seismic Province, likely corresponds to older basement below the Yamarna Terrane, indicated by the isotopic data and xenocrystic zircons, described above, with the Ziggy Monzogranite possibly representing a surface expression of this seismic province.

The origin of the gently-dipping to subhorizontal fabric of the Babool Seismic Province imaged in the YOM seismic line is an enigma, but possibly could be due to large-scale, crustal extension. Analogue centrifuge modelling by Harris et al. (2002) and Bédard et al. (2013) have produced scenarios which resemble the current seismic architecture of the Babool Seismic Province. One problem is that to produce the current thickness of the seismic province only by extension, the crust would have to have been originally of Himalayan thickness. A possible solution is that large-scale extension of a crust of normal thickness was followed by later contraction, which thickened the crust to about its current thickness.

Our interpretation of the YOM seismic section suggests that the Yilgarn Craton and underlying Babool Seismic Province extend much farther to the east than previously suggested, effectively to the southwest edge of the Musgrave Province. This is supported by the trends observed in the magnetic anomaly map (Milligan et al., 2010).

Manunda Basin

The Manunda Basin is an older, sedimentary basin, which developed on top of the Yilgarn Craton, and locally forms the basement to the Officer Basin (Figure 9.5). It has been intersected in drill holes and imaged on previous seismic sections (Korsch et al., 2013a), but the YOM seismic section provides the best image, to date, of its architecture. The basin has been described by Korsch et al. (2013a) and consists of at least two graben, up to about 18 km wide, with thinner platforms extending to both sides

(Figure 9.5). This produces a geometry typical of a classic steer's head basin, with the subsidence being driven initially by mechanical extension, followed by thermal relaxation of the lithosphere (Dewey, 1982; White and McKenzie, 1988). The basin is also cut by a series of later minor extensional faults, best observed by displacements in the base of the basin.

The Manunda Basin can be subdivided into at least two, and possibly three, seismic stratigraphic sequences. The lower parts of both graben contain a weakly-layered sequence, which is overlain by a package of strong reflections, which also can be mapped as the basal unit on the side platforms. The upper part of the basin forms a third sequence which is only weakly to moderately reflective (Figure 9.5). The GSWA Empress 1A well (Figure 9.1), drilled at CDP 21960 on the seismic line, penetrated about 103 m of the basin, which included about 58 m of basalt (Stevens and Apak, 1999). A sample of the basalt from a depth of 1602.0 m has a K–Ar whole rock age of 1058 ± 13 Ma (Amdel Limited, in Stevens and Apak, 1999). It is uncertain whether the basalt is a flow forming part of the succession, or whether it is a younger sill intruding into an older succession. Detrital zircons from two sandstone samples from the drill core were analysed by SHRIMP for U–Pb geochronology, as part of our project. Both samples were stratigraphically above the dated basalt sample, from within the upper seismic stratigraphic sequence, and had very similar age distribution profiles, with maximum depositional ages of about 1310 Ma (Korsch et al., 2013a), significantly older than the age obtained from the basalt. There was only a negligible contribution of Archean grains from the Yilgarn Craton (<5% of the total population).

A sample from the WMC NJD 1 drill hole, about 100 km to the south of the YOM seismic line, showed a very similar age distribution to the two samples from the GSWA Empress 1A well, with a maximum depositional age also of about 1310 Ma (Korsch et al., 2013a). A very similar age profile, with a maximum depositional age of about 1305 Ma, was also found in a basement sandstone in GSWA Lancer 1, about 230 km to the north of the YOM seismic line (Wingate and Bodorkos, 2007), indicating that the Manunda Basin occupies an extensive area, at least 400 km long by 130 km wide.

A sandstone sample from the Salvation Group, collected about 330 km to the northwest of the YOM seismic line, also has a similar detrital zircon age distribution profile, with a maximum depositional age of about 1330 Ma, but with a large error (Nelson, 2002). Regional outcrop trends in the eastern Capricorn Orogen suggest the Salvation Group overlies, and may interfinger with, the upper Collier Group, rather than being equivalent, as suggested by Grey et al. (2005), and thus probably forms part of the Collier Basin. Additionally, detrital zircon age profiles in sandstones from the Collier Basin collected much farther to the west have quite different age profile patterns (Martin et al., 2008). The Salvation Group also has been intruded by dolerites with an age of 1066 ± 14 Ma (Wingate, 2003). Puzzlingly, no peperites have been found associated with dolerites intruding the Salvation Group, implying the dolerites significantly post-date deposition, although they were recorded for similarly-aged intrusions in the Collier Group far to the west (Martin, 2003). Nevertheless, the maximum depositional ages of the three samples analysed for this project indicate that they are too young to be correlatives of either the Earaheedy Basin (constrained to having been deposited between about 1840 Ma and 1740 Ma; Pirajno et al., 2009) or the Edmund Basin (constrained to having been deposited between 1620 Ma and 1465 Ma; Martin et al., 2007; Cutten et al., 2011).

In contrast to the samples from WMC NJD1 and GSWA Empress 1A, a sandstone sample from the base of the Kanpa 1A well (Figure 9.1), presumed to be Manunda Basin, has a significantly different age profile, with a maximum depositional age of about 1790 Ma, and an abundance of late Archean grains (~60% of the total population), presumably derived from the Yilgarn Craton (Korsch et al., 2013a). One possibility to explain the different detrital zircon age pattern in the sample from the Kanpa 1A well, compared to the other samples, is that Kanpa 1A could have sampled a different part of the

stratigraphic succession in the Manunda Basin. Very similar age profiles, with maximum depositional ages of about 1800–1770 Ma, were reported for some samples from the Edmund Group by Martin et al. (2008), and also from the lower part of the Collier Basin (constrained to having been deposited between ca. 1200 Ma and 1070 Ma; Martin et al., 2007; Cutten et al., 2011), and inferred to be recycled from the uplifted part of the Edmund Basin (Martin et al., 2008). A sandstone sample from the Mulgarra Sandstone, the youngest unit in the Earaheedy Basin, also has a similar detrital zircon age distribution profile, with a maximum depositional age of about 1800 Ma (Halilovic et al., 2004). Thus, the sample from Kanpa 1A well could be a correlative of sandstones in the Earaheedy, Edmund or Collier basins, or even recycled from such sandstones. The age pattern also shows a remarkable similarity to a compilation of SHRIMP zircon individual ages from the Gascoyne Province and the northern Yilgarn Craton by Nelson (2001), suggesting that this sample, at least in part, could have been derived from these provinces.

Assuming the age of the basalt in GSWA Empress 1A well is a crystallisation age, and is not due to later resetting, the basalt is equivalent in age to the Bentley Supergroup and the Giles Event of the west Musgrave Province, which has an age range of 1085–1040 Ma (e.g. Evins et al., 2010a, 2010b; Howard et al., 2011a, 2011b), and is slightly younger than the Warakurna Large Igneous Province defined by Wingate et al. (2004). To date, only three samples of clastic sedimentary rocks in the Bentley Supergroup have been dated using the U–Pb SHRIMP technique; all samples have a maximum depositional age of about 1175 Ma (Kirkland et al., 2010, 2011a, 2012a), and thus have a very different detrital age spectra to the samples from the Manunda Basin.

Zircons in the three samples from GSWA Empress 1A and WMC NJD1 with ages of about 1300 Ma could be derived from the 1345–1293 Ma Wankanki Supersuite of the west Musgrave Province (see Howard et al., 2013). A major problem, however, is to explain the source of the large population of 1800-1650 Ma zircons in these samples, as there are no rocks older than about 1600 Ma reported from the Musgrave Province. A possible source region for these three samples is the Albany-Fraser Orogen, where Spaggiari et al. (2011) reported magmatic rocks of c. 1800–1660 Ma (related to the Biranup Orogeny), 1330–1285 Ma (related to Albany-Fraser Orogeny Stage I) and 1200–1140 Ma (related to Albany-Fraser Orogeny Stage II). The 1200-1140 Ma zircon peak is absent from the three samples from the Manunda Basin, suggesting that deposition in the basin occurred prior to Stage II of the Albany-Fraser Orogeny.

One possibility is that deposition in the Manunda Basin occurred at about 1300 Ma, or slightly later, possibly related to post-collisional orogenic collapse following amalgamation of the West Australian Craton with the west Musgrave Province (see below). If this is correct, then the basalt in Empress 1A is a younger intrusive, related to the 1085-1040 Ma Giles Event. Deformation of the basin, seen in the 01AGS-NY1 seismic section (Goleby et al., 2003), could then have occurred either during the 1220–1150 Ma Musgrave Orogeny or during the Giles Event, prior to initiation of deposition of the Officer Basin at about 830 Ma.

Western Officer Basin

The YOM seismic line has provided an image across almost the entire western Officer Basin, from near its southwest margin, to its northeast margin just to southwest of outcrops of the Musgrave Province. The basin has been described in detail by Korsch et al. (2013a), and consists of a well-layered stratigraphic succession, which thickens gradually towards the northeast (Figure 9.5). At its thickest, the basin is about 2.6 s TWT (~5200 m) thick, at about CDP 14800, but here there is an incomplete stratigraphic succession, with several of the late Neoproterozoic and ?early to mid-Cambrian stratigraphic units being removed by erosion, prior to eruption of the late Cambrian Table

Hill Volcanics, the base of which is mapped as a prominent angular unconformity in the YOM seismic section (Figure 9.5). The thick succession, and growth of the stratigraphic packages towards the northeastern end of the Officer Basin, suggests that subsidence of the basin was initially controlled by mechanical extension, with the original northeastern margin probably being defined by a steep, southwest-dipping, extensional growth fault, which was active at least during the deposition of the lower sedimentary succession (Browne, Hussar and Kanpa formations). The Winduldarra Fault, mapped as a major boundary in the crust (see below), was possibly the major basin-bounding fault during the extension which initiated the basin.

In the YOM seismic section, several nonreflective areas cut across the stratigraphy and are interpreted as salt diapirs or walls mobilised from evaporitic horizons in the Browne Formation (Figure 9.5). The Browne salt wall, imaged on the seismic section between CDP 14200 and CDP 14400 has been intersected in the Browne 1 and Browne 2 wells, to the north of the line (Figure 9.1). The distinctive seismic character of this salt wall has been used to interpret the presence of several salt structures in the YOM seismic section, some of which are farther to the southwest than previously described (see Korsch et al., 2013a).

The Officer Basin experienced contractional deformation during the late Neoproterozoic Petermann Orogeny and/or the late Cambrian Delamerian Orogeny. Reactivation of the Winduldarra Fault partially inverted the basin, bringing the basal Townsend Quartzite to the surface at the northeastern margin of the basin, against the Musgrave Province. Shortening produced broad folds in the Neoproterozoic and early to mid-Cambrian succession, which are truncated below the unconformity at the base of the Table Hills Volcanics. Several thrust faults displace the stratigraphy, often producing hangingwall anticlines in the upper part of the Neoproterozoic succession (Figure 9.5).

Northeastern half of the YOM Seismic section

In the northeastern half of the YOM seismic section, four layers can be seen in the crust (Figure 9.5):

1. An upper crust, which is weakly to strongly reflective, and quite variable in thickness, ranging from ~0.4 s TWT (~1 km) at about CDP 9200 to ~6.3 s TWT (~19 km) at about CDP 3600,
2. A moderately reflective middle crust, with the reflections generally being subhorizontal to gently-dipping. The middle crust is of variable thickness, ranging from ~4.7 s TWT (~14 km) at about CDP 3600 to ~10.3 s TWT (~31 km) at about CDP 10200,
3. A weakly to moderately reflective lower crust, with a relatively constant thickness, ranging from ~3.8 s TWT (~11 km) at about CDP 2002 to ~7 s TWT (~21 km) at about CDP 8200, and,
4. A thin (~1–3 km) crust-mantle transition zone at the base of the lower crust, which is usually more reflective than the lower crust above it. This contrasts with the crust below the Yilgarn Craton on the YOM seismic line, where a highly reflective crust-mantle transition zone has not developed. Nevertheless, the crust-mantle transition zone beneath the west Musgrave Province is similar to that imaged on seismic lines father to the west in the Yilgarn Craton, such as on line 01AGS-NY1 (Goleby et al., 2003) and on the Youanmi seismic lines (Korsch et al., 2013b).

West Musgrave Province

The Musgrave Province is a large east-west trending Mesoproterozoic basement terrane surrounded by younger sedimentary basins (Edgoose et al., 2004; Howard et al., 2011a, 2011b). Within Western Australia, the west Musgrave Province consists predominantly of rocks related to three major orogenic

events (see details in Howard et al., 2011a, 2011b). The 1345–1293 Ma Wankanki Supersuite and the 1340–1270 Ma Wirku Metamorphics formed during the Mount West Orogeny, possibly related to subduction and accretion (Smithies et al., 2010; Evins et al., 2012). This was followed by emplacement of the Pitjantjatjara Supersuite during the 1220–1150 Ma Musgrave Orogeny, in an intracontinental setting (Smithies et al., 2011). Finally, the Bentley Supergroup and related magmatic rocks of the Warakurna Supersuite formed during the 1085–1040 Ma Giles Event. A fourth event, the late Neoproterozoic to early Cambrian (580–530 Ma) Petermann Orogeny, in places strongly deformed parts of the west Musgrave Province, including the Bentley Supergroup and the Warakurna Supersuite, but produced virtually no new crust. There was also a magmatic event at ca. 1400 Ma, the Papulankutja Supersuite, which is very limited in areal extent, but possibly formed in a continental magmatic arc setting (Kirkland et al., 2012b, 2013a). In the South Australian and Northern Territory components of the Musgrave Province, there is 1600–1550 Ma basement present (e.g. Edgoose et al., 2004; Wade et al., 2006), but this is yet to be found in the Western Australian part of the province.

In the northeastern half of the YOM seismic line, between the Winduldarra Fault and the Woodroffe Thrust, the upper crust is interpreted to consist of the Bentley Supergroup and related magmatic rocks of the Warakurna Supersuite (Figure 9.5), and has been described in detail by Howard et al. (2013). The Bentley Supergroup usually consists of strong reflections forming a layered succession, for example, where it is exposed near the southwest margin of the province (between about CDP 12500 and CDP 12800). To the southwest of the Woodroffe Thrust, the Bentley Supergroup has been complexly faulted (Figure 9.5), usually by northeast-directed thrust faults, although some have an extensional sense of movement and may be related to the extensional event which formed the Ngaanyatjarra Rift (Evins et al., 2010a, 2010b), into which the Bentley Supergroup was deposited.

At the northeastern margin of the YOM seismic line, northeast of the Woodroffe Thrust, between CDP 2002 and CDP 4500, the upper crust consists of highly reflective subhorizontal reflections, along with smaller, usually pancake-shaped, weakly reflective to nonreflective bodies (Figure 9.5). This region is interpreted to consist predominantly of highly-reflective, amphibolite facies rocks of the Pitjantjatjara Supersuite along with nonreflective plutons, which intruded during the Giles Event (Howard et al., 2013).

The middle crust consists of subhorizontal to gently-dipping, moderate to strong reflections forming basement to the Bentley Supergroup south of the Woodroffe Thrust, and basement to amphibolite facies rocks of the Pitjantjatjara Supersuite north of the thrust (Figure 9.5). It is interpreted to consist of granulite facies rocks mainly formed during the Mount West Orogeny, but also including rocks of the Pitjantjatjara Supersuite, along with the Papulankutja Supersuite, and possibly some 1600–1550 Ma basement, which have not yet been found in the west Musgrave Province. Together, the upper and middle crust is taken to represent the Musgrave Province (*sensu stricto*), but also see Howard et al. (2013).

In recent years, there has been a marked increase in the amount of geochronological and isotopic data from the west Musgrave Province, including U–Pb SHRIMP geochronology and Nd and Hf isotopes, contributing to a greater understanding of the province (e.g. Howard et al, 2011a; Kirkland et al., 2013a). Zircon inheritance older than 1600 Ma in magmatic rocks from the Musgrave Province is extremely rare (Edgoose et al., 2004; Gum and Belousova, 2006; Howard et al., 2011a; Kirkland et al., 2013a). Nevertheless, Nd and Hf data suggest that there were possibly two major crustal forming events, at about 1950–1900 Ma and 1600–1550 Ma (Kirkland et al., 2013a; see also Wade et al., 2006). Thus, as indicated by the isotopic data, the middle crust could also correspond, at least in part, to this older basement.

Tikelmungulda Seismic Province

Below the Musgrave Province (*sensu stricto*), a weakly-reflective lower crust has a distinctively different seismic character to that of the middle and upper crust above it (Figure 9.5), and we use the term Tikelmungulda Seismic Province to refer to it in the region of the YOM seismic line. Here, we include the relatively thin crust-mantle transition zone in this seismic province. As we have not been able to track these rocks to the surface, we have no direct constraints on their lithology or age. We are not able to demonstrate that this rock package forms part of the Musgrave Province, but with a different seismic character. Hence, at this stage, we treat this seismic province as a discrete package of rocks which forms the current basement to the Musgrave Province. Also, the Tikelmungulda Seismic Province has a significantly different seismic character to that of the Babool Seismic Province to the southwest, beneath the Yamarna Terrane of the Yilgarn Craton (Figure 9.5).

The Musgrave Orogeny generated the Pitjantjatjara Supersuite, was dominantly an intracontinental extensional event, and is interpreted to have seen ultra-high temperature conditions (UHT) from about 1220 Ma to 1120 Ma (Smithies et al., 2011). This resulted in extreme crustal thinning and elevation of the asthenosphere. Smithies et al. (2011) suggested that a large mantle-derived component was required to produce the Pitjantjatjara Supersuite. Also, extensive mantle-derived magmatism occurred during the Giles Event (Howard et al., 2013). Thus, Smithies et al. (2013a) and Howard et al. (2013) suggested that the Tikelmungulda Seismic Province, forming the lower crust, consists predominantly of mafic underplate produced during the Musgrave Orogeny and Giles Event.

The present-day crust beneath the west Musgrave Province is very thick (Figure 9.5), which, coupled with the regional gravity low to the north of the Woodroffe Thrust, would suggest that the whole crust is predominantly felsic, at least in the region to the north of the thrust. This would imply that there is a significant amount of felsic material in Tikelmungulda Seismic Province mixed in with the mafic underplate. The gravity high between the Winduldarra Fault and the Mitika Fault could be explained by a relatively thin crust, but the seismic interpretation shows a relatively thick crust here (Figure 9.5). Alternatively, the gravity high could be explained by a thick crust (in agreement with the seismic interpretation) along with a significant amount of mafic material in the upper crust, that is, the mafic Giles intrusions and mafic components of the Bentley Supergroup. Thus, the Tikelmungulda Seismic Province in this region could also consist of mafic underplate mixed with felsic material.

Crustal sutures and major faults

Relationship between Yamarna Terrane and Musgrave Province

Basement units below the Officer Basin, and to the northeast of it, have seismic characteristics which are quite different to each other. The Babool Seismic Province beneath the Yilgarn Craton can be tracked as far towards the northeast as about CDP 15600, and the Musgrave Province can be tracked as far towards the southwest as about CDP 13600 (Figure 9.5). Hence, there is a gap of about 40 km where, beneath the Officer Basin, seismic resolution is poor, and it is not possible to determine definitively the nature of the boundary between the Yilgarn Craton and the Musgrave Province. In our interpretation, we have defined the boundary between the two provinces as a fault with an apparent dip to the southwest, here termed the Winduldarra Fault (new name, after Winduldarra Rockhole). In the vicinity of the YOM seismic section, the fault is not exposed, but is interpreted to be the faulted boundary between the Townsend Quartzite, the basal unit of the Officer Basin, and the Bentley Supergroup. It truncates a near complete succession of the Bentley Supergroup before cutting deeper

into the crust, reaching the Moho at about CDP 17600 (Figure 9.5). This interpretation is supported by the magnetotelluric conductivity model for the YOM seismic line (Duan et al., 2013), which shows that there is a significant change in conductivity in the vicinity of the fault (Figure 9.6). Alternatively, the boundary between the two provinces could dip to the northeast, but this is problematic if our interpretation of the faulted Moho in the vicinity of CDP 13400 is valid; also, based on the conductivity model, this alternative is less likely. A further alternative is that the boundary could be a broad zone of weak reflectivity, possibly due to extensive alteration and/or homogenisation of the crust.

Irrespective of whichever alternative is valid, the boundary between the Yilgarn Craton and the Musgrave Province is a major crustal break separating provinces of distinctly different lithological ages and geological histories. As well, there is a major change in crustal architecture across the boundary, with the dominant structures in the southwest dipping predominantly towards the northeast, and the dominant structures in the northeast dipping predominantly towards the southwest (Figure 9.5).

Significance of the Woodroffe Thrust

In the YOM seismic section, the Woodroffe Thrust, which here is internal within the Musgrave Province, is a major crustal structure forming part of a complex fault system, the major component of which is a listric fault, with an apparent dip to the southwest (Figure 9.5). Its surface trace is at about CDP 4550, and it reaches the Moho at about CDP 12600, where the crust is at its thickest in the YOM seismic section (~59 km). Here, we suggest that the Moho has been cut, and a thrust sense of movement shows displacement horizontally of about 20 km, and vertically of up to nearly 9 km (Figure 9.5). It is likely that the Woodroffe Thrust has had a long and complicated movement history, but there was a significant amount of movement on it after the formation of the Bentley Supergroup, possibly during the late Neoproterozoic-early Cambrian Petermann Orogeny, which significantly deformed and metamorphosed the Bentley Supergroup elsewhere. There is also a minor amount of fault reactivation in the Cenozoic.

About 500 km to the east, the Woodroofe Thrust was crossed by the deep seismic profile 08GA-OM1, where it forms the northern margin to the eastern Musgrave Province (Korsch et al., 2010b). Here the Musgrave Province consists of a two-layered crust, with a reasonably reflective upper crust and a weakly reflective lower crust, similar to the west Musgrave Province and the Tikelmungulda Seismic Province interpreted in the YOM seismic section. There, the crust is much thinner, however, only about 12 s TWT (~36 km) thick under the Musgrave Province. Nevertheless, the orientation and geometry of the Woodroffe Thrust is very similar in both seismic lines, with the Moho also being displaced by a similar amount (compare Figure 5 with Korsch et al., 2010b).

Geodynamic Implications

The new deep seismic imaging, extending from the northeastern Yilgarn Craton to the west Musgrave Province, provides, for the first time, a holistic view of the crustal architecture across this poorly exposed part of Western Australia. Based on the nature of the seismic reflectivity, the Yamarna Terrane is here confined to the upper crust. The crust which underlies it is seismically distinct, and cannot be tracked anywhere to the surface. Therefore, a new seismic province, the Babool Seismic Province, is proposed for the middle to lower crust in this region. Similarly, the Musgrave Province is here confined to the upper and middle crust. The crust which underlies it is also seismically distinct, and cannot be tracked anywhere to the surface. Therefore, a new seismic province, the Tikelmungulda Seismic Province, is proposed for the lower crust in this region. The seismic images, combined with geological and geophysical data, can be used to help constrain geodynamic models for the region.

Amalgamation of the west Musgrave Province and the West Australian Craton

The ca. 1400 Ma Papulankutja Supersuite and the 1345–1293 Ma Wankanki Supersuite are calcalkaline suites, which have been interpreted to be possibly subduction-related, with characteristics of an Andean-type continental margin magmatic arc (Smithies et al., 2010; Evins et al., 2012; Kirkland et al., 2012b, 2013a). Thus, the Mount West Orogeny is possibly related to a collisional event following ocean closure and cessation of subduction. The arc rocks of the Papulankutja and Wankanki supersuites are confined geographically to the west Musgrave Province, as rocks of these ages have yet to be found in the Musgrave Province in South Australia and the Northern Territory. This suggests that the west Musgrave Province was on the upper plate and that the subduction zone, or zones, dipped towards the north under the southern margin of the west Musgrave continental mass (Figure 9.8). The Winduldarra Fault is interpreted to be the current boundary between the Musgrave Province and the Yilgarn Craton, and is a possible candidate for the location of the suture zone. Nevertheless, this fault has the opposite dip to the inferred dip of the subduction zone, suggesting that, if it was the site of the suture, during collision the northeastern margin of the Yilgarn Craton could have been obducted onto the southwestern margin of the Musgrave Province.

In the southeastern Northern Territory, the Woodroffe Thrust marks the boundary between the eastern Musgrave Province and the Warumpi Province, which is part of the Arunta Region in the southern North Australian Craton. Korsch et al. (2011) proposed that the eastern Musgrave Province was sutured to the Warumpi Province at about 1594 Ma. Arc magmatism continued in the Musgrave Province until about 1565 Ma, when a marginal sea to the south of the province was consumed, and the Gawler Craton of the South Australian Craton collided with the expanded North Australian Craton (Korsch et al., 2011; see also Wade et al., 2006). Thus, at about 1400 Ma, the west Musgrave Province faced an open ocean, or marginal sea, whereas the eastern Musgrave Province was already part of the amalgamated North Australian–South Australian Craton.

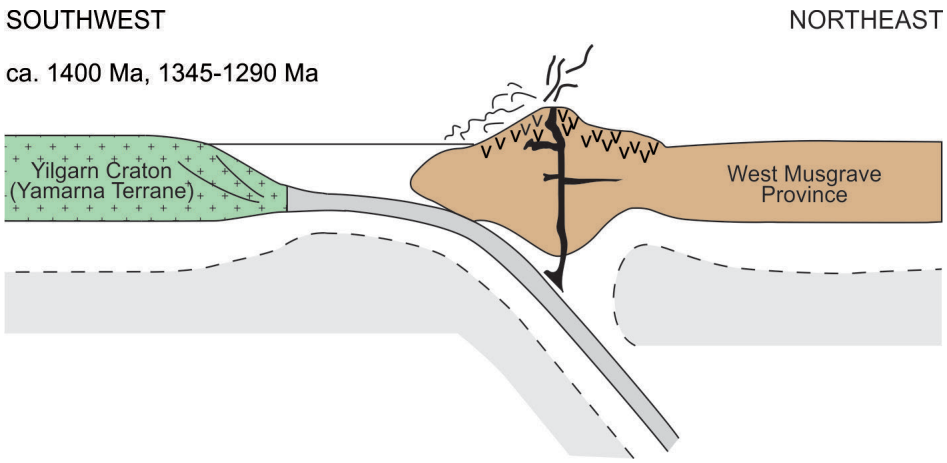

Figure 9.8 *Schematic cross section, showing a possible scenario for the formation of the 1400 Ma Papulankutja Supersuite and the 1345–1293 Ma Wankanki Supersuite, with a northeast-dipping subduction zone beneath the west Musgrave Province, prior to collision with the Yamarna Terrane of the Yilgarn Craton.*

There is some debate as to the nature and timing of the relationship between the Archean Yilgarn Craton and, to its south and southeast, the Paleoproterozoic–Mesoproterozoic Albany–Fraser Orogen. Previous plate tectonic models have proposed that the Albany–Fraser Orogen was separated by oceanic crust from the Yilgarn Craton, and that a southeast-dipping subduction system closed the ocean between them, with collision and amalgamation occurring at about 1345–1300 Ma (e.g. Myers

et al., 1996; Clark et al., 2000; Bodorkos and Clark, 2004; Spaggiari et al., 2009). More recently, however, Kirkland et al. (2011b, 2011c) and Spaggiari et al. (2011) have proposed that formation of the Albany–Fraser Orogen commenced at ca. 1710 Ma to ca. 1665 Ma within extended and thinned crust of the southeast Yilgarn Craton, with a northwest-dipping subduction located to the southeast.

Kirkland et al. (2011b, 2011c) and Spaggiari et al. (2011) further inferred that immediately prior to Stage I of the Albany–Fraser Orogeny (ca. 1345–1260 Ma), a northwest-dipping subduction zone was also located to the east, outboard of the Biranup Zone, and presumably east of the Nornalup Zone. This has a similar polarity to the earlier (ca. 1710–1665 Ma) subduction event, and the resulting oceanic closure led to the amalgamation of the southeast margin of the West Australian Craton and the combined South Australian Craton–Mawson Craton (see also Bodorkos and Clark, 2004; Giles et al., 2004). Gabbro in the Fraser Zone, dated at about 1300 Ma, has been interpreted by Smithies et al. (2013b) possibly to have formed in a distal backarc environment, again suggesting that the subduction zone was located well to the east.

Thus, between about 1345 Ma and 1290 Ma, there was a north-dipping subduction zone to the south of the West Musgrave Province, and a northwest-dipping subduction zone to the southeast of the combined Yilgarn Craton–Albany–Fraser Orogen. This would result in a complicated geometry, with opposing polarities for the two subduction systems. Nevertheless, possible analogues of similar complicated plate geometries can be seen in the Cenozoic of the western Pacific Ocean (e.g. Hall, 2002; Crawford et al., 2003).

An alternative scenario is that the subduction zone south of the west Musgrave Province and the one to the southeast of the Albany–Fraser Orogen are part of the same subduction system which dipped to the northwest, and hence the west Musgrave Province and the Albany–Fraser Orogen were part of the same continental landmass at this time. Nevertheless, according to Kirkland et al. (2012b, 2013a), Hf isotopic data indicates that, at least prior to 1400 Ma, the Musgrave Province and the Albany–Fraser Orogen were different in composition and probably evolved in different tectonic regimes. This alternative implies that the suture was probably not the Winduldarra Fault but that it was located farther to the east, now hidden beneath the west Musgrave Province, which later has been thrust some distance to the south during the Neoproterozoic Petermann Orogeny. This scenario, however, does not resolve the issue of the timing of the amalgamation of the northeast Yilgarn Craton with the west Musgrave Province, and the role of the Winduldarra Fault.

There is also a question as to what becomes of the subduction zone to the northwest of the west Musgrave Province in the first scenario, or northwards beneath the west Musgrave Province in the second scenario. Previously, workers have correlated the west Musgrave Province with the Rudall Complex of the Paterson Province to the northwest, often linking them by the Anketell Regional Gravity Ridge (e.g. Myers et al., 1996; Bagas, 2004; Bagas and Nelson, 2007). This implies that the key boundary would be to the southwest of the Rudall Complex. Nevertheless, the west Musgrave Province and the Rudall Complex have Paleoproterozoic–Mesoproterozoic geological histories which are virtually mutually exclusive (e.g. Betts and Giles, 2006; Neumann and Fraser, 2007; Fraser et al., 2007). Recently, Kirkland et al. (2013b) considered that the Rudall Complex was authochthonous with the eastern Pilbara Craton, implying that any convergent margin must lie somewhere outboard (that is, to the northeast) of the Rudall Complex. Collision between the West Australian Craton and the North Australian Craton, and their amalgamation, generally is considered to have occurred during the 1800–1765 Ma Yapungka Orogeny (Bagas and Smithies, 1997; Tyler, 2000; Bagas, 2004). This orogeny is at least 200 Ma older than any known rocks from the Musgrave Province, and thus the relationship between the Rudall Complex and the Musgrave Province is yet to be clarified.

Transect across Western Australia

It is now possible to combine the interpreted seismic section from the current YOM survey with seismic sections from earlier deep seismic surveys to produce a ~1800 km traverse across almost the entire southern half of Western Australia, from near the coast to within about 80 km of the border with the Northern Territory (Figure 9.9). Although there have been several previous deep seismic surveys in, and adjacent to, the Yilgarn Craton (Figure 9.7), the key surveys of interest here are:

1. the Eastern Goldfields survey, acquired in 1991 (line BMR91-EGF01, commonly known as EGF1; Drummond et al., 1993, 2000; Swager et al., 1997),
2. the Northeast Yilgarn survey, acquired in 2001 (lines 01AGS-NY1 and 01AGS-NY3; Goleby et al., 2004, 2006), and,
3. the Youanmi and Southern Carnarvon surveys (lines 10GA-YU1, 10GA-YU2 and 11GA-SC1; Korsch et al., 2013b).

The overall architecture of the Yilgarn Craton is dominated by a central nucleus, consisting of the Youanmi Terrane and the underlying Yarraquin Seismic Province (Korsch et al., 2013b). Based on Nd isotopic data, it has been proposed that the Youanmi Terrane has behaved as a coherent crustal block since at least 3000–2900 Ma (Champion and Cassidy, 2010; Ivanic et al., 2012; Van Kranendonk et al., 2013). Following this, the Youanmi Terrane acted as a nucleus, or protocraton, onto which the Narryer Terrane was accreted in the northwest and the Eastern Goldfields Superterrane developed to the east (e.g. Cassidy et al., 2006; Wyche et al., 2012). Terranes on either side of the Youanmi Terrane are seen to be bounded by crustal-scale faults which dip away from the nucleus, towards the west and northwest on the northwestern side, and towards the east on the eastern side (Figure 9.9; see also Korsch et al., 2013b).

Using a convergent plate tectonic model, based on analogies with modern day plate tectonic processes, several groups of workers (e.g. Barley et al., 1989; Myers, 1995; Krapez and Barley, 2008; Korsch et al., 2011) have proposed geodynamic models for the Eastern Goldfields Superterrane of the Yilgarn Craton which involve the accretion of allochthonous continental slivers as discrete terranes. Cassidy et al. (2006) considered that formation of the Eastern Goldfields Superterrane by amalgamation of a series of terranes to form the composite Yilgarn Craton was completed by about 2655 Ma (e.g. Korsch et al., 2013b). Alternatively, it has been proposed that, rather than a series of allochthonous continental slivers, the Eastern Goldfields Superterrane represents the extended margin of the Youanmi Terrane (Czarnota et al., 2010; Pawley et al., 2012; Van Kranendonk et al., 2012). In this scenario, the older Burtville Terrane would be analogous to a horst of the basement, whereas the greenstone rocks of the younger terranes were deposited in a series of basins following <2720 Ma extension.

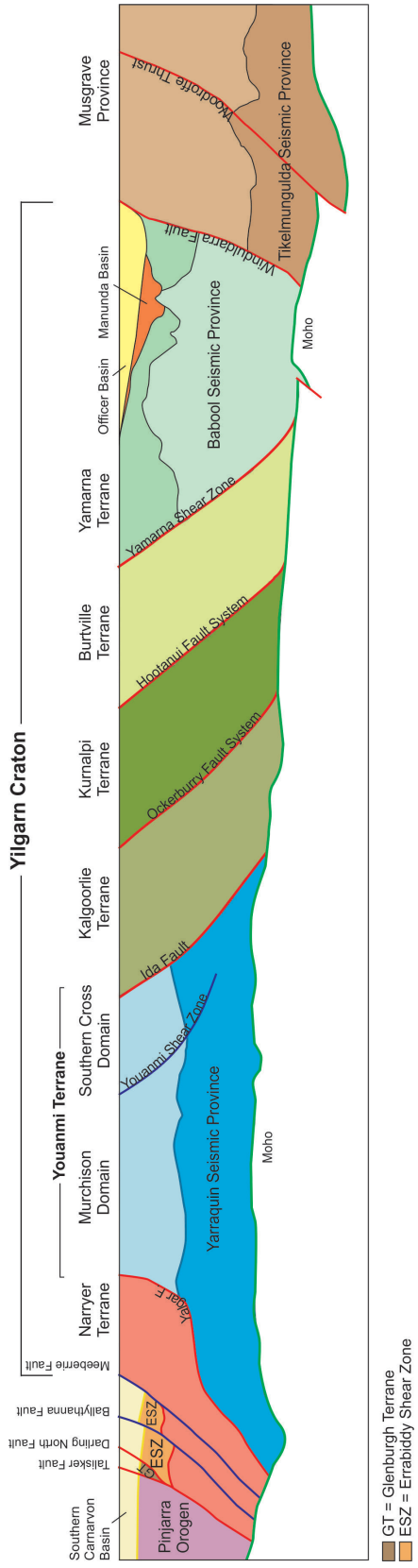

Figure 9.9 *Cartoon of the present day architecture of the crust in Western Australia, based on deep seismic reflecting profiling. The cross section extends from the Pinjarra Orogen near the coast in the west, across the Yilgarn Craton, from the Narryer Terrane to the Yamarna Terrane, and then to the west Musgrave Province in the east, showing the key provinces, terranes, basins and significant faults.*

To the northwest of the Yilgarn Craton, the Glenburgh Terrane and the Pinjarra Orogen were then accreted to the Narryer Terrane in the Proterozoic, at about 1965 Ma and 1080 Ma, respectively (see references in Korsch et al., 2013b). To the northeast of the Yilgarn Craton, the Wankanki Supersuite (1345–1293 Ma) is interpreted to have formed in a continental margin magmatic arc setting, with the subduction zone located to the south. Thus, closure of the ocean basin and accretion of the Musgrave Province to the Yilgarn Craton probably occurred at about 1300 Ma.

Summary

In our interpretation of the YOM seismic line, 11GA-YO1, we have investigated the crustal architecture of an area in Western Australia which is very poorly exposed, extending from the northeastern part of the Yilgarn Craton, across the younger Officer Basin, to the west Musgrave Province. Our preliminary interpretation defines two new seismic provinces, which are probably older basement beneath both the northeastern Yilgarn Craton and the west Musgrave Province. Neither is exposed. We define the Winduldarra Fault as the likely boundary between the northeastern Yilgarn Craton and the west Musgrave Province. The Woodroffe Thrust, within the west Musgrave Province, is shown to be a major, crustal-penetrating fault, cutting the entire crust and displacing the Moho.

A new Mesoproterozoic basin, the Manunda Basin, was imaged in the seismic profile. It has a steer's head geometry and sits unconformably on the Yilgarn Craton, but is completely covered by the Neoproterozoic–Paleozoic Officer Basin. New U–Pb SHRIMP dating of detrital zircons provide a maximum depositional age for the Manunda Basin of about 1310 Ma. The Officer Basin has an extensional geometry, thinning towards the southwest, with numerous salt diapirs locally affecting the succession.

The YOM seismic section, combined with previous deep seismic traverses, provides an almost completed transect across southern Western Australia, and our first view of the present day crustal architecture of this part of the continent. It consists of a series of terranes which have been accreted over a period of nearly two billion years, to form the composite West Australian Craton, which was then sutured to the North Australian Craton.

Acknowledgements

This paper forms part of a collaborative project between Geoscience Australia and the Geological Survey of Western Australia. We thank the following for their contributions to the project: Jenny Maher and Tristan Kemp for project management during the planning, acquisition and processing phase of the seismic data; Lindsay Highet, Weiping Zhang, Daniel McIlroy and Natalie Kositcin for producing the maps, digital versions of the interpretations of the seismic sections, seismic and MT figures, and cartoons, respectively; and David Champion and Natalie Kositcin for their reviews of the manuscript. RHS, RQdeG, HMH and RMH publish with permission of the Executive Director of the Geological Survey of Western Australia.

References

Bacchin, M., Milligan, P.R., Wynne, P., and Tracey, R., 2008. Gravity anomaly map of the Australian region (Third Edition), scale 1:5 000 000. *Geoscience Australia, Canberra*.

Bagas, L., 2004. Proterozoic evolution and tectonic setting of the northwest Paterson Orogen, Western Australia. *Precambrian Research*, 128, 475–496.

Bagas, L., and Smithies, R.H., 1997. Palaeoproterozoic tectonic evolution of the Rudall Complex, and comparison with the Arunta Inlier and Capricorn Orogen. *Geological Survey of Western Australia*, *Annual Review* 1996–97, 110–115.

Bagas, L., and Nelson, D.R., 2007. Provenance of Neoproterozoic sedimentary rocks in the northwest Paterson Orogen, Western Australia. In: Munson, T.J. and Ambrose, G.J. (editors), Proceedings of the Central Australian Basins Symposium (CABS), Alice Springs Northern Territory, 16–18 August 2005. *Northern Territory Geological Survey, Special Publication*, 2, 1–10.

Barley, M.E., Eisenlohr, B.N., Groves, D.I., Perring, C.S., and Vearncombe, J.R., 1989. Late Archean convergent margin tectonics and gold mineralization: a new look at the Norseman–Wiluna Belt, Western Australia. *Geology*, 17, 826–829.

Bédard, J.H., Harris, L.B., and Thurston, P.C., 2013. The hunting of the snArc. *Precambrian Research*, 229, 20–48.

Betts, P.G., and Giles, D., 2006. The 1800–1100 Ma tectonic evolution of Australia. *Precambrian Research*, 144, 92–125.

Black, L.P., Champion, D.C., and Cassidy, K.F., 2002. Compilation of SHRIMP U–Pb geochronology data, Yilgarn Craton, Western Australia, 1998–2000. *Geoscience Australia, unpublished report*.

Bodorkos, S., and Clark, D.J., 2004. Evolution of a crustal-scale transpressive shear zone in the Albany Fraser Orogen, SW Australia: 2. Tectonic history of the Coramup Gneiss and a kinematic framework for Mesoproterozoic collision of the West Australian and Mawson cratons. *Journal of Metamorphic Geology*, 22, 713–731.

Cassidy, K.F., Champion, D.C., Krapez, B., Barley, M.E., Brown, S.J.A., Blewett, R.S., Groenewald, P.B., and Tyler, I.M., 2006. A revised geological framework for the Yilgarn Craton, Western Australia. *Geological Survey of Western Australia, Record* 2006/8, 8p.

Champion, D.C., and Cassidy, K.F., 2007. An overview of the Yilgarn Craton and its crustal evolution. In: Bierlein, F.P. and Knox-Robinson, C.M. (editors), Proceedings of Geoconferences (WA) Inc. Kalgoorlie '07 Conference. *Geoscience Australia, Record* 2007/14, 8–13.

Champion, D.C., and Cassidy, K.F., 2008. Geodynamics: using geochemistry and isotopic signatures of granites to aid mineral systems studies: an example from the Yilgarn Craton. In: Korsch, R.J. and Barnicoat, A.C. (editors), New Perspectives: The foundations and future of Australian exploration: Abstracts for the June 2008 pmd*CRC Conference. *Geoscience Australia, Record*, 2008/09, 7–16.

Champion, D.C., and Cassidy, K.F., 2010. Granitic magmatism in the Yilgarn Craton: implications for crustal growth and metallogeny In: Yilgarn–Superior Workshop — Abstracts, Fifth International Archean Symposium, 10 September 2010. *Geological Survey of Western Australia, Record* 2010/20, 12–18.

Clark, D.J., Hensen, B.J., and Kinny, P.D., 2000. Geochronological constraints for a two stage history of the Albany–Fraser Orogen, Western Australia. *Precambrian Research*, 102, 155–183.

Clowes, R.M., and Oueity, J., 2010. The nature of the Moho transition in NW Canada from combined near-vertical and wide-angle seismic reflection studies. In: Finlayson, D.M. (compiler), 14th International Symposium on Deep Seismic Profiling of the Continents and their Margins. *Geoscience Australia, Record* 2010/24, 40.

Crawford, A.J., Meffre, S., and Symonds, P.A., 2003. 120 to 0 Ma tectonic evolution of the southwest Pacific and analogous geological evolution of the 600 to 220 Ma Tasman Fold Belt system. *Geological Society of Australia, Special Publication*, 22, 377–397.

Cutten, H.N., Thorne, A.M., and Johnson, S.P., 2011. Geology of the Edmund and Collier groups. In: Johnson, S.P., Thorne, A.M. and Tyler, I.M. (editors), Capricorn Orogen seismic and magnetotelluric (MT) workshop 2011: extended abstracts. *Geological Survey of Western Australia, Record* 2011/25, 41–48.

Czarnota, K., Champion, D.C., Goscombe, B., Blewett, R.S., Cassidy, K.F., Henson, P.A., and Groenewald, P.B., 2010. Geodynamics of the eastern Yilgarn Craton. *Precambrian Research*, 183, 175–202.

Dewey, J.F., 1982. Plate tectonics and the evolution of the British Isles. *Journal of the Geological Society, London*, 139, 371–412.

Drummond, B.J., Goleby, B.R., Swager, C.P., and Williams, P.R., 1993. Constraints on Archaean crustal composition and structure provided by deep seismic sounding in the Yilgarn Block. *Ore Geology Reviews*, 8, 117–124.

Drummond, B.J., Goleby, B.R., and Swager, C.P., 2000. Crustal signature of Late Archaean tectonic episodes in the Yilgarn craton, Western Australia: evidence from deep seismic sounding. *Tectonophysics*, 329, 193–221.

Duan, J., Milligan, P.R., and Fomin, T., 2013. Electrical resistivity distribution from magnetotelluric data in the Yilgarn Craton, western Officer Basin and western Musgrave Province. In: Neumann, N.L. (editor), *Yilgarn Craton–Officer Basin–Musgrave Province (YOM) Seismic and MT Workshop*. Geoscience Australia Record 2013/28, 9–23.

Edgoose, C.J., Scrimgeour, I.R., and Close, D.F., 2004. Geology of the Musgrave Block, Northern Territory. *Northern Territory Geological Survey, Report* 15, 44p.

Evins, P.M., Smithies, R.H., Howard, H.M., Kirkland, C.L., Wingate, M.T.D., and Bodorkos, S., 2010a. Redefining the Giles Event within the setting of the 1120–1020 Ma Ngaanyatjarra Rift, west Musgrave Province, Central Australia. *Geological Survey of Western Australia, Record* 2010/6, 36p.

Evins, P.M., Smithies, R.H., Howard, H.M., Kirkland, C.L., Wingate, M.T.D., and Bodorkos, S., 2010b. Devil in the detail: The 1150–1000 Ma magmatic and structural evolution of the Ngaanyatjarra Rift, west Musgrave Province, Central Australia. *Precambrian Research*, 183, 572–588.

Evins, P.M., Kirkland, C.L., Wingate, M.T.D. Smithies, R.H., Howard, H.M., and Bodorkos, S., 2012. Provenance of the 1340–1270 Ma Ramarama Basin in the west Musgrave Province, Central Australia. *Geological Survey of Western Australia, Report* 116, 39p.

Fraser, G.L., Huston, D.H., Gibson, G.M., Neumann, N.L., Maidment, D., Kositcin, N., Skirrow, R.G., Jaireth, S., Lyons, P., Carson, C., Cutten, H., and Lambeck, A., 2007. Geodynamic and Metallogenic Evolution of Proterozoic Australia from 1870–1550 Ma: a discussion. *Geoscience Australia Record*, 2007/16, 76p.

Geological Survey of Western Australia, 2008. 1:500 000 interpreted bedrock geology of Western Australia, 2008 Update. *Geological Survey of Western Australia, Perth.*

Giles, D., Betts, P.G., and Lister, G.S., 2004. 1.8–1.5-Ga links between the North and South Australian Cratons and the early-middle Proterozoic configuration of Australia. *Tectonophysics,* 380, 27–41.

Goleby, B.R., Blewett, R.S., Groenewald, P.B., Cassidy, K.F., Champion, D.C., Jones, L.E.A., Korsch, R.J., Shevchenko, S., and Apak, S.N., 2003. The 2001 Northeastern Yilgarn deep seismic reflection survey. *Geoscience Australia Record*, 2003/28, 143p.

Goleby, B.R., Blewett, R.S., Korsch, R.J., Champion, D.C., Cassidy, K.F., Jones, L.E.A., Groenewald, P.B., and Henson, P.A., 2004. Deep seismic reflection profiling in the Archaean northeastern Yilgarn Craton, Western Australia: implications for crustal architecture and mineral potential. *Tectonophysics,* 388, 119–133.

Goleby, B.R., Blewett, R.S., Fomin, T., Fishwick, S., Reading, A.M., Henson, P.A., Kennett, B.L.N., Champion, D.C., Jones, L.E.A., Drummond, B.J., and Nicoll, M., 2006. An integrated multi-scale 3D seismic model of the Archaean Yilgarn Craton, Australia. *Tectonophysics*, 420, 75–90.

Goodwin, J., Jones, T., Brennan, T., and Nicoll, M., 2013. 3D Geological Model and Geophysical Investigation of the Yilgarn Craton–Officer Basin–Musgrave Province Region. In: Neumann, N.L.

(editor), *Yilgarn Craton–Officer Basin–Musgrave Province (YOM) Seismic and MT Workshop*. Geoscience Australia Record 2013/28, 96–129.

Grey, K., Hocking, R.M., Stevens, M.K., Bagas, L., Carlsen, G.M., Irimies, F., Pirajno, F., Haines, P.W., and Apak, S.N., 2005. Lithostratigraphic nomenclature of the Officer Basin and correlative parts of the Paterson Orogen, Western Australia. *Geological Survey of Western Australia, Report* 93, 89p.

Gum, J., and Belousova, E., 2006. Musgrave Province reconnaissance using TerraneChron. *Australian Earth Sciences Convention, Melbourne, Extended Abstracts* 1, 1–7.

Halilovic, J., Cawood, P.A., Jones, J.A., Pirajno, F., and Nemchin, A.A., 2004. Provenance of the Earaheedy Basin: implications for assembly of the Western Australian Craton. *Precambrian Research*, 128, 343–366.

Hall, R., 2002. Cenozoic geological and plate tectonic evolution of SE Asia and the SW Pacific: computer-based reconstructions, model and animations. *Journal of Asian Earth Sciences*, 20, 353–431.

Hammer, P.T.C., and Clowes, R.M., 1997. Moho reflectivity patterns – a comparison of Canadian Lithoprobe transects. *Tectonophysics*, 269, 179–198.

Harris, L.B., Koyi, H., and Fossen, H., 2002. Mechanisms for folding of high-grade rocks in extensional tectonic settings. *Earth-Science Reviews*, 59, 163–210.

Howard, H.M., Smithies, R.H., Evins, P.M., Kirkland, C.L., Werner, M, Wingate, M.T.D., and Pirajno, F., 2011a. Explanatory notes for the west Musgrave Province. *Geological Survey of Western Australia, 1:100 000 Geological Series Explanatory Notes,* 349p.

Howard, H.M., Werner, M, Smithies, R.H., Kirkland, C.L., Kelsey, D.L., Hand, M., Collins, A., Pirajno, F., Wingate, M.T.D., Maier, W.D., and Raimondo, T., 2011b. The geology of the west Musgrave Province and the Bentley Supergroup – a field guide. *Geological Survey of Western Australia, Record* 2011/4, 119p.

Howard, H.M., Quentin de Gromard, R., Smithies, R.H., Kirkland, C.L., Korsch, R.J., Aitken, A.R.A., Gessner, K., Wingate, M.T.D., Blewett, R.S., Holzschuh, J., Kennett, B.L.N., Duan, J., Goodwin, J.A., Jones, T., Neumann, N.L., and Gorczyk , W., 2013. Geological setting and interpretation of the northeastern half of deep seismic reflection line 11GA-YO1: west Musgrave Province and the Bentley Supergroup. In: Neumann, N.L. (editor), *Yilgarn Craton–Officer Basin–Musgrave Province (YOM) Seismic and MT Workshop*. Geoscience Australia Record 2013/28, 51–95.

Ivanic, T.J., Van Kranendonk, M.J., Kirkland, C.L., Wyche, S., Wingate, M.T.D., and Belousova, E.A., 2012. Zircon Lu–Hf isotopes and granite geochemistry of the Murchison Domain of the Yilgarn Craton: Evidence for reworking of Eoarchean crust during Meso–Neoarchean plume-driven magmatism. *Lithos*, 148, 112–127.

Kennett, B.L.N., 2013. The nature of the lithosphere in the vicinity of the Yilgarn Craton–Officer Basin–Musgrave Province (11GA-YO1) seismic line. In: Neumann, N.L. (editor), *Yilgarn Craton–Officer Basin–Musgrave Province (YOM) Seismic and MT Workshop*. Geoscience Australia Record 2013/28, 158–168.

Kirkland, C.L., Wingate, M.T.D., and Evins, P.M., 2010. 194420: feldspathic sandstone, Mount Blyth. *Geological Survey of Western Australia, Geochronology Record* 923, 5p.

Kirkland, C.L., Wingate, M.T.D., and Evins, P.M., 2011a. 190292: metasandstone, Mount Finlayson. *Geological Survey of Western Australia, Geochronology Record* 935, 5p.

Kirkland, C.L., Spaggiari, C.V., Pawley, M.J., Wingate, M.T.D., Smithies, R.H., Howard, H.M., Tyler, I.M., Belousova, E.A., and Poujol, M., 2011b. On the edge: U–Pb, Lu–Hf, and Sm–Nd data suggests reworking of the Yilgarn Craton margin during formation of the Albany–Fraser Orogen. *Precambrian Research*, 187, 223–247.

Kirkland, C.L., Spaggiari, C.V., Wingate, M.T.D., Smithies, RH., Belousova, E.A., Murphy, R., and Pawley, M.J., 2011c. Inferences on crust–mantle interaction from Lu–Hf isotopes: a case study from the Albany–Fraser Orogen. *Geological Survey of Western Australia, Record* 2011/12, 25p.

Kirkland, C.L., Wingate, M.T.D., Evins, P.M., Smithies, R.H., and Howard, H.M., 2012a. 190233: phyllite, Prostanthera Hill. *Geological Survey of Western Australia, Geochronology Record* 1065, 5p.

Kirkland, C.L., Smithies, R.H., Woodhouse, A.J., Howard, H.M., Wingate, M.T.D., Belousova, E.A., Cliff, J.B., Murphy, R.C., and Spaggiari, C.V., 2012b. A multi-isotopic approach to the crustal evolution of the West Musgrave province, Central Australia. *Geological Survey of Western Australia, Report* 115, 47p.

Kirkland, C.L., Smithies, R.H., Woodhouse, A.J., Howard, H.M., Wingate, M.T.D., Belousova, E.A., Cliff, J.B., Murphy, R.C., and Spaggiari, C.V., 2013a. Constraints and deception in the isotopic record; the crustal evolution of the west Musgrave Province, central Australia. *Gondwana Research*, 23, 759–781.

Kirkland, C.L., Johnson, S.P., Smithies, R.H., Hollis, J.A., Wingate, M.T.D., Hickman, A.H., Tyler, I.M., Tessalina, S.G., Cliff, J.B., Belousova, E.A., and Murphy, R., 2013b. Not-so-suspect terranes of the Rudall Province. *Geological Survey of Western Australia, Record* 2013/2, 31–34.

Korsch, R.J., Goleby, B.G., Leven, J.H., and Drummond, B.J., 1998. Crustal architecture of central Australia based on deep seismic reflection profiling. *Tectonophysics*, 288, 57–69.

Korsch, R.J., Preiss, W.V., Blewett, R.S., Cowley, W.M., Neumann, N.L., Fabris, A.J., Fraser, G.L., Dutch, R., Fomin, T., Holzschuh, J., Fricke, C.E., Reid, A.J., Carr, L.K., and Bendall, B.R., 2010a. Deep seismic reflection transect from the western Eyre Peninsula in South Australia to the Darling Basin in New South Wales: Geodynamic implications. In: Korsch, R.J. and Kositcin, N. (editors), South Australian Seismic and MT Workshop, extended abstracts. *Geoscience Australia, Record* 2010/10, 105–116.

Korsch, R.J., Blewett, R.S., Giles, D., Reid, A.J., Neumann, N.L., Fraser, G.L., Holzschuh, J., Costelloe, R.D., Roy, I.G., Kennett, B.L.N., Cowley, W.M., Baines, G., Carr, L.K., Duan, J., Milligan, P.R., Armit, R., Betts, P.G., Preiss, W.V., and Bendall, B.R., 2010b. Geological interpretation of the deep seismic reflection and magnetotelluric line 08GA–OM1: Gawler Craton–Officer Basin–Musgrave Province–Amadeus Basin (GOMA), South Australia and Northern Territory. In: Korsch, R.J. and Kositcin, N. (editors), GOMA (Gawler Craton–Officer Basin–Musgrave Province–Amadeus Basin) Seismic and MT Workshop 2010: Extended Abstracts. *Geoscience Australia, Record* 2010/39, 63–86.

Korsch, R.J., Kositcin, N., and Champion, D.C., 2011. Australian island arcs through time: geodynamic implications for the Archean and Proterozoic. *Gondwana Research*, 19, 716–734.

Korsch, R.J., Huston, D.L., Henderson, R.A., Blewett, R.S., Withnall, I.W., Fergusson, C.L., Collins , W.., Saygin, E., Kositcin, N., Meixner, A.J., Chopping, R., Henson, P.A., Champion, D.C., Hutton, L.J., Wormald, R., Holzschuh, J., and Costelloe, R.D., 2012. Crustal architecture and of North Queensland, Australia: insights from deep seismic reflection profiling. *Tectonophysics*, 572–573, 76–99.

Korsch, R.J., Blewett, R.S., Pawley, M.J., Carr, L.K., Hocking, R.M., Neumann, N.L., Smithies, R.H, Quentin de Gromard, R., Howard, H.M., Kennett, B.L.N., Aitken, A.R.A., Holzschuh, J., Duan, J., Goodwin, J.A., Jones, T., Gessner, K., and Gorczyk, W., 2013. Geological setting and interpretation of the southwest half of deep seismic reflection line 11GA-YO1: Yamarna Terrane of the Yilgarn Craton and the western Officer Basin. In: Neumann, N.L. (editor), *Yilgarn Craton–Officer Basin–Musgrave Province (YOM) Seismic and MT Workshop*. Geoscience Australia Record 2013/28, 24–50.

Korsch, R.J., Blewett, R.S., Wyche, S., Zibra, I., Ivanic, T.J., Doublier, M.P., Romano, S.S., Pawley, M.P., Johnson, S.P., Van Kranendonk, M.J., Jones, L.E.A., Kositcin, N., Gessner, K., Hall, C.E., Chen, S.F., Patison, N., Kennett, B.L.N., Jones, T., Goodwin, J.A., Milligan, P.M., and Costelloe, R.D., 2013b. Geodynamic implications of the Youanmi and Southern Carnarvon deep seismic reflection surveys: a ~1300 km traverse from the Pinjarra Orogen to the eastern Yilgarn Craton. In: Wyche, S., Ivanic, I.J. and Zibra, I. (compilers), Youanmi and Southern Carnarvon seismic and magnetotelluric (MT) workshop. *Geological Survey of Western Australia, Record* 2013/6, 141–158.

Krapez, B., and Barley, M.E., 2008. Late Archaean synorogenic basins of the Eastern Goldfields Superterrane, Yilgarn Craton, Western Australia. Part III. Signatures of tectonic escape in an arc-continent collision zone. *Precambrian Research*, 161, 183–199.

Lindsay, J.F., and Leven, J.H., 1996. Evolution of a Neoproterozoic to Palaeozoic intracratonic setting, Officer Basin, South Australia. *Basin Research*, 8, 403–424.

Martin, D.McB., 2003. Peperite in the Backdoor Formation and its significance to the age and tectonic evolution of the Bangemall Supergroup. *Geological Survey of Western Australia, Annual Review* 2003–03*,* 55–59.

Martin, D.McB., Sheppard, S., Thorne, A.M., Farrell, T.R., and Groenwald, P.B., 2007. Proterozoic geology of the western Capricorn Orogen – a field guide. *Geological Survey of Western Australia, Record* 2006/18, 43p.

Martin, D.McB., Sircombe, K.N., Thorne, A.M., Cawood, P.A., and Nemchin, A.A., 2008. Provenance history of the Bangemall Supergroup and implications for the Mesoproterozoic paleogeography of the West Australian Craton. *Precambrian Research*, 166, 93–110.

Milligan, P.R., Franklin, R., Minty, B.R.S., Richardson, L.M., and Percival, P.J., 2010. Magnetic anomaly map of Australia (Fifth Edition), 1:5 000 000 scale. *Geoscience Australia, Canberra*.

Myers, J.S., 1995. The generation and assembly of an Archaean supercontinent: evidence from the Yilgarn Craton, Western Australia. In: Coward, M.P. and Ries, A.C. (editors), Early Precambrian Processes. *Geological Society, London, Special Publication* 95, 143–154.

Myers, J.S., Shaw, R.D., and Tyler, I.M., 1996. Tectonic evolution of Proterozoic Australia. *Tectonics*, 15, 1431–1446.

Nelson, D.R., 2001. Timing and distribution of events in the north-western Yilgarn Craton and southern Gascoyne Complex, Australia, inferred from statistical analysis of SHRIMP zircon and monazite U–Pb dates. In: Cassidy, K.F., Dunphy, J.M. and Van Kranendonk, M.J. (editors), Fourth International Archaean Symposium, Extended Abstracts. *AGSO–Geoscience Australia, Record* 2001/37, 183–185.

Nelson, D.R., 2002. 168983: metasandstone, Weld Spring; in Compilation of geochronology data, 2001: *Geological Survey of Western Australia, Record* 2002/2, 16–19.

Neumann, N.L., and Fraser, G.L. *(*editors*)*, 2007. Geochronological synthesis and time-space plots for Proterozoic Australia. *Geoscience Australia, Record,* 2007/06, 216p.

Pawley, M.J., Wingate, M.T.D., Kirkland, C.L., Wyche, S., Hall, C.E., Romano, S.S., and Doublier, M.P., 2012. Adding pieces to the puzzle: episodic crustal growth and a new terrane in the northeast Yilgarn Craton, Western Australia. *Australian Journal of Earth Sciences*, 59, 603–623.

Pirajno, F., Hocking, R.M., Reddy, S.M., and Jones, A.J., 2009. A review of the geology and geodynamic evolution of the Palaeoproterozoic Earaheedy Basin, Western Australia. *Earth-Science Reviews*, 94, 39–77.

Raymond, O.L. (coordinator), 2009. Surface geology of Australia 1:1 million scale digital geology data. *Geoscience Australia, digital geology map*. https://www.ga.gov.au/products/servlet/controller?event=GEOCAT_DETAILS&catno=69455

Sircombe, K.N., Cassidy, K.F., Champion, D.C., and Tripp, G., 2007. Compilation of SHRIMP U–Pb geochronological data, Yilgarn Craton, Western Australia, 2004–2006. *Geoscience Australia, Record* 2007/01, 182p.

Smithies, R.H., Howard, H.M., Evins, P.M., Kirkland, C.L., Kelsey, D.E., Hand, M., Wingate, M.T.D., Collins, A.S., Belousova, E.A., and Allchurch, S., 2010. Geochemistry, geochronology and petrogenesis of Mesoproterozoic felsic rocks in the western Musgrave Province of central Australia and implication for the Mesoproterozoic tectonic evolution of the region. *Geological Survey of Western Australia, Report* 106, 73p.

Smithies, R.H., Howard, H.M., Evins, P.M., Kirkland, C.L., Kelsey, D.E., Hand, M., Wingate, M.T.D., Collins, A.S., and Belousova, E.A., 2011. High-temperature granite magmatism, crust–mantle interaction and the Mesoproterozoic intracontinental evolution of the Musgrave Province, Central Australia. *Journal of Petrology*, 52 (5), 931–958.

Smithies, R.H., Howard, H.M., Kirkland, C.L., Medlin, C.C., and Wingate, M.T.D., 2013a. Western Australia's own super volcano: part of the torturous thermal history of the west Musgrave Province. *Geological Survey of Western Australia, Record* 2013/2, 23–26.

Smithies, R.H., Spaggiari, C.V., Kirkland, C.L., Howard, H.M., and Maier, W.D., 2013b. Petrogenesis of gabbros of the Mesoproterozoic Fraser Zone: constraints on the tectonic evolution of the Albany–Fraser orogen. *Geological Survey of Western Australia, Record* 2013/5, 29p.

Spaggiari, C.V., Bodorkos, S., Barquero-Molina, M., Tyler, I.M., Wingate, M.T.D., 2009. Interpreted bedrock geology of the South Yilgarn and central Albany–Fraser Orogen, Western Australia. *Geological Survey of Western Australia, Record* 2009/10, 84p.

Spaggiari, C.V., Kirkland, C.L., Pawley, M.J., Smithies, RH., Wingate, M.T.D., Doyle, M.G., Blenkinsop, T.G., Clark, C., Oorschot, C.W., Fox, L.J., and Savage, J., 2011. The geology of the east Albany–Fraser Orogen – a field guide. *Geological Survey of Western Australia, Record* 2011/23, 97p.

Stevens, M. K., and Apak, S.N. (compilers), 1999. GSWA Empress 1 and 1A well completion report, Yowalga Sub-basin, Officer Basin Western Australia. *Geological Survey of Western Australia, Record* 1999/4, 110p.

Swager, C.P., Goleby, B.R., Drummond, B.J., Rattenbury, M.S., and Williams, P.R., 1997. Crustal structure of granite–greenstone terranes in the Eastern Goldfields, Yilgarn Craton, as revealed by seismic reflection profiling. *Precambrian Research*, 83, 43–56.

Tyler, I.M., 2000. Paleoproterozoic orogeny in Western Australia. *Geological Survey of Western Australia, Record* 2000/8, 7–8.

Van Kranendonk, M.J., Ivanic, T.J., Wingate, M.T.D., Kirkland, C.L., and Wyche S., 2013. Long-lived, autochthonous development of the Archean Murchison Domain, and implications for Yilgarn Craton tectonics. *Precambrian Research*, 229, 49–92.

Wade, B.P., Barovich, K.M., Hand, M., Scrimgeour, I.R., and Close, D.F., 2006. Evidence for Early Mesoproterozoic arc magmatism in the Musgrave Block, Central Australia: Implications for Proterozoic crustal growth and tectonic reconstructions of Australia. *Journal of Geology*, 114, 43–63.

White, N., and McKenzie, D., 1988. Formation of the "steer's head" geometry of sedimentary basins by differential stretching of the crust and mantle. *Geology,* 16, 250–253.

Wingate, M.T.D., 2003. Age and palaeomagnetism of dolerite intrusions of the southeastern Collier Basin, and the Earaheedy and Yerrida Basins, Western Australia. *Geological Survey of Western Australia, Record* 2003/3, 35p.

Wingate, M.T.D., and Bodorkos, S., 2007. 181873: quartz sandstone, Lancer 1. *Geological Survey of Western Australia, Geochronology Record* 685, 6p.

Wingate, M.T.D., Pirajno, F., and Morris, P.A., 2004. Warakurna large igneous province: A new Mesoproterozoic large igneous province in west-central Australia. *Geology*, 32, 105–108.

Wyche, S., Kirkland, C.L., Riganti, A., Pawley, M.J., Belousova, E., and Wingate, M.T.D. 2012. Isotopic constraints on stratigraphy in the central and eastern Yilgarn Craton, Western Australia. *Australian Journal of Earth Sciences*, 59, 657–670.

10 The YOM seismic survey: Implications for mineral systems in the Yilgarn Craton–Officer Basin–Musgrave Province region

A.R.A. Aitken[1], R.S. Blewett[2], R.H. Smithies[3], A. Joly[1], R. Quentin de Gromard[3], H.M. Howard[3], M.J. Pawley[3], N.L. Neumann[2], R.J. Korsch[2], I.M.Tyler[3]

[1] Centre for Exploration Targeting, School of Earth and Environment, The University of Western Australia, 35 Stirling Highway, Crawley, WA 6009.
[2] Geoscience Australia, Cnr Jerrabomberra Avenue and Hindmarsh Drive Symonston ACT, GPO Box 378 Canberra ACT 2601 Australia.
[3] Geological Survey of Western Australia, Department of Mines and Petroleum, 100 Plain Street, East Perth, WA 6004.

alan.aitken@uwa.edu.au

Introduction

The 484 km Yilgarn Craton–Officer Basin–Musgrave Province (YOM) seismic line was undertaken as a collaborative initiative between the Geological Survey of Western Australia and Geoscience Australia and funded under the Australian Government's Onshore Energy Security Program (http://www.ga.gov.au/energy/energy-security-program/onshore-energy-security.html) and the Western Australian Government's Royalties for Regions Exploration Incentive Scheme (http://www.dmp.wa.gov.au/7743.aspx). In addition to exploring the frontier western Officer Basin, this transect crosses through several regions that may possess significant mineral resources, but remain little developed (Figure 10.1). Through helping develop a better understanding of crustal architecture and geodynamic processes the YOM seismic reflection transect can be used to re-assess the mineral potential in these regions.

The seismic transect starts in relatively thin successions of the Officer Basin that overlie the Yilgarn Craton, which is well-endowed in Archean orogenic gold and komatiite-hosted nickel deposits. The seismic line traverses the Officer Basin and the west Musgrave Province, which is endowed in Proterozoic magmatic Ni-Cu and PGEs and gold. This transect crosses the boundary between a stable Archean craton and a Proterozoic orogenic belt. Such boundaries separating differing lithospheric elements tend to be regions where energetic geodynamic systems and hence mineral systems may be focussed (Leahy et al., 2005).

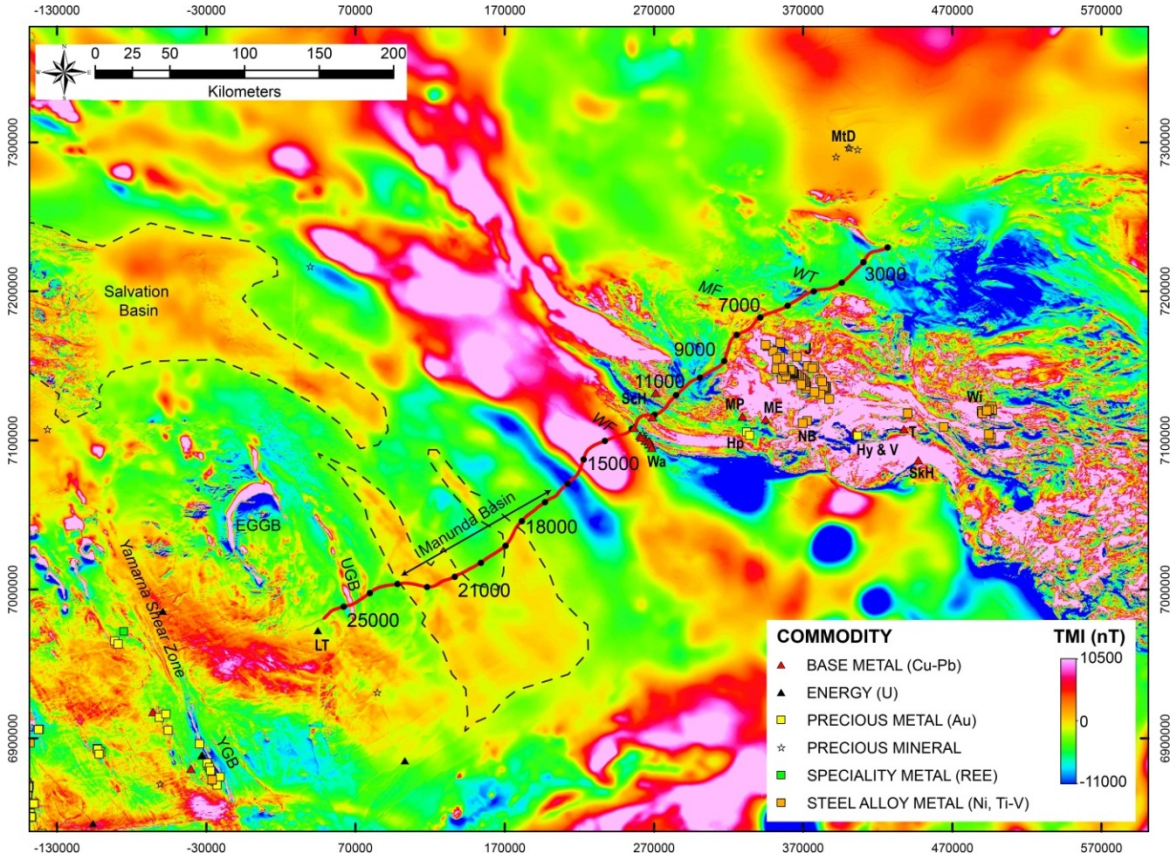

Figure 10.1 *The YOM seismic line overlain on total magnetic intensity data, with annotations. Dashed lines indicate inferred extent of magnetised sills within the Manunda and Salvation basins. YGB- Yamarna Greenstone Belt, EGGB – Ernst Giles Greenstone Belt, UGB – Unnamed Greenstone Belt; WF – Winduldarra Fault, MF- Mann Fault, WT – Woodroffe Thrust. Occurrences: LT – Lake Throssell, Wa –Warburton, ScH – Scamp Hill, Hp – Handpump/Primer, MP –Mount Palgrave, ME – Mount Eliza, NB – Nebo Babel, Hy – Halleys, V – Voyager, SkH – Skirmish Hill, T – Tollu, Wi – Wingellina, MtD – Mt Destruction.*

Mineral Systems

A mineral system is a holistic term to describe all components of the geological system, including lithospheric and crustal characteristics, active and past tectonics and transport and depositional processes. Mineral systems can be analysed with a process-oriented understanding by 'asking' five questions that characterise the ore-forming system, viz: what was the 1) geodynamic evolution; 2) architecture; 3) sources and reservoirs of fluids and metals; 4) fluid pathways and drivers; and 5) transport and metal depositional processes. The post-mineralization history, including preservation potential, is also an important part of a mineral systems analysis.

The benefit to an explorer in thinking in terms of a mineral system is one of scale. A mineral system operates at scales many orders of magnitude larger than the mineral deposit itself, which is just a favourable symptom of an effective system. For example, a deposit only 500 m wide may have a fluid outflow zone many tens of kilometres wide, such as in the Eastern Goldfields. Similarly, the zone of depletion of the metal-rich source rock may be many tens of kilometres wide, such as in Broken Hill. This scale factor makes selecting favourable tracts of ground on the basis of a mineral system more effective and tractable, especially undercover. The new data collected and synthesised through the YOM survey provide specific insights into these systems questions, especially geodynamics, architecture and fluid pathways.

Gold and Komatiite-hosted Nickel in the Yamarna Terrane

The Yamarna Terrane, is the easternmost tectonic subdivision of the Yilgarn Craton (Pawley et al., 2009). The greenstones of the Yamarna Terrane appear to consist of a single cycle of mafic-ultramafic-felsic volcanic and siliciclastic rocks dated between 2711 Ma and 2677 Ma (Pawley et al., 2012; Sircombe et al., 2007). This age range is consistent with stratigraphic ages in the Kalgoorlie Terrane. Korsch et al. (2013) have described the regional geology.

The Yamarna terrane is entirely buried beneath the Neoproterozoic Officer Basin, and in part, the Mesoproterozoic Manunda Basin. The Yamarna Terrane is underlain by a distinctly reflective mid-to lower crust, the Babool Seismic Province. The YOM seismic line shows that both the Yamarna Terrane and the underlying Babool Seismic Province extend beneath the Officer Basin to the Winduldarra Fault which defines the southwestern margin of the Musgrave Province. The Yilgarn Craton has a characteristic crustal-scale architecture of east-dipping faults that extend almost to the Winduldarra Fault in the east. At its most westerly end, the Yamarna Terrane is concealed beneath ~480 m (0.3 s TWT) of Officer Basin and younger sedimentary rocks so the precise age, origins and tectonic events of these concealed rocks are hard to characterise.

The character and trends in magnetic and gravity data suggest that the far eastern margin of the Yamarna Terrane is dominated by granitic rocks with two minor greenstone belts (Figure 10.1). Along strike to the northwest, on the ROBERT 1:250 000 sheet, lie two greenstone belts: the western hook-shaped belt is the Ernest Giles greenstone belt; the north-northwest–trending belt is unnamed, but may have been part of the Ernest Giles greenstone belt now displaced by a north-northwest striking fault. Greatland Gold has drilled through 170–300 m of sedimentary cover into the Ernest Giles greenstone belt, which they interpreted to have a stratigraphy similar to the greenstone package in the gold-rich Mount Magnet area of the Youanmi Terrane (Greatland Gold, 2010). This also implies that the Ernest Giles greenstone belt is older than the Yamarna Greenstone Belt, and may represent part of the older crust that underlies the Yamarna Terrane (Pawley et al., 2012). The unnamed easterly greenstone belt is crossed by the YOM line (labelled UGB on Figure 10.1), but it has not been drilled, so the nature of this belt is unknown.

Gold mineral systems

The Yilgarn Craton is extremely well endowed in gold, but its distribution is not equal in all terranes. A first-order empirical relationship with gold endowment is defined by the isotopic age of the crust, particularly between narrow terranes whose isotopic boundaries represent large gradients in age. The reasons for this relationship are unclear; the boundaries in crustal age data may simply be mapping the deep-cutting discontinuities in the lithosphere, and/or they may also be mapping different source regions for gold.

The most endowed regions of the Yilgarn Craton, such as the Kalgoorlie Terrane and the eastern Kurnalpi Terrane, have a crustal age in the intermediate range (Sm–Nd T_{DM} model age of 3.0 Ga to 2.9 Ga), which are adjacent to much older and much younger aged terranes. The Kalgoorlie Terrane has a 300 Ma time gradient between the older western Youanmi Terrane and the younger western Kurnalpi Terrane. The limited Sm–Nd data available for the Yamarna Terrane show that the region has an intermediate crustal age, adjacent to a more juvenile region within the Burtville Terrane to the west. More samples are needed, however, to improve the picture for the far east of the craton.

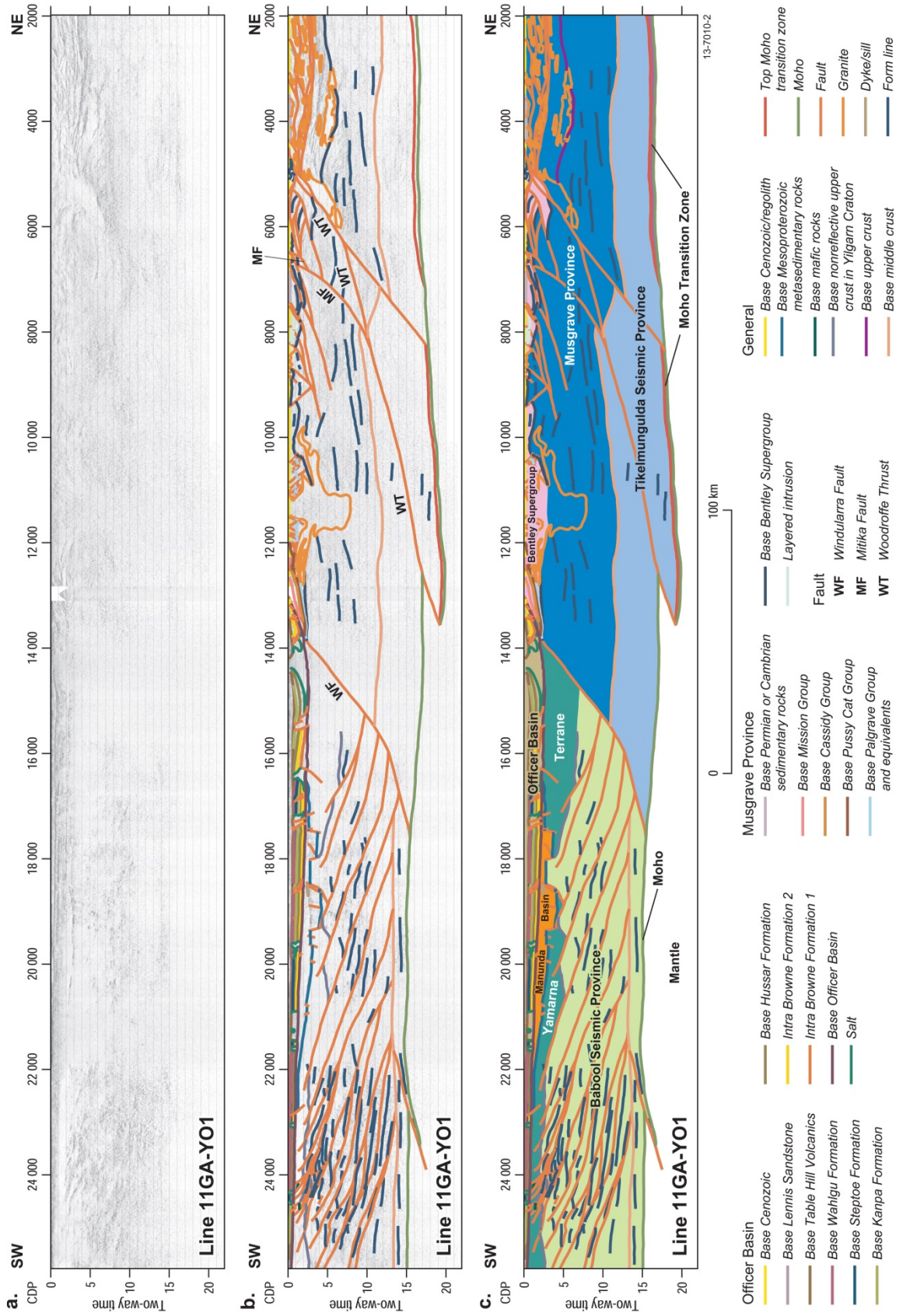

Figure 10.2 *Summary of the Yilgarn Craton–Officer Basin–Musgrave Province seismic section, with annotations.*

Large crustal-scale fault networks are interpreted to be important fluid pathways, and seismic reflection studies provide an excellent capacity to image these (Figure 10.2). Previous crustal-scale seismic reflection studies to the west, on lines 01AGS-NY1, 01AGS-NY3 and BMR91-EGF01 (Goleby et al., 2004), identified the Ida Fault, Ockerberry Fault, Hootanui Shear Zone as the major Moho-penetrating structures. The Yamarna Shear Zone appears to be crustal in scale, but because of the change in the orientation of the 01AGS-NY1 seismic line to a strike section it appears to sole out into the lowermost crust (Goleby et al., 2004), but it is likely that this structure extends to the Moho. Each of these major fault zones has many splays, some of which were interpreted to be pathways for migrating gold-rich fluids, and may be the preferential second- and third-order structures that controlled deposition of the gold (Groves, 1993; Groves et al., 2000; Micklethwaite and Cox, 2006). Domes provide an additional architectural focus to fluid flow in many of the Eastern Goldfields gold deposits (e.g. Kanowna Belle, Kalgoorlie, St Ives. (Blewett et al., 2010).

The seismic data show that the crustal-scale faults in the Yamarna Terrane dip consistently east, but do not offset the Moho. The major fault networks disrupt the Yamarna-Babool boundary, and are projected to intersect the Officer Basin unconformity at approximately ~CDPs 17400, 17900, 18700, 19200, 20300, 22700, 23200, 23800, 24000–24900, 25700. The region between CDP 22700 and CDP 24900 is particularly associated with a broad damage zone. This damage zone occurs at the culmination of a broad domal high, within which many smaller domes are located.

The deep-penetrating faults on the western end of the YOM seismic line project to the present-day surface along strike from the domal or hook-shaped Ernest Giles greenstone belt. If these deep faults link to the shear zones bounding the greenstone belt then the prospectivity of this region is enhanced.

Komatiite-related nickel mineral systems

The second major resource for which the Yilgarn Craton is remarkable is komatiite-associated nickel deposits. These deposits are typically considered to form when extremely hot komatiite lavas thermomechanically erode their substrate and mineralisation is localised in the channels (Barnes and Fiorentini, 2012; Fiorentini et al., 2010). Subsequent tectonic processes may however have reworked these primary deposits leading to dislocation, and remobilisation of nickel, sometimes leading to unconventional deposit geometries and locations (Collins et al., 2007).

Lithospheric architecture plays a fundamental role in the formation of these deposits (Barnes and Fiorentini, 2012; Fiorentini et al., 2010; McCuaig et al., 2010; Mole et al., 2010; Mole et al., 2012). Recent work suggests that, in terms of regional prospectivity within the Yilgarn Craton, the unusual endowment of the Kalgoorlie Terrane relates mostly to sustained high rates of magma flux (Barnes and Fiorentini, 2012), countering an earlier argument that distinctive mantle sources differentiate endowed regions from barren regions (Zhang et al., 2008). Mole et al. (2010) have suggested that lithospheric architecture controls the nature and style of komatiite volcanism. Their model suggests that the margins of crustal blocks, which form preferential pathways used by plume-derived magmas to access the surface, shifted as the Yilgarn Craton evolved and the lithosphere thickened. These intraplate crustal discontinuities were the sites of focused melting, extension and crustal thinning/rifting during plume magmatism, and facilitated the rapid emplacement of highly-primitive mantled-derived magmas. The present-day lithospheric architecture within the Yamarna Terrane is generally consistent, implying that there is only limited scope for grossly differing lithospheric processes within the region, although the paucity of isotopic data means that the paleo-lithospheric architecture at the time of ore-formation is not known well.

To reach the surface, komatiitic magmas also require a trans-lithospheric plumbing system that permits the entire crustal column to sustain the pressure gradient necessary to overcome the negative buoyancy of these magmas. The greenstone belt at CDP 24000–25000 is correlated to a major crustal-scale shear zone (Korsch et al., 2013). The only clear Moho-cutting fault in the Babool Seismic Province has generated a low-angle west-dipping offset centred on CDP 23000, and this may also form part of a potential magma pathway.

The Manunda Basin

The Manunda Basin is most likely Mesoproterozoic in age, with a maximum depositional age of 1310 Ma (Korsch et al., 2013). On the YOM seismic profile, the basin extends from ca. CDP 16500 to ca. CDP 22800, with two major graben and an intervening horst characterising the deepest part of the basin between CDP 17600 and CDP 19200. In its deepest graben, it is 2.4 s (TWT) thick, approximately 6 km (Korsch et al., 2013). The basin contains at least two, and possibly three seismic stratigraphic successions, including a weakly-layered lowermost package, only present within the graben, a strongly reflective middle package, and a weakly to moderately reflective upper package (Korsch et al., 2013). Along the seismic line, the depth of the Manunda Basin is probably prohibitive for economic exploration; although it is still useful to review the characteristics of this basin, with the potential for remobilization of metals into the overlying Officer Basin, and in the anticipation of less deeply buried parts of the basin elsewhere.

The lateral extent of the Manunda Basin along the YOM profile can be correlated with a long-wavelength low-amplitude magnetic high that extends for ca. 90 km to the southeast and up to 100 km to the northwest (Figure 10.1). Based on the aeromagnetic data, this magnetic character could be interpreted to be caused by the Warakurna-LIP aged rocks similar to the Glenayle dolerite sills that intrude the Earaheedy Basin, Collier Basin and Salvation Basin to the northwest. This may suggest similarity to the Collier and/or Salvation basins.

The Collier Basin includes the Backdoor, Calyie and Ilgarari formations, and is well exposed in the central Capricorn Orogen. The Backdoor Formation is characterised by ~1500 m of laminated siltstones, with some fine-grained sandstone and thin-bedded mudstone (Cutten et al., 2011), and the Calyie Formation is characterised ca. 200m of interbedded medium- to coarse-grained sandstone and siltstone (Cutten et al., 2011). The Ilgarari Formation consists of up to 700m of planar-laminated pyritic and carbonaceous siltstone and fine-grained sandstone, with minor limestone, calcareous siltstone and chert. The Collier Basin is widely intruded by the ca. 1070 Ma Kulkatharra Dolerite. The Collier Basin is prospective for several commodities, including base metals, especially shear-zone hosted and potentially stratiform copper (historically mined at Ilgarari and Kumarina), and manganese.

The Salvation Basin overlies the Collier Basin, and is prominently intruded by the ca. 1070 Ma Glenayle Dolerite, which dominates the magnetic signal, and constitutes > 50% of outcrop. The Salvation Basin preserves a succession of late Mesoproterozoic siliciclastic sedimentary rocks, including the Glass Spring, Brassey Range, Jilyili, and Coonabildie formations. To date, very little mineralisation has been identified within either the Salvation Group or the Glenayle Dolerite, with just the Bandit 2 manganese prospect, and several diamond occurrences at McConkey Hill.

In summary, the minerals potential of the newly defined Manunda Basin remains ill defined. Its geology is probably very similar to that of the Collier and Salvation basins, and as such should share many components of the mineral systems of these basins. Currently, the Collier and Salvation basins host only relatively minor mineralisation, however there is potential in those basins for large sediment-hosted base

metal mineralisation, which would also apply to the Manunda Basin. Basaltic layers within the Manunda Basin, K-Ar dated at 1058 ± 13 Ma (Stevens and Apak, 1999) are interpreted to cause a magnetic anomaly that has similar character to the Glenayle Dolerite within the Salvation Basin (Figure 10.1), and the Manunda Basin may be closely linked with the Giles Event and/or the Warakurna LIP.

Giles Event & Warakurna LIP magmatic Ni-Cu-PGE mineral system

The 1085 Ma to 1040 Ma Giles Event emplaced an extraordinary volume of magmatic material concentrated into the Musgrave Province (Aitken et al., 2013a; Evins et al., 2010). Overlapping this event, the 1078 Ma to 1073 Ma Warakurna LIP is associated with a late-Mesoproterozoic magmatic event that emplaced mafic rocks over a vast portion of central and western Australia (Wingate et al., 2004). In a variety of locations, most notably at Nebo-Babel (Godel et al., 2011; Seat et al., 2011), but also at numerous other prospects within the west Musgrave Province (Abeysinghe, 2003; Joly et al., 2013) and also in the Yilgarn Craton (Wyche et al., 2013) mafic rocks of this age are associated with Ni±Cu mineralisation.

Platinum-Group-Element (PGE) mineralisation is also associated with the Giles Complex magmatism. There are some occurrences in the uppermost parts of the Jameson Intrusion (Figure 10.1), and elevated PGE levels have been reported from the Wingellina Intrusion. Enhanced PGE potential is also suggested by similarities in cumulate stratigraphy between ultramafic-mafic Giles intrusions and the Bushveld and Great Dyke (Maier et al., in prep). These intrusions also contain economically significant nickeliferous laterite deposits at Wingellina and vanadiferous titanomagnetite deposits in the Jameson Range (Howard et al., 2011). PGEs have also been discovered in significant quantities within smaller “chonoliths” including Nebo-Babel but also Halleys.

The orthomagmatic nickel-sulphide mineral system requires several key components (Naldrett, 1999). A high degree of partial melting of the mantle is required (Li et al., 2001), so as to generate a high-MgO magma capable of carrying metals into the crust. Magma flow must be focused along dynamic pathways that permit rapid fluid migration to the accessible crust. Sulphur saturation is required at some point, often, but not always, from interaction with upper crustal country rocks. Mid-level, high-energy staging chambers also provide opportunities for assimilation, fractionation and contamination, and may provide further opportunity to achieve sulphur saturation. Deep-crustal magmatic ponding sites may also fulfil a potentially important role. They may explain the long-lasting heat flux in the Musgrave Province expressed by UHT metamorphism and near continuous magmatism over nearly 200 Ma. Finally, to form a deposit, this metal-rich sulphur-saturated magma must be suitably trapped in a concentrated form, often within a magma conduit, or chonolith (Barnes and Lightfoot, 2005).

To date, the majority of orthomagmatic Ni-Cu prospects associated with the Giles Event are in the Musgrave Province, and the extensive sills of the Warakurna LIP, where they extend into the Bangemall Basin are apparently barren. Significant potential may still exist within the extensive Warakurna-aged sills within the Yilgarn Craton (Wyche et al., 2013). The Cu-Mo-Ni Earoo project indicates some mineralisation associated with these sills.

The YOM seismic line images a fundamental difference in crustal character across the Winduldarra Fault that may relate to the Mesoproterozoic geodynamic setting of this region. The Babool Seismic Province is strongly reflective and extends to the base of the crust. The Musgrave Province basement is less reflective and is underlain by the Tikelmungulda Seismic Province. This deep seismic province is interpreted to represent a 20 km thick magmatic underplate at the base of the Musgrave Province. The age of this underplate is equivocal, but it could represent extensive magmatic additions during either the

Musgrave Orogeny or the Giles Event. Continent-scale gravity modelling indicates dense and thick crust in this region, with a geometry which suggests that a similar underplate exists throughout the eastern Warakurna LIP region but not beneath the West Australian Craton (Aitken et al., 2013c).

This postulated underplate is not unusual, considering the enormous volumes of magma production in the west Musgrave Province during the Musgrave Orogeny and Ngaanyatjarra Rift. Preliminary estimates for the latter event indicate preserved volumes of >40,000 km^3 of mafic and ultramafic rocks (Aitken et al., 2013b) and >20,000 km^3 of felsic volcanic rocks (Smithies et al., 2013), with a total magmatic pile at least 20 km thick. These volumes are consistent with the dimensions of the Tikelmungulda Seismic Province. Furthermore, the magmatic system appears to have been essentially static, with net extension in the order of 10 ± 30 km and little migration of the locus of magmatism (Aitken et al., 2013a; Smithies et al., 2013).

Large magmatic events are particularly prospective for magmatic ore deposits as they may result in large sill-like intrusions hosting PGE-bearing reefs, dynamic magma feeder conduits hosting Ni-Cu deposits, and trigger large scale crustal heating and melting, potentially providing external sulphur to the magmas to trigger sulphide saturation.

Orthomagmatic nickel-copper deposits are found primarily in dolerite intrusions of the Alcurra Dolerite Suite. This magmatic event is contemporaneous with a series of rapidly evolving deformation events, involving major shortening, basin forming and shearing events (Aitken et al., 2013a). These events involved movements of several kilometres to tens of kilometres on the major crustal scale faults of the region including the Cavenagh Fault and Mount West Shear Zone and the reactivation of early rift-related growth faults that accommodated intrusion emplacement and volcanic fill. These large-scale structures are essential to allow the primitive magmas to reach the surface, and in a rapidly changing stress field, provide opportunities for physical traps to develop.

The Nebo-Babel deposit (1068 ± 4 Ma; Seat et al., 2011) is located in the hanging wall of the northwest-dipping Cavenagh Fault, 2.5 km from the near-surface trace. This fault zone is up to 8 km wide, and, based on a strong magnetotelluric response extends at least to the lower crust, and probably into the upper mantle, separating more conductive lithosphere to the northwest from highly resistive lithosphere to the southeast (Aitken et al., 2013b). The vicinity of this deposit is characterised by structure developed during the latter part of the rift event, which was characterised by several tectonic events closely spaced in time, and which display rapid switching between different stress-states. This is well demonstrated by an analysis of the Cavenagh Fault.

This fault zone experienced a series of deformational events throughout the later part of the Giles Event. The first was activation as a sinistral strike-slip structure that accommodated the north-eastwards motion of the southeast Mamutjarra Zone by ~10 km in the shortening event that formed the Blackstone syncline. There is no folding to the northwest of the Cavenagh Fault, suggesting it was a passive structure, and that motion was northeast-directed. Subsequently, a switch to extension, but with similarly oriented principal stresses, meant that the region was subjected to northwest-southeast extension. During this phase the Cavenagh Fault bounded the deposition of the upper part of the Talbot Sub-basin, which is only observed to the northwest of the fault. Northwest-down normal motion is currently estimated at several kilometres based on apparent offsets to the Mount Palgrave Group strata (Aitken et al., 2013a). The final period of late-Giles Event tectonics involved a change in the principal stress orientation, and involved dextral movement on east-southeast trending faults and sinistral motion on north-south trending faults. One of the north-south faults (the Jameson Fault) cuts Nebo-Babel suggesting that emplacement occurred before, or perhaps during, the stress-field change.

Some reverse movement on the Cavenagh Fault may have occurred at this time. Post Ngaanyatjarra Rift motion on the Cavenagh Fault is estimated at 4 km sinistral slip.

Godel et al. (2011) suggested that mineralisation at Nebo-Babel was the result of mixing between two different magma types. The first of these were mafic dykes compositionally similar to the Alcurra Dolerite suite that dominates the slightly older, regional, Warakurna LIP magmatism. The second was what Howard et al. (2009) referred to as the 'plagioclase-rich dykes', which crop-out mainly in the eastern part of the west Musgrave Province, in the vicinity of the Bell Rock intrusion. Mixing occurred within major mantle-tapping crustal structures.

The Halleys copper-PGE-nickel mineralisation on the southeast flank of the Saturn gabbroic intrusive complex, dated at 1072 ± 8 Ma (Howard et al., 2011), occupies a quite different setting. It is located above a fault that is interpreted to have formed the bounding fault to the ~8 km thick Blackstone intrusion during its emplacement. The Tollu granite pluton is symmetrical across this fault, suggesting that early-rift structures played a key role in controlling magma ascent later in the event. Like the Cavenagh Fault, these east-southeast trending early-rift structures were reactivated several times, forming the boundaries of the Talbot Sub-basin and being reactivated during later events.

Hydrothermal gold and base-metal mineral systems in the Bentley Supergroup

The Bentley Supergroup describes the extensive and voluminous volcanic-sedimentary sequence emplaced on the Musgrave Province synchronous with the Giles Event. The basins are dominated by rhyolites, with minor basalt and sedimentary rocks (Howard et al., 2011). The recent discovery of the Handpump deposit, 55 km southeast of the seismic line at CDP 117500 has sparked much interest in the potential for the Bentley Supergroup to host hydrothermal gold deposits. The Bentley Supergroup has been prospective for base-metal and minor gold deposits, including hydrothermal mineralisation at Tollu (Cu-Co-Ni-PGE-Ag-Au-Pb), Skirmish Hill (Cu-Au) and Voyager (Au-Cu), and stratabound base metal mineralisation at Pussy-Cat Hill (Cu), Scamp Hill (Cu), Mount Eliza (Cu-Pb-Zn) and Mount Palgrave (Cu-Pb-Zn) (Abeysinghe, 2003).

The Handpump deposit is hosted within a series of steeply north-dipping magmatic hydrothermal breccia zones within rhyolite of the Mount Palgrave Group (Howard et al., 2011). Relative to the majority of the Bentley Supergroup, which is intensely magnetised and strongly textured, this region is characterised by low-amplitude, smooth aeromagnetic character, likely indicative of extensive hydrothermal alteration. In the seismic line, the corresponding region is characterised by a large (>3000 km^2 in cross section) 'ghost' shaped Warakurna Supersuite granite body, that may be very similar to the Winburn Granite (1077 ± 6 Ma), which underlies the Mount Palgrave Group to the east. The Tollu prospect is hosted in altered gabbros and felsic volcanic rocks within a dilation zone between north-south oriented shear-zones, interpreted to be active at ca. 1067 Ma (Aitken et al., 2013a). Tollu prospect is located on the northern margin of the shallowly north-dipping Tollu Pluton (1076 ± 9 Ma), which intruded into the basal parts of the Blackstone sub-basin.

These deposits suggest that there may be an intimate relationship between granitic intrusions within the Bentley Supergroup and hydrothermal gold and copper ore-deposits hosted within the felsic volcanic and volcaniclastic rocks. The seismic line shows that granitic intrusions are very common within the Bentley Supergroup, especially in the thick successions to the northeast of, and in the footwall of, the Woodroffe Thrust, where several intrusions are interpreted (e.g. CDP 5000–6000, CDP 3400–4800).

The enormous size of the volcanic system associated with deposition of the Bentley Supergroup (in particular in the Talbot Sub-basin), which includes super-volcano sized eruptions, a silicic LIP, several caldera structures, high-temperature rhyolitic ignimbrites, and voluminous syn-volcanic granite intrusion (Smithies et al., 2013) suggests the potential for extensive hydrothermal alteration. Primary magmas of the Bentley Supergroup were typically reduced and water-poor but were halogen-rich (Howard et al., 2011). In addition, volcanic deposition was typically sub-aqueous and so deep circulation of surface water is potentially important. Preliminary isotopic data suggest that all of the felsic magmas in the Talbot Sub-basin were interacting, at an early stage, with deep hydrothermal fluids. Although we have not identified any regional-scale alteration overprint (other than pervasive but weak sericite-pyrite), the eastern contact between rhyolites of the Mount Palgrave Group and the Winburn granite, in particular, is a northerly-trending zone cut by several east-trending zones of strong silicification, cleavage development and locally brecciation, resembling in many ways the mineralising environment at Handpump.

Iron Oxide Copper-Gold (IOCG) mineral systems

Conceptually, IOCG potential in the west Musgrave Province is high. The region has abundant A-type and also voluminous mafic magmatism reflecting intraplate magmatic processes from the Musgrave Orogeny and Giles Event; underwent major thermal events during the aforementioned events; possesses many crustal-scale fault zones; is not too deeply eroded for preservation, especially in the southwest; and, crucially, occupies a position adjacent to a craton margin (the Winduldarra Fault). These are similar to the first-order characteristics of the world-class Olympic Dam IOCG deposit (Hayward and Skirrow, 2010).

Despite this conceptual favourability, the existence of IOCG mineralisation in the west Musgrave Province has yet to be demonstrated. The strongest candidate targets for IOCG are likely to be associated with Warakurna Supersuite A-type granites, which have intruded at mid-to-upper crustal levels as part of a major, high temperature rifting event (Smithies et al., 2009). Strong compositional similarities with granites and rhyolites of the Hiltaba Supersuite and Gawler Range Volcanics (Smithies et al., 2011), however, suggest that the Pitjantjatjara Supersuite, emplaced during the Musgrave Orogeny, might also be highly prospective for IOCG deposits.

Summary

The YOM seismic traverse has crossed one of the greatest unknown regions in Australia, not coincidentally a region with very few mineral deposits, and has provided immensely valuable knowledge on the crustal architecture and the likely geodynamic processes of this region. As many mineral systems are heavily reliant on crustal and lithospheric scale architecture studies of this sort are important components in our efforts to “open-up” greenfields areas through better informed area selection. The fundamental crustal-scale boundary between the Archean Yilgarn Craton and the Proterozoic Musgrave Province is delineated. This boundary is associated with fundamentally different crustal structure, and also potentially different mineral systems.

We have focused here on some of the potential implications of the newly revealed crustal structure for well-established mineral systems, such as Archean orogenic gold and komatiite related nickel in the Yilgarn Craton and orthomagmatic Ni-Cu±PGE associated with the Giles Event and Warakurna LIP. Nevertheless, we have also considered some less well understood systems, such as IOCG,

hydrothermal gold and copper in the Bentley Supergroup and the potential for mineralization in the Manunda basin, based on similarities with other basins of the northern Yilgarn Craton.

Acknowledgements

This paper forms part of ongoing collaboration between the Centre for Exploration targeting at UWA, the Geological Survey of Western Australia and Geoscience Australia. The work was funded by the Australian Government's Onshore Energy Security Program (http://www.ga.gov.au/energy/energy-security-program/onshore-energy-security.html) and the Western Australian Government's Royalties for Regions Exploration Incentive Scheme (http://www.dmp.wa.gov.au/7743.aspx). We thank all in these organisations for their input to the project. Wolfgang Maier and David Mole are thanked for their contributions to the orthomagmatic and komatiite related nickel sections respectively.

References

Abeysinghe, P.B., 2003. Mineral occurrences and exploration activities in the Arunta–Musgrave area. *Geological Survey of Western Australia Record* 2002/9, Perth, 33p.

Aitken, A.R.A., Smithies, R.H., Dentith, M.C., Joly, A., Evans, S., and Howard, H.M., 2013a. Magmatism-dominated intracontinental rifting in the Mesoproterozoic: The Ngaanyatjarra Rift, central Australia. *Gondwana Research* (in press).

Aitken, A.R.A., Joly, A., Dentith, M.C., Evans, S., Gallardo, L., Thiel, S., Smithies, R.H., and Tyler, I.M., 2013b. Imaging crustal structure in the west Musgrave Province from magnetotelluric and potential field data. *Geological Survey of Western Australia Report*.

Aitken, A.R.A., Salmon, M.L., and Kennett, B.L.N., 2013c. Australia's Moho: a test of the usefulness of gravity modelling for the determination of Moho depth. *Tectonophysics* (in press).

Barnes, S.-J., and Lightfoot, P.C., 2005. Formation of magmatic nickel sulfide deposits and processes affecting their copper and platinum group element contents. *Economic Geology*, 100, 179–213.

Barnes, S.J., and Fiorentini, M.L., 2012. Komatiite magmas and sulfide nickel deposits: A comparison of variably endowed archean terranes. *Economic Geology*, 107, 755–780.

Blewett, R.S., Henson, P.A., Roy, I.G., Champion, D.C., and Cassidy, K.F., 2010. Scale-integrated architecture of a world-class gold mineral system: The Archaean eastern Yilgarn Craton, Western Australia. *Precambrian Research*, 183, 230–250.

Collins, J.E., Hagemann, S.G., McCuaig, T.C., Frost, K.M., and Sharp, D., 2007. Geological History of the Flying Fox Nickel Deposit, Forrestania Greenstone Belt, Yilgarn Craton, Western Australia: A Preliminary Assessment. Digging Deeper, Vols 1 and 2, 1567–1570.

Cutten, H.N., Thorne, A.M., and Johnson, S.P., 2011. Geology of the Edmund and Collier Groups. In: Johnson, S.P., Thorne, A.M., Tyler, I.M. (editors.), Capricorn Orogen seismic and magnetotelluric (MT) workshop 2011: extended abstracts. *Geological Survey of Western Australia, Record* 2011/25, 27–40.

Evins, P.M., Smithies, R.H., Howard, H.M., Kirkland, C.L., Wingate, M.T.D., and Bodorkos, S., 2010. Devil in the detail; The 1150-1000Ma magmatic and structural evolution of the Ngaanyatjarra Rift, west Musgrave Province, Central Australia. *Precambrian Research*, 183, 572–588.

Fiorentini, M.L., Beresford, S.W., Rosengren, N., Barley, M.E., and McCuaig, T.C., 2010. Contrasting komatiite belts, associated Ni-Cu-(PGE) deposit styles and assimilation histories. *Australian Journal of Earth Sciences*, 57, 543–566.

Godel, B., Seat, Z., Maier, W.D., and Barnes, S.J., 2011. The Nebo-Babel Ni-Cu-PGE sulfide deposit (West Musgrave Block, Australia): Pt. 2. Constraints on parental magma and processes, with implications for mineral exploration. *Economic Geology*, 106, 557–584.

Goleby, B.R., Blewett, R.S., Korsch, R.J., Champion, D.C., Cassidy, K.F., Jones, L.E.A., Groenewald, P.B., and Henson, P., 2004. Deep seismic reflection profiling in the Archaean northeastern Yilgarn Craton, Western Australia: Implications for crustal architecture and mineral potential. *Tectonophysics*, 388, 119–133.

Greatland Gold, 2010. Proof of concept in initial drilling at Ernest Giles, A new large greenstone sequence discovered in the Eastern Goldfields of Western Australia. Greatland Gold Exploration Update 10 November 2010, http://www.greatlandgold.com/pdfs/20101110%20Exploration%20Update.pdf.

Groves, D.I., 1993. The crustal continuum model for late-Archean lode-gold deposits of the Yilgarn Block, Western Australia. *Mineralium Deposita*, 28, 366–374.

Groves, D.I., Goldfarb, R.J., Knox-Robinson, C.M., Ojala, J., Gardoll, S., Yun, G.Y., and Holyland, P., 2000. Late-kinematic timing of orogenic gold deposits and significance for computer-based exploration techniques with emphasis on the Yilgarn Block, Western Australia. *Ore Geology Reviews*, 17, 1–38.

Hayward, N., and Skirrow, R., 2010. Geodynamic Setting and Controls on Iron Oxide Cu-Au (±U) Ore in the Gawler Craton, South Australia. In: Porter, T.M. (editor), Hydrothermal Iron Oxide Copper-Gold & Related Deposits: A Global Perspective. PGC Publishing, Adelaide, 9–31.

Howard, H.M., Smithies, R.H., Kirkland, C.L., Evins, P.M., and Wingate, M.T.D., 2009. Age and geochemistry of the Alcurra Suite in the west Musgrave Province and implications for orthomagmatic Ni-Cu-PGE Mineralization during the Giles Event. *Geological Survey of Western Australia Report*.

Howard, H.M., Werner, M., Smithies, R.H., Evins, P.M., Kirkland, C.L., Kelsey, D.E., Hand, M., Collins, A.S., Pirajno, F., Wingate, M.T.D., Maier, W.D., and Raimondo, T., 2011. The geology of the west Musgrave Province and the Bentley Supergroup - a field guide. *Geological Survey of Western Australia Report*, 119p.

Joly, A., Aitken, A.R.A., Dentith, M., Porwal, A.K., and Smithies, R.H., 2013. Mineral prospectivity analysis of the West Musgrave Province. *Geological Survey of Western Australia Report*.

Korsch, R.J., Blewett, R.S., Smithies, R.H., Quentin de Gromard, R., Howard, H.M., Pawley, M.J., Carr, L.K., Hocking, R.M., Neumann, N.L., Kennett, B.L.N., Aitken, A.R.A., Holzschuh, J., Duan, J., Goodwin, J.A., Jones, T., Gessner, K., and Gorczyk, W., 2013. Geodynamic implications of the Yilgarn Craton–Officer Basin–Musgrave Province (YOM) deep seismic reflection survey: part of a ~1800 km transect across Western Australia from the Pinjarra Orogen to the Musgrave Province. In: Neumann, N.L. (editor), *Yilgarn Craton–Officer Basin–Musgrave Province (YOM) Seismic and MT Workshop*. Geoscience Australia Record 2013/28, 169–197.

Leahy, K., Barnicoat, A.C., Foster, R.P., Lawrence, S.R., and Napier, R.W., 2005. Geodynamic processes that control the global distribution of giant gold deposits. *Geological Society, London, Special Publications*, 248, 119–132.

Li, C., Maier, W.D., and De Waal, S.A., 2001. Magmatic Ni-Cu versus PGE deposits: Contrasting genetic controls and exploration implications. *South African Journal of Geology*, 104, 309–318.

Maier, W.D., Howard, H.M., Smithies, R.H., Yang, S., and Barnes, S.-J., in prep. Mafic-ultramafic intrusions of the Giles Event, Western Australia: Petrogenesis and prospectivity for magmatic ore deposits. *Geological Survey of Western Australia Report.*

McCuaig, T.C., Beresford, S., and Hronsky, J., 2010. Translating the mineral systems approach into an effective exploration targeting system. *Ore Geology Reviews*, 38, 128–138.

Micklethwaite, S., and Cox, S.F., 2006. Progressive fault triggering and fluid flow in aftershock domains: Examples from mineralized Archaean fault systems. *Earth and Planetary Science Letters*, 250, 318–330.

Mole, D.R., Fiorentini, M.L., Thebaud, N., McCuaig, T.C., Cassidy, K.F., Barnes, S.J., Belousova, E., Mudrovska, I., and Doublier, M.P., 2010. Lithospheric controls on the localization of komatiite-hosted nickel-sulfide deposits., 5th International Archean Symposium. *Geological Survey of Western Australia Record* 2010/18, 101–103.

Mole, D.R., Fiorentini, M.L., Thebaud, N., McCuaig, T.C., Cassidy, K.F., Kirkland, C.L., Wingate, M.T.D., Romano, S.S., Doublier, M.P., and Belousova, E.A., 2012. Spatio-temporal constraints on lithospheric development in the southwest-central Yilgarn Craton, Western Australia. *Australian Journal of Earth Sciences*, 59, 625–656.

Naldrett, A.J., 1999. World-class Ni-Cu-PGE deposits: Key factors in their genesis. *Mineralium Deposita*, 34, 227–240.

Pawley, M.J., Romano, S.S., Hall, C.E., Wyche, S., and Wingate, M.T.D., 2009. Article in Ann Rev 07-08: The Yamarna Shear Zone: a new terrane boundary in the northeastern Yilgarn Craton? In: Australia, G.S.o.W. (editor.), *GSWA Annual Review*, 2007-2008, 27–32.

Pawley, M.J., Wingate, M.T.D., Kirkland, C.L., Wyche, S., Hall, C.E., Romano, S.S., and Doublier, M.P., 2012. Adding pieces to the puzzle: Episodic crustal growth and a new terrane in the northeast Yilgarn Craton, Western Australia. *Australian Journal of Earth Sciences*, 59, 603–623.

Seat, Z., Mary Gee, M.A., Grguric, B.A., Beresford, S.W., and Grassineau, N.V., 2011. The Nebo-Babel Ni-Cu-PGE sulfide deposit (West Musgrave, Australia): Pt. 1. U/Pb zircon ages, whole-rock and mineral chemistry, and O–Sr–Nd isotope compositions of the intrusion, with constraints on petrogenesis. *Economic Geology*, 106, 527–556.

Sircombe, K.N., Cassidy, K.F., Champion, D.C., and Tripp, G., 2007. Compilation of SHRIMP U–Pb geochronological data, Yilgarn Craton, Western Australia, 2004-2006.

Smithies, R.H., Howard, H.M., Evins, P.M., Kirkland, C.L., Bodorkos, S., and Wingate, M.T.D., 2009. The west Musgrave Complex - new geological insights from recent mapping, geochronology, and geochemical studies. *Geological Survey of Western Australia Record* 2008/19, 20p.

Smithies, R.H., Howard, H.M., Evins, P.M., Kirkland, C.L., Kelsey, D.E., Hand, M., Wingate, M.T.D., Collins, A.S., and Belousova, E., 2011. High-temperature granite magmatism, crust-mantle interaction and the mesoproterozoic intracontinental evolution of the Musgrave Province, Central Australia. *Journal of Petrology*, 52, 931–958.

Smithies, R.H., Howard, H.M., Kirkland, C.L., Medlin, C.C., and Wingate, M.T.D., 2013. Western Australia's own super volcano: part of the torturous thermal history of the west Musgrave Province. *Geological Survey of Western Australia, Record* 2013/2, 23–26.

Stevens, M.K., and Apak, S.N., 1999. GSWA Empress 1 and 1A well completion report, Yowalga Subbasin, Officer Basin, Western Australia. *Geological Survey of Western Australia Record* 1999/4, 110p.

Wingate, M.T.D., Pirajno, F., and Morris, P.A., 2004. Warakurna large igneous province: A new Mesoproterozoic large igneous province in west-central Australia. *Geology*, 32, 105–108.

Wyche, S., Ivanic, T.J., and Zibra, I., 2013. Youanmi seismic and magnetotelluric (MT) workshop 2013: extended abstracts Preliminary edition. *Geological Survey of Western Australia Record* 2013/6.

Zhang, M., O'Reilly, S.Y., Wang, K.L., Hronsky, J., and Griffin, W.L., 2008. Flood basalts and metallogeny: The lithospheric mantle connection. *Earth-Science Reviews*, 86, 145–174.